Novel Hydrogels For Keratoprosthesis

JIFAN LI

Doctor of Philosophy

ASTON UNIVERSITY

December 2001

NOVEL HYDROGELS FOR KERATOPROSTHESIS

JIFAN LI

Submitted for the degree of December 2001

Doctor of Philosophy

Hydrogels may be described as cross-linked hydrophilic polymers that swell but do not dissolve in water. They have been utilised in many biomedical applications, as there is the potential to manipulate the properties for a given application by changing the chemical structure of the constituent monomers. This project is focused on the development of novel hydrogels for keratoprosthesis (KPro).

The most commonly used KPro model consists of a transparent central stem with a porous peripheral skirt. Clear poly (methyl methacrylate) (PMMA) core material used in the Strampelli KPros prosthesis has not been the cause of failure found in other core and skirt prostheses. However, epithelialization of this kind of solid, rigid optic material is clearly impossible. The approach to the development of a hydrogel for potential KPro use adopted in this work is to develop soft core material to mimic the properties of the natural cornea by incorporating some hydrophilic monomers, such as N, N-dimethyacrylamide (NNDMA), N-vinyl pyrrolidone (NVP) and acryloylmorpholine (AMO) with methyl methacrylate (MMA). Most of these materials have been used in other ophthalmic applications, such as contact lens. However, an unavoidable limitation of simple MMA copolymers as conventional hydrogels is poor mechanical strength. The hydrogel for use in this application must be able to withstand the stresses involved during the surgical procedure involved with KPro surgery and the *in situ* stresses such as the deforming force of the eyelid during the blink cycle. Thus, semi-interpenetrating polymer networks (SIPNs) based on ester polyurethane, AMO, NVP and NNDMA were examined in this work and were found to have much improved mechanical properties at water contents between 40% and 70%. Polyethylene glycol monomethacrylate (PEG MA) was successfully incorporated in order to modulate protein deposition and cell adhesion. Porous peripheral skirts were fabricated using different types of porosigen. The water content, mechanical properties, surface properties and cell response of these various materials have been investigated in this thesis.

These studies demonstrated that simple hydrogel SIPNs, which show isotropic mechanical behaviour, are not ideal KPro materials since they do not mimic the anisotropic behaviour of natural cornea. The final stage of the work has concentrated on the study of hydrogels reinforced with mesh materials. They offer a promising approach to making a hydrogel that is very flexible but strong under tension, thereby having mechanical properties closer to the natural cornea than has been previously possible.

Keyword: hydrogel, semi-interpenetrating polymer network, mesh reinforced, keratoprosthesis

For my family

ACKNOWLEDGEMENTS

I would like to take this opportunity to express my thanks to the following:

Firstly, to my supervisor Professor Brian Tighe for his guidance, encouragement, enthusiasm and financial support throughout the course of this project.

To Mr. Richard Edwards for checking my thesis, and his support, assistance and many useful discussions throughout the course of this work!

To Dr. Val. Franklin for completing the *in vitro* ocular spoilation studies, and her help.

To Dr. Fiona Lydon for completing the rheometer test on natural human cornea.

To the Department of Pharmacy and Biomolecular Sciences at the University of Brighton for carrying out the cell test work.

To everyone in the Biomaterials Research Unit who has made my time at Aston so enjoyable. With them, I found the pleasures of drinking "Gin and Tonics" and "Coke and Rum". Cheers, mate!

And finally special thanks go to my family and friends for their support and encouragement.

LIST OF CONTENTS

LIST OF TABLES

LIST OF FIGURES

LIST OF ABBREVIATIONS

AMO	Acryloylmorpholine	θ	Contact Angle
NNDMA	N, N-dimethylacrylamide	NVP	N-vinyl pyrrolidone
EWC	Equilibrium Water Content	AZBN	Azo-bis-isobutyronitrile
THEMA	Tetrahydrofurfuryl methacrylate	DSC	Differential Scanning Calorimetry
MMA	Methyl methacrylate	EGDMA	Ethylene glycol dimethacrylate
SIPNs	Semi Interpenetrating Polymer Network	PEG MA	Polyethylene glycol methacrylate
γ	Surface Tension	KPro	Keratoprosthesis
OOKP	Osteo-odonto keratoprosthesis	PU	Polyurethane
HEMA	2-Hydroxyethyl Methacrylate	ABH	Aston Biomimetic Hydrogel
MAA	Methacrylic acid	Q	Reactivity of monomer
e	Charge on radical	E.Mod	Elastic Modulus
Ts	Tensile Strength	Eb	Elongation at break
THF	Tetrahydrofuran	FCS	Foetal Calf Serum
UV	Ultra Violet	NMP	N-methyl pyrrolidone
DPBS	Dulbecco's Phosphate Buffered Saline	IPN	Interpenetrating Polymer Network
NMR	Nuclear Magnetic Resonance Spectroscopy	BAC	Biomaterial-associated calcification
PK	Penetrating Keratoplasty	OCP	Ocular Cicatricial Pemphigoid
PTFE	Polytetrafluoroethylene	PDMS	Polydimethylsiloxane
CAB	Cellulose Acetate Butyrate	SJS	Stevens-Johnson Syndrome
HDI	Hexamethylenediisocyanate	Ig	Immunoglobulin
Calcein AM	Calcein acetoxy methyl ester	FWC	Freezing water content

Chapter 1

Introduction

A biomaterial is a nonviable material used in a device, intended to interact with biological systems[1]. The goal of biomaterials science is that of "biocompatibility". Biocompatibility is the ability of a material to perform with an appropriate host response in a specific application[1]. In many tissues acceptable prosthetic materials are available (*e.g.* dental implants, artificial hip joints, intraocular lenses) and research focus has shifted to developing surfaces which function effectively in the long term. However, there remain certain tissues which pose severe challenges in the development of short to medium term material replacements. Chief among these remains the human cornea because of a combination of its relatively poorly understood basic biology and inadequate understanding and optimisation of the materials requirements of the polymeric implant.

This project is centred on the development of novel hydrogels for use in corneal surgery, in particular, to produce synthetic analogues of natural cornea for use in corneal replacement (improved keratoprosthesis for corneal blindness).

1.1 Hydrogels

Hydrogels are water-swellable, three-dimensional polymeric networks possessing both the cohesive properties of solids and diffusive transport properties of liquids. The three-dimensional networks of a hydrogel are formed by either reversible bonds (physical bonds), which can be made or broken under certain environment, or covalent bonds (chemical bonds). If the crosslinks are based on physical bonds, such as hydrogen, ionic, or Van der Waal's bonds, the responses of the hydrogels to external stimuli are often reversible. They can contain 20-98% water, and it is the water that has a major influence on the transport, mechanical and surface properties of the hydrogel. A range of water contents and therefore resulting properties are possible to achieve by varying the quantity and type of monomer, amount of crosslinking agent, initiator and any possible diluent.

Hydrogels were first proposed for biomaterials in 1960 by Wichterle and Lim[2], who developed poly(2-hydroxyethyl methacrylate), poly(HEMA), as contact lens material. Since then, hydrogels have been in utilized in many sites in the body, fulfilling many roles, including heart valves[3], joint replacement[4, 5], membrane oxygenators[6], haemodialysis membranes[7], intraocular lenses[8] and contact lenses[9, 10].

1.2 Interpenetrating Polymer Networks

An interpenetrating polymer network, IPN, can be defined as a combination of two polymers in network form, at least one of which is synthesized and/or crosslinked in the immediate presence of the other[11]. An IPN can be distinguished from simple polymer blends, blocks and grafts in two ways: (1) An IPN swells, but does not dissolve in solvents, and (2) creep and flow are suppressed. The formation of IPNs can greatly enhance the mechanical properties of polymers.

The first IPN known was invented by Aylsworth[12] in 1914. This was a mixture of natural rubber, sulphur, and partly reacted phenol-formaldehyde resins. However, the first use of the term "interpenetrating polymer network" was by Millar in 1960, who also carried out the first serious scientific study of IPNs[11].

There are several types of IPNs depending upon the methods of the formation: simultaneous, sequential, semi-IPNs, and homo-IPNs. Simultaneous IPNs begin with a mutual solution of both monomers and their respective crosslinkers, which are then polymerised simultaneously by noninterfering methods. Sequential IPNs begin with the synthesis of a crosslinked polymer I, monomer II, plus its own crosslinker and initiator, are swollen into polymer I, and polymerised *in situ*. Semi-IPNs are produced when one of the components is linear and the other is a crosslinked polymer. Homo-IPNs consist of polymers that are chemically identical but retain their specific properties. Figure 1.1 illustrates a semi-IPN.

Interpenetrating polymer networks have been utilized for many functions, including biomedical applications. Corkhill *et al*[13] had used this technology to produce a synthetic articular cartilage. Conventional synthesis hydrogels can have high water content, but the mechanical properties are often poor. IPNs can be produced that have similar water contents but much improved mechanical properties, as they are stronger and stiffer, and so mimicking more closely the natural tissue.

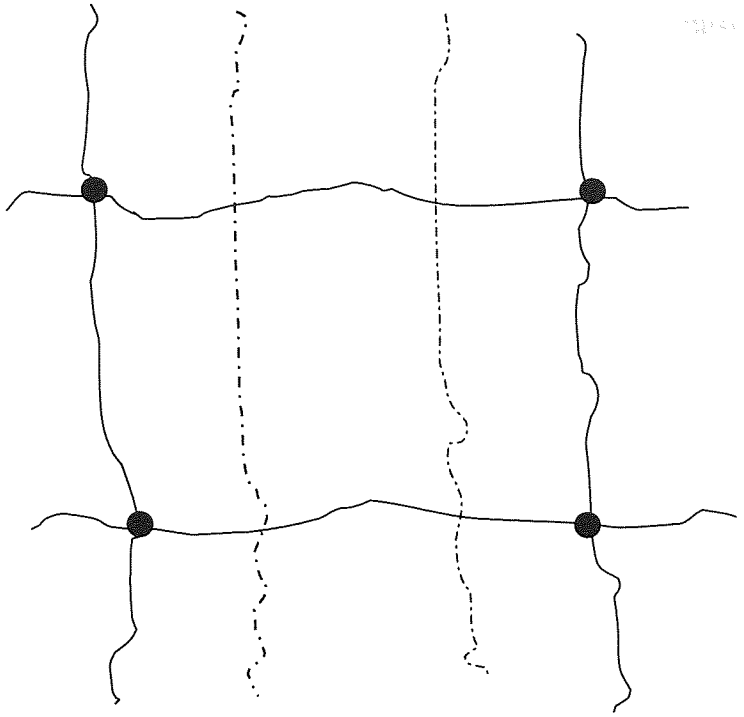

Figure 1.1 Semi-interpenetrating polymer networks

1.3. Characterization of Hydrogels

1.3.1 Equilibrium Water Content

When a hydrogel is placed in water, it will swell absorbing water until an equilibrium is reached. The equilibrium water content (EWC) is the most important single property of the hydrogel, as it governs the mechanical properties, surface properties, permeability to biological solutes and behaviour at a biological interface. It can be defined as:

$$\text{EWC}\,(\%) = \frac{\text{Weight of water in the gel}}{\text{Total weight of the hydrated gel}} \times 100\% \qquad (1.1)$$

The EWC is influenced by the nature of the monomers used, the crosslink density and the temperature, pH and tonicity of the hydrating media. Water is able to have such a high affinity for a hydrogel because it can permeate the loosely crosslinked three-dimensional structure and interact with the hydrophilic groups within.

However, the EWC does not give a full indication of the many states in which water can exist within the hydrogel. It is not the only structural factor that must be taken into account.

1.3.2 Water in Polymers

Translucence in hydrated system is generally due to the preferential water clustering around the more hydrophilic moieties to the exclusion of hydrophobic blocks, causing light to scatter.

The water present in the hydrogel network also influences the properties of the hydrogels. The water in the hydrogel performs two other functions. It acts as a bridge between the natural and the synthetic systems giving greater biocompatibility, or perhaps more properly biotolerance, and confers membrane properties on the hydrogel, allowing transport of oxygen and water soluble metabolites through the polymer matrix. Polar groups in hydrogel polymers interact more strongly with water than nonpolar fragments.

Previous work[14] carried out indicates that water exists in a continuum of states between two extremes in a hydrogel, ranging from freezing, or 'free' water, which is water that does not interact with the polymer matrix, to non-freezing, or 'bound' water, which is water that has direct hydrogen bonding with polar groups of the polymer matrix, or which strongly interacts with ionic residues of the matrix[15]. Polymer combined with freezing water has a lower density than polymer combined with strongly bonded water and this is reflected in the densities of the hydrated copolymers. The freezing water can also be regarded as plasticizing water in view of its greater relative effect on chain mobility. It is the amount of free water that is crucial for oxygen transport. The ratio of freezing to non-freezing water in the polymer still influences the properties of hydrogels.

The techniques that have been used to study water binding in hydrogel systems include ^{1}H nuclear magnetic resonance spectroscopy (NMR)[16, 17, 18, 19, 20], specific conductivity[21] and differential thermal analysis[22]. Each technique has some influence on the water structuring, the dynamic and thermodynamic properties of the water present and hence on the ratio of freezing to non-freezing water obtained[23]. This project utilizes differential scanning calorimetry, DSC, to enable an easy, quantitative determination of the relative amount of freezing water to be made[24, 25, 26, 27].

1.3.2.1 Differential Scanning Calorimetry

Differential Scanning Calorimetry, DSC, was developed in 1964 by Perkin-Elmer. The working principle is that measured energy is required to keep the reference holder and sample holder at the same temperature. If the temperature is varied and a transition occurs, energy will be supplied to either reference or sample to keep them at the same temperature. If energy needs to be inputted into the sample holder, the transition is endothermic, and if energy needs to be inputted into the reference holder, the transition is exothermic. The energy inputted can be measured directly as the area under the peak. The schematic for the measuring system is shown in Figure 1.2.

Differential Scanning Calorimetry is a relatively quick method of determining the ratio of water states present in the hydrogel. This is obtained as even at very low temperatures only part of the water in the polymer will freeze, allowing a quantitative determination of the relative amounts of freezing and non-freezing water to be obtained. Further information about the structuring of water in the gel can be obtained from the fine structure of the thermogram. In general, water bound to the backbone by hydrogen bonding will not freeze, whilst the more mobile water which is unaffected by the polymeric environment will freeze. The chemical constituents, chain flexibility, water binding properties, and pore size and distribution all influence the properties of a hydrogel.

1.3.3 Mechanical Testing

The mechanical properties of the hydrogels are measured by tensile testing. The standard testing conditions were determined by Trevett and Tighe[28] to overcome the difficulties encountered in testing a hydrogel in a non-aqueous environment, and allow for comparative (but not absolute) data to be obtained.

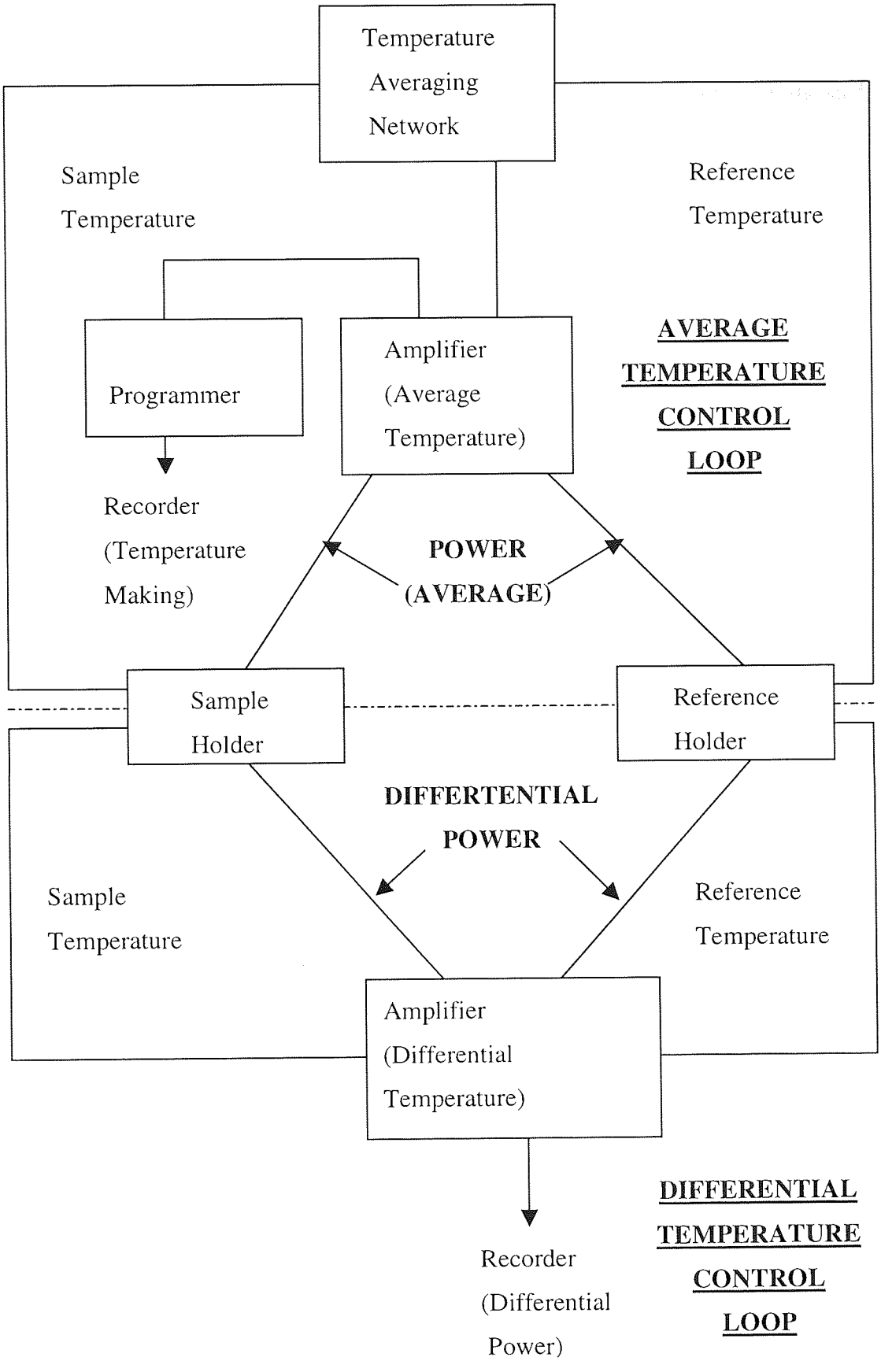

Figure 1.2. Schematic representation of a differential scanning calorimeter

1.3.4 Wettability

Wettability is the ability of a liquid to adhere to a solid and spread over its surface to varying degrees. It is considered to be a surface property as opposed to hydrophilicity which is thought of as a bulk property. For the fabrication of biomaterials that come into contact with blood and tissue, it is usually desirable to utilise materials that exhibit very high degrees of wettability. This is due to the fact that most of the internal biological environments, with the exception of lipids, are hydrophilic in nature and biocompatibility appears to correlate directly with the degree of hydrophilicity that a surface exhibits[29]. Thus the practice of incorporating hydrophilic materials into the designed biomaterials to enhance their wettability has arisen. However, the hydrophilic material does not mean that the surface is automatically hydrophilic as well. The polymer chain at the solid-air boundary orientates itself into a position of lowest free energy, i.e., hydrophobic groups pointing out, hydrophilic groups buried into the material. Efforts to reduce or even prevent chain rotation must be an integral part of controlling wettability and deposition.

The property of wettability can be characterised by several methods including the measurement of contact angles and the surface tension of solids and liquid. The measured value of the contact angle will vary depending on whether the liquid is advancing initially over a dry surface or receding from a wetted surface. This is referred to as the contact angle hysteresis and the values of the receding and advancing contact angles may vary by as much as 50°. The divergence of these two values is enhanced by surface heterogeneity and surface roughness.

Using the sessile drop and captive bubble methods it is often difficult to estimate the angle between a bubble or drop and the solid surface, resulting in poor reproducibility of the measurements. Many researchers[30, 31] employed the Wihelmy technique which is a more objective method of assessing contact angle and operates by alternately immersing and withdrawing the sample from a test liquid to examine the hysteresis of polymers. This requires a mechanical testing device, an electrobalance, and a means of graphical output. The solid test sample is attached to the electrobalance and the test solution (usually water) is raised or lowered on a scissor jack with a motorised micropositioner in order to immerse and then remove the sample. The advancing contact angle is measured as the solution is moved over a previously unwetted surface (during immersion) and the receding angle when

the sample is withdrawn from the liquid (during withdrawal). The microbalance is used to measure the weight of the sample as it is moved into and out of the fluid.

The force exerted by the test sample is proportional to the apparent weight of the sample, and this in turn, is defined by the height of the meniscus of liquid adhered to the sample (a product of wetting) and the buoyancy. The contact angle at the instant of insertion and removal from the test liquid, when there are no buoyancy effects, can be calculated using the following formula:

$$\cos\theta = \frac{F}{\sigma \times P} \qquad (1.2)$$

Where: θ = advancing or receding contact angle

F = measured force (dynes)

σ = surface tension of probe solution (dynes/cm) (or mN/m)

P = perimeter of test sample (cm)

Many polymer systems display some degree of contact angle "hysteresis", defined as the difference between the advancing and receding contact angles. A typical dynamic hysteresis profile is illustrated in Figure 1.4. On most surfaces, the advancing contact angle exceeds the receding contact angle. Contact angle hysteresis can be subdivided into two types: thermodynamic hysteresis, where the hysteresis curve is reproducible over many cycles and is independent of time and frequency, and kinetic hysteresis, where the curve changes with the time and conditions.

Thermodynamic hysteresis on a clean surface is thought to be due to surface roughness (rugosity) and surface heterogeneity[32]. Surface heterogeneity is a second cause of thermodynamic hysteresis. Patches of different surface energies produce metastable differences when the contact line moves.

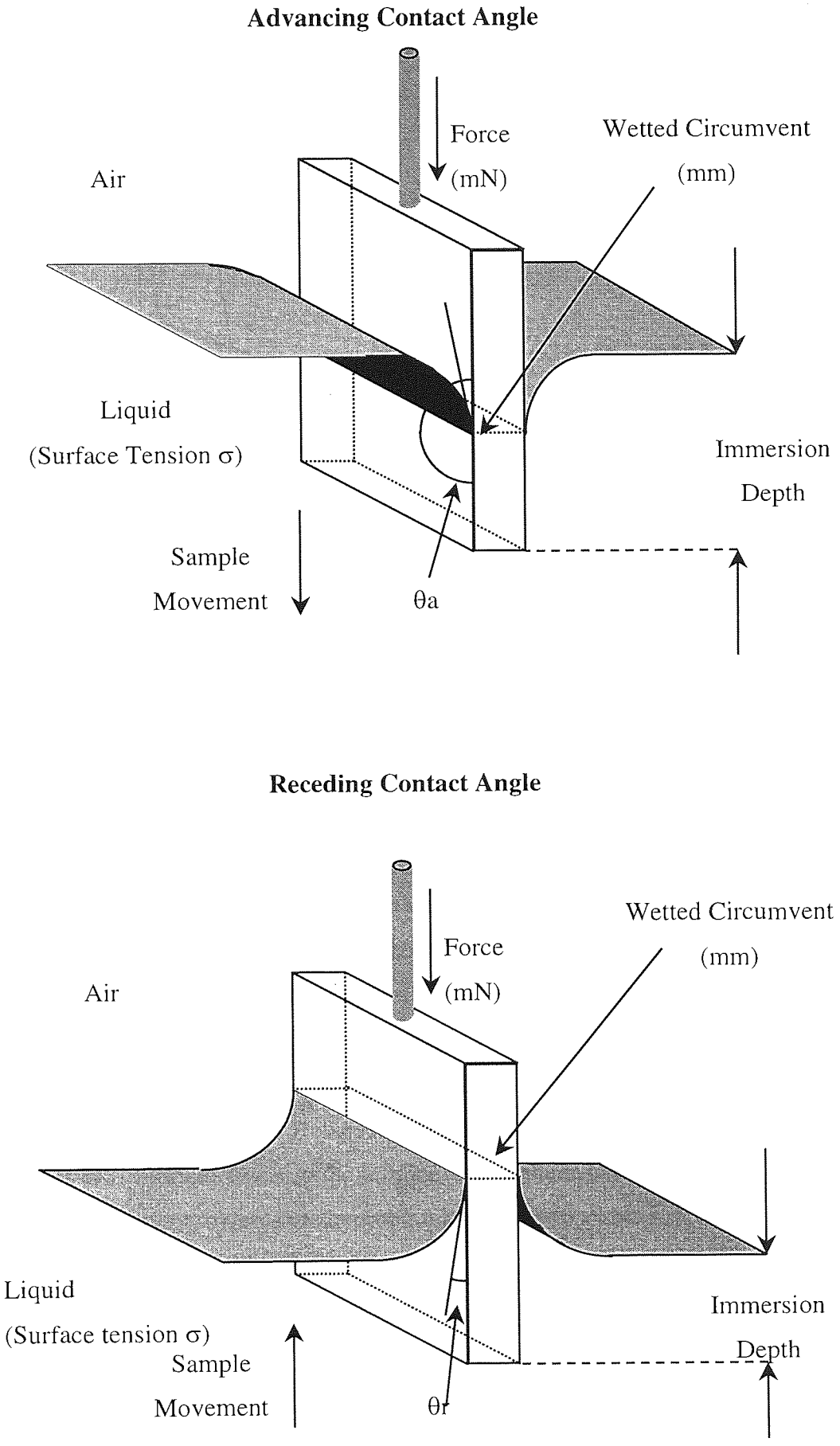

Figure 1.3 Advancing and receding contact angles

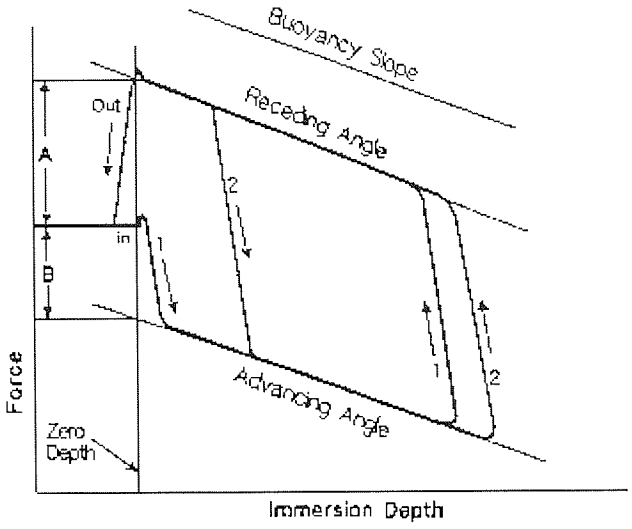

Figure 1.4 Diagram of a dynamic contact angle hysteresis curve, illustrating a two immersion cycle

Kinetic hysteresis is usually accounted for by time or rate dependent processes, such as swelling, liquid penetration into the surface region and surface reorientation of functional groups[32] (such that the conformation of the polymer changes to minimise the interfacial energy between itself and the adjacent phase). The large hysteresis observed for polymers containing hydrophilic functional groups is mainly due to the high rotational mobility of macromolecules at the surface[33]. The rate of reorientation is likely to be particularly fast within hydrogel materials, where flexibility of the polymer network enables free motion of such functional groups. A hydrogel polymer in air will tend to orient its polar groups into the structure of the hydrogel, towards the imbibed water, and the hydrophobic groups will tend to be at the surface. However, when the polymer is placed in water, the hydrophilic groups will reorient towards the surface where there is more water, and the hydrophobic groups will orient towards the hydrophobic polymer backbone.

The phenomenon of surface mobility is related to the mobility of the hydrophilic and hydrophobic groups on the backbone of the polymer. If a sample is unwettable this suggests that the hydrophobic groups prefer the phase (air) on the surface of the gel and the hydrophilic groups prefer to be away from the surface and associate with water molecules already trapped within the polymer bulk.

Incomplete wetting is characterised by the contact angle θ of the liquid on the solid surface. If an initially unwettable sample is dipped into an aqueous solution, the advancing angle is high. The hydrophilic groups will tend to associate with the water molecules and rotate around the backbone of the carbon to orientate themselves at the surface of the gel, while the hydrophobic groups move into the gel. The sample at this point will be wettable and the receding angle will be low, hence the hysteresis will be large. In this case there is a high surface mobility. On the other hand, if the sample is already wettable, the hydrophilic groups will already be present on the surface of the gel, so there is little mobility of the surface.

A low advancing angle combined with negligible hysteresis can therefore be considered to be an indication of excellent wettability.

Polymers containing anionic groups will tend to be wettable at high pH, and polymers containing cationic groups will be wettable at low pH. This is due to the repulsion of the ionic groups, which results in large pores in the matrix of the polymer. Water molecules in solution can then flood into the matrix and form a hydration shell around the charged groups, thus giving a wettable gel.

1.3.5 Contact Angle Measurement

The main factor in determining the wettability of a material is the chemical structure of the polymer at the air-sold-liquid interface. Polymer surfaces are mobile and the molecular orientation can be modified in response to the environment. When the sample in air, the hydrophobic groups are orientated towards the hydrophobic solid-air interface. When the liquid comes into contact with the sample, the hydrophilic groups reorientate themselves towards the liquid-solid interface. The wettability of sample can be measured in terms of contact angles, θ. The greater the degree of wettability of the surface, the lower the value of θ.

Hydrogels used for biomedical applications come into contact with biological fluid, so the surface free energy of the material is an important parameter in determining its biotolerance. The surface free energy of the materials can be obtained by analysing the interface between a drop of wetting liquid or vapour on a solid surface. The surface free energy is formed

from polar and dispersive components and the polar component in particular is important in that it determines the wettability of a material.

Contact angles are generally measured in the dehydrated state using the sessile drop technique and in the hydrated state using Hamilton's method and captive bubble technique. Results are obtained via the resolution the forces at a three-phase interface, formed either by a drop of liquid on a solid surface in air or by a drop of liquid or vapour on a solid surface immersed in a liquid. The theories used to determine the surface free energy of polymers from contact angle measurements is shown below.

1.3.5.1 Dehydrated Surfaces

When a drop of liquid is placed on a smooth solid surface, the shape of the drop is determined by the wettability of the solid surface (Figure 1.5). The contact angle θ is the angle between the surface of the solid and the tangent to the liquid surface.

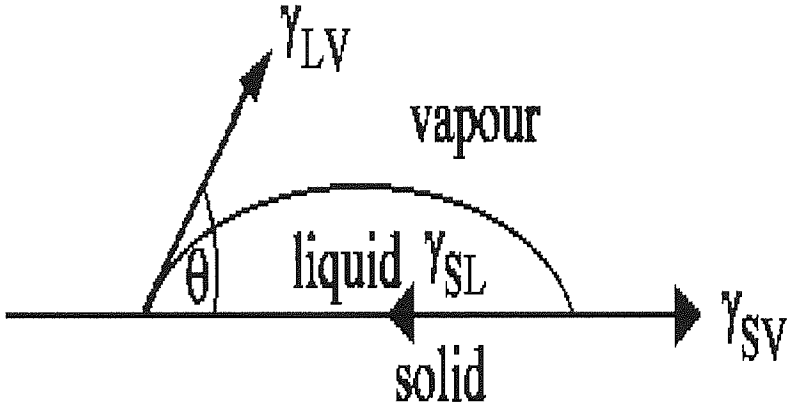

Where: γ_{SV} is the surface free energy of the solid

γ_{LV} is the surface free energy of the liquid

γ_{SL} is the interfacial free energy of the solid and liquid

Figure 1.5 Components of solid surface free energy

In 1805 Young derived an equation[34] that involves the resolution of the forces at a point of contact of a sessile drop and a solid, as demonstrated in Figure 1.5.

$$\gamma_{SV} = \gamma_{SL} + \gamma_{LV} \cos\theta \tag{1.3}$$

More than sixty years later, Dupre[35] expressed the reversible work of adhesion of a liquid and a solid as:

$$W_{SL} = \gamma_{SV} + \gamma_{LV} - \gamma_{SL} \tag{1.4}$$

Combining these two equations gives the Young-Dupre equation:

$$W_{SL} = \gamma_{LV} (1 + \cos \theta) \tag{1.5}$$

The spreading pressure π_e is the reduction of the surface tension of the solid due to vapour adsorption, and can be ignored for solids which give large values of θ.

$$\pi_e = \gamma_S - \gamma_{SV} \tag{1.6}$$

Fowkes[36] and Good[37] took into consideration polar (e.g. H-bonding) and dispersive (e.g. Van der Waals) forces and their equations can be combined to give:

$$W_{SL} = 2 [(\gamma_1^d \gamma_2^d)^{1/2} + (\gamma_1^p \gamma_2^p)^{1/2}] \tag{1.7}$$

where γ_1^d and γ_2^d are the dispersive components and γ_1^p and γ_2^p are the polar components of liquids 1 and 2. For a solid-liquid interface, combining this equation with Young's equation gives the Owens and Wendt equation[38]:

$$1 + \cos \theta = (2 / \gamma_{LV}) [(\gamma_{LV}^d \gamma_{SV}^d)^{1/2} + (\gamma_{LV}^p \gamma_{SV}^p)^{1/2}] \tag{1.8}$$

This expression may be used to determine the surface free energies of polymers in the dehydrated state. Two wetting liquids which have been fully characterised for polar and dispersive components are used. By measuring the contact angles of the liquids on the polymer surface and solving the equations simultaneously, γ_S^p and γ_S^d, the polar and

dispersive components of the surface free energy of the polymer may be determined. Water and diiodomethane are usually used as wetting liquids because of their high total surface free energies and their balance of polar and dispersive forces.

Table 1.1 shows the surface free energies and the polar and dispersive components of several liquids that may be used.

Liquid	γ^d (mN/m)	γ^p (mN/m)	γ^t (mN/m)
Water	21.8	51.0	72.8
Glycerol	37.0	26.4	63.4
Formamide	39.5	18.7	58.2
Diiodomethane	48.5	2.3	50.8
n-Hexane	27.6	0.0	27.6
n-Octane	21.8	0.0	21.8

Table 1.1 Polar and dispersive components of some wetting liquids commonly used for contact angle studies

1.3.5.2 Hydrated Surfaces

The sessile drop technique is an unsatisfactory method for measuring hydrated surfaces because hydrated hydrogels begin to lose water by evaporation as soon as they are placed in air. It is therefore difficult to measure the contact angle accurately because the angle will change according to the state of dehydration of the sample. In addition, there exists no efficient and reproducible way to remove the surface water from the sample before measurement. Two techniques have been developed to overcome these problems, Hamilton's method[39, 40] and the captive air bubble technique, which allow the surface energy of a polymer to be determined in the fully hydrated state.

1.3.5.2.1 Hamilton's Method

Hamilton's method involves measuring the contact angles of small n-octane droplets on solid surfaces under water as shown in Figure 1.6.

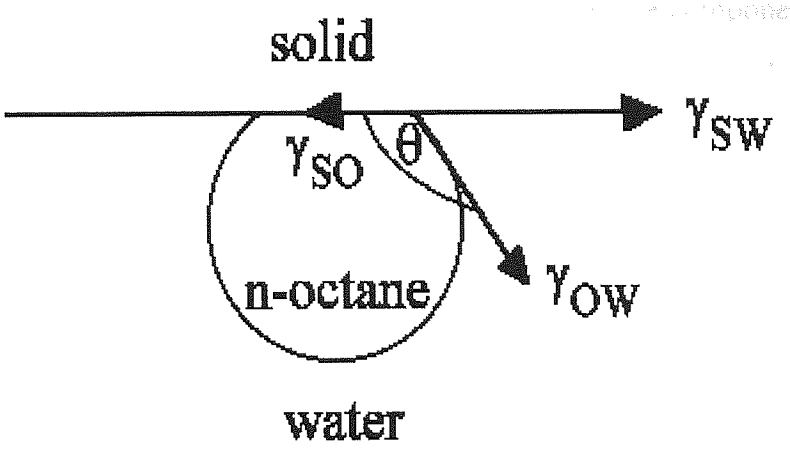

where: γ_{SW} = solid - water interfacial free energy

γ_{SO} = solid - octane interfacial free energy

γ_{OW} = octane - water interfacial free energy

Figure 1.6 The free energy components for Hamilton's method

Fowkes[41] developed an equation for the work of adhesion at a solid – liquid interface, assuming that the sum of the surface free energies of the two separate phases would be offset by the stabilization from dispersive forces (universal Van del Walls forces) to give the interfacial free energy between the solid and the liquid.

$$\gamma_{SL} = \gamma_S + \gamma_{LV} - 2\,(\gamma_{LV}^{d}\,\gamma_S^{d})^{0.5} \qquad (1.9)$$

This equation does not take into account the polar forces acting across the interface. So a modified form of this equation was developed by Tamai *et al*[42] which accounted for stabilisation by non-dispersive forces.

$$\gamma_{SL} = \gamma_S + \gamma_{LV} - 2(\gamma_{LV}^{d}\,\gamma_S^{d})^{0.5} - I_{SL} \qquad (1.10)$$

where:

$$I_{SL} = 2\,(\gamma_{LV}^{p}\,\gamma_S^{p})^{0.5} \qquad (1.11)$$

n-Octane has no polar component and the dispersive components for n-octane and water are identical (both 21.8 mN/m), thus it is possible to combine Young's equation with Tamai's equation to give an expression for I_{SW}, the polar stabilisation energy between water and the solid. The subscripts O for n-octane and W for water have been used.

$$I_{SW} = \gamma_{WV} - \gamma_{OV} - \gamma_{OW}\cos\theta \qquad (1.12)$$

Where: I_{SW} = polar stabilization energy between water and the solid

γ_{WV} = surface tension of n-octane saturated water

γ_{OV} = surface tension between n-octane and its vapour

γ_{OW} = surface tension between n-octane and water

Once the components γ_{OV} and γ_{OW} have been determined experimentally by Fowkes' method, I_{SW} can be calculated. γ_S^p, the polar component of surface free energy can now be determined by substituting the final value of I_{SL} into equation 1.11.

1.3.5.2.2 Captive Air Bubble Technique

This technique uses the same experimental procedure as Hamilton's method, using a bubble of air instead of a drop of n-octane on the solid surfaces as shown in Figure 1.7[43].

Andrade *et al*[44] showed that by using data from Hamilton's method and also the captive air bubble technique, it is possible to find values for γ_{SV}, γ_{SV}^p, γ_{SV}^d and γ_{SW} for the hydrogel water interface. Applying Young's equation (1.3) with water as the liquid phase gives:

$$\gamma_{SV} - \gamma_{SW} = \gamma_{WV}\cos\theta \qquad (1.13)$$

γ_{WV} is known to be 72.8 mN/m and θ is the contact angle of the captive air bubble, thus (γ_{SV} - γ_{SW}), the adhesion tension can be calculated.

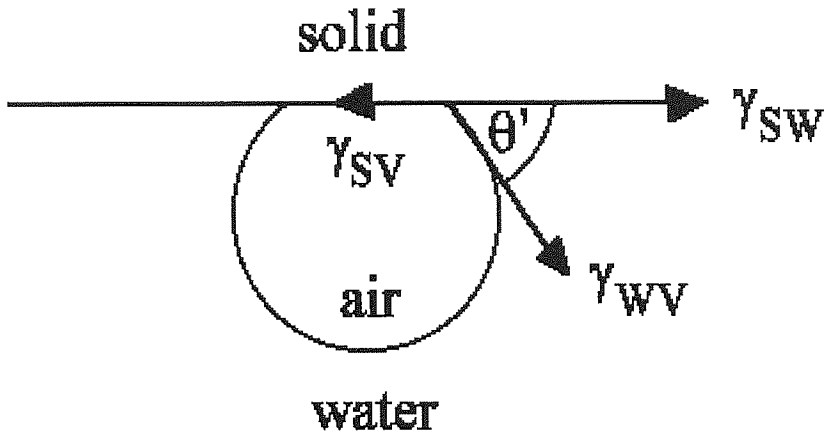

Where: γ_{SW} = solid – water interfacial free energy

γ_{WV} = water – vapour interfacial free energy (i.e. the surface tension of water)

γ_{SV} = solid – vapour interfacial free energy $\approx \gamma_S$ = solid surface free energy

Figure 1.7 Individual free energy components for the captive air bubble technique

An equation for the polar stabilisation parameter has already been derived

$$I_{SW} = \gamma_{WV} - \gamma_{OV} - \gamma_{OW} \cos\theta \qquad (1.14)$$

Knowing that γ_{WV} = 72.8 mN/m, γ_{OV} = 21.8 mN/m and γ_{OW} = 51.0 mN/m, this equation can be rewritten:

$$I_{SW} = 51.0\,(1 - \cos\theta) \qquad (1.15)$$

I_{SW} can now be calculated. Combining Tamai's and Andrade's equations gives:

$$(\gamma_{SV} - \gamma_{SW}) = 2\,(\gamma_{WV}^{d}\,\gamma_{SV}^{d})^{0.5} + I_{SW} - \gamma_{WV} \qquad (1.16)$$

Rearranging this equation gives an expression for the dispersive component, (γ_{SV}^{d}) of the hydrogel:

$$\gamma_{SV}^{d} = [\{(\gamma_{SV} - \gamma_{SW}) - I_{SW} + \gamma_{WV}\} / 2 (\gamma_{WV}^{d})^{0.5}]^2 \quad (1.17)$$

The polar component, (γ_{SV}^{p}) can also be derived by rearranging the equation for I_{SL} to give:

$$\gamma_{SV}^{p} = I_{SW}^{2} / (4 \gamma_{WV}^{p}) \quad (1.18)$$

A spreadsheet application has been programmed so that (γ_{SV} - γ_{SW}), I_{SW}, γ_{SV}^{p}, γ_{SV}^{d}, γ_{SV} and γ_{SW} may be calculated upon entry of θ.

An alternative method of calculating the dispersive component can be used based on the Owens and Wendt equation (1.8). The polar component is obtained by using Hamilton's method and by inserting this value into the Owens and Wendt equation, together with the measured water-air contact angle, the dispersive component can be calculated. Corkhill[15] has shown that the results obtained for the dispersive component using both methods have been shown to be within 0.2 mN/m.

1.3.6 *In Vitro* Spoilation

The principle of ocular spoilation is common to other instances where materials contact biological fluids, i.e., thrombosis at foreign surfaces, the formation of dental plaque in saliva. These all involve the adsorption of protein at a solid surface. *In vitro* spoilation can give us a guide as to the indication of the biocompatibility of the synthetic material. The Aston tear model was specifically designed and developed[45] to mimic the ocular environment, by replicating the tear-contact lens interaction, so as to give an indication of performance[46].

The critical surface tension of solid surfaces is sometimes used as an indicator of biocompatibility. This is defined as the surface tension of a liquid that will just wet the surface and spread[47]. Interfacial tension is the difference between the critical surface tension of the surface and the surface tension of the liquid. Some researchers have suggested that for maximum biocompatibility, an interfacial tension of less than 5 dyn cm^{-1}

is needed. The corneal epithelium has a surface tension of approx. 30 dyn cm^{-1} but the natural wetting agents in tears (mucins) reduces the surface tension of water (72.8 dyn cm^{-1}) to 40-46 dyn cm^{-1} and increases the critical surface tension of the cornea to about 40 dyn cm^{-1} by adsorption on to its surface, both effects combine to facilitate a continuous tear film.

Protein adsorption studies can also be used to assess biocompatibility but moreover they can also give us some idea of the surface structure of a material at a molecular level. Protein adsorption is a thermodynamic process, one of two types: 1. hydrophilic, exothermic and reversible, 2. hydrophobic, endothermic and irreversibly bound. Protein absorption is influenced by EWC and the nature of the water structuring in polymers, so protein studies will give an indication of the surface structure of the material at a molecular level[48, 49].

Lipids interact either via the carbonyl groups of fatty acids interacting with hydrogen bonding sites at the hydrogel surface, or via penetration into the hydrogel matrix because molecules have a greater solubility in the organic backbone than in water. Deposition arises with the regular collapse of the tear films and is independent of the ongoing interfacial process of protein adsorption[50]. Penetration of lipid into the polymer matrix modifies the interface and changes the course of biological conversion.

1.3.7 Biocompatibility

When a synthetic material is placed into a biological fluid, a complex set of interactions occurs, regardless of the material or fluid into which it has been placed[51]. Biocompatibility is concerned with the interactions that take place between synthetic materials and the body fluids which they are in contact with. The interactions that occur are dominated by initial events at a molecular level at the interface between the material and body fluids, thus it is primarily the surface properties of a material that govern its degree of biocompatibility although it is also important to consider the effect of molecular architecture and monomer sequence distribution on biocompatibility. An understanding of biocompatibility is required to enable the design of materials which are accepted by the bodily environment and do not undergo adverse reactions which result in rejection, or failure of the material in its application.

Protein deposition onto the surface of the synthetic substrate is usually the first stage of interaction between material and biological fluid illustrating that the surface properties of a material control its biocompatibility. Biological fluid such as tears contains proteins which are found to exist in aqueous solution. When in contact with another phase proteins tend to accumulate at the interface resulting in adsorption onto any surfaces present such as the surface of contact lens. A review of protein deposition onto surfaces has been compiled by Baker and Tighe[51]. Protein adsorption is caused by the resultant interactions of polar and dispersive components acting across the interface. The surface energy of a material and the interfacial tension between the material and the biological environment are also highly influential factors.

Several theories have been proposed as to the factors which are important in predicting whether a material would be non-thrombogenic (blood compatible) or not[14, 52]. Baier *et al*[53] suggested that for a material to exhibit non-thrombogenic characteristics it should have a critical surface tension in the region of 20-30 mN/m. Andrade[54] proposed that minimum interfacial tension should exist between an implant material and its environment to improve biocompatibility. However, later work carried out by the same research workers on a range of hydrogel copolymers produced results that could not be explained in terms of this hypothesis[55]. Ratner *et al*[56] reported that a balance of polar and non-polar groups increased blood compatibility.

The composition and relative hydrophilicity of regions on the surface are also important in controlling the blood compatibility of a material. It has been shown that regions of hydrophilicity and hydrophobicity at the polymer surface control the composition of the adsorbed proteins from the biological fluid. Work on the protein adsorption indicates that globulin and fibrinogen adhere to the hydrophobic domains and albumin adheres to the hydrophilic domains[57]. The formation of ordered areas of adsorbed protein is thought to suppress platelet adhesion.

1.3.8 Copolymer Sequence Distribution

Work carried out previously at Aston[58, 59] has shown that synthetic polymers with large irregular molecular domains in which components of the same chemical type tend to become aggregated, have a greater tendency to show non-specific protein adsorption than

polymers that mimic naturally occurring polymers with regular chemical variations. It would be useful to predict the order of chemical constituents at different compositions in a copolymer so that the formation of blocks of one component is avoided. This resulted in the development of a computer simulation program which allows the sequence distribution to be predicted for copolymerisation reactions, based on the concentration and reactivity ratios of the monomers used. Although the reactivity ratios for a pair of monomers are fixed, optimisation of the concentration of monomers of specific reactivity ratios enables copolymers with short repeat units to be produced.

1.3.8.1 The Terminal Model of Copolymerisation

The standard kinetic treatment of free radical polymerisation is the terminal model of copolymerisation[60, 61]. The reactivity of an active centre is dependent only on the monomer unit in the copolymer chain on which the radical is located in this model. For the copolymerisation of two monomers, the growth of the polymer chain, the monomer consumption and the development of the microstructure can be given by four propagation equations:

$$\sim\sim M_1\bullet + M_1 \xrightarrow{} \sim\sim M_1\bullet \qquad rate_{11} = k_{11}\,[M_1\bullet]\,[M_1] \tag{1.19}$$

$$\sim\sim M_1\bullet + M_2 \xrightarrow{} \sim\sim\sim M_2\bullet \qquad rate_{12} = k_{12}\,[M_1\bullet]\,[M_2] \tag{1.20}$$

$$\sim\sim M_2\bullet + M_1 \xrightarrow{} \sim\sim\sim M_1\bullet \qquad rate_{21} = k_{21}\,[M_2\bullet]\,[M_1] \tag{1.21}$$

$$\sim\sim M_2\bullet + M_2 \xrightarrow{} \sim\sim\sim M_2\bullet \qquad rate_{22} = k_{22}\,[M_2\bullet]\,[M_2] \tag{1.22}$$

Where:

M	=	monomer
M•	=	monomer radical
k	=	rate constant
[ ]	=	concentration of individual species

The rate of consumption of the two monomers can be expressed as,

$$-d[M_1]/dt = k_{11}[M_1\bullet][M_1] + k_{21}[M_2\bullet][M_1] \quad (1.23)$$

$$-d[M_2]/dt = k_{12}[M_1\bullet][M_2] + k_{22}[M_2\bullet][M_2] \quad (1.24)$$

The mole ratio of the monomers in the copolymer is given by,

$$\frac{d[M_1]/dt}{d[M_2]/dt} = \frac{k_{11}[M_1\bullet][M_1] + k_{21}[M_2\bullet][M_1]}{k_{12}[M_1\bullet][M_2] + k_{22}[M_2\bullet][M_2]} \quad (1.25)$$

If a steady state is reached instantly after polymerisation starts, the total concentrations of $M_1\bullet$ and $M_2\bullet$ will remain constant and the rate of conversion of $M_1\bullet$ to $M_2\bullet$ will equal the rate of conversion of $M_2\bullet$ and $M_1\bullet$, i.e.:

$$k_{21}[M_2\bullet][M_1] = k_{12}[M_1\bullet][M_2] \quad (1.26)$$

The individual reactivity ratios of monomers M_1 and M_2 are defined as the ratio of the rates of reaction of a polymer chain ending in a radical of one type adding to itself, to the rate of its reaction with the second monomer in the copolymer system. As such,

$$r_1 = k_{11} / k_{12} \quad (1.27)$$

$$r_2 = k_{22} / k_{21} \quad (1.28)$$

Equation 1.25 reduces to,

$$\frac{d[M_1]}{d[M_2]} = \frac{[M_1](1 + r_1[M_1]/[M_2])}{[M_2](r_2 + [M_1]/[M_2])} \quad (1.29)$$

The monomer reactivity ratio r_1 and r_2 are the ratios of the rate constant for a given radical adding to its own monomer, to the rate constant for its adding to the other monomer. It is a

measure of the preference for its own kind of monomer to that of the other, thus if $r_1>1$, radical $M_1\bullet$ prefers to add to monomer M_1 and if $r_1<1$, radical $M_1\bullet$ prefers to add to the monomer M_2.

An ideal copolymerisation is where the radicals have the same preference of addition to each of the monomers and $r_1r_2 = 1$. The arrangement of the monomer units is completely random along the chain. When $r_1 = r_2 = 0$, each radical shows a strong preference for cross-propagation which results in the monomers alternating regularly regardless of the monomer feed ratio until one monomer is completely consumed. Where $r_1 = r_2 = 1$, neither radical centre shows a preference for either monomer and the rates of consumption are determined by the relative concentrations of monomer in the initial feed. If $r_1 >> r_2$, the polymerisation produces large blocks of M_1 with small segments of M_2 between the blocks until M_1 is completely consumed.

1.3.8.2 Computer Copolymer Sequence Distributions

The terminal model is very useful for explaining the structure of copolymers prepared from various vinyl monomers whose reactivity ratios are known. A computer program based on this model provides an illustration of the sequence distribution of copolymers whilst allowing alterations in key parameters such as monomer type and initial feed concentration. The approximate sequence distributions of various copolymers can be determined easily without the need for producing the polymer and performing detailed structural analysis required for determination of the sequence distribution.

Computer simulation of the sequence distribution is carried out using two computer programs. The program 'COPOL' provides analysis for binary systems and 'TERPOL' for ternary systems. Both methods are based on the terminal model of copolymerisation and make use of the Monte Carlo method of statistical trials. An approximation relieves the need for producing the polymer and performing detailed structural analysis to resolve the sequence. Ashraf[59] studied the viability of using these computer simulation programs. Computer simulations were prepared using a number of methacrylate based comonomer systems together with the experimental preparation of the same copolymers. It was found that the sequence lengths determined using the methods of ^{13}C NMR and elemental analysis were within 3% of the sequence lengths produced by the computer simulation. It is

therefore assumed that the computer simulation is accurate enough to simulate the reactivity of comonomers in a free radical polymerisation. An example of a sequence simulation for a hydrogel copolymer is listed below:

80 mole % of monomer A, NVP

20 mole % of monomer B, MMA

r (AB) = 0.01 r (BA) = 4.04

In the simulated copolymer NVP is represented by O and MMA is represented by X

XXOXOXXXOXXOXOXXXOXOXOOXXOXXOXXXOXXOXXXOXOXOXOXO

XOXXXXOXOXXXXXXXXOXXXOXOXXXXXXXXOXXXOXXXOXXOXXXOXXOX

OXXOXOXOXOXXXOXXXXXOXXXOXXOXXOXXXOXOXOXOXOXXXOXOXOX

OXXOXXXXOXXOXOXXOXOXOXOOXOXXOXOXXOXOXXXOXOXOXOXXXXO

XOXOXOOOXOXXOXXOXOXOXOXXOXXXXOXOOXOXXXOXOXOXXOXXOXO

XXXOXXOXXXXXXOXOXOXXOXOXXOXOXXOXOXXXOXXOXXOXXOXOOXX

XXXXOXXOXOXXXXOXOXOXOXOXXOXOXOXOXOXOXOXXOXOXOXOXX

XOXXOXOXOXOXXXXXXOXXOXOXXOOXXXXXOXOXOXXOXXXOXXOXOXX

OXOXXXOXXOXOXOXOXOOXXOXOOXOXXXXOXOXXOXXOXOXOXOXOXOX

OXOOXXXOXOXXXOXOXXOXOOXXOXOXXOXOXOXOXOXOXOXOXXXOX

OXOXOXOOOXOXOOXOXOXXOXOXOOXOOXXOXOXOOXOXOXOXOXOXOXO

XOXOXXOOXOXOXOOXOXOXOXOXOOOXOXOXOXOXOOXOOOXOXOXOXOX

OOXOXOXOXOXOOXOXOXOXOOOXOXOXOOXOXOOOXOOXOXOXOOXOOXO

XOOOXOXOXOXOOXOXXOOOOOOXOXOXOXOXOOOOOOOOOOOOOOOOOOO

OOOOOOOOOOOOOOOOOOOOOOOOOOOOOOOOOOOOOOOOOOOOOOOOOO

OOOOOOOOOOOOOOOOOOOOOOOOOOOOOOOOOOOOOOOOOOOOOOOOOO

OOOOOOOOOOOOOOOOOOOOOOOOOOOOOOOOOOOOOOOOOOOOOOOOOO

OOOOOOOOOOOOOOOOOOOOOOOOOOOOOOOOOOOOOOOOOOOOOOOOOO

OOOOOOOOOOOOOOOOOOOOOOOOOOOOOOOOOOOOOOOOOOOOOOOOOO

OOOOOOOOOOOOOOOOOOOOOOOOOOOOOOOOOOOOOOOOOOOOOOOOOO

OOOOOOOOOOOOOOOOOOOOOOOOOOOOOOOOOOOOOOOOOOOOOOOOOO

OOOOOOOOOOOOOOOOOOOOOOOOOOOOOOOOOOOOOOOOOOOOOOOOOOOO

OOOOOOOOOOOOOOOOOOOOOOOOOOOOOOOOOOOOOOOOOOOOOOOOOOOO

OOOOOOOOOOOOOOOOOOOOOOOOOOOOOOOOOOOOOOOOOOOOOOOOOOOO

OOOOOOOOOOOOOOOOOOOOOOOOOOOOOOOOOOOOOOOOOOOOOOOOOOOO

OOOOOOOOOOOOOOOOOOOOOOOOOOOOOOOOOOOOOOOOOOOOOOOOOOOO

OOOOOOOOOOOOOOOOOOOOOOOOOOOOOOOOOOOOOOOOOOOOOOOOOOOO

OOOOOOOOOOOOOOOOOOOOOOOOOOOOOOOOOOOOOOOOOOOOOOOOOOOO

OOOOOOOOOOOOOOOOOOOOOOOOOOOOOOOOOOOOOOOOOOOOOOOOOOOO

OOOOOOOOOOOOOOOOOOOOOOOOOOOOOOOOOOOOOOOOOOOOOOOOOOOO

OOOOOOOOOOOOOOOOOOOOOOOOOOOOOOOOOOOOOOOOOOOOOOOOOOOO

OOOOOOOOOOOOOOOOOOOOOOOOOOOOOOOOOOOOOOOOOOOOOOOOOOOO

OOOOOOOOOOOOOOOOOOOOOOOOOOOOOOOOOOOOOOOOOOOOOOOOOOOO

OOOOOOOOOOOOOOOOOOOOOOOOOOOOOOOOOOOOOOOOOOOOOOOOOOOO

OOOOOOOOOOOOOOOOOOOOOOOOOOOOOOOOOOOOOOOOOOOOOOOOOOOO

OOOOOOOOOOOOOOOOOOOOOOOOOOOOOOOOOOOOOOOOOOOOOOOOOOOO

OOOOOOOOOOOOOOOOOOOOOOOOOOOOOOOOOOOOOOOOOOOOOOOOOOOO

OOOOOOOOOOOOOOOOOOOOOOOOOOOOOOOOOOOOOOOOOOOOOOOOOOOO

OOOOOOOOOOOOOOOOOOOOOOOOOOOOOOOOOOOOOOOOOOOOOOOOOOOO

OOOOOOOOOOO

The simulated copolymer contains 1600 NVP units and 400 MMA units

Sequence Length	NVP	MMA
1	222	171
2	23	48
3	7	22
4	0	6
5	0	2
6	1	3
7	0	1
8	0	1
1305	1	0

Figure 1.8 Example of a sequence simulation for a hydrogel copolymer

1.3.8.3 The Alfrey-Price Q-e Scheme

The reactivity ratios of monomers are required to allow the computer simulations described previously to be utilised. For many monomers the reactivity ratios have been determined experimentally but there are still a number of monomers for which this process has not been carried out. The Alfrey-Price Q-e scheme[62] may be used to approximate reactivity ratios without the need for lengthy experimental procedures. The scheme attempts to quantify reactivity by considering the polar and resonance stabilisation effects of the monomer and their influence on the copolymerisation process[63, 64].

The two reactants in a radical / monomer addition are assigned values e_1 and e_2 to represent their charges, identical charges being assumed for a monomer and its derived radical. The general reactivities of radicals and monomers were denoted by P and Q respectively. The rate of reaction is considered to be determined by the four quantities P, Q, e_1 and e_2 as indicated in equation 1.30:

$$K_{12} = P_1 Q_1 \exp(-e_1 e_2) \tag{1.30}$$

The equations, applied to each of the propagation steps outlined previously in equations 1.19 to 1.22, are combined and re-arranged to give.

$$r_1 = (Q_1 / Q_2) \exp [-e_1(e_1-e_2)] \tag{1.31}$$

$$r_2 = (Q_2 / Q_1) \exp [-e_2(e_2-e_1)] \tag{1.32}$$

The multiplication of the two relative reactivities leads to a simplified expression involving only the difference in polarity, which can be used to determine an unknown e value from which than a Q value may be established, where r_1 and r_2 are known.

$$r_1 r_2 = \exp [-(e_1-e_2)^2] \tag{1.33}$$

1.4 Cornea

The cornea is a unique portion of the outer, fibrous ocular tunic that is transparent and serves a refractive function while maintaining a mechanically tough and chemically impermeable barrier between the eye and the environment. In concert with the evolutionary development of vision, the cornea became structurally and functionally specialized to achieve the required optical properties. It evolved as an avascular structure that meets its oxygen requirements largely from the atmosphere via the anterior corneal surface and most of its additional nutritional requirements from the aqueous humour via the posterior corneal surface. Some of the protective functions and optical properties of the cornea are derived from adjacent tissues, such as the conjunctiva and lacrimal glands, which provide secretions that are spread over the cornea by the blinking action of the eyelids, resulting in a smooth anterior corneal surface. The mechanical strength of the cornea is provided by its collagen matrix, which is different from that of skin or the contiguous sclera and which requires the presence of mechanisms that regulate hydration to maintain transparency. For protection, the cornea is endowed with exquisitely sensitive nerves.

1.4.1 Anatomy of the Cornea

The cornea protects the eye by acting as a tough membrane between the external environment and the ocular environment. The cornea can be divided into five layers, as shown below in Figure 1.8: the epithelium, Bowman's layer, stroma, Descemet's membrane, and the endothelium.

The layer of stratified squamous epithelium can be regarded as a continuation of the conjunctival epithelium. It consists of four to six layers of cells and is approximately 50 μm thick, representing nearly10 percent of the total corneal thickness. The epithelium is divided morphologically into three layers: the superficial or squamous cell layer, the middle or wing cell layer, and the deep or basal cell layer. The deepest of these, the basal cells, stand in perfect alignment on a basement membrane, and are continuous at the corneal periphery with the same layer in the conjunctiva. The daughter cells thus formed push anteriorly and change their shape, conforming to the contiguous wing cells, which are defined by the way they overlap onto the apices of the underlying basal cells. As the cells continue to move anteriorly, they become the superficial cells, after which they disintegrate

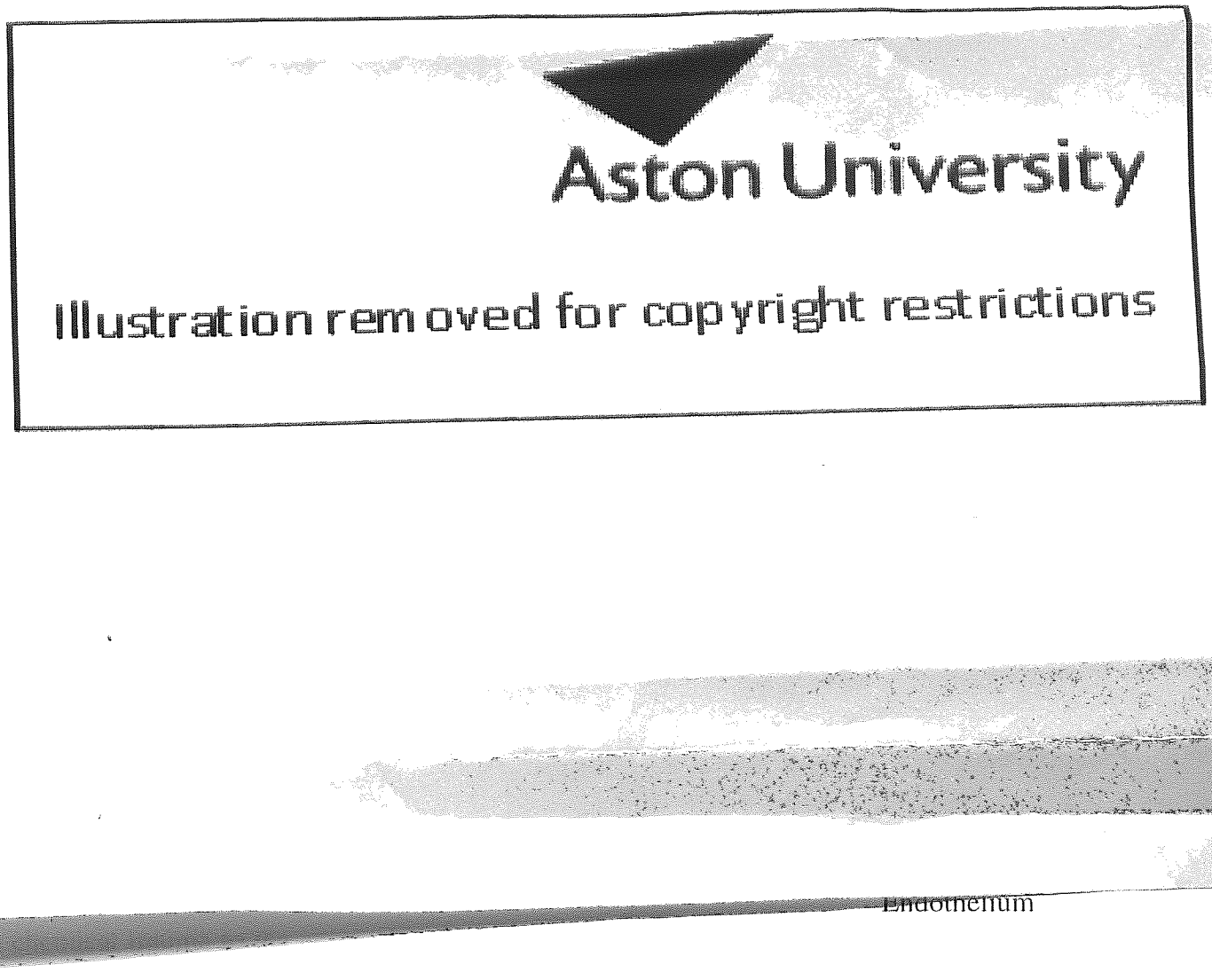

Figure 1.9 Structure of the cornea[65]

and are shed into the tear film in a process known as desquamation. The superficial cells represent the highest level of differentiation and are, chronologically, the oldest epithelial cells. The epithelium is nonkeratinizing and turns over approximately every 7 days. The epithelium is compact with no gap between cells, thus enhancing its strength. The corneal epithelium fulfils a number of vital functions. For a healthy cornea and maintenance of normal vision, the epithelium must provide an effective barrier to injury. It must be strong enough to withstand the rubbing of eyes and the presence of a contact lens or other foreign body within the eye. The epithelium must also resist microorganism and fluid entry. For good vision, the epithelium must be transparent, and have a smooth surface to provide an ideal refractive surface. It is covered by an intensely hydrophilic submicron-sized coating

of hydrated mucous gel[66], glycocalyx, which increases the surface area, provides a roughened surface to assist the adherence of the precorneal tear film.

The anterior limiting lamina, or Bowman's membrane, is a thin homogenous sheet, 8-14 μm thick, between the basement membrane and the stroma. It is composed of randomly arranged collagen fibrils that are interwoven proteoglycans; it separates the keratocytes and the stroma from the corneal epithelium residing at the outer surface of the globe. It has a small degree of elasticity and does not regenerate once it has been destroyed, but it does show good resistance to injury and infection.

The substantia propria, or stroma, is about 0.5mm thick, forming approximately 90% of the corneal thickness, and composed of a modified connective tissue, consisting of alternating lamellae of collagenous tissue, the planes of which are parallel to the surface of the cornea. The layered network organization of the collagen lamellae imparts considerable mechanical strength to the stroma. It was estimated[67] that the network gives the cornea 100 times more strength than is necessary to withstand the maximum intraocular pressure under physiological conditions. An isolated mounted cornea can withstand pressures 600 times higher than the maximum intraocular pressure. The collagen fibrils are embedded in a fluid consisting of proteins, glycoproteins and mucopolysaccharides. The gross physical or chemical trauma to the cornea is largely repaired by the keratocytes which synthesise and degrade extracellular matrix material in the stroma in a manner analogous to fibroblasts in the skin[68]. Thus, the regularity of the extracellular material constituting the stroma determines many features of the corneal tissue including corneal transparency under normal fluid conditions and the capacity of the structure to withstand the abrasive force of the eyelids. The stroma permanently displays a tendency to swell in water or aqueous solutions. The degree of swelling differs between species. This swelling tendency is largely due to the presence of proteoglycans (more exactly, of their glycosaminoglycan moieties), and the intraocular pressure also contributes by forcing aqueous humour into the stroma. Generally, the stroma is responsible for the optical properties, while the protective capability of the cornea is a result of the limiting layers. Transparency requires an avascular stroma, maintained in a relatively dehydrated state. With normally hydrated stromal tissue, the spacing of collagen lamellae is less than one wavelength of light, such that light scattering is cancelled by destructive interference, thus following transparency. Swollen corneas are no longer transparent because the orderly spacing of the lamellar collagen fibrils is

disturbed and increased, and the scattering of light rises dramatically. The maintenance of a normal degree of stromal hydration is therefore a task that the cornea must perform continuously.

The posterior limiting lamina, or Descemet's membrane, is a strong, homogenous and very resistant membrane. It is 10-12 μm thick, being thinner centrally and thickest near the periphery. Unlike Bowman's membrane, Descemet's membrane will regenerate following injury. It is composed of very regular strata of fine collagenous fibres, and displays elastic characteristics.

The endothelium consists of a single layer of flattened cells and is separated from the stroma by Descement's membrane, measuring 4-5 μm thick. The cells exhibit a high degree of metabolic activity. It is critical to the maintenance of transparency in the corneal stroma both by actively pumping water out, via a sodium-potassium adenosine triphosphate (ATP) ase and a coupled bicarbonate pump, and by serving as a tight barrier to fluid entry[69]. In human eye, the endothelial cell layer, although capable of division, has a relatively low fraction of cells traversing the cell cycle *in vivo* compared to lower mammals[70]. This means that the principal process of endothelial layer repair is by cell enlargement rather than sustained division[71]. A severely compromised endothelial layer leads to corneal deturgescence and loss of clarity often referred to as corneal decompensation. Minimisation of endothelial cell damage is thus an obligate requirement in the development of ocular biomaterials that may come into contact with the inner surface of the cornea[72]. The endothelium is not alone in performing this task: the epithelium acts as a semipermeable membrane, creating a barrier to the flow of water into the cornea from the tears.

1.4.2 Functions of the Cornea

The cornea performs many varied functions. It acts as a tough protective membrane between a potentially damaging environment and the internal sensory ocular elements. Because of its elasticity and thickness, the cornea can withstand and contain the intraocular pressure from within the eye. The containment of the intraocular pressure and good mechanical properties are required to deal with the deforming force of the eyelid during the blink cycle. Approximately 75% of the total dioptric power of the human eye is due to the

interface between the cornea and air, so the cornea serves as the major optical component in the eye by transmitting and refracting light. The cornea also performs a photoprotective function by absorbing ultraviolet radiation of wavelengths between 200 and 300 nm (most of UV-C and UV-B), preventing it from reaching and damaging the posterior ocular elements. Transparency and refraction require a thin avascular tissue of uniform refractive index and a smooth surface. This demands a thick elastic tissue, preferably with the capability for vascularisation which would allow it to regenerate easily. The human cornea appears to be an idea; compromise able to fulfil all functional requirements[73].

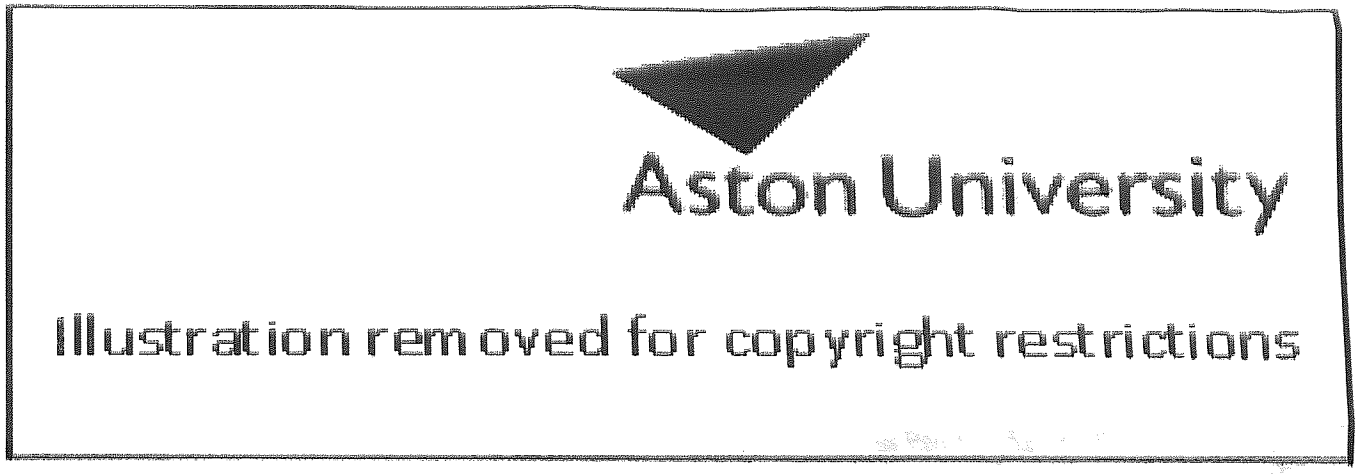

Table 1.2 Table showing some properties of the cornea and its environment[74]

The maintenance of the strength and transparency of the cornea is essential for its good performance and normal vision. The cornea maintains its normal characteristics through a complex set of processes. However, the cornea is the most vulnerable portion of the outer tunic of the eye, and in certain situations, its defence capability is overwhelmed. Under pathological conditions or as a consequence of insult from the outside habitat, any of the complex processes governing the performance of the cornea can be disrupted and the resulting changes may be incompatible with normal vision. Of particular importance are the insults that may affect the endothelium, which is the metabolic pump primarily responsible for the maintenance of the normal corneal deturgescence. When this pump is compromised, the aqueous fluid penetrates the barrier in a quantity that exceeds the capacity of the pump, and induces stromal, and ultimately epithelial, swelling. This

condition is known as corneal oedema, which always results in reduced vision. These processes can be dramatically altered if the cornea is diseased, or as a result of injury. The resulting degenerated, scarred or opacified cornea leads to problems with vision which may require surgery, of varying degrees of complexity and severity, to correct.

The cornea can be affected by a wide variety of disorders[75, 76, 77, 78], some of which, despite treatment, may cause partial or total loss of vision; others have minor or reversible effects. Corneal disorders are currently the second most common cause of blindness in the world population, with only cataract prevailing. The factors responsible for these disorders can be hereditary, age-related, traumatic or infectious, the latter being especially important in underprivileged areas.

The traumatic disorders are produced by mechanical thermal or chemical injuries. Most blunt mechanical injuries result in little damage to the cornea. Perforating injuries may cause scarring but serious visual consequences are generally due to the additional involvement of other ocular tissues. While thermal burns are relatively uncommon and usually not severe, some chemical burns are able to produce extensive destruction of the cornea. In particular, alkaline and acidic materials can cause severe damage to the cornea which usually results in permanent loss of vision. The alkaline hydroxides are particularly dangerous; they saponify the fatty components of cell membranes and modify chemically both collagen and proteoglycans, with devastating results. The nature of acid damage differs from acid to acid (irritative action, specific action on tissues, charring effect and denaturation of proteins), but tends to be less serious because the acids coagulate proteins and limit deeper penetration. The corneas affected by moderate burns usually respond to treatment by topical medication and the eyes recover partially or totally within weeks. More severe burns leave the cornea irreversibly opaque, encourage vascularization and conjunctivalization, and often cause additional disorders such as glaucoma.

The corneal diseases are usually classified into inflammations, dystrophies and degenerations. While the inflammatory reactions have many causes, predominantly infective, the dystrophies are regarded as a result of genetically defective processes, they are usually bilateral (i.e. occurring in both eyes) and are not associated with prior inflammation or systemic disease. The degenerations are the result of biological changes or

occurrence of abnormal matter in the cornea, associated with aging, systemic diseases or exposure to a hostile environment.

1.5 Keratoprosthesis

The surgical replacement of a cornea with a donor cornea is called penetrating keratoplasty. The restoration of vision in patients with corneal blindness has become increasingly successful because of advances in standard penetrating keratoplasty (PK) and ocular surface reconstruction achieved during the past century. The success rate for PK is currently in the order of 90%[79] for those patients whose disorder is uncomplicated by other facts, such as tear deficiency, vascularization, inflammation, or uncontrollable intraocular pressure. However, there are remains a subset of patients with severe corneal opacity in whom PK and ocular surface reconstruction techniques have failed, or carry a poor prognosis, owing to past or ongoing chronic inflammation. Such cases include Stevens-Johnson syndrome (SJS), chemical burns, ocular cicatricial pemphigoid (OCP), severe keratoconjunctivitis sicca, stem cell deficiencies, and severe vascularization resulting from other causes. In addition, there exists another, larger group of patients with repeated graft failures for unknown reasons, in whom the likelihood of successful subsequent corneal allografting is low. For these two categories of patients with complicated corneal blindness, keratoprosthesis (KPro) surgery may be the only hope of any visual improvement for these patients. Keratoprosthesis is an artificial cornea, designed to replace the defective natural cornea. A world shortage of donated corneas has increased further the need for KPro.

The prognosis of keratoprosthesis (KPro) procedures depends on the preoperative diagnosis: graft failure-noncicatrizing disease < ocular cicatricial pemphigoid < chemical burns < Stevens-Johnson syndrome. The likelihood of failure after KPro surgery follows this scheme[80].

1.5.1 Historical Background

A brief history of KPro which was introduced by several review papers[121, 169] outlined below.

Guillaume Pellier de Quengsy was the first person[81] who proposed an artificial cornea in his two-volume book *Precis ou cours d'operations sur la chirurgie des yuex*, published around 1789 by Didot publishers (Paris). He suggested replacing a completely opaque cornea with a silver-rimmed glass window in 1796, but his designs were not developed further.
None of the ophthalmologists of the period followed his suggestion. It was nearly 60 years later that Nussbaum, in Germany, experimented with a glass stud in the rabbit eye in 1853[82]. He had first implanted in his own body small spheres of wood, glass, iron, copper and other materials, and concluded that only glass produced no irritation. Following this painful experience, Nussbaum made a glass keratoprosthesis and implanted it into the rabbit cornea. The first prototype was too large and was extruded[83] in less than 2 weeks. His next model, much smaller and of an oblong shape, was so successful in animals, that Nussbaum decided to use it in human patients. According to other authors[84, 85], Nussbaum's new model was maintained for 3 years in a rabbit and for 7 months in a human patient.

Heusser in Switzerland was the first to follow Nussbaum's example and implanted a quartz keratoprosthesis into the eye of a blind girl in 1859[86]. After 6 months, the prosthesis was still in place and the patient had significantly recovered her vision.

In 1862, Abbate presented a report on his experiments at the Periodical International Congress of Ophthalmology in Paris, which was published the following year in the congress proceedings. Details of Abbate's work can be found in one of the early reviews on corneal surgery[87]. The French surgeon used a keratoprosthesis consisting of a glass disc surrounded by a skirt made of two successive rings, the first of gutta-percha and the next of casein. Both these materials are natural polymers: gutta-percha is the *trans*-isomer of natural rubber isolated from the exudates of various trees of the genera *Palaquium* and *Payena* (Malaya), while casein is a mixture of phosphoproteins precipitated from milk or cheese. This device was implanted in dog and cat corneas where it was maintained for one week before extrusion. Although the choice of peripheral prosthetic materials was not the most fortunate (casein is brittle and gutta-percha becomes so when exposed to air and light), this keratoprosthesis is an indication of Abbate's understanding of the need for a skirt made of a material different from glass, able to promote a better incorporation of the prosthesis into the host cornea.

In 1886 Baker[88] implanted a glass keratoprosthesis into one eye of a patient whose corneas and lids were completely destroyed by an acid splash. Following the operation, vision was restored in part and, despite later signs of tissue melting around the prosthetic rim, this device was maintained in the eye for almost 2 years.

Dimmer[89, 90] made a keratoprosthesis manufactured from a material different from glass or quartz at the end of last century. He made a keratoprosthesis in the shape of a hat from 0.1 mm thick sheet of celluloid, and implanted it in four human patients. Celluloid was the first commercial plastic in the world. It is a molecular complex of nitrocellulose (of low nitrogen content) with camphor and also contains stabilizing agents. Celluloid might not have been the best choice for a biocompatible material because within 3-17 weeks, the celluloid devices had to be removed from the eyes because of infection and extrusion. Despite this outcome, Dimmer remained optimistic about celluloid as a prosthetic material and apparently his work triggered its use in cranioplasty[90]. This is the only use of a polymer in KPro during the early history period of KPro, and probably is the first use of a polymeric material as a biofunctional prosthetic device. A few years earlier in London, Lang had used celluloid balls as orbital implants after removal of the eye globe[91], a prosthesis which is rather cosmetic than biofunctional. Dimmer was not aware of this work.

Salzer in Germany was the last ophthalmologist of the nineteenth century to make serious efforts to design a functional keratoprosthesis. After many experiments on animal corneas, he developed a model made of a quartz disc surrounded by a platinum ring with prongs and implanted it in four human patients[92]. While in three of them the prosthesis was extruded in 9 weeks, 9 months and 1 year respectively, in one patient it lasted almost 3 years. Even by today's standards, this was a truly remarkable performance. Salzer made two revolutionary suggestions in a later account of his past contributions to corneal surgery[93]: that keratoprostheses should be made from materials lighter than glass, and that the prosthetic rim should be made from a material able to incorporate the host tissue.

In the early part of the 20th century growing success with PK diverted attention from KPro research due to a low rate of success, until it was realized that PK would never be successful in all cases. Among the very few notable achievements of this period, the experiments performed by Hess[94, 95] are worthy of mention. He implanted a quartz disk

surrounded by a platinum ring in rabbit eyes; although the device was maintained for 1 year in one case, he discontinued his experiment[96].

Sommer[97] implanted a glass keratoprosthesis in three human patients. Their vision was significantly improved and the prostheses were apparently well integrated with the host tissue, but all were extruded after 1 month due to complications.

In 1951, Anderson[98] suggested that the nature of the metals used as peripheral attachments may be responsible for the previous lack of success, and he recommended the use of tantalum. He described in detail the design and manufacture of a device consisting of a central convex glass disk mounted into a tantalum flange provided with anchorage lugs. There is no indication that this keratoprosthesis has ever been evaluated *in vivo*.

The use of glass keratoprostheses was eventually resurrected a decade ago by Worst's group in the Netherlands. Their first prototypes[99] were shaped as a mushroom and consisted of a glass core mounted in a metal (platinum or a Cr-No-Co alloy) cylinder provided with a flange. Four stainless steel wires were passed through the flange and used for the fixation of keratoprostheses to the sclera. Only the platinum-glass keratoprosthesis was successful in animals at the end of the experiments (7 months). Subsequent models had the shape of a "champagne cork" and no metal enclosure. Up to eight stainless steel wires were provided for deep fixation to the sclera[100]. The champagne cork keratoprosthesis, known as Worst-Singh-Angel keratoprosthesis, was implanted in hundreds of human patients in Punjab, India. The high rate of success which was reported[101, 102], however, is questionable when considering the long history of failure of glass devices in the cornea, the possible damage to the optic nerve and blood vessels by the steel wires, and the poor clinical follow-up of the operated patients in this instance, since most of them never came back for examination. The latter was regarded as an evidence for success[102], based on the rationale that the patients did not turn up because their vision recovered. On the background of the fatalistic character of most religious beliefs in India, the opposite alternative is more probable, and this evidence appears tenuous.

The modern period in the history of the keratoprosthesis began with the use of poly(methyl methacrylate) as a material for keratoprostheses, which was subsequently followed by the use of other synthetic polymers. During World War II it was noticed that poly (methyl

methacrylate) (PMMA) fragments from shattered airplane canopies embedded in pilots' corneas were well tolerated. In the early 1950s it was found that full-thickness PMMA implants in rabbits extruded after just 2 weeks, although intralamellar implants were tolerated for up to 24 months. The importance of a periphery which allowed tissue ingrowth was appreciated by Stone and Herbert[103] and was encouraged by trephination of the plastic. Their prostheses were made as buttons, and some of them had a peripheral tantalum meshwork or roughed edges.

Ridley was the first, in 1949, to implant PMMA intraocular lenses into human patients[104, 105], and opened the era of one of the safest surgical procedures on the human body.

Strictly chronologically, other ophthalmologists reported the use of PMMA keratoprosthesis[97, 106] before Stone did. Gottfried Wunsche in Germany[107] was the first surgeon who reported in print the use of keratoprostheses made from PMMA. There are some remarkable aspects of Wunshce's work performed in rather inauspicious circumstances. He was on the battlefield in 1943 when, with no knowledge of any previously published work, he implanted into the rabbit cornea pieces of PMMA obtained from the canopy of a fallen aeroplane. To check the stability of the material, he treated samples of polymer with a concentrated solution of sodium chloride. Wunsche further tested the tissue tolerance to PMMA by implanting a piece under his own skin and observing its behaviour for 6 weeks. A keratoprosthesis was then manufactured in the garrison's field workshop and implanted in 10 rabbits during 1944. In one animal, the device was maintained for almost 2 months without complications. Eventually, with the retreat of the defeated German army, the experiments were discontinued. In Hungary, Gyorffy implanted a PMMA keratoprosthesis in a human patient, which was extruded within 2 weeks. Sommer implanted PMMA keratoprostheses in animal eyes in 1946. Franceschetti did the same in 1947. Macpherson and J. Anderson also implanted a full-thickness PMMA device in a blind patient. The vision was recovered significantly, and 2 years after the operation this situation was still maintained.

In the 1950s the idea occurred[108] to use an interlamellar supporting plate (flange) around the PMMA optical cylindrical core which led to the development of "core-and-skirt" keratoprostheses. There plates were either perforated or fenestrated, or made of meshworks. PMMA was used initially for their manufacture but later the range of materials diversified.

1.5.2 Current Research

Synthetic polymers and copolymers offer certain advantages in the making of devices for keratoprosthesis applications. These include the reduced risk of transmission of infectious agents, an unlimited supply, improved optical properties and avoidance of postoperative remodelling[109]. The design of polymers for these applications has been directed primarily at anchorage of the peripheral portion of the device in the corneal stroma. Results from *in vivo* studies show some success in terms of this aspect of the design, although optimisation of a polymer to support epithelial growth over the central optical portion of these devices remains a challenge[110, 111, 112].

There are two basic types of KPro designs. The most commonly used type consists of a transparent central stem anchored to the cornea with a peripheral skirt, which is implanted in an intralamellar location within the corneal stroma and occasionally covered by transplanted autologous tissue or eyelid skin. The second, and less commonly used, design is a collar-button shaped device that consists of two plates joined by a central optical stem. It is implanted such that the plates sandwich the cornea between them and is sewn into place like a standard PK graft.

1.5.2.1 Improving the Core-skirt Junction and Reducing Optic Rigidity

1.5.2.1.1 Poly (methyl methacrylate)

The materials used for the central optical stem of a KPro (and the entire KPro when using the collar button design) traditionally has been poly (methyl methacrylate) (PMMA) based, a material introduced 50 years ago. Those incorporating a peripheral skirt in the design have, through the years, used a variety of porous polymers, such as perforated grids of PMMA, nylon, ceramics, and Teflon (polytetrafluoroethylene). Such varied materials have been used in an attempt to overcome inflammatory complications caused by what many believe to be bioincompatibility between the implant and the surrounding tissues, by promoting "biointegration" of host keratocytes into the implanted material so that the implant becomes an integral part of the cornea.

1.5.2.1.2 Polytetrafluoroethylene / Polyurethane Elastomer

Jacob-LaBarre and Caldwell experimented with potential materials for a flexible core-and skirt KPro[113]. They selected a porous polytetrafluoroethylene (PTFE) with 60 μm pores as the skirt and a transparent polyurethane elastomer for the optic. They preferred a chemical fusion between the two flexible polymers over any mechanical junction involving rigid materials and developed a method of polymerisation of the optic polymer within the porous skirt, allowing blending with the junctional area.

1.5.2.1.3 Carbon Fibre / Silicone

Kain and Thoft appreciated the benefits of using a material more elastic than PMMA as an optic and recognized the advantages of having a core and skirt of similar elasticity[114]. Their KPro comprised a silicone optic and a carbon fibre haptic. They confirmed *in vitro* and *in vivo* that fibroblasts invaded the carbon fibre skirt, but anchorage proved to be insufficient.

1.5.2.1.4 Poly (vinyl alcohol) Copolymer Hydrogels

Trinkaus-Randall *et al* are working on a KPro with a skirt to allow fibroblastic ingrowth and an optically transparent, epithelialized core[115, 116]. They reported that poly (vinyl alcohol) copolymer hydrogels were transparent materials with twice the tensile strength of corneal tissue on which seeded epithelial cells could grow. They selected a polypropylene/polybutylene copolymer fibrous web (fibre diameter 2-12 μm) as the skirt material[117] and demonstrated that stromal keratocytes could penetrate it, proliferate, and synthesize collagen.

1.5.2.1.5 Poly (2-hydroxyethyl methacrylate)

Poly (2-hydroxyethyl methacrylate) (polyHEMA) was selected because it made a composite core-and-skirt KPro possible, in which both optic and sponge surround are chemically identical and able to be permanently fused, eliminating potential interface problems. It is flexible, thus preventing mechanical stresses at the implantation site. Additionally, homogeneous hydrated polyHEMA gels have a similar refractive index to corneal stroma. When polymerisation is carried out in the presence of more than 45%

water, a solvent for HEMA but not for polyHEMA phase separation occurs, resulting in opaque, heterogeneous, macroporous polyHEMA sponges[118]. Sponge structure and characteristics can be manipulated by changing the initiator, crosslinker, and initial water content[119].

1.5.2.1.6 Epithelialization of a Keratoprosthesis

Epithelialization of a solid, rigid optic material, such as PMMA, is impossible and remains problematic even when permeable polymers are used. Adhesion and spread of epithelial cells onto hydrogels *in vitro* do not imply that an epithelialized KPro would be able to maintain a stable epithelium *in vivo*. The long-term survival of an epithelial layer depends on nutrients and growth factors from underlying mesenchymal tissue and in the ocular environment. A patient with a dry eye or a dysfunctional limbus would be no more able to epithelialize a KPro than to maintain donor tissue in a healthy state, and a KPro with a nonepithelialized optic would be more appropriate. A beneficial epithelium must be complete and stable. An unstable epithelium is undesirable, because of its capacity for collagenolytic enzyme production and because an injured epithelium may induce keratocyte apoptosis via the intermediary actions of IL-1 alpha, IL-1 beta, and the Fas receptor-Fas ligand system[120].

1.5.2.1.7 Topograpy and Surface Modification

It has been suggested[121] that an accurate replication of the topography of the extracellular matrix that underlies the corneal epithelium might enhance cell adhesion to synthetic polymers.

1.5.2.2 Skirt Materials

The "core and skirt" keratoprostheses did not significantly reduce the rate of implant extrusion despite a large variety of materials being utilised for the skirt, including polymers, ceramics, metals and preserved autologous tissues. It became evident that the peripheral prosthetic material should be incorporated into the host biological substrate through a more intimate process, such as cellular invasion and growth across the interface between material and tissue. The tissue proliferation should occur within voids of confined width but

unlimited length (i.e. contiguous) that are large enough to accommodate the stromal fibroblasts. A tight interpenetration of the tissue and material should result, which was never achieved within large voids such as those offered by holes or meshworks. The attempts to achieve this led relatively recently to the use of porous polymers as materials for the prosthetic skirt.

1.5.2.2.1 Carbon Fibres

It appears that Kain *et*[122] were the first to advocate the use of porous skirts. Their keratoprosthesis consisted of a transparent silicone core, surrounded by a skirt of carbon fibres. Like other polymeric carbons, the carbon fibres display a fibrous structure able to accommodate the large stromal fibroblasts. The latest model consists of four parts. The nontransparent parts are made from silicone rubber coated with a 200 µm thick layer of carbon fibres, and the posterior components extend beyond the equator of the eye. The keratoprosthesis itself (silicone core and carbon-fibre-coated silicone skirt) is usually implanted one month later and connected through an interface to the preimplanted component.

1.5.2.2.2 Polybutylene / Polypropylene

Trinkaus-Randall's group chose for the skirt a melt-blown fibrous web of a polybutylene / polypropylene (80/20) blend, which has a fibrous structure with contiguous pores of between 10 µm and 100 µm. It was demonstrated both *in vitro*[117, 123] and *in vivo*[124] that this material was invaded by stromal fibroblasts, and that the cellular proliferation, the synthesis of extracellular matrix proteins and the wound healing rate were enhanced when the web was impregnated with basement membrane proteins (collagens I and IV, laminin, fibronectin)[125], or pro seeded with stromal fibroblasts[126]. In order to impart hydrophilic properties to the central polymers they had to be subjected to chemical treatment after attachment to the skirt. This treatment consisted of solvolysis in methanolic solutions of either ammonium hydroxide or ethylenediamine, followed by extraction in methanol. Prior to implantation, the core must be proceeded with epithelial cells, for which a special device had to be designed[127]. The authors also recommended the treatment of the skirt with fibrin adhesives in order to retard the epithelial downgrowth.

1.5.2.2.3 Polytetrafluoroethylene

Polytetrafluoroethylene is today one of the most extensively used materials as a porous skirt in keratoprosthesis. Lamberts and Grandon suggested that Proplast™, a combination of polytetrafluoroethylene (PTFE, Telfon™) and vitreous carbon, might be utilized as a skirt material[128]. This porous (100-500 μm) material is wettable, stable and easy to handle, although somewhat rough when cut. It has been successfully used in dentistry and other surgical applications[129]. Proplast™ was tested as full-thickness buttons in the rabbit cornea and demonstrated to be well tolerated, showing fibrovascular ingrowth but also encapsulation. A more detailed study was performed independently by Barber *et al*[130] who implanted Proplast™ disks into rabbit corneas. White and Gona[131] designed a keratoprosthesis having a PMMA cylinder as the optical core and a Proplast™ (pore size 80-400 μm) discs as the skirt. The joining of the two polymers was achieved either by gluing them with cyanoacrylate adhesives during surgery, or by screwing a pre-threaded PMMA cylinder into the trephined Proplast™ disk that had been implanted 2 months previously. Caldwell and Jacob-LaBarre[113, 132, 133] designed a keratoprosthesis that is anchored deeply into the sclera through a six-pronged skirt. After an extensive assessment in rabbit eyes of seven porous materials including hydrophobic polymers (mesh or sponge) and ceramics, as well as transparent flexible polymers, they concluded that the most suitable materials included a porous PTFE (pore size 15-90 μm), commercially available as Gore-Tex® (from W.L.Gore and Associates, Flagstaff, USA), for the skirt, and a polyurethane elastomer for the optic core. The union between the two polymeric components was achieved by performing the polymerisation of polyurethane precursors within the circular cavity surrounded by the porous PTFE rim. Along the boundary, the liquid polymerisation mixture penetrated the porous material to a certain distance and assured a mechanical interpenetration of the two polymers. Porous PTFE was also the material of choice for the skirt in the so-called "Seoul keratoprosthesis" developed in Korea[134]. The device was made using circular 0.6 mm thick sheets (diameter 8-13 mm) of Gore-Tex®, in which 2 mm large windows were perforated centrally, and onto which PMMA lenses (diameter 6-11 mm) were then glued with cyanoacrylate adhesives. Legeais and his coworkers in Paris developed[135] a keratoprosthesis consisting of a skirt made from porous PTFE and a cylindrical PMMA core. The two polymers were joined together by clamping the PTFE rim between the jaws of the PMMA central piece and of a titanium ring. In experiments in the rabbit cornea[136], a porous PTFE available as IMPRA® (IMPRA, Inc.,

Tempe, USA) offered the best results, both clinically and histopathologically, when compared to Proplast™ or Gore-Tex®. Another surprising result of Legeais' group was the observation[136, 137, 138] that the opaque, hydrophobic porous PTFE became progressively transparent and wettable after intralamellar insertion into the cornea, owing to its invasion by the stromal collagen.

1.5.2.2.4 Polyurethane

Ikada's group[139] developed " core and skirt" keratoprostheses in which the skirt is made from nonwoven polyurethane fabrics manufactured by Kanebo, Inc., Japan. This is a fibrous material displaying a porosity of 90%. Two keratoprosthetic models were developed. In one, a 250 μm thick polysiloxane core was enclosed by a 250 μm thick fibrous polyurethane skirt, and the *posterior* surface was coated with a 50 μm thick layer of polysiloxane. In the second prototype, all elements were made from polyurethanes, i.e. the transparent core (450 μm), the skirt (450 μm) and the coating of the *anterior* surface (30 μm). The joining of various polymer parts and coating was thought to be performed by gluing.

1.5.2.2.5 Polyethylene

A group at the Fitzsimons Army Medical Centre in Colorado reported[140] recently the use of a brand of porous polyethylene (Medpor®, Porex Surgical, College Park, USA) as a skirt in keratoprostheses. Annular skirts (8 mm in diameter, 800 μm thick with a 3 mm central hole) were implanted intralamellarly into 10 rabbit corneas.

1.5.2.2.6 Poly (ethylene terephthalate)

Pintucci *et al* have produced a KPro with a PMMA optic 5.4 mm long and a flexible poly (ethylene terephthalate) (Dacron™) skirt[141]. It is preimplanted in the patient's eyelid so that biocolonization will occur and later implanted into the eye in a manner similar to the OOKP technique (see Section 1.5.3.1), with the skirt fixed to the corneal surface and covered with buccal mucosa. The nature of the optic-skirt junction is not disclosed, but due to the dissimilarity of the two materials it is likely to rely upon a mechanical feature or glue.

1.5.2.2.7 Poly (2-hydroxyethyl methacrylate)

Chirila's group in Perth, Australia developed a device in which both components were made from crosslinked polyHEMA, and therefore chemically identical[142, 143, 144]. The skirt is made from polyHEMA sponges, which were produced by phase separation polymerisation in aqueous solution. Since water is a nonsolvent for polyHEMA, it is expected that when its concentration in the initial monomer mixture exceeds a critical value, the effect of the unfavourable thermodynamic interaction between diluent (water) and polymer network will prevail during polymerisation[145, 146]. Indeed, when the water concentration in the monomer mixture was higher than the equilibrium water uptake of polyHEMA, phase separation occurred during the polymerisation process[118]. By varying the amount of water in the initial monomer mixture, a large range of porosities can be attained. It was demonstrated[147, 148], both *in vitro* and *in vivo,* that the sponges synthesized in more than 75% water in the monomer mixture, displaying contiguous pores larger than 10 μm (but generally between 20 – 30 μm), were biocolonized through cellular invasion and growth, when pre-impregnated with collagen.

1.5.2.2.8 Other Materials

Metal[149], plastic[150, 151], and ceramic keratoprosthesis supporting elements[150, 152, 153, 154, 155] are rigid and covered by fibroblasts that cannot colonize them in three dimensions because of a lack of suitable empty spaces. Heterotissues, autotissues, and homotissues (dentin, cartilage, and bone)[156, 158, 159] keratoprosthesis supporting elements are mechanically anchored to the eye wall (sutured or screwed) and can be reabsorbed. Nevertheless, several authors[103, 149, 150, 154, 157, 158] suggested that the mechanical stress may lead to inflammation with tissue melting, necrosis, and the formation of empty spaces at the implant-eye interface. As a consequence, aqueous humour leakage, infections[155, 159, 160, 161, 162], and reparative epithelial and connective tissue proliferation[164, 165] may occur and lead to keratoprosthesis encapsulation[156, 157, 158, 159] or to the formation of retroprosthetic membrane with consequent keratoprosthesis extrusion[149, 150, 156, 157, 158, 165, 166].

Kornmehl[167] developed the rabbit derived collagen allograft as a material for an artificial cornea. Collagen is the primary structural protein of the cornea and collagen allografts are readily available, disease free and optically clear. Extrusion did not occur but epithelial

coverage over the clear central zone was poor, and necrosis occurred. However, Kornmehl believed that these problems could be overcome.

Recently Green[168] has developed a keratoprosthesis using biocoral though this has not yet to be implanted in an eye.

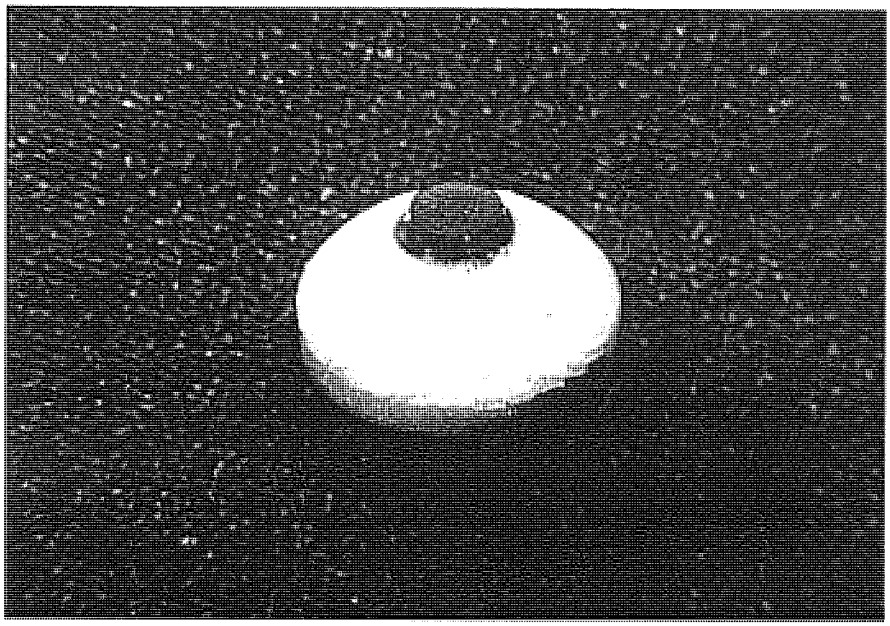

Figure 1.10 Biocoral KPro

There is a major problems[169] with the "core-and-skirt" keratoprostheses, pertaining to polymers. The attachment of the porous peripheral polymer to the transparent central polymer can be quite difficult to achieve, since they are usually different in their chemical structure and physical properties.

1.5.3 Keratoprosthesis Models in Current Clinical Use

1.5.3.1 Osteo-odonto-keratoprosthesis (OOKP)

The most successful KPro to date is the osteo-odonto-keratoprosthesis (OOKP) which consists of tooth and bone supporting frame and a polyMMA core[170, 171] (see Figure 1.11). Strampelli *et al*[156] selected tooth as a material surrounding the optical cylinder in a novel approach in the early 1960s. It involves complex, staged surgery over many months, but

some patients have been reported to maintain a device for more than 20 years. The first and second stages of the surgery involve corneal epithelial strip, suturing of buccal mucosa over the cornea and replacement of Tenon's capsule and the conjunctiva. A tooth, preferably an autologous canine, is harvested with its alveolar dental ligament intact, and one-half of the root is sectioned to obtain a lamina comprising alveolar bone and half the dental root. A hole is then drilled through this into which the acrylic cylinder is secured, and the assembled device is placed in a lower eyelid subcutaneous pocket. In the final stage, up to 1 year later, the implant is retrieved, the cornea is uncovered and opened, and iridectomy is performed. The smaller end of the conical optic, which is 9 mm in length, perforates the cornea, protruding 3.5 mm into the anterior chamber. Its anterior end passes through a hole in the buccal mucosa.

An independent analysis of the work of Falcinelli was made by Liu *et al*[172] and the success rate was confirmed to be very high. 77% of eyes could see 6/12 or better and no KPros had extruded from the body. The reason for these results is attributed to the function of the cementum in preventing epithelial downward growth and, hence, expulsion.

1.5.3.2 Seoul Type KPro

Lee *et al*[173] have described a new KPro model, the "Seoul type KPro" (S-KPro), which consists of three parts: a long cylindrical PMMA optical surrounded by a mushroom shaped anterior flange of fluorinated silicone; a "biointegratable" skirt for corneal fixation (either porous polytetrafluoroethylene (expanded-PTFE) of 20 micron pore size or polyurethane of 40 micron pore size); and monofilament polypropylene haptics for scleral fixation. The primary difference between the standard KPro and the S-KPro is the manner of fixation to the eyeball.

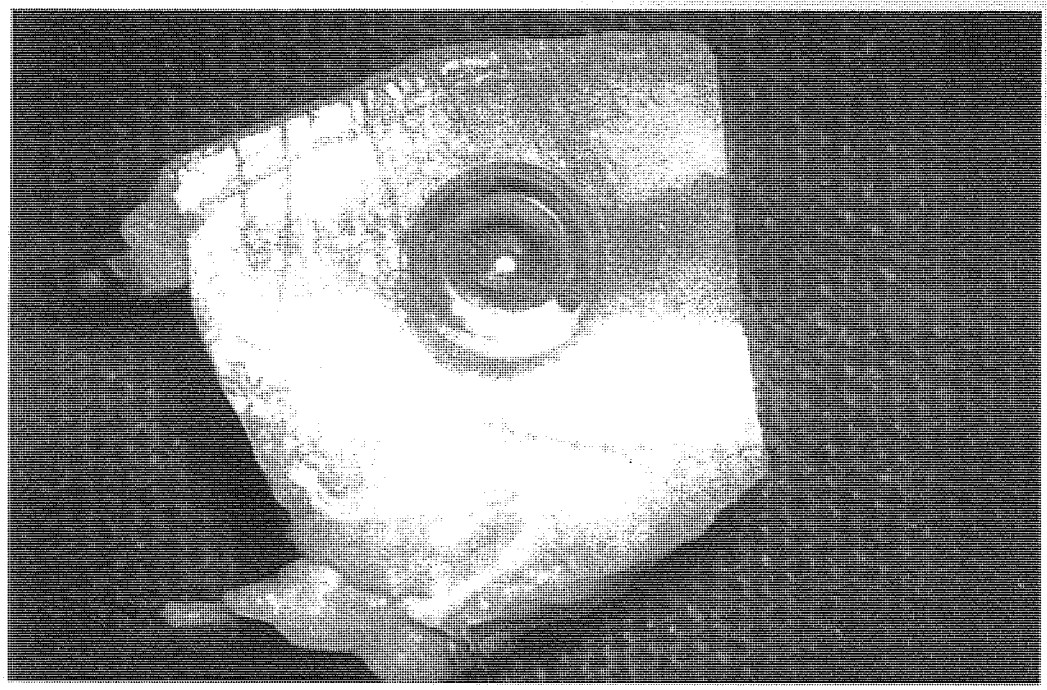

Figure 1.11 Osteo-odonto-keratoprosthesis (OOKP)

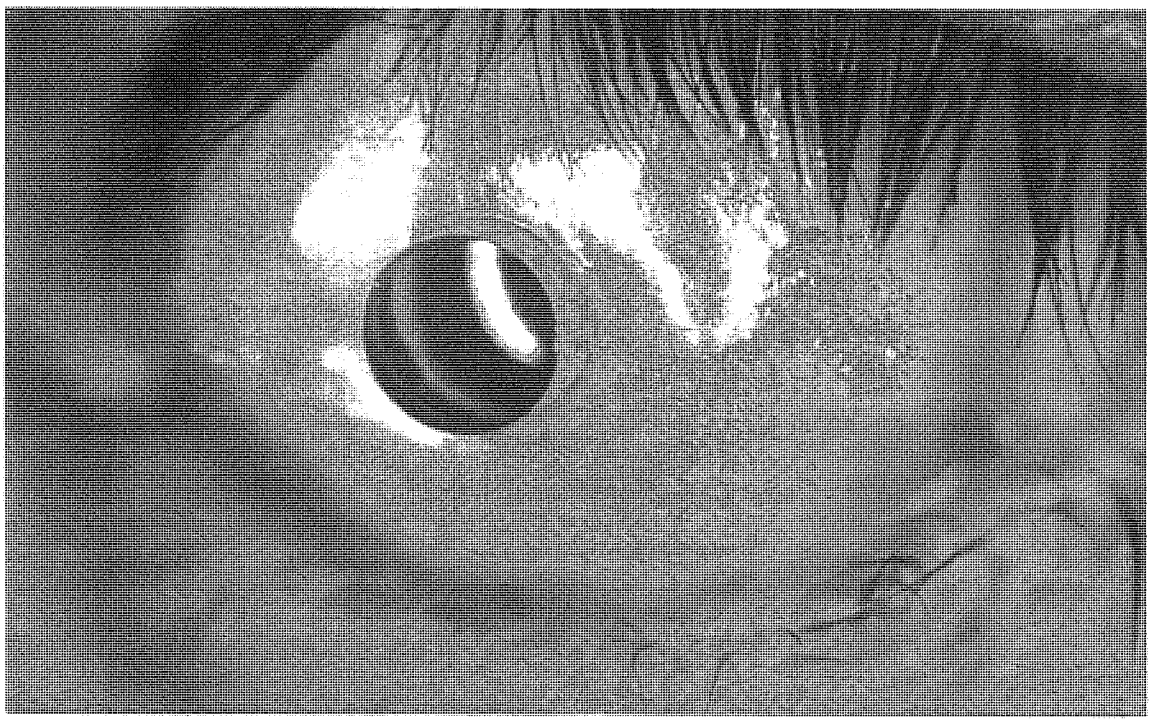

Figure 1.12 Implanted OOKP

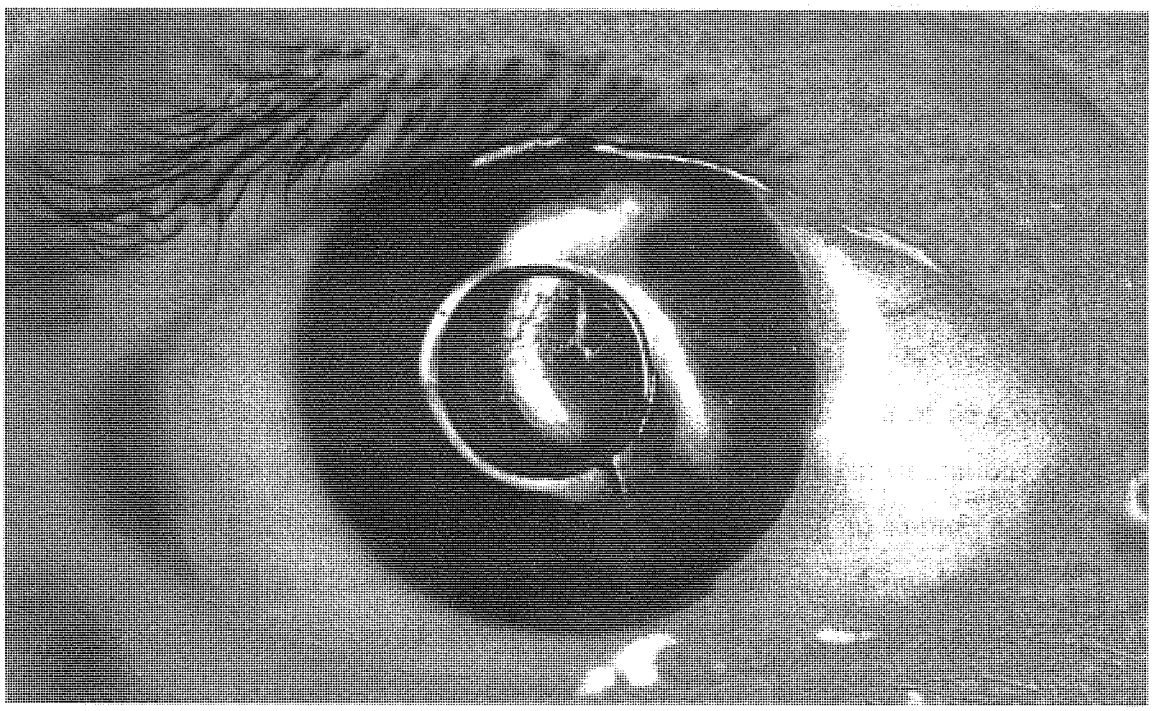

Figure 1.13 Implanted OOKP with cosmetic iris

When implanting an S-KPro, the skirt is anchored to the cornea, and the polypropylene haptics are anchored to the sclera to improve its stability, even in cases where corneal integrity may be poor. The S-KPro was used in 25 rabbit eyes and 2 humans (one patient with Steven-Johnson syndrome (SJS) received an S-KPro with the ePTFE skirt and a second patient with a chemical burn received an S-KPro with a polyurethane skirt). There were no reported complications in either of the human patients, after 18 months follow-up in the SJS patient and 8 months follow-up in the patient with chemical burns. The S-KPros reportedly maintained stable fixation to the eye during the follow-up period with visual improvements from HM(hand movement)/LP(light perception) to 20/100 and 20/50, respectively. These preliminary results suggest that the micro porous polymers ePTFE and polyurethane may be well tolerated in the human eye with the possibility of "biointegration". Further study is required to determine long-term integration and stability of these materials in the eye and of the novel haptic fixation method.

1.5.3.3 Chirila KPro

The Type I Chirila KPro[169] is a "true artificial corneal button", 9 mm in diameter, implanted by passing sutures through the sponge skirt in a manner similar to standard penetrating

keratoplasty. A complete conjunctival cover was required, which was later opened in a second surgery. The Type II Chirila KPro[169] is similar in design but somewhat smaller than Type I and is implanted in a small lamellar corneal pocket after a scleral incision and removal of the posterior layer of the pocket (2-3 mm hole) posterior to the KPro optic. Anteriorly, it is covered by a corneal layer and subsequently by a conjunctival flap. An opening typically is made in the conjuctival flap, followed by the anterior corneal layer at about 4 months postoperatively[174]. Both the PHEMA based types were implanted in 7 patients. No infection, extrusion, retinal detachment, or evidence of new onset glaucoma was present after implantation of either KPro type. The current limitations of the Chirila KPro include suboptimal mechanical strength predisposing to suture related tears, the possibility of calcium deposition within PHEMA materials and dependence on conjunctival coverage for maintenance of ocular integrity (Type I). Careful alignment of the anterior and posterior corneal openings is essential for successful application of the Type II device, which, of the two, may prove to be the model choice, especially where conjunctival health is questionable or poor. Increasing the posterior opening to 4 mm was also suggested for this model. In addition, because of the softness of the materials, this device may allow for the possibility of direct intraocular pressure measurement in the future. The patient base for Chirila KPro is limited by the need for a good tear pool.

Figure 1.14 Chirila KPro

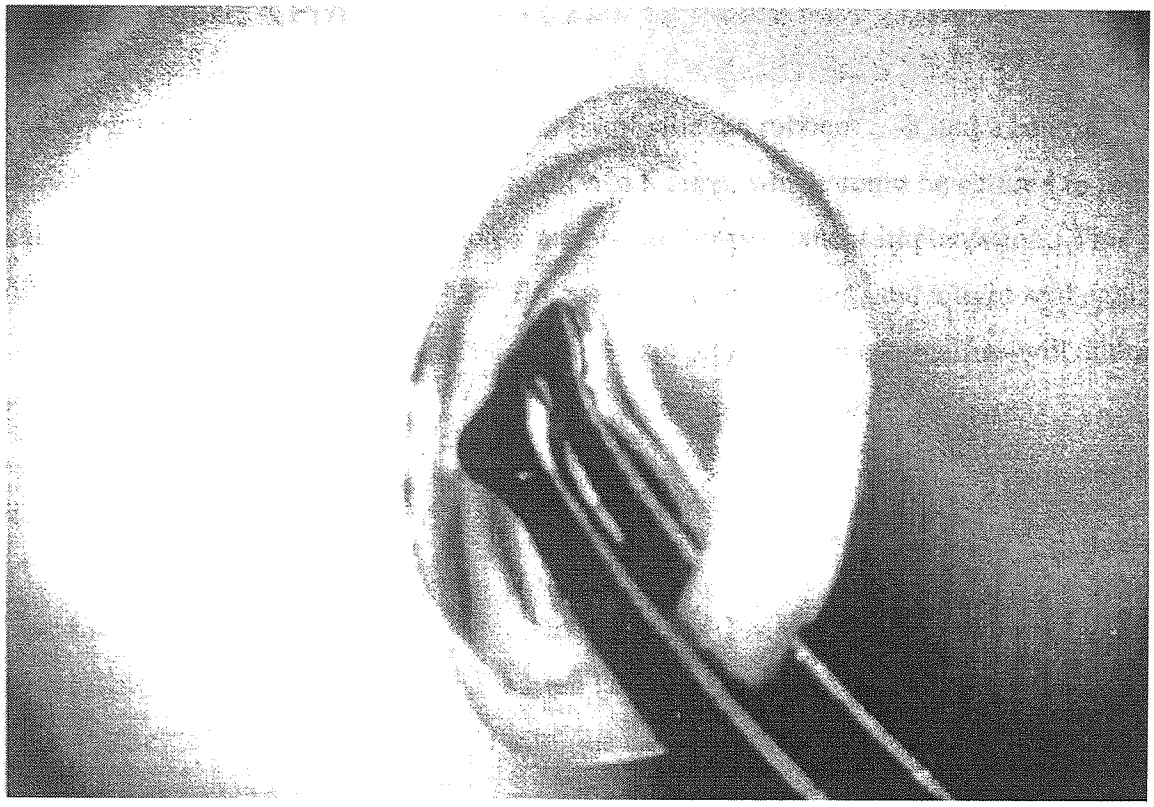

Figure 1.15 Chirila KPro before implantation

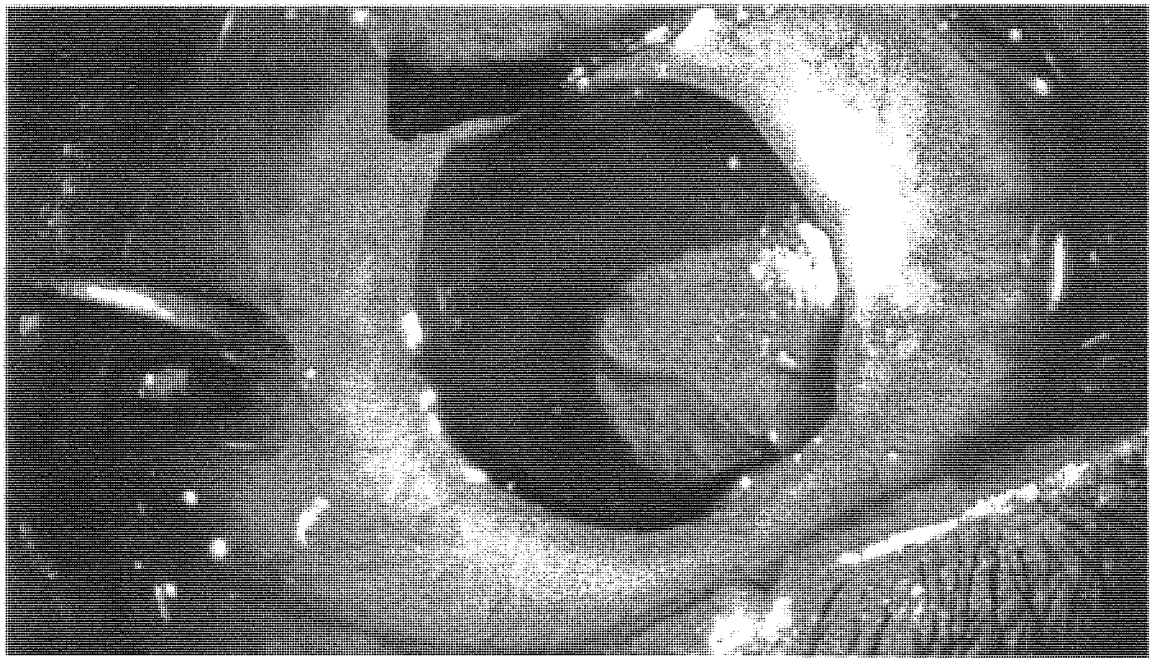

Figure 1.16 Chirila KPro during surgery

1.5.3.4 Aachen KPro

The original Aachen KPro was made entirely of silicone rubber[175]. It had a central cylinder, which fits into a 6.8 mm trephined hole. It had 8 arms, which could be sutured to the sclera and covered by conjunctiva or Tenon's membrane for permanent implantation. This device offered good optical clarity, good handling with ease of suturing, and a tight seal against the host rim, allowing for scleral depression during surgery. Future evaluations will address the performance of this device during longer periods of implantation.

1.5.3.5 Dohlman-Doane KPro

The Dohlman-Doane KPro was a "collar-button" of PMMA[176]. The anterior plate had a stem, which pierced a donor corneal button, and a back plate was either threaded onto it or glued. The carrier graft was sutured into place in the manner of a PK. Conjunctival flaps were employed where possible and opened centrally up to 1 month later. Dohlman *et al*[176] developed also an "artificial corneal endothelium" consisting of transparent silicone rubber (Silastic MDX) membranes sutured to the posterior surface of the cornea or corneal donor grafts in order to provide a fluid barrier against oedema, especially when the corneal endothelium was damaged.

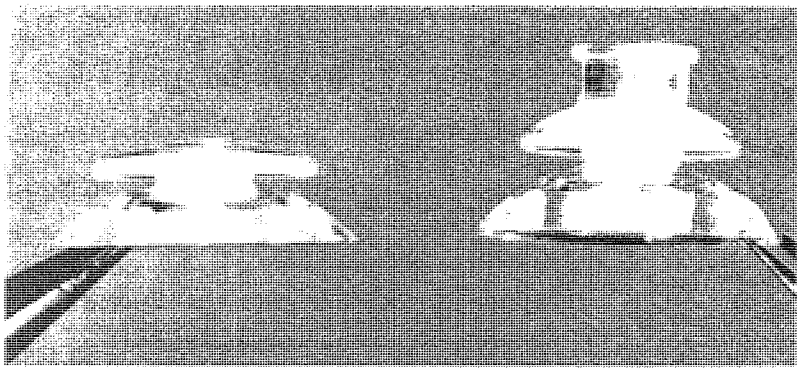

Figure 1.17 Dohlman-Doane KPro

1.5.3.6 Cardona KPro

Cardona designed a combined intralamellar/perforating KPro with a transparent central perforating cylinder and a holding lamellar plate, which proved to have an extrusion rate of

up to 20%, and later a "nut-and-bolt" KPro[177, 178]. The latter consisted of an external cosmetic contact lens of coated PMMA and a PMMA cylinder, which screwed into the contact lens and also into the PMMA nut that was placed against the endothelium. The extrusion rate for this device was about 21%, but its advantages over the earlier model included reduced evaporation, thicker supporting tissue, a covered junction between the cylinder and the host stroma, and the fact that there is no need for donor corneal tissue.

Cardona described his latest KPro and least invasive surgical technique in 1991[119]. The front plate has a Teflon™ skirt, 8.5 mm in diameter and 0.3 mm thick, perforated with 1.8 mm and 0.5 mm diameter holes to allow tissue ingrowth and the placement of sutures. Centrally, there is a threaded hold to accommodate the optical cylinder. The surgical procedure involves harvesting periosteum or fascia lata, de-epithelialization of the cornea and total peritomy. Panforniceal dissection is done and the upper lid orbicularis is resected if through-the-lid placement is intended. The visual axis is marked and a partial 3.5 mm trephine is made centrally with a lateral cut to facilitate cataract extraction or lensectomy. Radial iridotomies and anterior vitrectomy are performed and the cylinder introduced. The Teflon™ plate is sutured to the external cornea and sclera with interrupted 7/0 polypropylene. Dacron ™ mesh is placed over the Teflon™ skirt and a flexible polyester mesh may be added. Fascia or periosteum is sutured over the outside, with the cylinder protruding through it, and covered with conjunctiva.

1.5.3.7 Legeais KPro

Legeais and his coworkers[112] have designed a second generation KPro substituting the PolyMMA optic with an optic made from polydimethylsiloxane (PDMS) coated with polyvinylpyrrolidone. PTFE with a pore diameter of 80 μm is used for the skirt material. The optic still does not support epithelial cell coverage, a feature considered desirable by Legeais. However, most of the eyes were clinically stable after 7 months follow up and the new material appears to show advantages such as better surface properties compared to polyMMA.

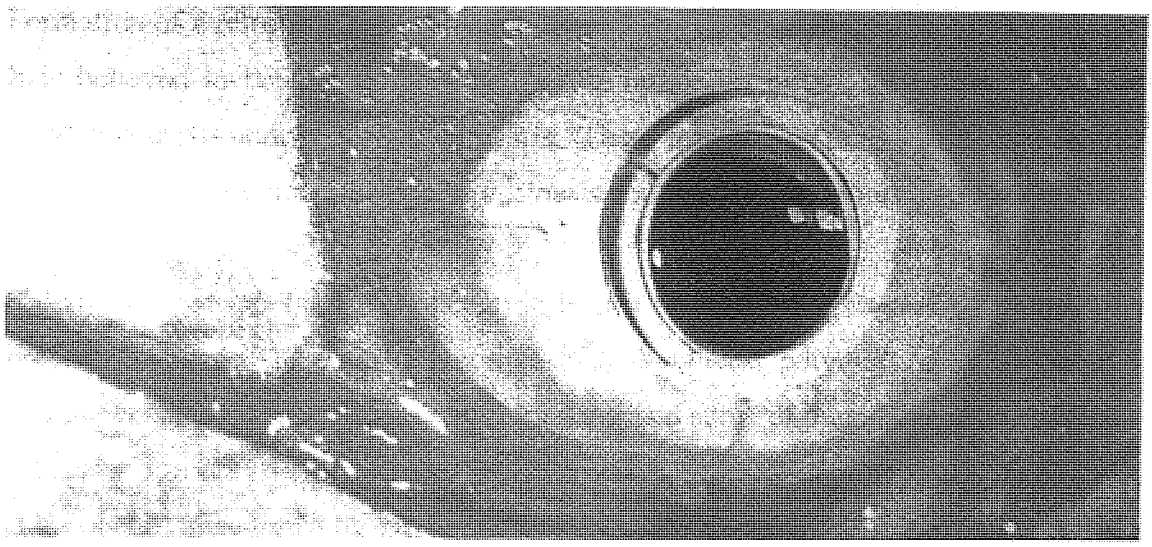

Figure 1.18 Legeais KPro

1.5.4 KPro Complications

The best of the available KPros are prone to serious complications, such as extrusion, infection, intraocular inflammation, membrane formation, and glaucoma. These problems may be difficult to diagnose and to treat, resulting in high morbidity. Rigid components cause mechanical stresses that facilitate ulceration. Glued or threaded interfaces between KPro components and the interface between the KPro and host tissue, constitute sites where epithelial downgrowth, leakage, and infection can occur. The lack of an epithelialized external surface predisposes the optic to extrusion and infection. The complexity of implantation surgery may provoke inflammation, glaucoma, and retroprosthetic membrane formation. Examination of KPro components that are buried under layers of tissue is difficult, limiting IOP measurement to digital estimation.

Keratoprostheses fail mainly because of postoperative complications. One of the most devastating complications is extrusion of the keratoprosthesis. Extrusion is usually preceded by the gradual ulceration and subsequent loss of the host tissue around the prosthesis (tissue melting), dislocation of keratoprosthesis, and leakage of aqueous humour. Epithelial downgrowth along the prosthesis can also occur, aggravating the consequences. Tissue melting was originally believed to be an aseptic necrosis, but it is now known that this is caused by the digestion of collagen by the proteolytic enzymes released at the site of implantation[169].

Formation of a retroprosthetic membrane is a frequent complication of prosthokeratoplasty. It is believed to be related to postoperative inflammation and/or to the contact between keratoprosthesis and vitreous body or iris. These membranes may thicken and may contract, exerting a pressure upon the keratoprosthesis and thereby contributing to its extrusion.

Calcification at the site of implantation is one of the leading causes of failure of several prosthetic devices and artificial organs[179]. Synthetic polymers calcify when used as components in various cardiovascular implants and some of them in locations different from the circulatory system[180]. Biomaterials imbibed with physiological fluids which are subsequently penetrated by growing tissues may then undergo calcification. It is associated with substrate not initially part of the implant. The condition for the occurrence of this type of calcification is a loose structure of the biomaterials, such as in porous materials. It was surmised[111] that microscopic manufacturing defects in gels might become supersaturating centres for calcium and phosphate ions, from which nucleation ensues.

The negative effects of calcification in the components of the keratoprosthesis should not be underestimated. The calcium salts deposited in either a gel or a sponge can cause brittleness, thus affecting the long-term clinical stability of the whole prosthesis, while the deposits in/on the core hydrogel can irreversibly affect the quality of the patients' restored vision. The calcium ions are bound through complexation or chelation to polar groups, such as carbonyl, until the positive charge repulsion balances out the affinity of the substrate. Once bound, calcium ions will attract phosphate anions until the positive charges are neutralized, which then allows more calcium to be bound, and so on.

The affinity of calcium for certain organic structures was also central to other 'chemical' hypotheses on biomaterial-associated calcification (BAC). The polymers[179] containing polarizable ether oxygen atoms may form cyclic structures that have a great tendency to chelate calcium, and the resulting structural units may function as initial nucleation sites. The cyclic ether structures are not actually essential: a linear macromolecular chain is also a valid alternative, provided it can 'wrap' around the calcium ions by assuming a helical conformation[181]. Calcification of the implanted biomaterials causes stiffening and tearing, thus limiting the functional longevity of the devices.

Localised tissue melting at the tissue-polymer interface could result in failure of the implant. Tissue melting is a result of chronic enzymatic activity that degrades the collagens of the stroma and basement membrane and is a common sequel to alkali burn injury[182].

Mechanical disruptions of the interface coupled with the use of materials that do not allow tissue growth into the supporting rim have led to an unacceptably high rate of implant extrusion[112].

Other complications of prosthokeratoplasty include inflammation (vitritis, uveitis, orbital cellulites), glaucoma, retinal detachment, hemorrhage, and cataract.

1.5.5 Requirements of KPro

The KPro material should have the following properties:

1. The material should be noninflammatory, should not permit the deposition of lipid, must allow keratocyte ingrowth & collagen synthesis to anchor the KPro within the cornea. It should also suppress epithelial downgrowth.
2. The core material should posses optical clarity, tensile strength & refractive power similar to a natural cornea and be able to form an image at or near the retina. It should also function as a UV radiation filter.
3. Surface modification of the material should be possible, either to promote or inhibit cell adhesion.
4. Under normal circumstances the anterior face of the material should be readily colonised by the corneal epithelium. A lack of such a surface predisposes to extrusion and infection. In dry eyes inhibition of epithelial colonisation is desirable since the eye fails to maintain epithelium normally. A compromised epithelium causes apoptosis in the underlying stroma and leads to extrusion.
5. Inhibition of cell adhesion on the posterior face is required. This prevents retroprosthetic membrane formation. On the internal face the implant should either permit the restablishment of an endothelial cell layer, to avoid excess fluid flow into the stroma or, if an impermeable implant, be highly biocompatible to avoid protein deposition or cell attachment compromising visual clarity.
6. The material should allow adequate nutrients to reach invading or overlying cells and also permit intercellular communication between the surviving cell layers of the

cornea. This is an important feature since studies have demonstrated that de-epithelialization of the cornea results in the apoptosis of the underlying keratocytes [183]. Failure to do so compromises the healing capacity and the integrity of a KPro.

7. When keratocyte invasion has taken place the collagens synthesized should be closely reflective of those made in the unwounded state and be arranged in similar arrays to ensure optical clarity.
8. It should be sufficiently soft for suture needles to pass through but strong enough so that suture materials do not cheesewire.
9. The prosthesis should be flush with the rest of the ocular surface to enhance comfort and to reduce mechanical shearing forces on it.
10. The skirt material must be made of a material that is highly biocompatible, causes minimal tissue swelling, and which is not reabsorbed. The skirt should also allow fibroblast ingrowth and collagen deposition sufficient to provide a permanent, firm anchorage without the need for additional mechanical features, such as lamellar spoke haptics. Additionally, the peripheral material must act as a barrier against epithelial downgrowth and be sufficiently porous to allow for keratocyte ingrowth[184].

1.5.6 Management of the Patient with a Keratoprosthesis

In addition to optimising the prosthesis, complications can be minimized by adequate preoperative assessment and pre- and postoperative management. Patient selection involves the following strict criteria[121].

1. Bilateral blindness (hand movements or less).
2. Severe, debilitating corneal disease with no realistic chance of a successful outcome from penetrating or lamellar keratoplasty.
3. Evidence of retinal function, such as light perception, papillary responses if ascertainable, normal electrophysiological findings, ultrasound excluding retinal detachment.
4. Normal intraocular pressure. Previous/current glaucoma must be well controlled without reliance upon topical medication if through-the-eyelid implantation is planned.
5. No current ocular inflammation.
6. Adult, well-motivated patient prepared to attend for regular follow-up and aware of the risk associated with prosthokeratoplasty.

The total diameter of the implant and the relative size of the skirt were critical components in encouraging fibroplasias. A diameter greater than 8 mm was found to be too great an insult to the cornea and resulted in extrusion. The range of successful devices ranged in diameter from 5 to 7 mm. In addition, the increased skirt size enhanced the surface area for possible fibroplasias and was found to be optimal at 0.5 mm[185].

1.6 Scope and Objectives of this Work

Hydrogels have been utilised in many biomedical applications, as there is the potential to manipulate the properties for a given application by changing the chemical structure of the constituent monomers. The work in this thesis is concerned with the development of novel hydrogels for keratoprosthesis.

The most commonly used KPro model consists of a transparent central stem with a porous peripheral skirt. Clear PMMA core materials have been used in KPro for many years, such as in the Strampelli keratoprosthesis (OOKP) which have not caused the failure found in other core and skirt prostheses; the OOKP approach has been particularly valuable when there is tear film dysfunction. However, epithelialization of this kind of solid, rigid optic material is clearly impossible and thus it is not ideal for patients with a stable tear film. The approach to the development of a hydrogel for potential KPro application adopted in this work is to develop soft core materials to mimic the properties of the natural cornea; this can then be used in patients with a good tear film. This studies have been based on hydrophilic monomers, such as N,N-dimethyacrylamide (NNDMA), N-vinyl pyrrolidone (NVP) and acryloylmorpholine (AMO) in combination with methyl methacrylate (MMA). They may therefore be regarded as an extension of the PMMA-based prosthesis to soft hydrogel corneal analogue.

The hydrogel for use in this keratoprosthesis must be able to withstand the stresses involved in the surgical procedure involved with the KPro and the *in situ* stresses such as the deforming force of the eyelid during the blink cycle. Conventional synthetic hydrogels such as simple MMA copolymers can be produced with a similar high water content to that of biological organ, but the mechanical properties are poor. Semi-interpenetrating networks were produced in this work to obtain much improved mechanical properties with similar water contents to conventional hydrogels. An ester-based polyurethane (PU), hydrophilic

monomers, AMO, NVP and NNDMA, and THFMA were used to produce SIPNs in this work for the synthetic cornea.

The core material in the KPro should inhibit the deposition of lipid and protein and should either not promote cell adhesion at all or be able to support a functioning epithelium. Polyethylene glycol (PEG), known as an effective monomer to modulate protein deposition and cell adhesion, was incorporated with SIPNs in this work.

The porous peripheral skirt is an important component in the "core and skirt" KPro. In the work described in this thesis, the porous peripheral skirt was synthesized using different porosigens with different pore sizes.

The studies stated above demonstrated that simple hydrogel SIPNs, which show isotropic mechanical behaviour, are not ideal KPro materials since they do not mimic the anisotropic behaviour of natural cornea. The final stage of the work has concentrated on the study of mesh reinforced hydrogels. They offer a promising approach to making a hydrogel that is very flexible but strong under tension, thereby having mechanical properties closer to the natural cornea than has been previously possible.

Several techniques were utilised in this work to investigate the properties of the novel hydrogels. The equilibrium water content, mechanical properties, surface properties and cell adhesion of the hydrogels were measured.

Chapter 2

Materials And Methods

This chapter deals with the identification and source of raw materials, the preparation and characterisation techniques of the hydrogel samples derived for use as keratoprosthesis.

2.1 Reagents

All reagents used are shown in Table 2.1, with structures shown in Figure 2.1.

Monomers were purified by reduced pressure distillation before use[186], and stored in a refrigerator where appropriate.

Reagent	Abbreviation	Molecular weight	Supplier
Acryloylmorpholine	AMO	141	Vista Optics
N-vinyl pyrrolidone	NVP	111	Vista Optics
N,N- dimethylacrylamide	NNDMA	74	Aldrich
Azo-bis-isobutyronitrile	AZBN	164	Aldrich
Ethylene glycol dimethacrylate	EDGMA	198.2	BDH
Tetrahydrofurfuryl methacrylate	THFMA	170	Polysciences
Poly (ethylene glycol)$_n$ Monomethacrylate	PEG MA		Polysciences
Polyurethane 5 Cat. #5706	PU5		B.F. Goodrich
Dextran		19,500	Sigma
Dextrin			Sigma
Methyl methacrylate	MMA	100	Vista Optics
2-hydroxyehtyl methacrylate	HEMA	130	Vista Optics

Table 2.1 Molecular weights and supplier of reagents used

N-vinyl pyrrolidone (NVP)

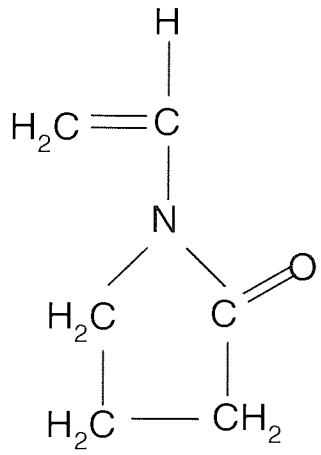

Acryloylmorpholine (AMO)

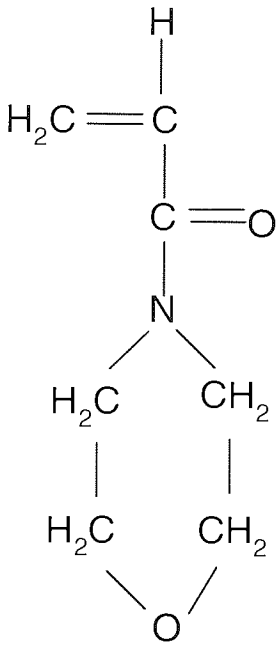

Tetrahydrofurfuryl methacrylate (THFMA)

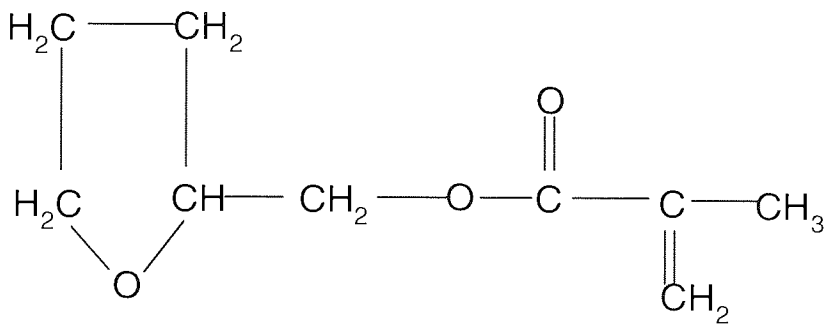

Figure 2.1 Structures of principle chemicals used

N,N-dimethylacrylamide (NNDMA)

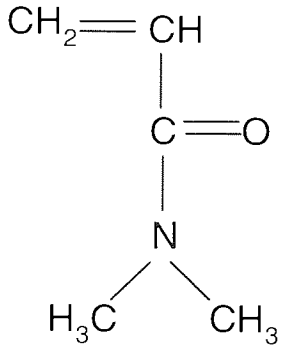

Azo-bis-isobutyronitrile (AZBN)

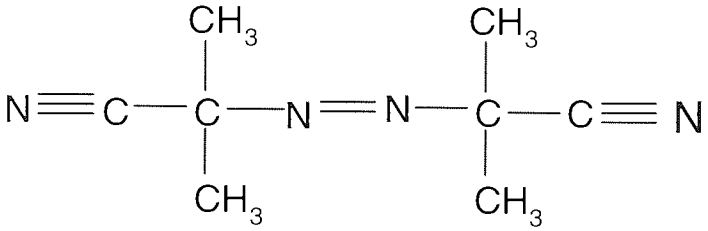

Ethylene glycol dimethacrylate (EDGMA)

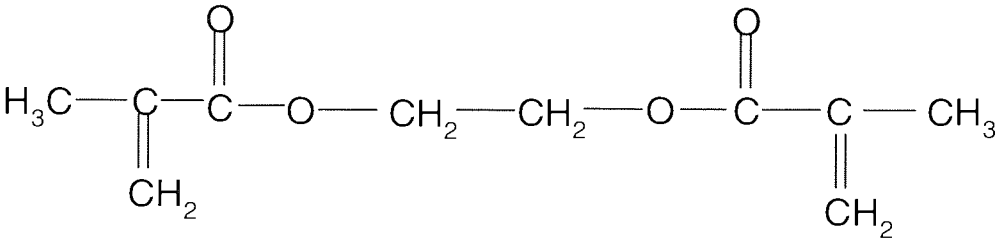

Polyurethane (general structure) (PU)

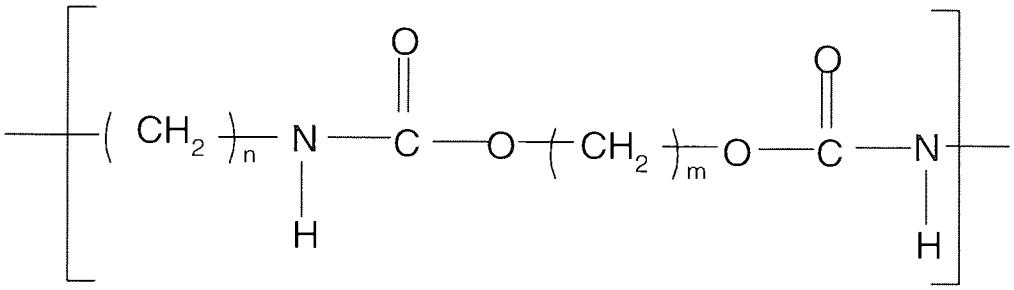

Figure 2.1 continued. Structures of principle chemicals used

Methyl methacrylate (MMA)

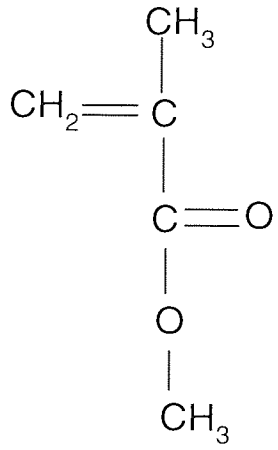

2-Hydroxyethyl methacrylate (HEMA)

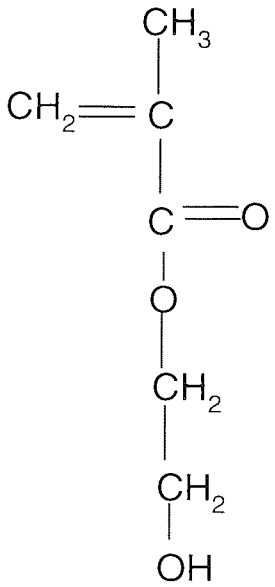

Poly(ethylene glycol)$_n$ monomethacrylate (PEG MA)

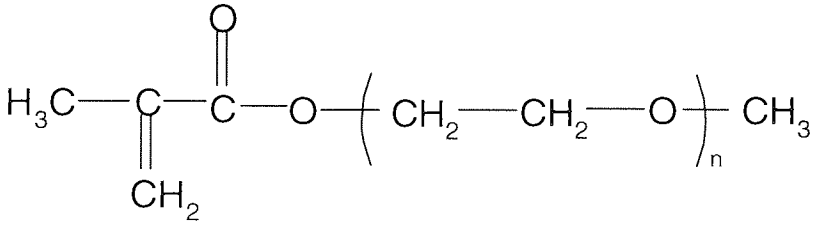

Methacrylic acid (MAA)

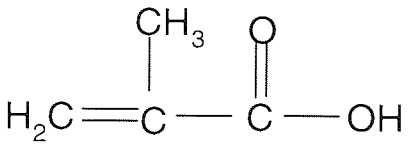

Figure 2.1 continued. Structures of principle chemicals used

2.2 Polymer Synthesis

2.2.1 Membrane Polymerisation

Polymers were produced in the form of a membrane sheet, using the mould shown in the following figure.

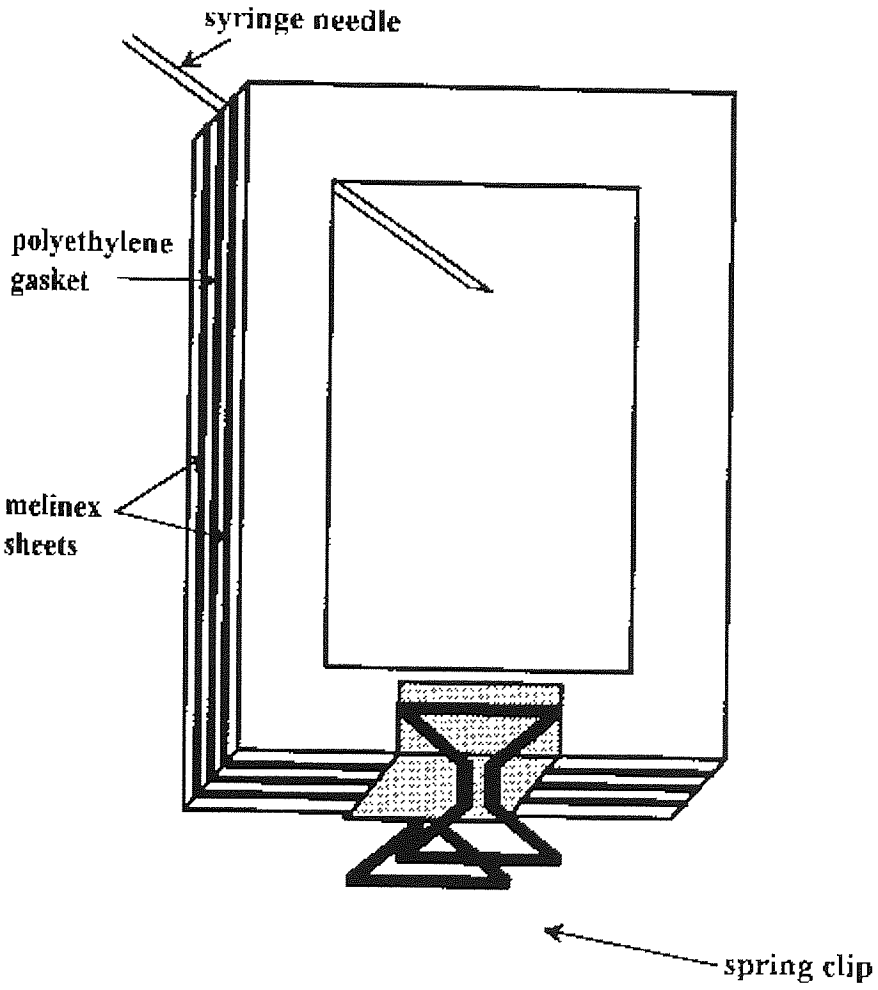

Figure 2.2 Diagram of a hydrogel membrane mould

Two glass plates (15cm x 10cm) were each covered with a sheet of Melinex (polyethylene terephthalate) secured by spraymount, and the surface cleaned by acetone. The Melinex can prevent the polymer adhering to the glass plates and allow for easy separation of the glass plates, as well as providing a clean, smooth surface. Then the plates were placed together with two polyethylene gaskets, each 0.2mm thick, separating the Melinex sheets (cavity 5 x 9 cm). The whole mould was held together by spring clips and the monomer mixture was injected into the mould cavity using a G22 syringe needle and syringe.

The standard comonomer mixture was made up to 5g in mass, with 1% w/w crosslinker (ethylene glycol dimethacrylate) and 0.5% w/w initiator (for thermal polymerisation this was azo-bis-isobutyronitrile). Then the mixture was degassed with nitrogen for 10 minutes prior to injection to make sure that all the oxygen is removed from the sample. The mixture was then introduced to the mould via the syringe and needle, the needle was removed so that the monomer mixture filled the mould cavity, and the mould tapped gently to remove any air bubbles that may have been introduced. In this work, if not specially stated, the 1% w/w crosslinker and 0.5% w/w initiator were used to synthesis the hydrogels in order to make the data comparable.

The injected mould was then put into a 60°C oven for three days to effect polymerisation, followed by a three hours post-cure in a 90°C oven. Then the mould was removed and the spring clips were removed. The membrane was then removed from the mould and separated from the Melinex sheets carefully. The membrane was placed in distilled water to hydrate to equilibrium. The membrane was hydrated for at least one week, changing the water daily to remove any unreacted monomer or crosslinker.

2.2.2 Interpenetrating Polymer Networks

For semi-interpenetrating polymer networks (SIPNs), the linear or interpenetrating polymer was dissolved in the monomer or comonomer, with up to 20% w/w of the solvent tetrahydrofuran, THF, if necessary. Once a homogeneous mixture was obtained and degassed, it was poured into one half of the mould cavity directly and the second plate placed onto it as the mixture was too viscous to be injected into the mould.

2.2.3 Porous Membranes

A porous membrane was synthesized in the same method as above, with an added porosigen, usually dextrin (pore size < 38 μm). The required amount of porosigen was added to the monomer mixture prior to the addition of the crosslinker and initiator once a homogeneous mixture had been obtained. Dextrin is a particulate carbohydrate material (Sigma) and dextran is a more fibrous carbohydrate material.

2.2.4 Freeze-thaw Technique

The macroporous hydrogels can also be synthesized using freeze-thaw technique. Firstly freeze a monomer/crosslinker/ solvent mixture onto a cold plate, or by dropping the mixture into a cold non-solvent, to create a system which consists of a solid monomer matrix around and between solvent crystals. This monomer matrix is then polymerised using UV radiation. After polymerisation the solvent is removed by thawing and a macroporous film results.

2.3 Equilibrium Water Content

The equilibrium water content, EWC, was measured from weight differences. Small samples of the hydrated membrane sheet were cut with a size seven cork-borer, and the surface water was removed by filter paper carefully to ensure that the membrane was not squeezed. The weighed hydrated samples were then dehydrated in an 800W microwave for 15 minutes at high power. Then the samples were reweighed and dehydrated further if necessary, so that constant weight was reached. The EWC was calculated for a minimum of three samples from each membrane and the final value was given as an average.

$$EWC\ (\%) = \frac{\text{Weight of water in the gel}}{\text{Total weight of the hydrated gel}} \times 100\% \qquad (2.1)$$

2.4 Measurement of Mechanical Properties

Materials were tested in their fully hydrated state by static tensile testing. The mechanical properties of the hydrogel samples were investigated using a Hounsfield Hti tensometer which was interfaced to an IBM 55SX computer. The tensometer was fitted with a 10N load cell attached to the instrument crosshead which was able to move in a vertical plane. From the load cell, a clamp was suspended by a chain and was directly above a lower clamp permanently fixed to the tensometer. Samples to be tested were placed into the sample clamps in a vertical position. The crosshead speed and force exerted on the sample were set at 20mm/min and usually 1.0N respectively, to a maximum extension of 50mm. The samples were cut from hydrated membrane sheets using a purpose designed, dumbbell shaped, cutter of 8mm gauge length and 3.3mm width.

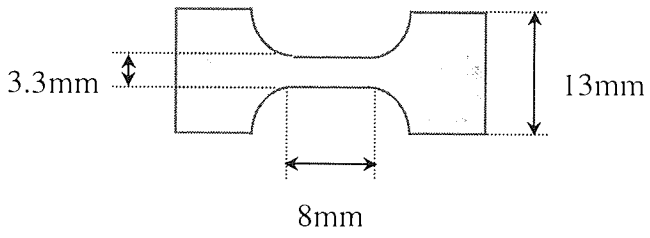

Figure 2.3 Dimensions of a hydrogel sample used in mechanical testing in tension

Equilibrated completely in distilled water, the test piece was then measured for its thickness using a micrometer and then placed between the clamps. Testing was carried out at room temperature and pressure. The test conditions and the sample dimensions were entered into the computer. Throughout the test, the sample was kept in a hydrated state by the application of a fine mist of water from an atomizer onto its surface. Upon completion, the computer program calculated Young's modulus (E.Mod), tensile strength at break (Ts) and elongation at break (Eb) using the following equations:

$$\text{Elastic modulus (E.Mod)} = \frac{\text{Stress}}{\text{Strain}} \qquad (2.2)$$

$$\text{Where: stress} = \frac{\text{Load}}{\text{Cross-sectional area}} \qquad (2.3)$$

$$\text{strain} = \frac{\text{Extension of gauge length}}{\text{Original gauge length}} \qquad (2.4)$$

$$\text{Tensile strength (Ts)} = \frac{\text{Load at break}}{\text{Cross-sectional area}} \qquad (2.5)$$

$$\text{Elongation at break (Eb)} = \frac{\text{Extension of gauge length}}{\text{Original gauge length}} \times 100\% \qquad (2.6)$$

Five samples of each polymer were tested and the final result stated was given as an average.

2.5 Differential Scanning Calorimetry

Differential Scanning Calorimetry (DSC) was used to determine the percentage of freezing water present in a hydrogel sample.

Thermograms were obtained using a Perkin-Elmer differential scanning calorimeter, DSC-7, in conjunction with a 7500 professional computer and liquid nitrogen cooling accessory. The program was run using Perkin-Elmer Pyris Software 2.01 on Windows NT on an interfaced P-133 PC. A hydrogel sample was cut from the hydrated membrane using a size 1 cork borer and the surface water was carefully removed using filter paper. The disc was then weighed to give a weight of sample in milligram and sealed in aluminium pans to prevent water evaporation during measurement. The sample's weight is about 4-7 mg. Then the sample was placed in the sample holder of the thermal analyser unit.

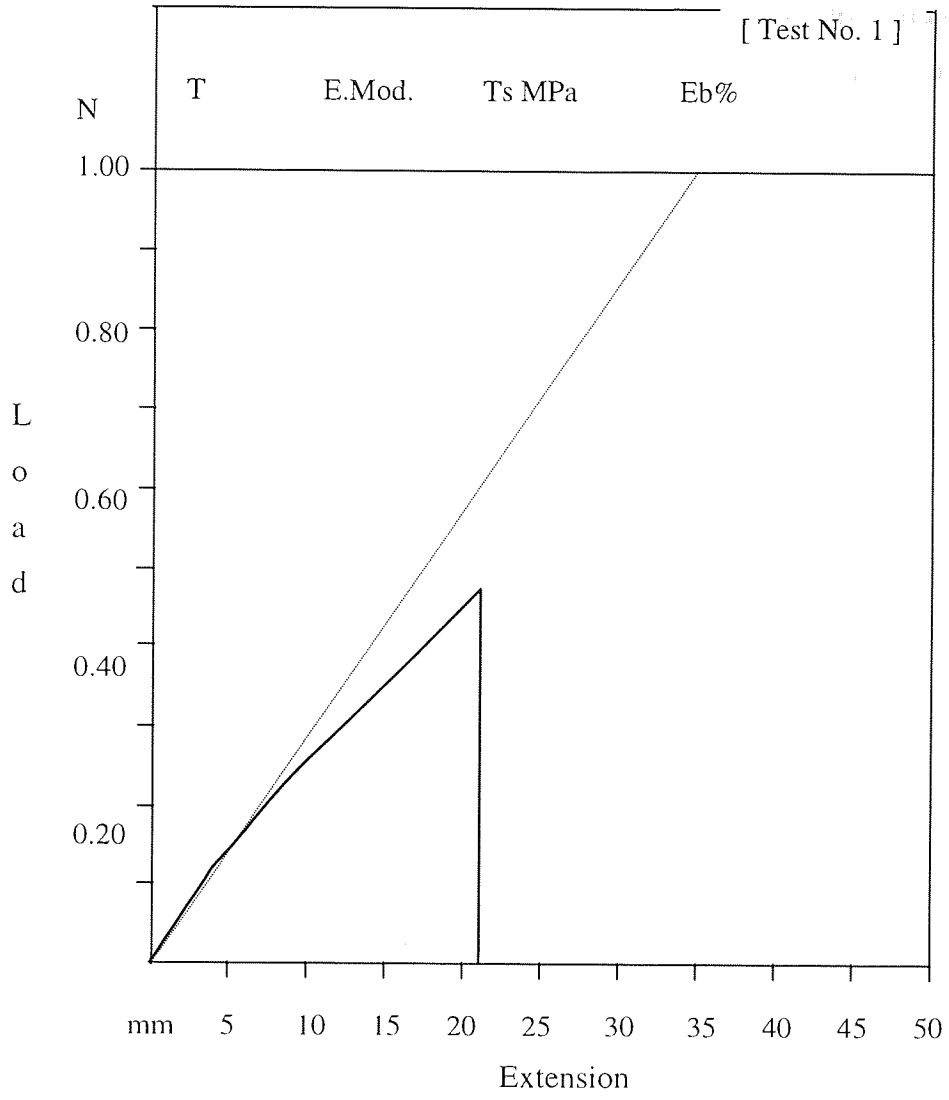

Figure 2.4 An example of a stress-strain curve obtained from a tensometer

The method steps used to supercool the water in the hydrogel and then slowly heat the sample to produce endothermic peaks in the region of the melting point of water are as follows:

1. cool from 20°C to –70°C at 100°C/min
2. hold for 5 minutes at –70°C
3. heat from –70°C to –25°C at 20°C/min
4. heat from –25°C to 20°C at 10°C/min

Using the calibration graph produced by pure water, the area under the endothermic peaks from step 4 was converted by the software to the weight of freezing water in the sample, expressed as a percentage of the sample weight. The proportion of freezing to non-freezing

water was calculated by the computer software from the resulting thermogram. The area under the melting peaks of the hydrogel sample was measured which enabled ΔH to be calculated. ΔH for the samples was obtained by the following equations:

$$\text{Freezing water (\%)} = \frac{\Delta H \text{ calculated}}{\Delta H \text{ for pure water}} \times 100\% \qquad (2.7)$$

$$\text{Where: } \Delta H = \frac{\text{Area under the peak}}{\text{Weight of the sample}} \qquad (2.8)$$

And ΔH for pure water = 333.77 Jg^{-1}

The process was repeated three times for each sample, and at least three separate samples from each hydrogel sheet were tested. The non-freezing water was then calculated as the difference between the EWC and the freezing water content (FWC).

2.6 Surface Properties

The surface energies of hydrogels can be calculated using the equations explained in Chapter 1.

1. in the hydrated state using the Hamilton and captive air bubble techniques
2. in the dehydrated state using the sessile drop technique.

Past researchers in our laboratory have cleaned samples using "Teepol L" or "Tween 20" detergent to remove any grease on the surface that may affect measurements and then rinsed thoroughly using distilled water. However, there is a high risk of traces of detergent remaining on the surface, and modification of the surface chemical groups by the detergent, especially with materials containing ionic monomers. It was decided, therefore, not to clean samples, but to use distilled water to rinse the surface to remove any dusts on the surface and to ensure that fingers did not touch them, so that the risk of contamination was reduced.

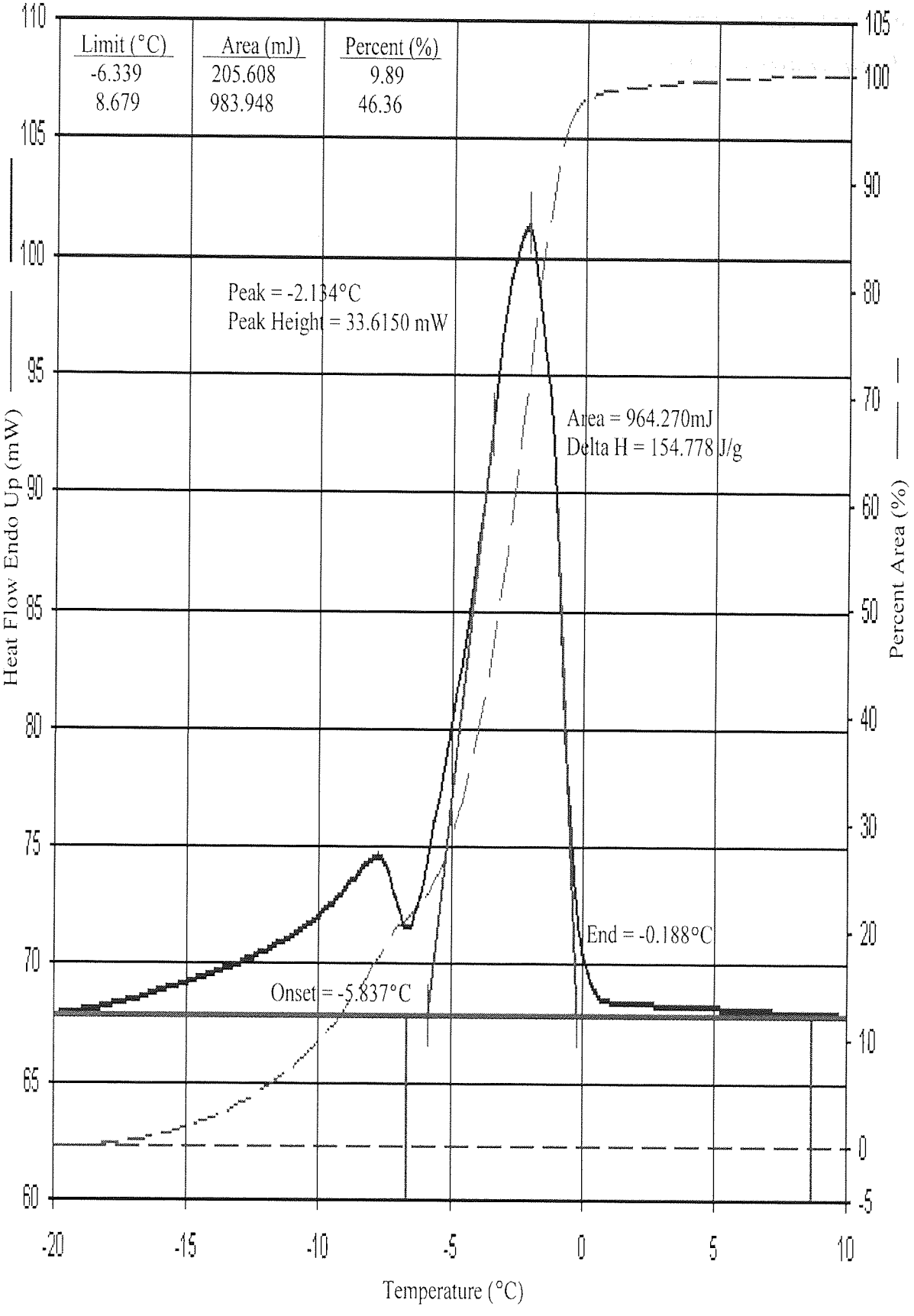

Figure 2.5 An example of a thermogram obtained by DSC

The contact angles are measured using a GBX contact angle measuring system. The system consists of a computer controlled stage, above which sits an automated syringe which is again controlled by the computer. A camera located within the instrument is used to view the stage and syringe tip with the image being sent to the computer. The system can be set to take an instantaneous image after a drop is placed on the surface of the material. The contact angle can then be measured from the image visible on the computer's monitor using the software installed into this computer. By the use of an automated syringe, the drop that is formed can be set to always be of the same volume. The computer controlled stage ensures that the drop formed by the syringe is placed on the material with a reproducible force. The polar, dispersive and total surface free energies could be calculated by Macintosh Works™.

2.6.1 Hamilton's Method

Discs were cut from the hydrated hydrogel membrane using a size seven cork-borer. Surface water was carefully removed from the sample using filter paper. The sample was then glued to an electron microscope stub using super glue, and inverted and suspended in an optical cell which was filled with distilled water. A small drop of N-octane was placed on the surface of the sample using a curved G25 syringe needle. This was repeated at least three times on three samples so as to reduce any errors arising from surface topology irregularities and operator error.

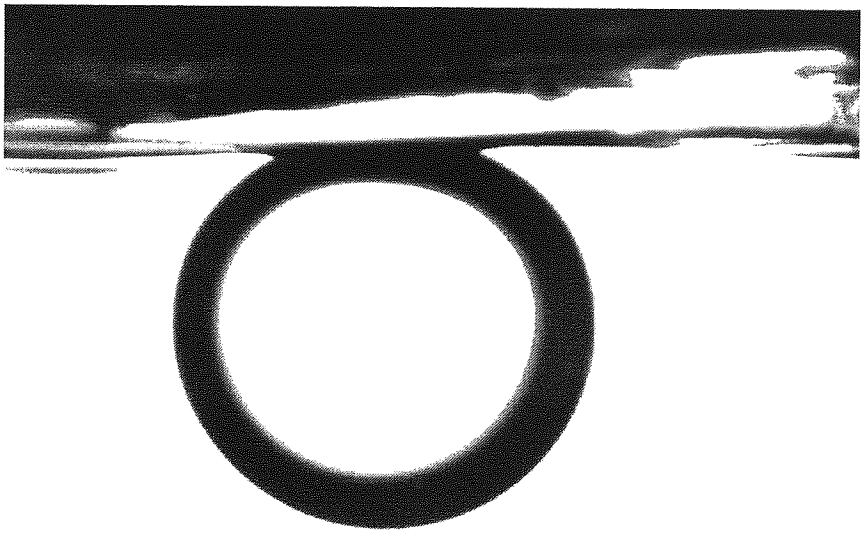

Figure 2.6 Example image produced by GBX goniometer for Hamilton's method

2.6.2 Captive Air Bubble Technique

Discs were cut from the hydrated hydrogel membrane using a size seven cork-borer. Samples were mounted as described above for Hamilton's method. Air bubbles were then released onto the surface using a specially curved syringe G25 needle. This allowed for accurate control of the bubble volume onto the surface of the sample. At least nine readings were taken to reduce errors.

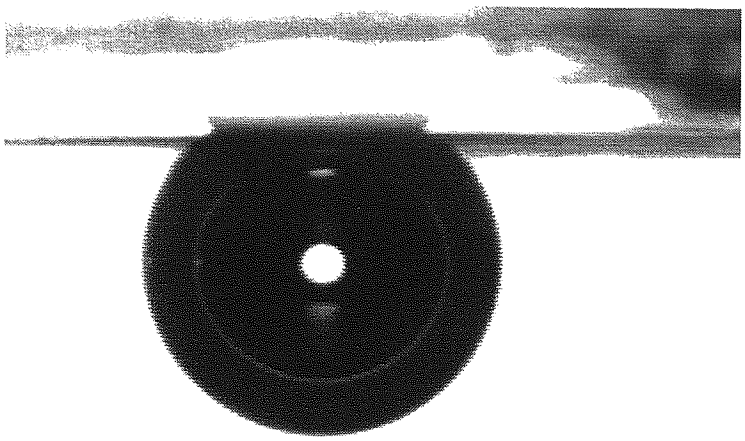

Figure 2.7 Example image produced by GBX goniometer for captive air bubble

2.6.3 Sessile Drop Technique

A size seven cork-borer was used to cut the discs out of a hydrogel membrane. Samples were dehydrated to constant weight in a microwave oven for approximately 15 minutes and kept in a desiccator until tested. The samples were kept flat by dehydrating between two blocks of PTFE. Then they were placed on a microscope slide which was placed on the support of the goniometer. The wetting liquids used were distilled water and diiodomethane. A drop of liquid was placed onto the surface of the sample using a straight G25 syringe needle. Several samples were tested to reduce errors.

.

2.7 Scanning Electron Microscopy

The surface of sample is viewed under very high magnification, using this well established technique. The samples are dehydrated in a microwave oven prior to being mounted onto an aluminium stub. Samples are then coated with gold in a sputter coater, placed in the Cambridge Instruments Stereoscan 5150 microscope and evacuated. A beam of electrons is fired at the sample and the reflected electrons are collected and an image formed on a cathode ray tube.

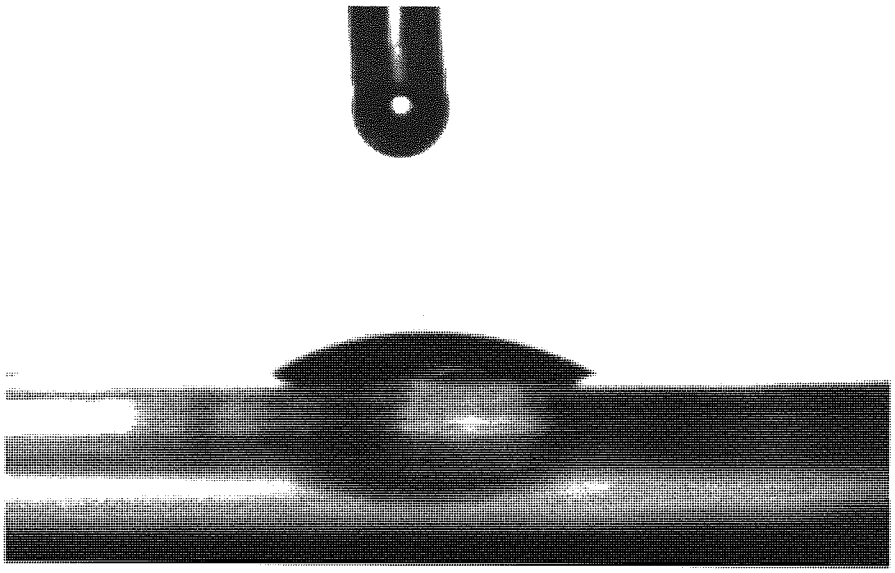

Figure 2.8 Example image produced by GBX goniometer for sessile drop

2.8 *In Vitro* Ocular Spoilation Model

The *in vitro* ocular model has been developed over several years at Aston in order to show the effects of lipid and protein deposition on a hydrogel sample[45].

This model depends upon having a suitable and stable tear substitute. The tear substitute was based on a 1:2 (v/v) solution of foetal calf serum (FCS) diluted with phosphate-buffered saline as a base. This was then 'spiked' with additional components such as mucin, lactoferrin and lysozyme in order to mimic the composition of tears.

The tear model enables controlled spoilation to be carried out by the 'shaker' model or the 'drop and dry' model. The 'shaker' was used in this work. A small number of glass beads were placed into a glass vial to provide an irregular surface on which the sample could sit, allowing contact with air and the artificial tear solution. The tear solution was pipetted into the vial to a level just below the top surface of the glass beads. Samples were cut from the hydrated hydrogel membrane using a size seven cork-borer and placed into the vial. These were then placed on a flatbed vibrating shaker, set at 200 cycles/minute, which enhanced the air and tear solution contact with the samples. The tear solution in the vial was replaced every 24 hours to maintain a fresh supply of protein and lipid components. The experiment was run over 28 days, which gave an accelerated spoilation profile equivalent to several times this period of normal contact lens wear and being representative of an extended wear regime. *In vitro* spoilation carried out at Aston has been found to give spoilation equivalent to six months wear, and removes the patient to patient variability that occurs *in vitro*[45]. Spoilation is patient, materials and wear regime dependent so no single spoilation correlation factor can be obtained. The spoilation model does not aim to mimic the tears but to mimic the proportional spoilation chemistry encountered from an array of proteins and lipids.

Lipid deposition was monitored on a modified Hitachi F-4500 fluorescence spectrophotometer. This is a non-destructive technique that relies on the fluorescence of lipoidal species (via the conjugation present in cholisterol esters and fatty acids) following excitation by UV light. Lenses were placed in distilled water in a specially designed quartz cell, which allowed reproducible orientation of the disc to the incident light beam to be achieved. An excitation beam wavelength of 360 nm was used and the height of the resulting emission peak monitored over the 400-600 nm range.

Protein adsorption was measured using a Hitachi UV spectrometer at 280 nm. The sample was placed right at the bottom of the UV cell, which was filled with distilled water for position consistency and the absorbance was measured against distilled water. The progressive accumulation of protein on the hydrogel was then calculated by referral to a standard Beer-Lambert curve. Multiplying the values obtained by 1.5 converted the units from mg/sample to mg/lens.

2.9 Calcein AM Assay for Viable Cell Adhesion

Hydrated hydrogels were cut into 13 mm diameters discs using a size ten cork-borer. Anchorage dependent cells have traditionally been grown on glass substrates, however, commercial tissue-culture plastics are now commonly used for convenience. Tissue-culture plastic was used as a positive control and poly HEMA was used as the negative control. Place sterilised 13 mm discs of each material in the wells of a 24 well plate (IWAKI) and incubate in Dulbecco's Phosphate Buffered Saline (DPBS) for at least 24 hours. Cells were passaged and resuspended to give a concentration of 1 to 4 x 10^4 cells/ml in working media. Add 1 ml of cell suspension to each well and incubate materials for 72 hours. A 0.5 μM solution of calcein AM in DPBS was then made up. Media was removed from the materials which were then washed in DPBS to remove serum esterase activity. 1 ml of the calcein AM solution was then added to each well and incubated at room temperature for 15 to 30 minutes. Each disc was transferred to a microscope slide and viewed under fluorescent microscope, counting the number of cells present in each of 20 fields for each material; 6 discs of each material were used.

2.10 Fluorescence Microscopy

Fluorescence studies were carried out with a Leitz Dialux 20 microscope fitted with a Ploempak 2.4 Fluorescence Vertical illuminator. A 50-watt ultra high pressure mercury lamp was employed as the light source. A H3 filter cube (BP 490 excitation filter and LP 515 suppression filter) was used for the calcein AM and ethidium homodimer-1 assays and an E3 filter cube (BP 436/7 excitation filter and LP 490 suppression filter) was used for the DAPI assays.

2.11 Bohlin Rheometer

Rheology is the study of the flow and deformation of materials. Newton was one of the first to define the forces behind material flow. The word 'rheology' was formally accepted at the inaugural meeting of the Society of Rheology (American) in 1929. However, practical study has only been possible in modern times with the advent of advanced technology. Bohlin CVO rheometer is used at Aston to study the dynamic mechanical properties of the hydrogels.

The Bohlin CVO rheometer is a controlled shear stress instrument, that is they apply a torque (force) and measure the resultant displacement (movement). Torque and displacement are converted to "rheological format" by means of the measuring system constants. This integrated system of Bohlin is consisted of the rheometer, temperature control unit, graphics output device, computer and printer.

There are three operation modes available in the Bohlin CVO rheometer:

Viscometry Mode: It measures viscosity as a function shear stress or shear rate. Shear rate sweep, shear stress sweep, time sweep (isothermal) and temperature sweep (gradient or step change) modes can all be programmed. A continuous ramp (yield stress) experiment is also available.

Oscillation Mode: It measures the dynamic viscoelastic properties as a function of frequency. Frequency sweep, stress sweep, time sweep and temperature sweep (gradient or step change) modes can all be programmed. Frequency, time and temperature sweeps can be programmed at constant stress or constant strain amplitude (autostress).

Creep Mode: It measures the creep compliance and recoverable compliance as a function of time to determine the elastic compliance as well as the zero viscosity. Flexible zoned sampling is user defined.

The test sample was placed on / in the lower measuring system. The correct gap was set for each measuring system because the correct gap between the upper and lower measuring system is essential for accurate measurements. Then slowly lower the upper measuring system into place. Select the operation mode as stated above and set up the required test parameters one by one. The results can be obtained from the software installed in the computer.

Chapter 3

Water Contents Of Novel Hydrogels

3.1 Introduction

This chapter investigates the water content of novel hydrogels for potential materials for keratoprosthesis. The amount of water absorbed by a hydrogel may be expressed as the equilibrium water content (EWC). The EWC is the single most important property of a hydrogel because it governs the permeability of the membranes, mechanical properties, surface properties and resultant behaviour at biological interfaces. Water plays an important role in determining the biocompatibility of the synthetic materials. Materials with high water contents possess similarities with normal tissues found in the biological environment (body). They also ensure a low interfacial tension with blood which reduces protein adsorption and cell adhesion. This advantage has been known as an essential requisite for the utilisation of synthetic material in contact with physiological fluids such as blood.

Water in the hydrogel structure also has an important influence on the gas permeability of the materials. In relation to biomaterial this is of great importance since a high permeability will permit the diffusion of molecular species vital to the processes of life, such as dissolved oxygen. The cornea is a naturally occurring hydrogel containing 81% water[74]. As the cornea is avascular and receives most of its oxygen supply direct from the atmosphere, adequate oxygen transport must be ensured to the corneal surface through any materials to prevent hypoxia, and allow sufficient carbon dioxide transport in the opposite direction to prevent acidosis, both of which would lead to physiological stress to the eye.

There is a great deal of evidence to suggest that water in polymers can exist in more than one physical state[15] and these states of water in the hydrogel will also affect its properties. This property can be investigated by calorimetric techniques[14] such as differential scanning calorimetry (DSC).

The daunting synthetic challenge involves choosing the right combination of monomers and controlling both the sequence distribution and molecular architecture of the resulting polymer. Some monomers have conventional vinyl functionality enabling them to be polymerised and copolymerised with other vinyl monomers, but they have pendant groups whose properties tend to dominate the surface water structuring properties of the resultant material. A range of hydrogels synthesized from a wide selection of hydrophilic and

hydrophobic monomers was prepared with this aim, with various water contents from 10% to 90%. This chapter attempts to illustrate the multi factors which affect the water content and water binding properties of the hydrogels. The results obtained are presented in this chapter in graphical form, to illustrate the trends in behaviour with changes in composition. The precise values of equilibrium, freezing and non-freezing water content can be found in appendix 1.

3.2 MMA Based Copolymer Clear Hydrogels

Because of its excellent optical clarity and moderate foreign-body reaction, poly (methyl methacrylate) (PMMA) has been widely used as a KPro optic portion since the 1950's[169]. It is particularly successful in Strampelli KPros prosthesis (OOKP) which has been valuable when there is tear film dysfunction. However, epithelialization of this kind of solid, rigid optic material is clearly impossible and thus it is not ideal for patients with a stable tear film. The approach to the development of a hydrogel for potential KPro application adopted in this work is to develop soft core materials to mimic the properties of the natural cornea; this can then be used in patients with a good tear film. These studies have been based on hydrophilic monomers, such as N,N-dimethyacrylamide (NNDMA), N-vinyl pyrrolidone (NVP) and acryloylmorpholine (AMO) in combination with methyl methacrylate (MMA). They may therefore be regarded as an extension of the PMMA-based prosthesis to soft hydrogel corneal analogues.

N,N-dimethylacrylamide (NNDMA) is the simplest of the N,N-disubstituted acrylamides, and can be polymerised radically or anionically to afford water soluble polymers as it offers a potential increase in equilibrium water content over HEMA. NNDMA which is used in contact lens compositions can prevent hydrolysis reactions[187]. It is a liquid with good solvent properties and has a structural resemblance to NVP; additionally, the presence of two methyl groups confers hydrolytic stability. Unfortunately, methyl groups lead to chain transfer reactions during copolymerisation, which are caused by hydrogen abstraction from the pendant methyl groups. This produces imperfect networks with lower than expected mechanical properties.

N-vinyl pyrrolidone (NVP), a lactam, is soluble in water and many other solvents. Its strong interaction with water creates advantages and disadvantages with respect to hydrogel

formation. However, homogeneous crosslinked polyNVP is difficult to prepare due to low reactivity ratio and low mechanical strength. NVP/MMA copolymers have a blocky sequence distribution rather than the desired alternating sequence distribution that has been demonstrated to show enhanced compatibility[188, 189]. N-vinyl pyrrolidone (NVP) and MMA copolymers had also previously been investigated for use in synthetic cartilage[13]. Previous work indicated that the leaching effect and poor polymerisation associated with NVP would lead to problems with long term wear in the eye due to the toxicity effects of the NVP[46] and the degree of spoilation caused by the "blocky" nature of the resulting copolymers. Not only does NVP form "blocky" sequences within copolymer networks, but gives rise to extra-network oligomeric material formed towards the end of the polymerisation which diffuses slowly out of the network. Both give potential problems in extended wear, since blocks of NVP are highly lipophilic and the oligomers gradually leach into the eye[190]. Studies have shown the potential for replacing NVP with AMO in hydrogels which would overcome these problems[23]. It contains a highly polar disubstituted amide group coupled with apolar methylene and methane groups. PolyNVP is interesting from the biological viewpoint, since it has structural features similar to those of proteins which have led to its being proposed on several occasions as a simple protein model. However, in contrast to proteins, polyNVP is physiologically inactive which has led to its use as a blood plasma substitute or blood volume expander[191], although these applications are now very much restricted since it is not metabolised or in any way degraded in the body. Moreover, polyNVP was the first synthetic polymer to be used for the modification of therapeutically useful enzymes[191] and it has been proposed as a soluble drug carrier[192, 193].

Acryloylmorpholine (AMO) was first synthesized by Parrod and Elles in 1957 and has been used to synthesise hydrophilic gels[194]. Previous work carried out suggested that AMO possessed similar properties to those of NVP[23]. Recent work at Aston has shown the potential of AMO for use in hydrogel systems for biomedical applications[23]. It is a hydrophilic monomer which shows a good alternating sequence distribution when copolymerised with MMA, water content and mechanical properties, along with promising *in vitro* spoilation studies.

3.2.1 Effect of Monomer Composition on EWC

As stated above, the equilibrium water content is the single most important property of the hydrogel. The effect of monomer composition on equilibrium water content of MMA based copolymers is displayed on Figure 3.1.

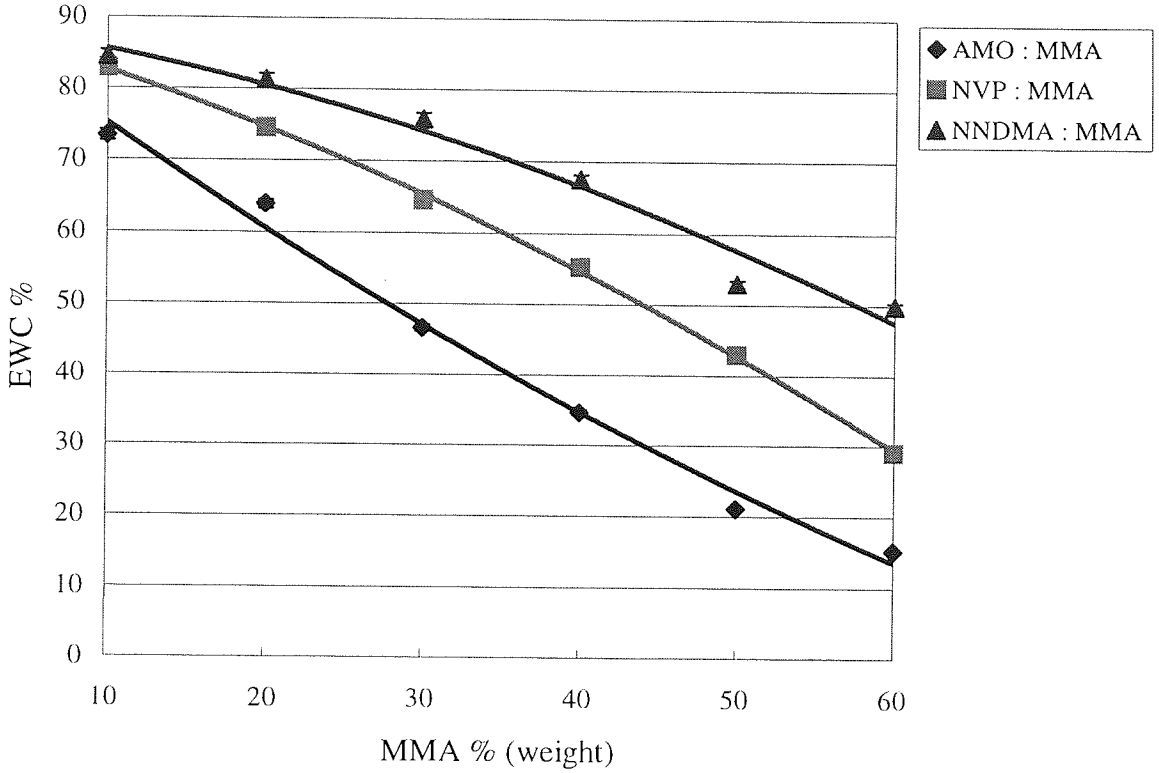

Figure 3.1 The effect of MMA content on the equilibrium water content of MMA based copolymers

It can be seen from Figure 3.1, that equilibrium water contents decrease as the amount of methyl methacrylate (MMA) increases. The structure of the monomers influences the ability of the resulting polymer to absorb water. MMA is much more hydrophobic than NNDMA, NVP and AMO. At the same composition, the NNDMA based copolymer hydrogel has the highest equilibrium water content and the AMO based copolymer hydrogel has the lowest. So the hydrophilic order of these four monomers is: NNDMA > NVP > AMO > MMA.

Previous work at Aston[195] indicated that AMO and NVP monomers produced polymers with a similar hydrophilicity when they were copolymerised with 2-hydroxyethyl methacrylate (HEMA). To minimise the steric interactions between the lactam heterocyclic rings polyNVP and polyAMO may coil in a staggered coil conformation. Water molecules can form a "bridge" between the polar groups on adjacent rings in this kind of conformation. However, the addition of any other monomer will disrupt the packing arrangement as the polar groups on NVP and AMO will interact with the polar groups on the comonomer. There are several possible explanations for the fact that AMO is much more hydrophobic than NVP when copolymerised with MMA rather than HEMA. One is that the effect of MMA on AMO is more marked than HEMA in the helical conformation of polyAMO. Another possible reason is that MMA incorporation will restrict access to the water binding sites on NVP; however, this may be compensated for, in part, by the formation of hydration clusters. Thirdly, the sequence distribution may affect the arrangement and conformation of polar group in the backbone chain, thereby influencing the water taken up.

NNDMA is undoubtedly the most hydrophilic monomer among these reagents because of its lower steric hindrance on the polymer backbone chain. With the addition of 10% weight MMA, the NVP-MMA copolymer has a similar water content of around 83% as the NNDMA-MMA copolymer. However, with more and more addition of MMA, the gap of EWC between these two kinds of copolymers becomes larger and larger. This may due to two possible reasons. MMA incorporation restricts access to the water binding sites on NNDMA, however, this may be compensated for, in part, by the formation of hydration clusters. Another possible reason is that the effect of MMA on NVP is more marked is the helical conformation of poly NVP as discussed previously.

3.2.2 Effect of Monomer Composition on FWC and Non FWC

The properties of hydrogels are influenced not only by their equilibrium water content (EWC) but also by the ratio of freezing to non-freezing water content in the polymer. The technique used to determine this property was DSC whose advantages and disadvantages were discussed in chapter 1 to determine this property. The effects of hydrophilic component on equilibrium water content, freezing water content and non-freezing water content of MMA based copolymer are displayed from Figure 3.2 to Figure 3.7.

Although expressing the water contents as percentages clearly illustrates the change in total water content and freezing water content, especially in hydrogels with a high equilibrium water content, the trend in non-freezing water can be obscured. Expressing the water content as grams of water / gram of polymer or moles of water / mole of repeat unit overcomes this problem and gives an indication of the water binding potential of a single monomer unit.

It has been shown in Figure 3.2 that equilibrium water content and freezing water content increase steadily in AMO-MMA copolymers when the amount of the hydrophilic component, AMO, increases. The same phenomenon can be observed in NVP-MMA and NNDMA-MMA copolymers. An increase in the AMO and NVP content leads to a slight increase in the non-freezing water content of the respective copolymers. The non-freezing water content of NNDMA-MMA copolymers does not change greatly when the NNDMA content increases. When these hydrophilic components increase from 40% to 50%, the equilibrium water content of AMO-MMA copolymer increases about 6%, the NNDMA-MMA copolymer increases about 3%, however, the equilibrium water content of NVP-MMA copolymer increases about 14%. From these figures, it can be seen that freezing water contents of these MMA based copolymers do not significantly change when the content of hydrophilic group, AMO, NVP and NNDMA, increases from 40% to 50%. So we can conclude that the non-freezing water content of NVP-MMA copolymers changes much more than those of AMO-MMA and NNDMA- MMA copolymers. As we have seen, non-freezing water is the water strongly associated with the polymer network through hydrogen bonding. It proves that the effect of MMA is more marked on the helical conformation of polyNVP than polyAMO.

Figures 3.3, 3.5 and 3.7 show the substantial water-binding ability that NNDMA and NVP have is over AMO. It could be possible that the sequence distribution of AMO-MMA copolymer is less advantageous to arrange the helical conformation of AMO to attract more water to polar groups via hydrogen bonding in a hydrating medium than NVP-MMA and NNDMA- MMA copolymers.

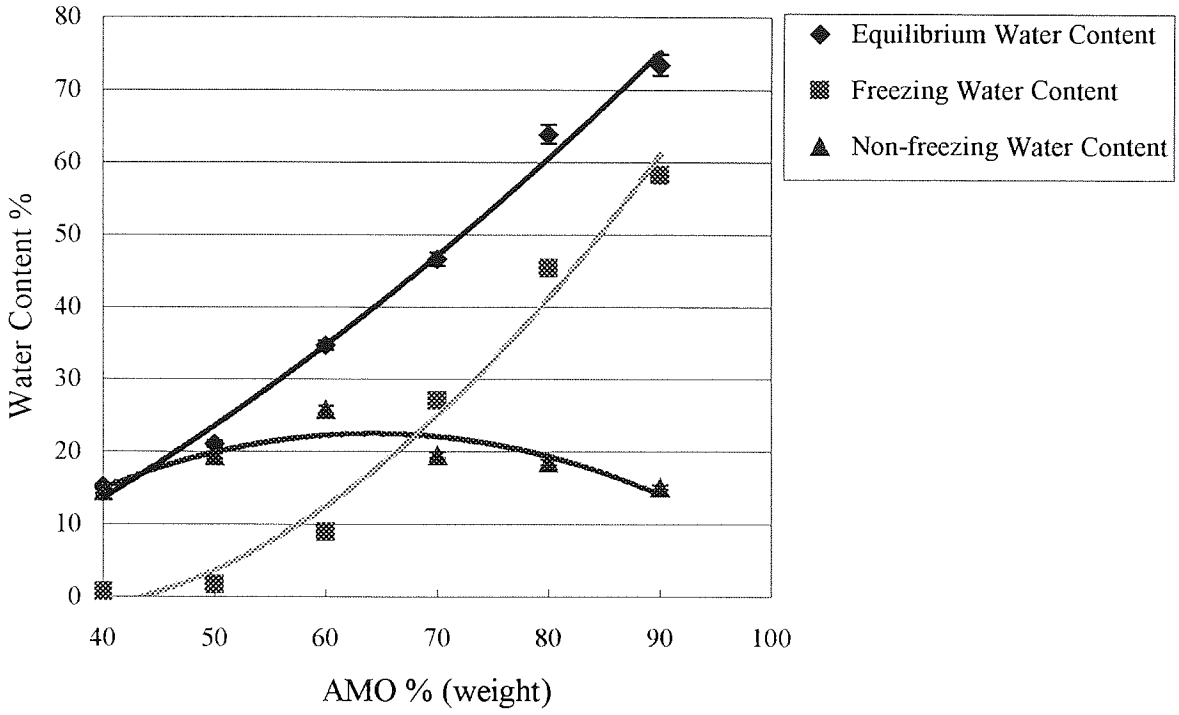

Figure 3.2 The effect of AMO content on the water contents of AMO-MMA copolymers

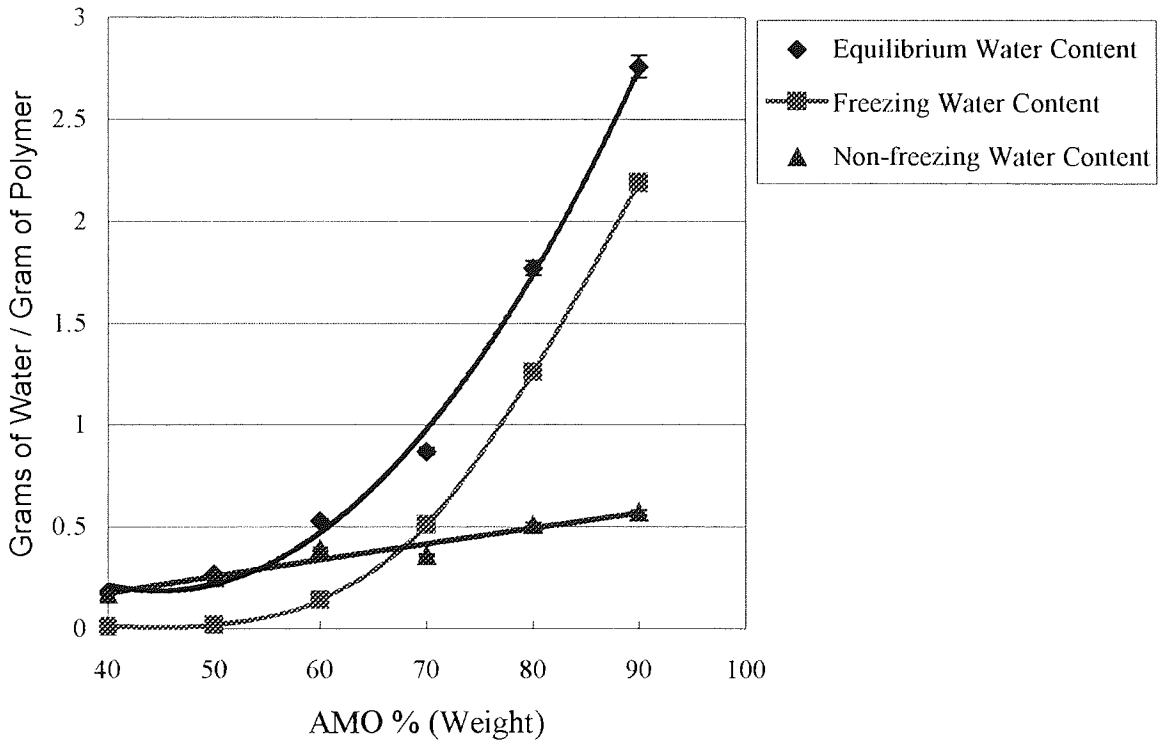

Figure 3.3 The effect of AMO content on the water binding properties of AMO-MMA copolymers

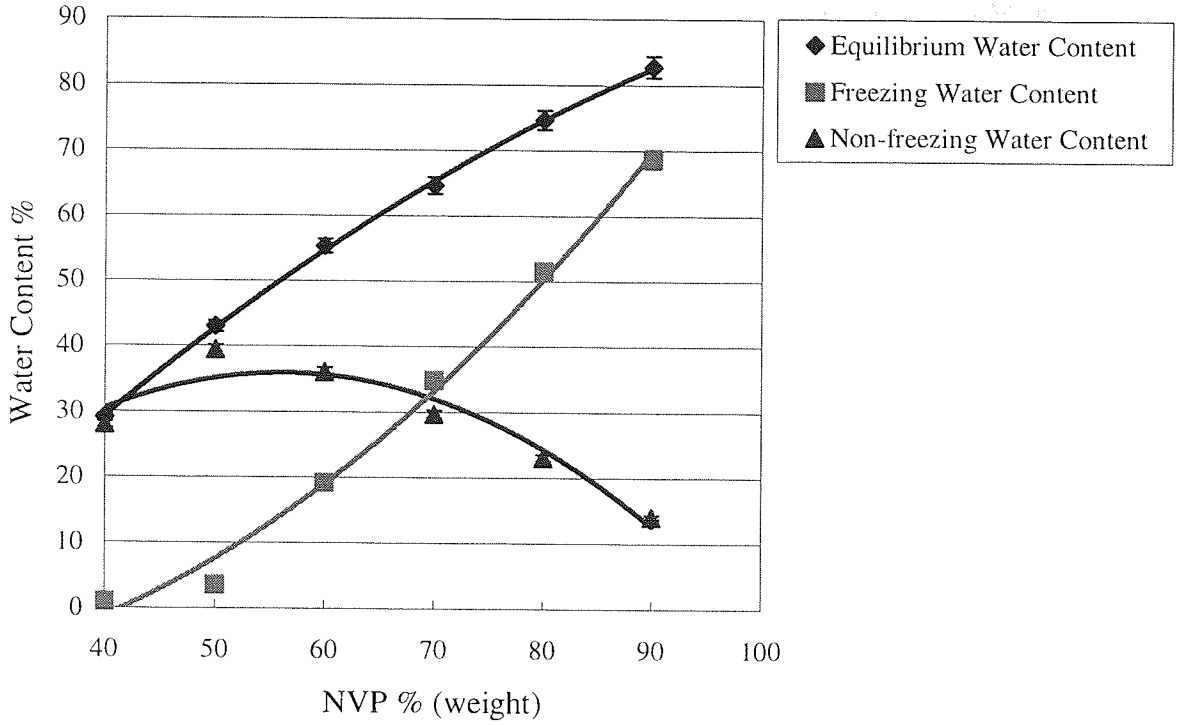

Figure 3.4 The effect of NVP content on the water content of NVP-MMA copolymers

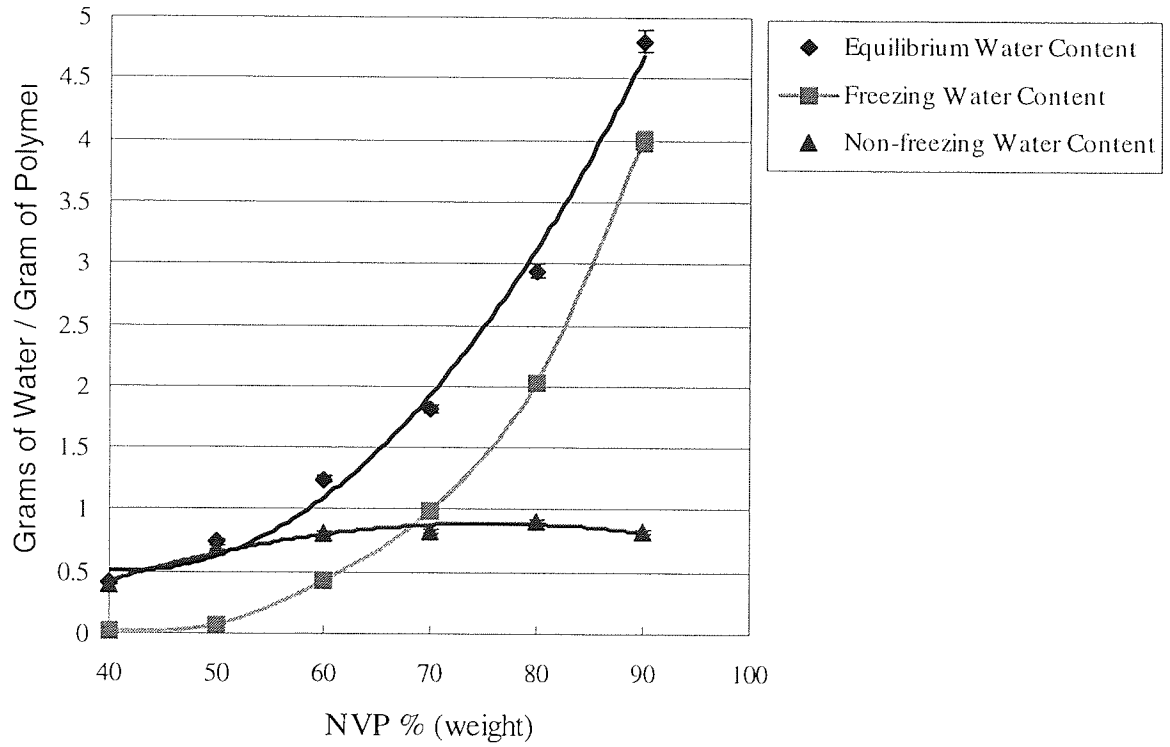

Figure 3.5 The effect of NVP content on the water binding properties of NVP-MMA copolymers

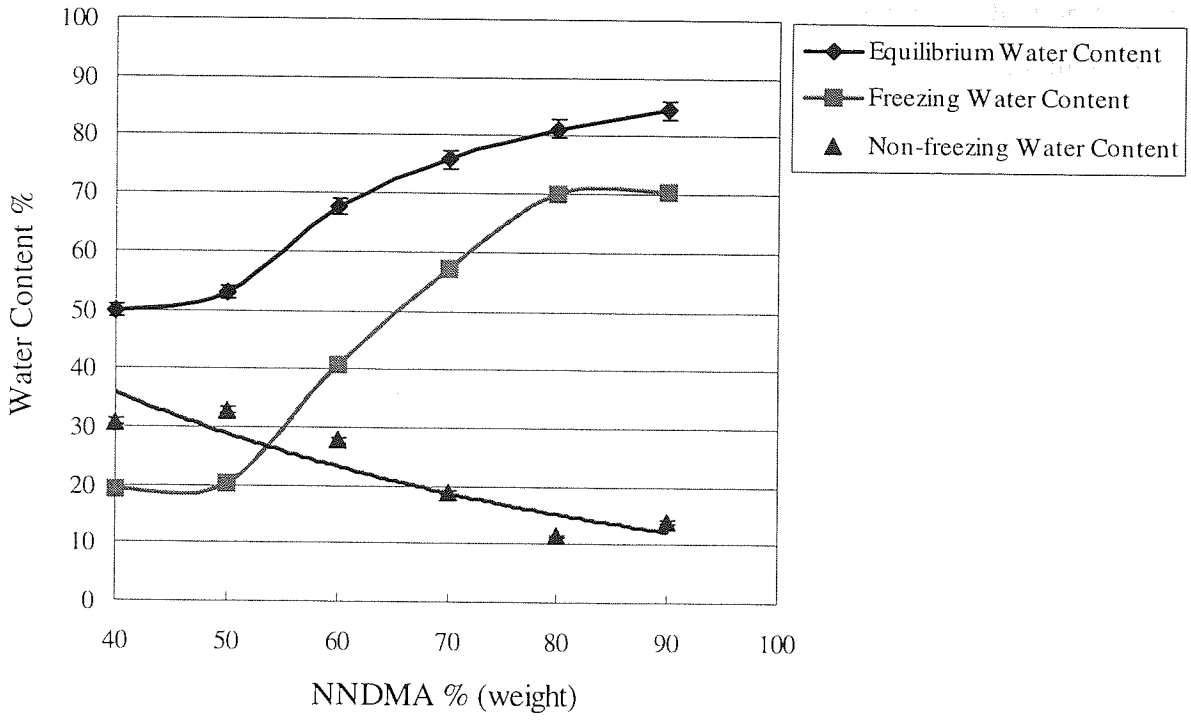

Figure 3.6 The effect of NNDMA content on water content of NNDMA-MMA copolymers

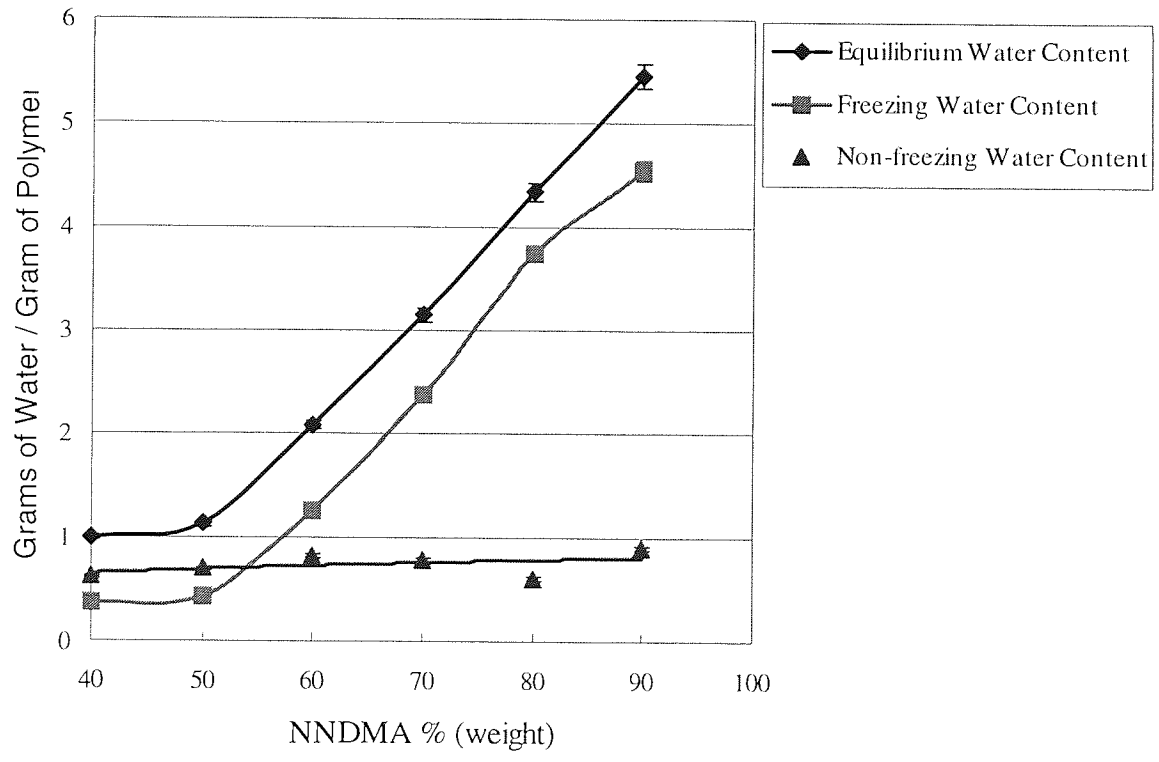

Figure 3.7 The effect of NNDMA content on the water binding properties of NNDMA-MMA copolymers

When expressing the water content as grams of water / gram of polymer, the non-freezing water content does not seem to significantly change with the increase in hydrophilic component. However, from Figure 3.2, 3.4 and 3.6, we see that the non-freezing water contents change greatly. In NNDMA-MMA copolymers, the difference between highest non-freezing water content and lowest is around 22%, from 33% to 11%. In NVP-MMA copolymers, the difference between these is about 15%, from 39% to 14%. The least difference in AMO-MMA copolymers between these two extremes of non-freezing water is about 11%, from 26% to 15%. Previous work[18, 196, 197, 198] states that in the hydrogels non-freezing water content will not change greatly even when equilibrium water content changes hugely and the non-freezing water content will not go below 18% although the different techniques used to measure the freezing water content can lead some deviations. This unusual phenomenon may be due to experimental system error because the curves of non-freezing water content displayed in the figures are all similar. The following items are the experimental system errors which possibly cause the irregular results.

1. Non-freezing water content is calculated by equilibrium water content minus freezing water content. The equilibrium water content, EWC, is measured from differences between the weight before dehydrated and after dehydrated. A small sample of the hydrated membrane sheet prepared for measuring EWC is cut with a size seven cork-borer. The sample prepared for measuring freezing water content by DSC is cut with a size one cork-borer. The difference between the diameters of these two sizes of cork borer causes the calculation error for non-freezing water content.
2. The sharpness of the rim of the core borer is an important factor in the accuracy of DSC experimental data. The minor loss of the hydrogel in the periphery of the sample will influence the result obtained from DSC.
3. Manual operation may affect the results to some extent. When the surface water is removed by filter paper, the membrane may be squeezed. Water loss may occur during the process of weighing the sample.
4. Inevitably the equipments, such as the DSC and the weight balance, have system errors themselves.

3.3 Semi-Interpenetrating Polymer Networks

The study of SIPNs has received considerable interest because most of them exhibit better mechanical properties than their individual networks, due to a synergistic effect induced by forced compatibility of the components[199].

Conventional synthetic hydrogels can be produced with a similar water content to that of biological organs, but the mechanical properties are poor. SIPNs were produced that had similar water contents and much improved mechanical properties, as they were stronger and stiffer, so mimicking more closely the natural hydrogel.

Corkhill *et al*[13] studied the use of semi-interpenetrating polymer networks (SIPNs) to enhance the mechanical properties of hydrogels for use as a synthetic articular cartilage. Evans[195] synthesized the same kind of materials for use as Keratoprosthesis (artificial cornea). In her research, she investigated the properties of a series of tetrahydrofurfuryl methacrylate (THFMA), polyurethane SIPNs, whose water contents ranged from 30% to 55%.

In the synthetic cartilage developed at Aston, cellulose acetate butyrate (CAB) was used as the interpenetrant. This produces materials with suitable mechanical properties but which are often translucent. Although this translucency is of no consequence in cartilage-related applications, if this technology were to be extended into the ocular environment optical clarity is a necessity. In order to identify an interpenetrant capable of producing suitable mechanical properties for an artificial cornea while producing optically clear materials, six different polyurethanes were investigated and compared to systems produced with CAB. Only one of the interpenetrants, an ester polyurethane (PU5), formed a clear system with AMO and THFMA[200]. Although the opaque systems may exhibit properties suitable for the porous periphery, at this stage, to eliminate complications at the join between the core and periphery it was desirable to use the same polymer constitutes. In this work, polyurethane 5 was used as the interpenetrant.

Polyurethanes (PUs) are multiblock copolymers usually consisting of hard segments and polyether or polyester soft segments. Polyurethanes have excellent mechanical properties, high elongation capacity, good abrasion resistance, high flexibility and hardness, and good

biocompatibility[201]. Their resistance to biological aggressions makes them good candidates for long-term implants. Polyurethanes are used extensively in the medical field as intravascular devices[201, 202], uretal stents[203], for meniscal reconstruction[204, 205], cartilage and bone repair[206, 207, 208, 209], and as vehicles for sustained delivery of biologically active agents.

Polyurethanes had been neglected as potential keratoprosthetic materials until Szycher[210, 211, 212] produced optically clear polyurethane from 4.4'-dicyclohexylmethane diisocyanate, poly(tetramethylene ether) glycol and ethylene oxide-capped trimethylolpropane (as a chain extender). A decade later, Pennings *et al*[213] developed transparent, highly crosslinked polyurethanes from low molecular weight polyols and hexamethylenediisocyanate (HDI). A polyurethane produced from tetrakis (2-hydroxypropyl)ethylenediamine (Quadrol) and HDI was implanted in rabbit corneas, either as discs, in three eyes, or in the form of a "champagne cork" keratoprosthesis, in one eye. No adverse reactions were observed, and at the time of reporting the keratoprosthesis had been maintained for 1 year without complications.

Heterocyclic monomers have been used in dental applications for many years[214, 215, 216, 217, 218]. Tetrahydrofurfuryl methacrylate, (THFMA), has been investigated as an alternative to PMMA in dental applications, and used in drug delivery systems that have been implanted in the cartilage of rabbits[215]. As such its biotolerance has been studied and was found to be relatively non-irritant in dental applications[216]. It is non-volatile, colourless, with a mild odour. It is miscible with the dimethacrylate oligomers in all molar fractions.

3.3.1 Effect of Monomer Composition on EWC of SIPNs

The literature values relating to the mechanical properties of the collagen cornea have caused some confusion. Papers in recent years have quoted the value of the shear modulus of the natural human cornea is 13 MPa[74]. Our initial work was based on this quoted value but the mechanical property of traditional hydrogels with high water content is much lower than this value, thus it is necessary to design and produce SIPNs hydrogels with a wide range of mechanical properties.

Based on the previous study[14], the optimum range of concentration of the ester-based polyurethane (PU5) used in SIPN is between 10% and 20% (by weight). If the

concentration of PU5 is lower than 10%, it does not contribute to enhance the mechanical properties of hydrogels significantly. If higher than 20%, it does not dissolve in the monomer solutions completely. The solvent tetrahydrofuran (THF) can be used to dissolve PU5 but it may cause chain transfer reactions, therefore decreasing the molecular weight and mechanical properties. Thus in the work described in this thesis, the concentration of PU5 is between 10% and 20% (by weight).

The interpenetrant PU5 not only gives clear compatible hydrogels, but also was found to contribute to the freezing water content. However, Corkhill[14] found some interpenetrants, such as CAB, do not affect the freezing water content. It appears that the polyurethane interpenetrant has greater molecular compatibility and behaves rather like a hydrophobic monomer, which do affect freezing water content. Thus it is useful to investigate the effect of the ratio of the hydrophilic and hydrophobic components in these three SIPNs families in various ways on the water properties. The ratios are displayed in Table 3.1

Gel ID	PU5 :AMO:THFMA (by weight)	EWC %	Hydrophilic component / (PU+THFMA)	Hydrophilic component / PU	Hydrophilic component / THFMA
J18	16.8 : 41.6 : 41.6	30.7	0.7	2.5	1.0
J19	21.8 : 41.6 : 36.6	35.8	0.7	1.9	1.1
A14	20 : 50 : 30	41.4	1.0	2.5	1.7
J1	10 : 55 : 35	44.2	1.2	5.5	1.6
J10	15 : 55 : 30	48.1	1.2	3.7	1.8
J11	10 : 60 : 30	51.1	1.5	6.0	2.0
J20	15 : 60 : 25	46.5	1.5	4.0	2.4

Gel ID	PU5 : NNDMA : THFMA (by weight)	EWC %	Hydrophilic component / (PU+THFMA)	Hydrophilic component / PU	Hydrophilic component / THFMA
J15	16.8 : 41.6 : 41.6	55.9	0.7	2.5	1.0
J16	21.8 : 41.6 : 36.6	55.2	0.7	1.9	1.1
J2	20 : 50 : 30	58.6	1.0	2.5	1.7
J3	10 : 55 : 35	70.3	1.2	5.5	1.6
J4	15 : 55 : 30	67.0	1.2	3.7	1.8
J5	10 : 60 : 30	72.6	1.5	6.0	2.0
J17	15 : 60 : 25	69.1	1.5	4.0	2.4

Table 3.1 The ratio of the hydrophilic component to hydrophobic components in various ways

Gel ID	PU5 : NVP :THFMA (by weight)	EWC %	Hydrophilic component / (PU+THFMA)	Hydrophilic component / PU	Hydrophilic component / THFMA
J12	16.8 : 41.6 : 41.6	45.9	0.7	2.5	1.0
J13	21.8 : 41.6 : 36.6	45.4	0.7	1.9	1.1
J6	20 : 50 : 30	51.3	1.0	2.5	1.7
J7	10 : 55 : 35	60.2	1.2	5.5	1.6
J8	15 : 55 : 30	58.3	1.2	3.7	1.8
J9	10 : 60 : 30	63.3	1.5	6.0	2.0
J14	15 : 60 : 25	62.1	1.5	4.0	2.4

Table 3.1 continued. The ratio of the hydrophilic component to hydrophobic components in various ways

A series of tetrahydrofurfuryl methacrylate (THFMA), polyurethane 5 (PU5) SIPNs, with N,N-dimethylacrylamide (NNDMA), acryloylmorpholine (AMO) and N-vinyl pyrrolidone (NVP) respectively were synthesized. It is shown that N,N-dimethylacrylamide (NNDMA), acryloylmorpholine (AMO) and N-vinyl pyrrolidone (NVP) are all hydrophilic monomers from the analysis of MMA based copolymers as stated above. In the section, unless otherwise stated, N,N-dimethylacrylamide (NNDMA), acryloylmorpholine (AMO) and N-vinyl pyrrolidone (NVP) are regarded as hydrophilic components.

3.3.1.1 Clear SIPNs

The equilibrium water contents of these series of SIPNs are displayed in Figure 3.8, the variation in EWC with various ratios of hydrophilic and hydrophobic components is shown.

It can be seen from Figure 3.8, that water contents increase as the amount of hydrophilic components increases. The predication stated above is proved, i.e. NNDMA, NVP and AMO are more hydrophilic than PU and THFMA. So in this thesis, PU and THFMA can be treated as the hydrophobic group together when they are used for these SIPNs. In the same composition with THFMA and PU, NNDMA SIPNs have the highest water content and AMO SIPNs have the lowest water content. So the hydrophilicity order of these three hydrophilic monomers is: NNDMA > NVP > AMO because of the steric effect arising from heterocyclic groups of AMO and NVP. It is the same conclusion as we found from the MMA based copolymers in section 3.2.

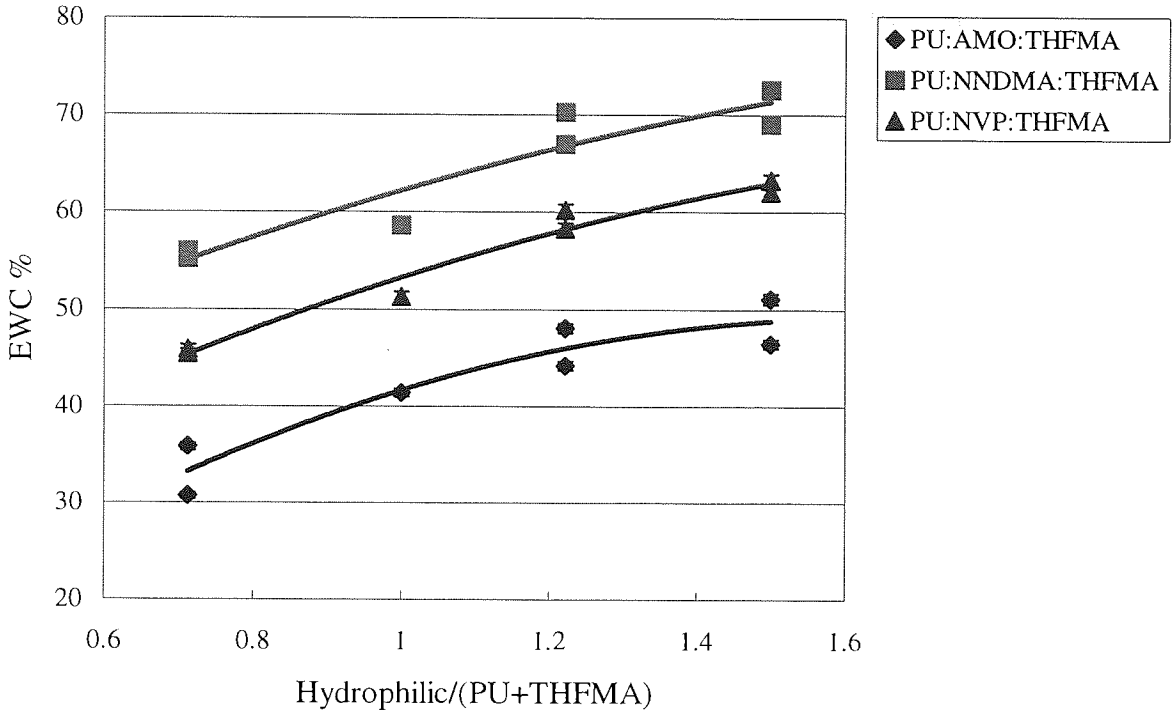

Figure 3.8 The effect of the hydrophilic component / PU+THFMA ratio on EWC (composition details shown in Table 3.1)

However, Evans[195] indicated that NVP has a similar hydrophilicity to AMO when they were copolymerised with 2-hydroxyethyl methacrylate (HEMA). This may be due to the better sequence distribution which arises by substituting NVP with AMO. Since these hydrogels formed are composed of three components, it is not easy to determine trends associated with changes in composition as more than one variable is altered.

It has been shown in Figure 3.1 and Figure 3.8 that with incorporation of 50% (by weight) NNDMA, the equilibrium water content of MMA-NNDMA copolymer (53%) is less than that of NNDMA SIPNs (59%). The same phenomenon can be found from hydrogels containing AMO or NVP. With incorporation of 50% (by weight) AMO or NVP, the equilibrium water content of MMA-AMO copolymer (21%) is much less than that of AMO SIPNs (41%). The equilibrium water content of MMA-NVP (43%) is less than that of NVP SIPNs (51%). So MMA is more hydrophobic than the combination of PU5 and THFMA. THFMA is more hydrophobic than MMA because the ring group in THFMA backbone causes more steric hindrance than the methyl group in the MMA backbone. As analysed

above, PU is more hydrophilic than THFMA. So PU is less hydrophobic than MMA. The order of hydrophilicity of these three components is: THFMA < MMA < PU5.

To obtain more information about this series of SIPNs, it is necessary to draw the graphs which describe the effect of ratio of hydrophilic components to PU and THFMA individually on the equilibrium water content (EWC).

In Figures 3.9 and 3.10, we can see that the increase in the hydrophilic component leads to an increase in the trend of equilibrium water content of these three different kinds of clear SIPNs. It indicates that the hydrophilic components, NVP, NNDMA and AMO are more hydrophilic than PU and THFMA, respectively because PU5 and THFMA have longer chains to restrict the mobility of polar groups. An increase in PU content and a corresponding decrease in THFMA results in an increase in water content, indicating that PU is more hydrophilic than THFMA because the steric effects arise from the large ring in the THFMA backbone. The water content is dependent upon the relative proportions of each of the components although the increase in the hydrophilic component causes the increase in water content.

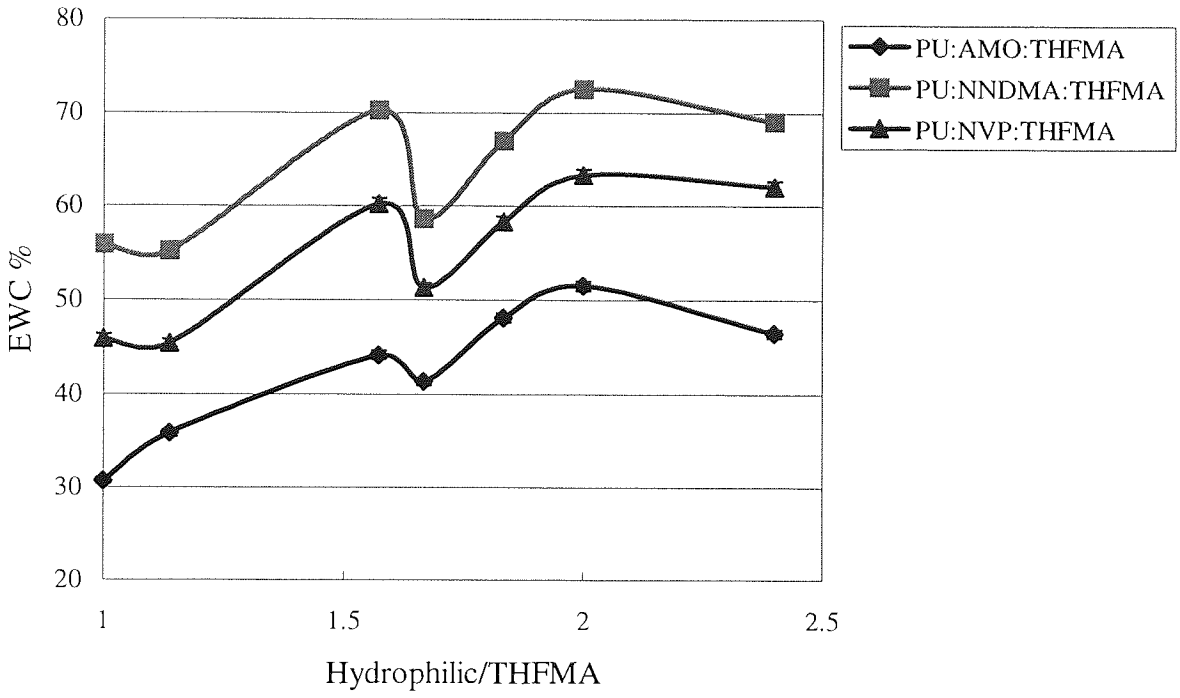

Figure 3.9 The effect of the hydrophilic component / THFMA on EWC (composition details shown in Table 3.1)

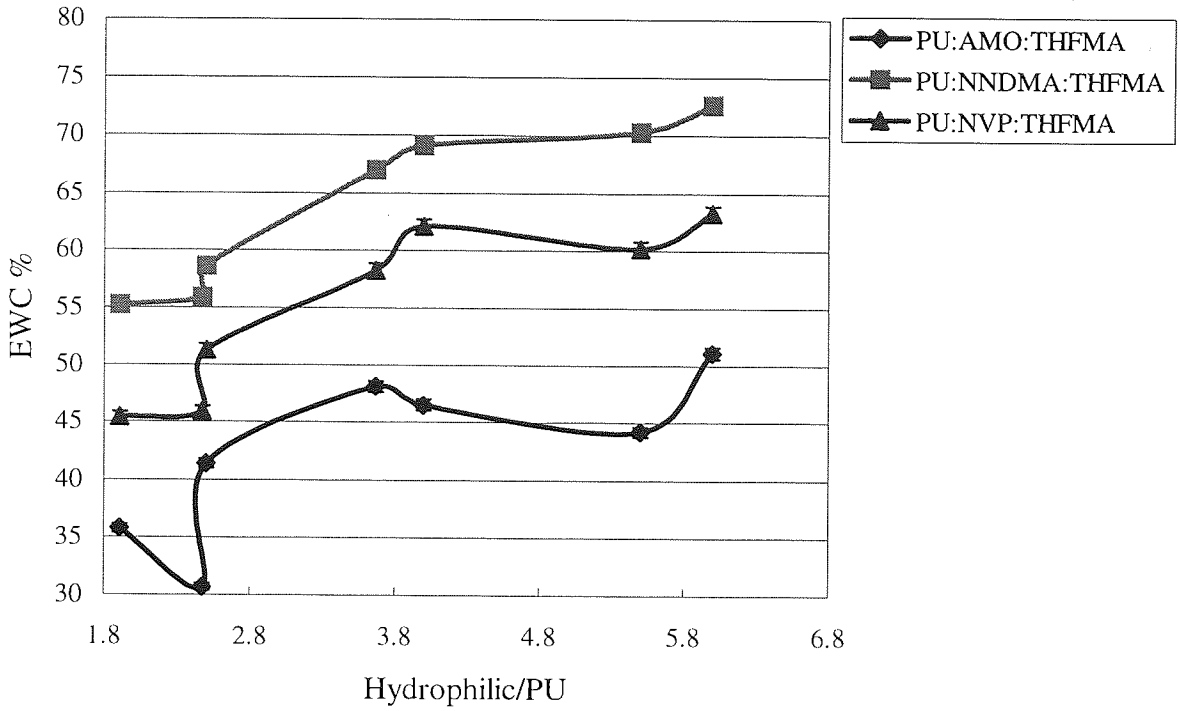

Figure 3.10 The effect of the hydrophilic component / PU on EWC (composition details shown in Table 3.1)

3.3.1.2 Porous SIPNs

The design of the "core and skirt" KPro consists of an optically clear central core, surrounded by a porous periphery. The synthetic cornea requires a porous peripheral skirt into which stromal fibroblasts (keratocytes) can penetrate coupled with an optically transparent centre and anterior surface that will either support the adherence and proliferation of corneal epithelial cells or resist substantial contamination by denatured tear component.

A major problem with the two-piece keratoprosthesis lay in the fusion between the porous peripheral materials and transparent central polymer, since they usually were quite different in their chemical nature[219]. A sound junction between the two components is easier to achieve if the materials for each portion is of the same basic material.

The use of a freeze-thaw technique (described in Chapter 2) presents interesting opportunities in biomaterials science and can be utilised to prepare membranes containing

interconnecting pores with diameters in the range 1-20 microns. Careful choice of monomers, solvents, crosslinking agents and polymerisation conditions leads to a variable and controlled distribution of pore size. Chirila's group[142, 143, 144] invented a device in which both components were made from crosslinked PHEMA, and therefore chemically identical. The skirt is made from PHEMA sponges, which were produced by phase-separation polymerisation in aqueous solution. However, these macroporous poly HEMA gels containing 5-10% crosslinking agent have mechanical properties which are quite inadequate for ophthalmic biomaterials since they are typically stiff and inflexible. There are also problems in extending the free-thaw technique to the SIPNs developed in this project. Therefore an alternative technique was developed for production of macroporous materials which utilises simple porosigen technology.

The usual polymerisation protocol was followed and in addition a water soluble porosigen of a known particle size was dispersed into mixture. A variety of porosigens have been explored, for example, NaCl, sucose, lactose and dextrin. Dextrin was found to give the best results. Polymerisation of this mixture produces SIPNs with the porosigen dispersed throughout the polymer network. The porosigen is then leached out of the network when the hydrogel is soaked in water to reach equilibrium. The porous surface can be examined using scanning electron microscopy (SEM).

A series of porous materials were synthesized with comparable compositions to the clear materials discussed above by the same method outlined in Chapter 2. The porosigens used here were dextrin and dextran.

Dextrin is an amorphous, soluble, carbohydrate with chemical formula $(C_6H_{10}O_5)n$, and is any one of a number of carbohydrates having the same general formula as starch but is a smaller and less complex molecule. They are polysaccharides and are produced as intermediate products in the hydrolysis of starch by heat, by acids, and by enzymes. Their nature and their chemical behaviour depend to a great extent on the kind of starch from which they are derived. For commercial use dextrin is prepared by heating dry starch or starch treated with acids to produce a colourless or yellowish, tasteless, odourless powder which, when mixed with water, forms a strongly adhesive paste.

Dextran has great potential as a biomaterial, but combining its properties can give a hydrogel that may be selectively enzymatically degradable but not hydrolytically degradable. Certain grades are used as blood plasma volume expanders[220]. Certain molecular weight fractions of dextran are very useful as blood plasma substitutes.

Dextrin and dextran were added on top of the 100% basic monomer mixture, as the dextran was subsequently dissolved out of the polymer along with the dextrin particles, the final material is chemically identical to the clear SIPNs. During hydration of the membranes, care must be taken to ensure that all of the porosigen is removed. With the thicker membranes required for the implantation work, however, residual porosigen may be detected if the membranes are cleaned with iodine and later observed in some of the sections under SEM[195]. Dextrin was used to produce the pores, and dextran to produce channels. The dextrin used here created pores whose size is smaller than 38 μm. The equilibrium water contents of these porous hydrogels are displayed in Figure 3.11 and Figure 3.12.

From Figures 3.11 and 3.12, we observed that the water content of porous materials with added dextrin or dextran and dextrin is similar to that of the clear materials because the small pore size of dextrin does not help to hold more water in the pore, neither do channels created by small amounts of dextran. And because dextrin and dextran do not interfere with the reaction of the monomers they were mixed with, it will not change the hydrophilicity of the hydrogels.

To improve the integration of the two components of the prosthetic devices, the core and skirt materials were made from the same basic composition. Hydrogels with very different EWC, and consequently different swelling ratios, would cause high stress at a join which would usually be formed in the dehydrated state. Therefore, it is important to be sure that the EWC of the optical core and periphery are not too dissimilar. The porous materials made from dextrin and dextran have good potential properties for the "core and skirt" KPro model because the equilibrium water contents of clear and porous materials are only slightly different. The swelling of the two components will therefore not be too different, which will minimise any effect on the junction between them.

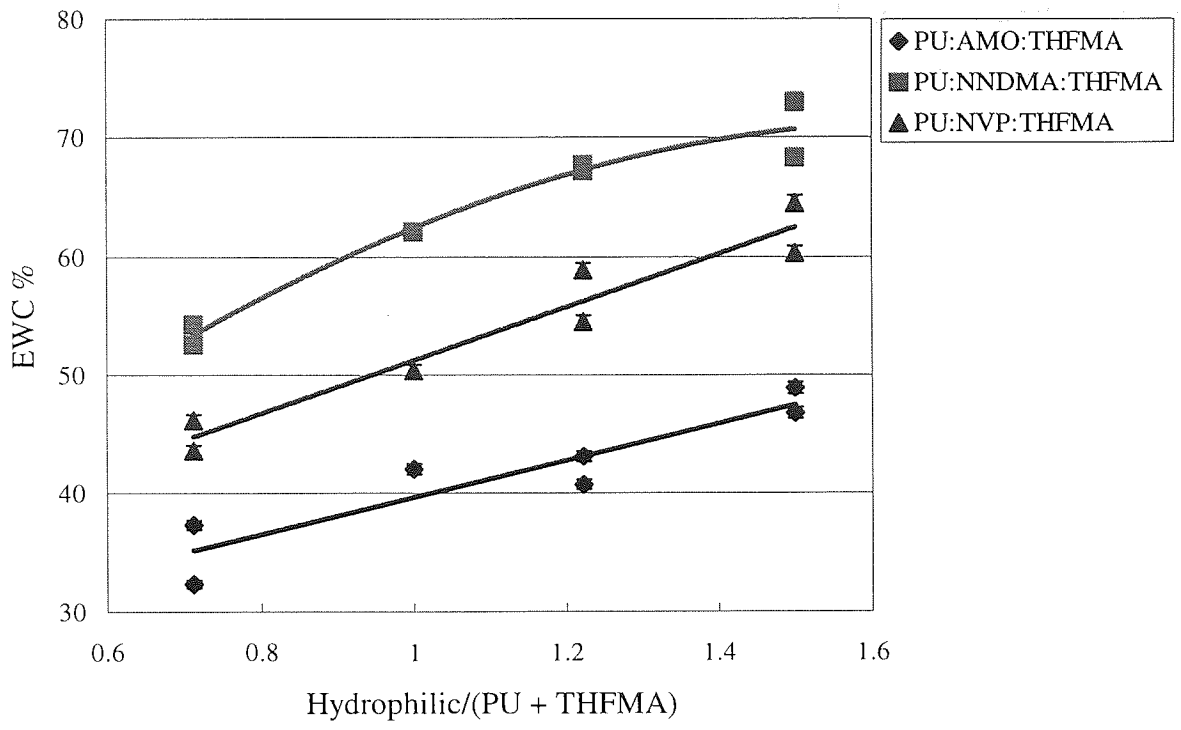

Figure 3.11 The effect of the hydrophilic components on equilibrium water content of porous (dextrin and dextran) SIPNs (composition details shown in Table 3.1)

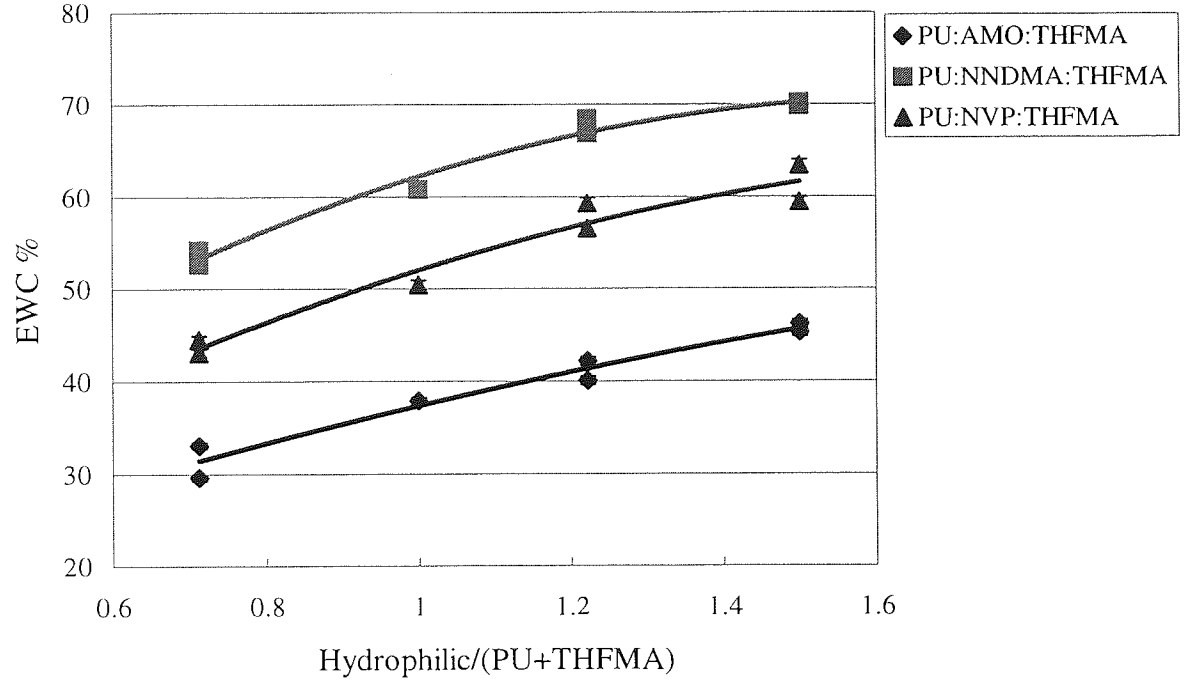

Figure 3.12 The effect of the hydrophilic components on equilibrium water content of porous (dextrin) SIPNs (composition details shown in Table 3.1)

The pore size of dextrin used in this project was smaller than 38 μm in diameter. It may encourage fibrous tissue ingrowth from the host cornea to a less extent than a larger pore size. The size of the pores is a key factor and a pore size less than 20 μm in diameter is simply too small to allow keratocyte to enter and synthesis the stromal matrix. By contrast, hydrogels with a pore size in excess of 20 μm are readily invaded by these stromal cells[137]. A detailed study of keratocyte invasion of custom-made Impra polytetrafluroethylene (PTFE) with a 50 μm pore size demonstrated a steady increase in the quantities of collagen laid down in the implanted materials and a transition toward the collagen subtypes and arrangement typical of untraumatised stroma[221]. Work previously carried out with chondrocytes at Aston[13] has shown that a pore size of 40-60 μm was preferred. In support of these findings is the work of Lee *et al*[173] whose "Seoul type KPro" (S-KPro) was implanted into 25 rabbit eyes: the results showed that rabbit fibroblasts invaded the polyurethane skirt with 40-micron pores more easily than they did in the 20-micron pore ePTFE.

So it is necessary to find an alternative porosigen which has larger pore size. Salt (NaCl) was considered to take the place of dextrin as the porosigen in this work. The salt is heated by the microwave to remove the water absorbed from the environment before being grounded by a pestle. The ground salt was then sieved using several grades of sieves, and grouped according to the pore size of networks from 38 μm to 125 μm. After sieving, the different pore sizes of salt obtained were: smaller than 38 μm, 38-63 μm, 63-90 μm, 90-125 μm and larger 125 μm. The porous hydrogels were made using the same technique as with the dextrin as stated above. The equilibrium water contents of these porous materials made from salt are displayed in the Table 3.1.

From the data obtained from J18, J2, J3, J7 and J13, it is shown that the incorporation of porosigen leads to a slight increase in the equilibrium water content. Even with a pore size between 90 μm to 125 μm, the equilibrium water content only increases by around 3%. So it can be concluded that a pore size in a certain range (smaller than 125 μm) has a minor effect on the equilibrium water content of porous materials. However, the equilibrium water content of the J10 series porous materials seems to be exception to this. With the addition of porosigen, regardless of the size of the pore the EWC does not increase but decreases. A possible explanation is that the randomly porous nature of the hydrogels causes inconsistencies in the results.

Salt as a porosigen is easier to create in several ranges of pore size. However, because the density of salt is much higher than that of the monomer solution and the salt does not disperse evenly in the monomer mixture, salt will precipitate on the bottom of the membrane which makes the surfaces of two sides of the membrane completely different, one smooth side and one coarse side although they all are chemically identical.

Gel ID	PU : AMO :THFMA (by weight)	EWC %
J10A	15 : 55 : 30	44.8
J10B	15 : 55 : 30	44.1
J10C	15 : 55 : 30	45.2
J10D	15 : 55 : 30	46.0
J10	15 : 55 : 30	48.1
J18A	16.8 : 41.6 : 41.6	31.7
J18B	16.8 : 41.6 : 41.6	30.9
J18C	16.8 : 41.6 : 41.6	33.2
J18D	16.8 : 41.6 : 41.6	33.4
J18	16.8 : 41.6 : 41.6	30.7

Gel ID	PU: NNDMA: THFMA (by weight)	EWC %
J2A	20 : 50 : 30	64.9
J2B	20 : 50 : 30	63.6
J2C	20 : 50 : 30	65.9
J2D	20 : 50 : 30	64.6
J2	20 : 50 : 30	58.6
J3A	10 : 55 : 35	71.4
J3B	10 : 55 : 35	73.0
J3C	10 : 55 : 35	73.0
J3D	10 : 55 : 35	73.2
J3	10 : 55 : 35	70.3

Gel ID	PU: NVP: THFMA (by weight)	EWC %
J7A	10 : 55 : 35	63.7
J7B	10 : 55 : 35	62.8
J7C	10 : 55 : 35	61.8
J7D	10 : 55 : 35	63.0
J7	10 : 55 : 35	60.2
J13A	21.8 : 41.6 : 36.6	46.7
J13B	21.8 : 41.6 : 36.6	45.5
J13C	21.8 : 41.6 : 36.6	45.2
J13D	21.8 : 41.6 : 36.6	48.4
J13	21.8 : 41.6 : 36.6	45.4

Table 3.2 Comparing the equilibrium water content for a series of porous materials made by salt and non-porous semi-IPN hydrogels

A: Add salt pore size between 38-63 μm 20% (by weight)

B: Add salt pore size between 63-90 μm 20% (by weight)

C: Add salt pore size between 90-125 μm 20% (by weight)

D: Add salt pore size between 38-63 μm 20% (by weight) + Dextran 4% (by weight)

Table 3.2 continued. Comparing the equilibrium water content for a series of porous materials made by salt and non-porous semi-IPN hydrogels

3.3.2 Effect of Monomer Composition on FWC and Non FWC of Clear SIPNs

The EWC of the clear SIPNs has been investigated above; it is now necessary to survey the freezing and non-freezing water contents in more detail to gain further understanding of the structure/property relationship. The effect of composition on the freezing water content and non-freezing water content is illustrated in Figures 3.13-3.18.

With the increase in hydrophilic components, AMO, NVP and NNDMA, the equilibrium water content and freezing water content increase steadily. The non-freezing water content changes slightly. From Figure 3.13 to Figure 3.15, it can be seen that the non-freezing water contents of these three series of SIPNs are all between 20% and 30%. At first glance, comparing the data obtained with MMA based hydrogels, the data for the semi-IPNs are very reasonable. However, one interesting finding is discovered. At 50% EWC, the AMO SIPN has a freezing water content of around 27% and the NVP SIPN has a freezing water content of around 23%. At 60% EWC, the NVP SIPN has a freezing water content of about 33% and the NNDMA SIPN has a freezing water content of about 34%. We can conclude that at the same EWC each of three interpenetrating network polymers has similar the freezing water content.

In contrast, at 60% EWC, the AMO-MMA copolymer has a freezing water content of 42% while the NVP-MMA and NNDMA-MMA copolymers have freezing water contents 28% and 30% respectively. Because the hydrophilicity order is NNDMA > NVP > AMO, the amount of hydrophilic component among these three copolymers is in the order: AMO > NVP > NNDMA. Therefore the order of the water binding properties of these three monomers is: NNDMA > NVP > AMO when they copolymerise with MMA. In addition,

at the same EWC AMO appears to produce polymers with much higher freezing water content than the corresponding NVP and NNDMA polymers.

Figure 3.16 to Figure 3.18 show the substantial water binding ability that NNDMA and NVP have over AMO. It is the same phenomenon shown in MMA based copolymers. The sequence distribution and conformation of the polymers are important factors in the water binding capabilities of the hydrogels because those affect the accessibility of the hydrophilic sites.

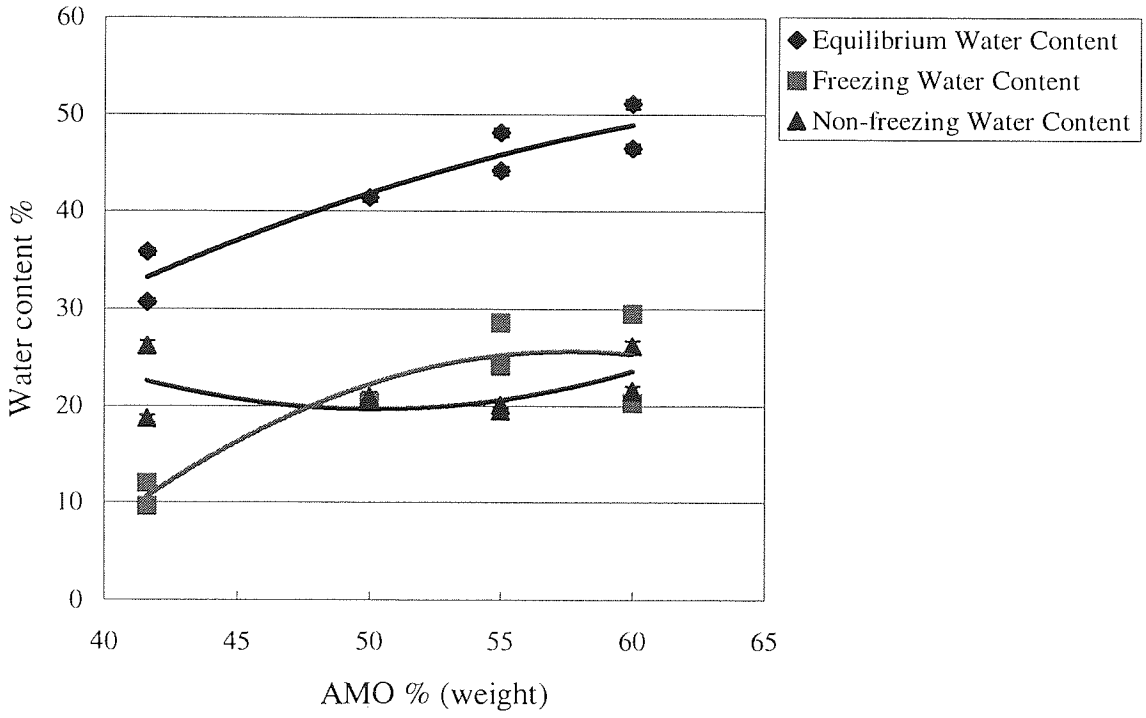

Figure 3.13 The effect of AMO content on the water content of AMO based SIPNs

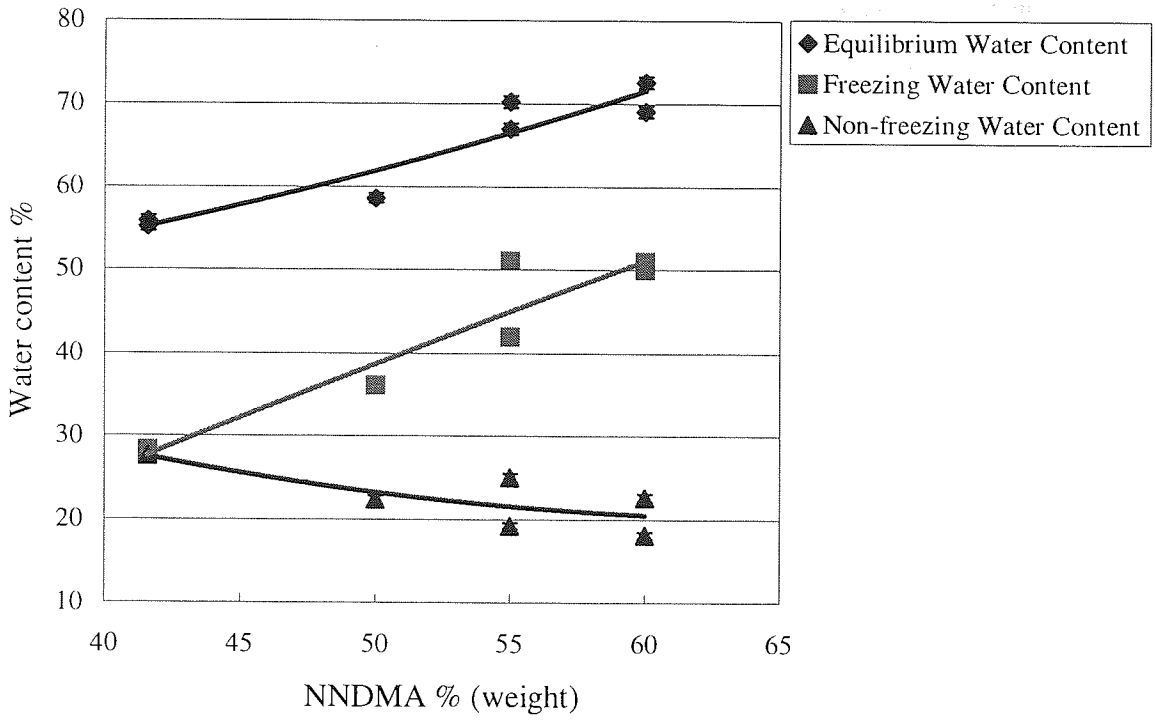

Figure 3.14 The effect of NNDMA content on water content of NNDMA SIPNs

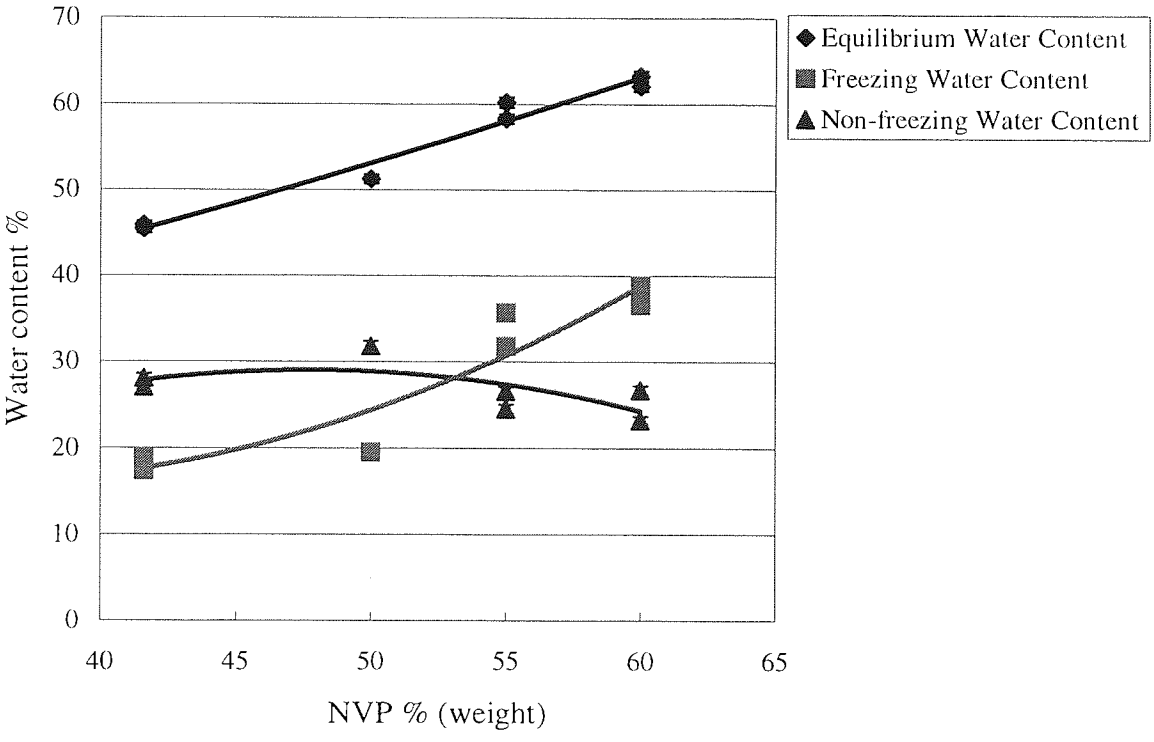

Figure 3.15 The effect of NVP content on water content of NVP based SIPNs

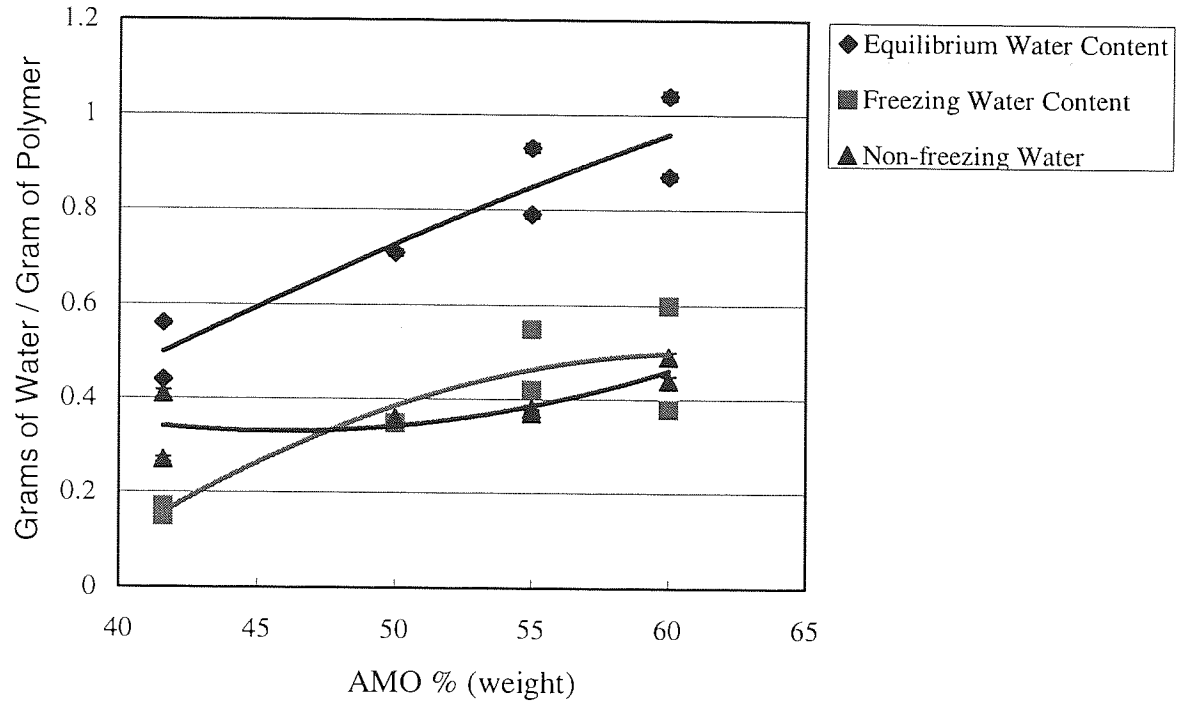

Figure 3.16 The effect of AMO content on the water binding of AMO based SIPNs

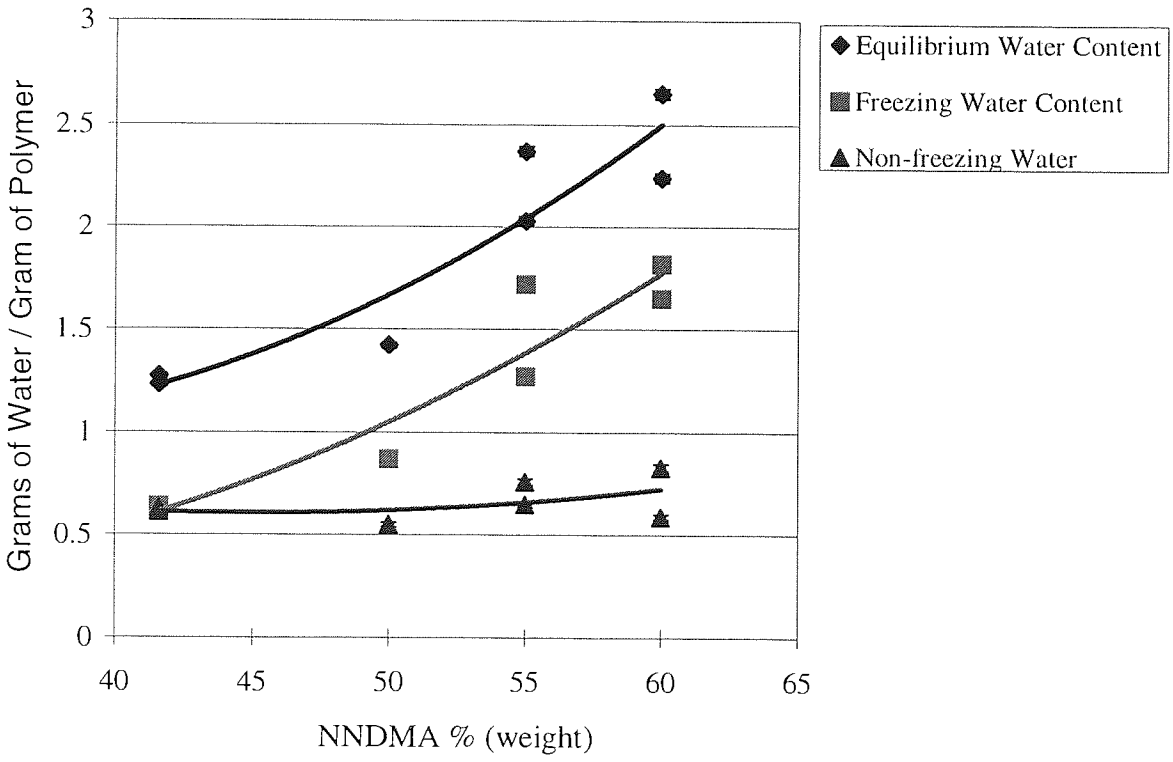

Figure 3.17 The effect of NNDMA content on water binding of NNDMA SIPNs

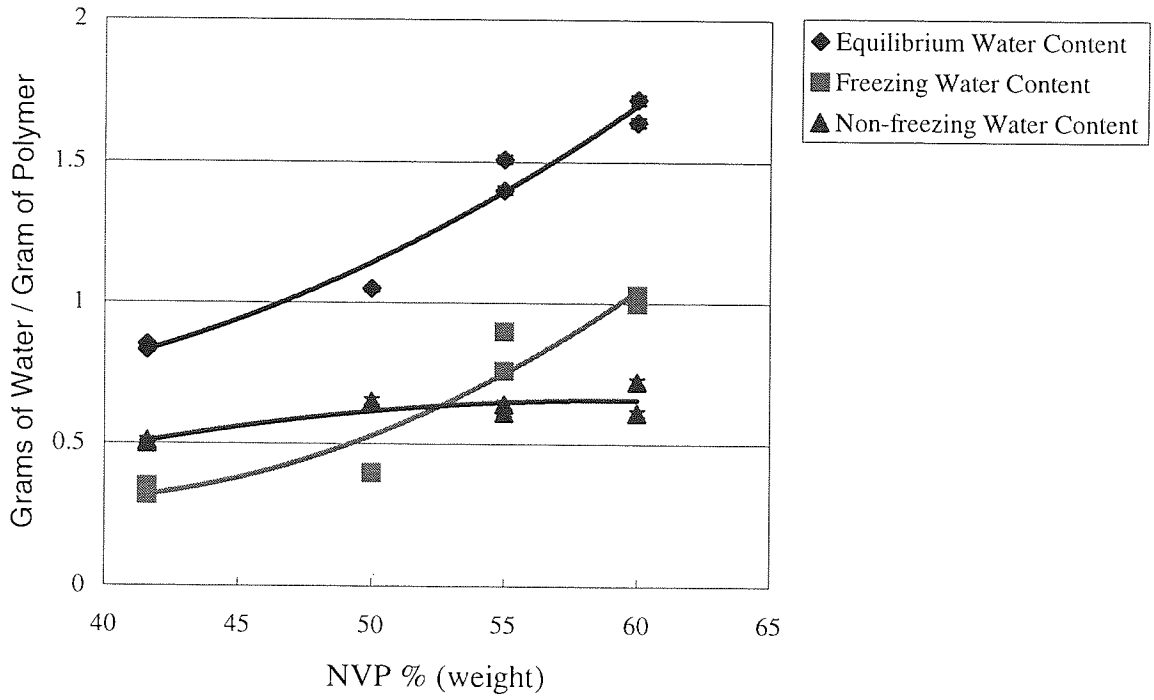

Figure 3.18 The effect of NVP content on water binding of NVP based SIPNs

3.4 Clear SIPNs with PEG MA

The current state-of-the-art in biomaterials involves the development of substrates that completely block non-specific protein adsorption but which may be additionally modified to present isolated peptide moieties to induce bioactivity[222, 223]. Polyethylene glycol (PEG) is known to effectively reduce protein deposition and cell adhesion[224]. Typically, PEG can be incorporated onto biomaterial surfaces through bulk incorporation via crosslinking[225].

The molecular weights of the polyethylene glycol monomethacrylate (PEG MA) used in this work were 200 and 440, although higher molecular weight PEG MA has been shown to reduce protein adsorption due to the more mobile and more hydrophilic surface presented, but longer chains have the consequence of increased calcium ion interaction in biological solutions[226].

3.4.1 Effect of Concentration of Crosslinker on EWC

The EWC is influenced by the nature of the monomers used, the crosslink density and the temperature, pH and tonicity of the hydrating media. The experiments in this section were designed to show the relative effect of increasing crosslink density on the equilibrium water contents of the materials. Different amounts of crosslinker were used in this experiment. One drop is equivalent to about 0.02g ethylene glycol dimethacrylate (EGDMA). The EWC of these materials were measured and the results are displayed in the Table 3.3 and Figure 3.19

In the case of all three hydrophilic monomers (NVP, AMO and NNDMA), a similar progressive effect of the crosslinking agent EGDMA is observed on the water content of the gel. It is shown than the equilibrium water content decreases with the increase in amount of crosslinker. The increase in amount of crosslinker leads to an increase in the crosslink density of the hydrogels, thereby restricting the mobility of the hydrogel chains, so reducing swelling in water.

Gel ID	PU5: AMO : THFMA = 10 : 55 : 35	EWC%
J1A	1 Drop Crosslinker (EGDMA)	49.0
J1B	2 Drop Crosslinker (EGDMA)	45.3
J1C	3 Drop Crosslinker (EGDMA)	43.3
J1D	4 Drop Crosslinker (EGDMA)	42.2
J1E	5 Drop Crosslinker (EGDMA)	40.5

Gel ID	PU5: NNDMA : THFMA = 10 : 55 : 35	EWC%
J3A	1 Drop Crosslinker (EGDMA)	77.2
J3B	2 Drop Crosslinker (EGDMA)	74.2
J3C	3 Drop Crosslinker (EGDMA)	71.5
J3D	4 Drop Crosslinker (EGDMA)	68.5
J3E	5 Drop Crosslinker (EGDMA)	65.9

Gel ID	PU5 : NVP : THFMA = 10 : 55 : 35	EWC%
J7A	1 Drop Crosslinker (EGDMA)	68.0
J7B	2 Drop Crosslinker (EGDMA)	66.2
J7C	3 Drop Crosslinker (EGDMA)	62.7
J7D	4 Drop Crosslinker (EGDMA)	61.1
J7E	5 Drop Crosslinker (EGDMA)	57.3

Table 3.3 Comparing equilibrium water content with different content of crosslinker

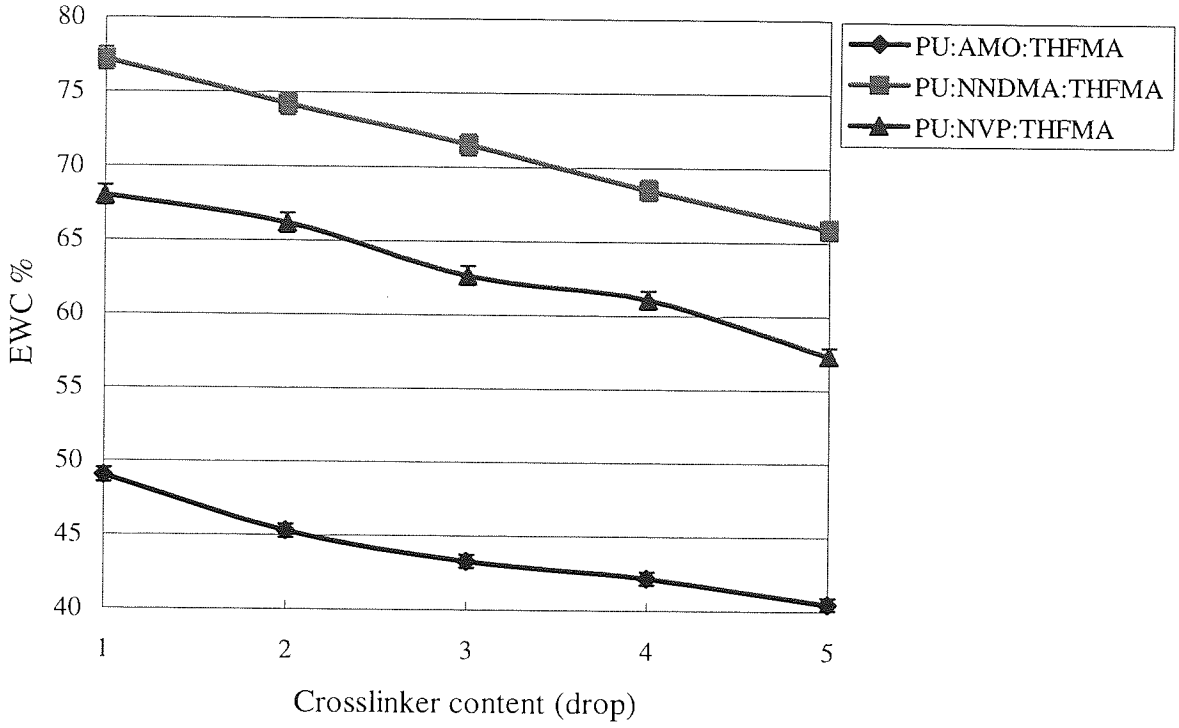

Figure 3.19 The effect of crosslinker content on equilibrium water content of hydrogels

3.4.2 Effect of PEG MA on EWC

Polyethylene glycol monomethacrylate (PEG MA) can be used as an alternative crosslinker to EDGMA since its structure also allows three-dimensional networks to be formed. A number of clear SIPNs were synthesized with PEG MA and/or ethylene glycol dimethacrylate as the crosslinker to compare the effect of PEG MA on EWC with that of EDGMA.

This information was required to assess the effect that difunctional (i.e. dimethacrylate) impurity would have on the PEG monomethacrylate used.

Because addition of the PEG MA has a dissimilar effect on the gels formed from these three hydrophilic monomers (in contrast to the effect found with EGDMA), it is reasonable to assume that there is a difference in the relative hydrophilicity of the PEG methacrylate used and each of the three monomers.

Gel ID		EWC%
J30B	PU5 : AMO : THFMA = 10 : 55 : 35	55.2
J33B	PU5 : NNDMA : THFMA = 10 : 55 : 35	76.6
J36B	PU5 : NVP : THFMA = 10 : 55 : 35	70.0

No EGDMA, Add PEG MA (440) 5% by weight

Gel ID		EWC%
J30	PU5 : AMO : THFMA = 10 : 55 : 35	47.8
J33	PU5 : NNDMA : THFMA = 10 : 55 : 35	71.5
J36	PU5 : NVP : THFMA = 10 : 55 : 35	63.8

1% EGDMA, Add PEG MA (440) 5% by weight

Table 3.4 Comparing the effect of EGDMA and/or PEG MA on the equilibrium water content

Thus, by comparing these results as above (Table 3.3 and 3.4), PEG MA is more hydrophilic than AMO, PEG MA is less hydrophilic than NNDMA and PEG MA is more hydrophilic than NVP. For NNDMA, the effect of 5% PEG MA on EWC is greater than 1 drop of crosslinker (EDGMA). For NVP, the effect of 5% PEG MA on EWC is less than 1 drop of crosslinker (EDGMA). If PEG MA is just as hydrophilic as NVP and NNDMA, the effect of 5% PEG MA as crosslinker on EWC would be the same as 1 drop of crosslinker (EDGMA). It appears that the PEG MA does contain a small amount of cross-linking agent

3.4.3 Test for MAA

The aim of this test is to determine if the PEG MA is contaminated with methacrylic acid (MAA). Methacrylic acid as an impurity can affect the water content and other properties of hydrogels made from it. It has already been demonstrated that very small amounts of MAA present in polyHEMA will affect the concentrations of protein adsorbed from the surrounding solution[46]. In particular it has been shown that FDA Group IV contact lens materials (high EWC, anionic), containing no more than 5% MAA increase the adsorption of the small positively charged tear protein, lysozyme, quite considerably[227].

A sample of each copolymer containing PEG MA was soaked in 1% sodium bicarbonate solution for one hour in order to fully ionise the carboxyl group and then transferred to saline or distilled water. If the water content of the hydrogel is increased after treatment, it

proves that small amounts of methacrylic acid are present in the polymer. The results are displayed in the following Table 3.5:

Gel ID		EWC%
J30A	PU : AMO : THFMA = 10 : 55 : 35	48.8
J33A	PU : NNDMA : THFMA = 10 : 55 : 35	71.6
J36A	PU : NVP : THFMA = 10 : 55 : 35	63.2

1% Crosslinker, PEG MA (440) 5%

Soak in 1% sodium bicarbonate solution for 1hour

Table 3.5 Equilibrium water content of hydrogels after being soaked in sodium bicarbonate solution for 1hour

Comparing the data in Table 3.4 with the data in Table 3.5, the EWC of the hydrogels has not changed. Therefore there is no appreciable MAA contamination in these hydrogels. This demonstrates that PEG MA (440) is not contaminated with MAA.

3.4.4 Effect of PEG MA on Equilibrium Water Content of Clear SIPNs

5%, 10% and 20% Polyethylene glycol monomethacrylate (PEG MA) were incorporated in the clear SIPNs as above. All contain 1% EDGMA crosslinker (3 drops). The equilibrium water contents of these materials are displayed from Figure 3.20 to Figure 3.22.

With the incorporation of PEG MA, the EWC of AMO SIPNs and NVP SIPNs increase steadily but the EWC of NNDMA SIPNs does not significantly change. Because the PEG MA is more hydrophilic than AMO and NVP but more hydrophobic than NNDMA as analysed above, the hydrophilicity of PEG MA does have some effect on the EWC of AMO and NVP SIPNs and has a minor effect on the EWC of NNDMA SIPNs. Although the incorporation of PEG MA leads to the increase in crosslink density, thereby reducing the EWC, the hydrophilicity of PEG MA can offset and even exceed this impact.

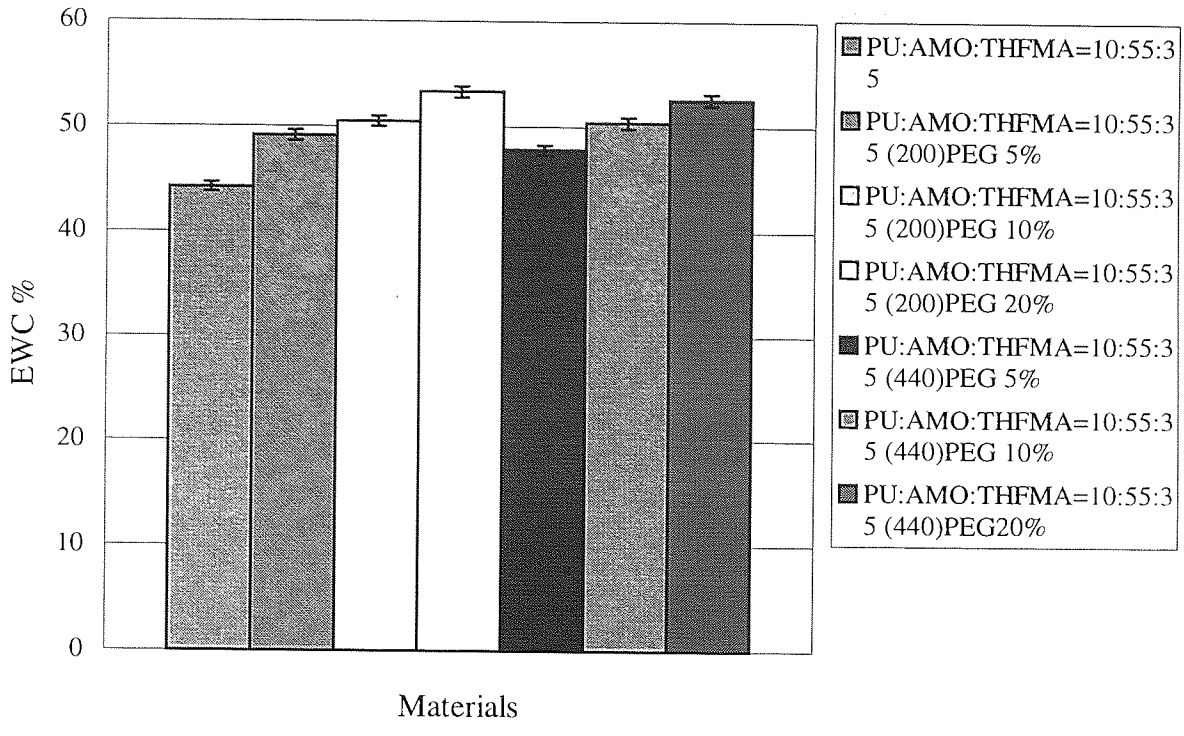

Figure 3.20 The comparison of EWC of AMO based SIPNs with and without PEG MA

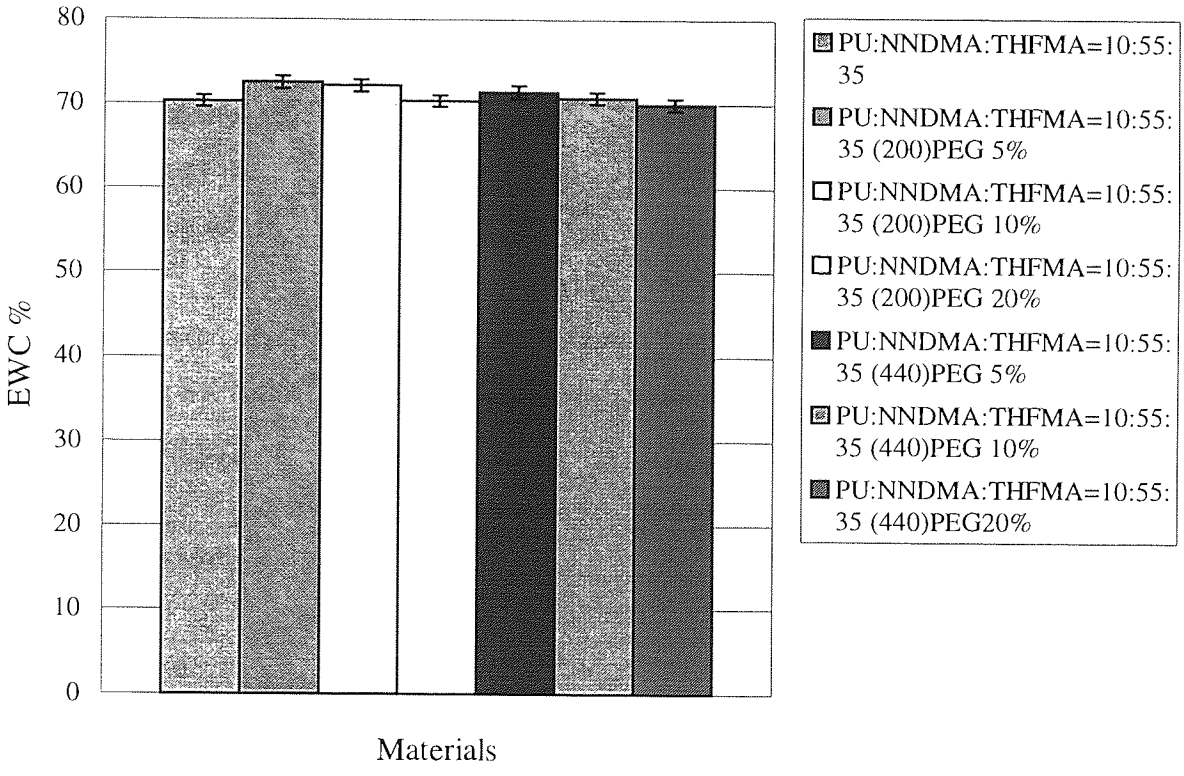

Figure 3.21 The comparison of EWC of NNDMA based SIPNs with and without PEG MA

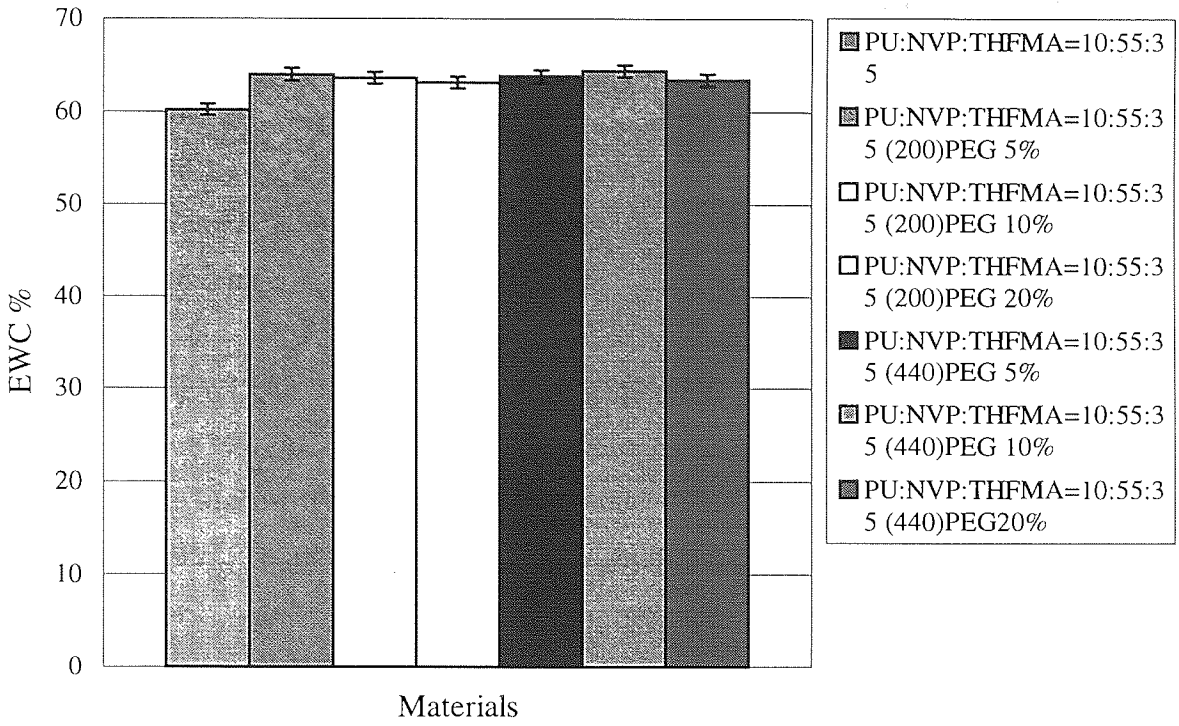

Figure 3.22 The comparison of EWC of NVP based SIPNs with and without PEG MA

In AMO SIPNs, the increase in the PEG MA contents leads to the increase in the EWC. However, for NNDMA and NVP SIPNs, it does not change significantly with the increase in PEG MA content. The effect of hydrophilicity of PEG MA on EWC in NNDMA and NVP copolymers is offset by the effect of increased crosslink density with the incorporation of PEG, thereby reducing the EWC.

The difference in chain length of the two PEG MA does not affect the EWC greatly in these three kinds of SIPNs because the difference of chain length between these two weights of PEG MA is not large enough to affect the EWC.

3.5 Conclusions

The water binding properties of a range of copolymers and semi-interpenetrating network polymers, with a wide range of EWC have been examined. The balance of hydrophilicity / hydrophobicity in the hydrogel, the crosslink density and, in particular, the steric and polar contributions of backbone substituents clearly influence the EWC and water binding properties.

The hydrophilicity order of the monomers used in this work is: NNDMA > PEG MA > NVP > AMO > PU5 > MMA > THFMA. Increasing the proportion of hydrophilic monomer in both copolymers and semi-interpenetrating networks increases the value of the EWC as would be expected, and also increases the value of the freezing water content. The order of water binding properties is: NNDMA > NVP > AMO. The non-freezing water content tends to remain at the same level.

The highest EWC of the MMA based copolymer synthesized in this work was approximately 83%. High water content hydrogels can also be created using the SIPN technique. The highest EWC of the SIPNs produced was 73%. The natural cornea contains about 81% water, so these hydrogels have good potential as the suitable material for keratoprosthesis.

Porous SIPN hydrogels were made for a potential skirt material by adding porosigens. Two different porosigens, dextrin and salt were employed and several ranges of pore sizes of salt were used to create the different pore sizes in the porous hydrogels. The incorporation of porosigen only slightly increases the EWC of porous hydrogels compared to the clear materials having the same chemical composition. Dextrin produced polymers with too small pore size and the high density of salt can lead to precipitation at the underside of the membrane so as to create two completely different surfaces of the membrane. Other porosigens should therefore be considered for the continuation of this project.

In order to reduce protein deposition on the surface of the hydrogel, PEG MA was incorporated onto SIPN surfaces through bulk incorporation via crosslinking. PEG MA contains a little crosslinking agent, so PEG MA can be used as a crosslinker to add to the crosslink density. On the other hand, PEG MA is also a hydrophilic monomer. The incorporation of PEG into AMO and NVP SIPN does lead to the increase in the EWC but will not affect the EWC of NNDMA SIPN. The chain length of PEG MA (200) and PEG MA (440) has little effect on the EWC of hydrogel.

Chapter 4

Mechanical Properties Of Novel Hydrogels

4.1 Introduction

An important consideration when selecting a material for use as a keratoprosthesis is the mechanical strength of the polymer. The hydrogel for use in this application must be able to withstand the stresses involved in the surgical procedure involved with the KPro and the *in situ* stresses such as the deforming force of the eyelid during the blink cycle.

It is not surprising that with higher equilibrium water contents, mechanical properties will suffer, but although water content has a marked effect on mechanical strength, the chemical structure of the polymer can also play a large part in determining its value. The strength and to a lesser extent the modulus depend upon the molecular weight of the polymers. The elastic behaviour and rigidity of the materials will be governed by monomer structure and crosslink density, polar and steric interchain forces.

The mechanical properties of hydrogel polymers are not easy to measure. The very act of deformation involved in such testing causes a redistribution of the water in the sample and so the properties of the sample at the end of the test will not be identical to those of the untested hydrated polymer. Nonetheless, such measurements are made and give useful comparative information. We have, in previous work[49], constructed test cells which enabled tensile testing to be carried out with complete immersion in the appropriate aqueous medium. Perhaps surprisingly, the form of the tensile stress-strain curves produced did not show appreciable differences from measurements made in air, provided sufficient speed and care were taken to prevent premature dehydration of the sample.

The EWC of the hydrogels synthesized for a potential keratoprosthesis in the work described in this thesis has been discussed in Chapter 3. This chapter mainly investigates the mechanical properties of these hydrogels. Results for tensile strength (Ts), Young's modulus (E.Mod) and elongation at break (Eb) of each series of hydrogels are illustrated graphically and numerical values are presented in Appendix 2.

4.1.1 Experimental Measurement Error

As stated in Chapter 2, the stress–strain curve like that shown by Figure 4.1 can be constructed by subjecting the specimen to a tensile force applied at a uniform rate and

measuring the resulting deformation. The shape of such a curve is dependent on the rate of testing. The initial portion of the curve is linear and the elastic modulus is obtained from its slope. In the work described in this thesis, the mechanical properties of the hydrogel samples were investigated using a Hounsfield Hti tensometer which was interfaced to an IBM 55SX computer and the results were calculated by the program installed on this computer.

However, because the tangent made for the calculation of elastic modulus by computer sometimes departs from the slope (shown in Figure 4.1), the value of elastic modulus calculated by the program automatically is not correct. Therefore, it is necessary to make the correction. A tangent is drawn manually and the elastic modulus can be calculated by the following equation:

$$\text{Elastic modulus} = \frac{Y/(T \times W)}{X/8} \qquad (4.1)$$

Where: X, Y = The intercepts on the X and Y axis, respectively
T = Thickness of the sample (mm)
W = Width of the sample (mm)
8mm is the gauge length of the sample

The results obtained from this equation may not be as precise as those obtained from the computer, but has the advantage that minor experimental error can be reduced. In this work, all graphs were checked and modified if their tangents departed from the slope.

4.2 MMA Based Copolymer Clear Hydrogels

The mechanical properties of the same MMA based copolymers as described in Chapter 3 were measured by the technique described in Chapter 2 and the results are displayed graphically from Figure 4.2 to Figure 4.10. This section attempts to illustrate in turn the effect of monomer composition, equilibrium water content and freezing water content, on the mechanical properties of the MMA based copolymers.

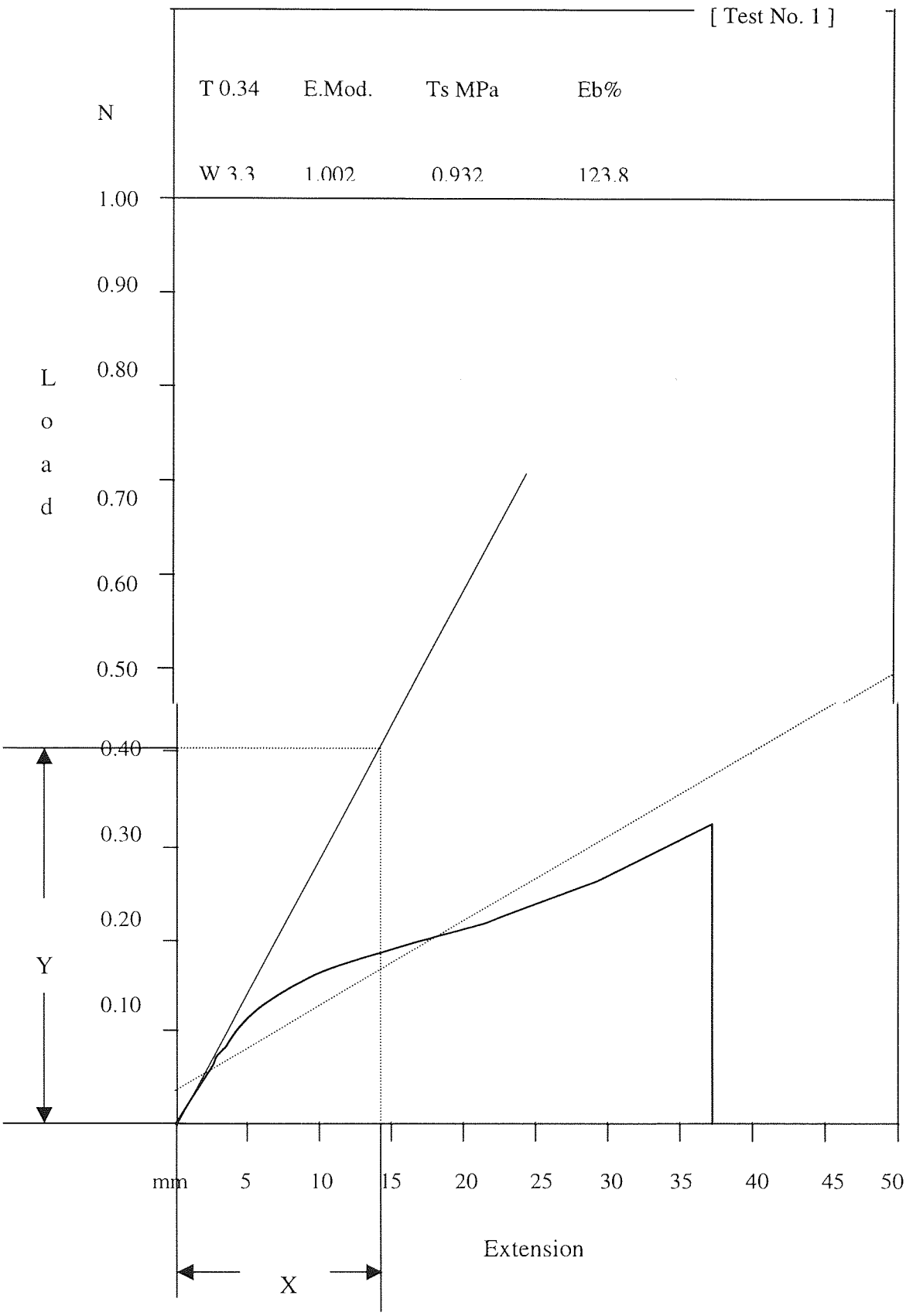

Figure 4.1 An example of the correction on the elastic modulus of the hydrogel

4.2.1 Effect of Monomer Composition on Mechanical Properties

The effect of incorporation of the hydrophobic monomer methyl methacrylate on the mechanical properties of three series of copolymers, AMO-MMA, NVP-MMA and NNDMA-MMA, is illustrated in from Figure 4.2 to Figure 4.3.

An increase in the concentration of MMA leads to an increase of both tensile strength and elastic modulus for the AMO-MMA and NVP-MMA copolymers but has no obvious effect on the NNDMA-MMA copolymers. At concentrations of MMA less than 40%, the values of the elastic modulus for the AMO-MMA and NVP-MMA copolymers are all quite low (less than 0.5 MPa) and do not change greatly with the increase in concentration of MMA. However, a massive increase occurs with increasing concentration of MMA above 40%. The elastic modulus of the AMO-MMA copolymers even reaches and exceeds 300 MPa with the addition of 60% MMA (by weight).

The elastic modulus is a measure of the stiffness of the polymer, which can be related to the chain mobility of the network. So with the addition of the heterocyclic ring contained in NVP and AMO, there is less rotation about the carbon backbone due to the increase in steric interaction because of the large ring, thereby increasing the elastic modulus.

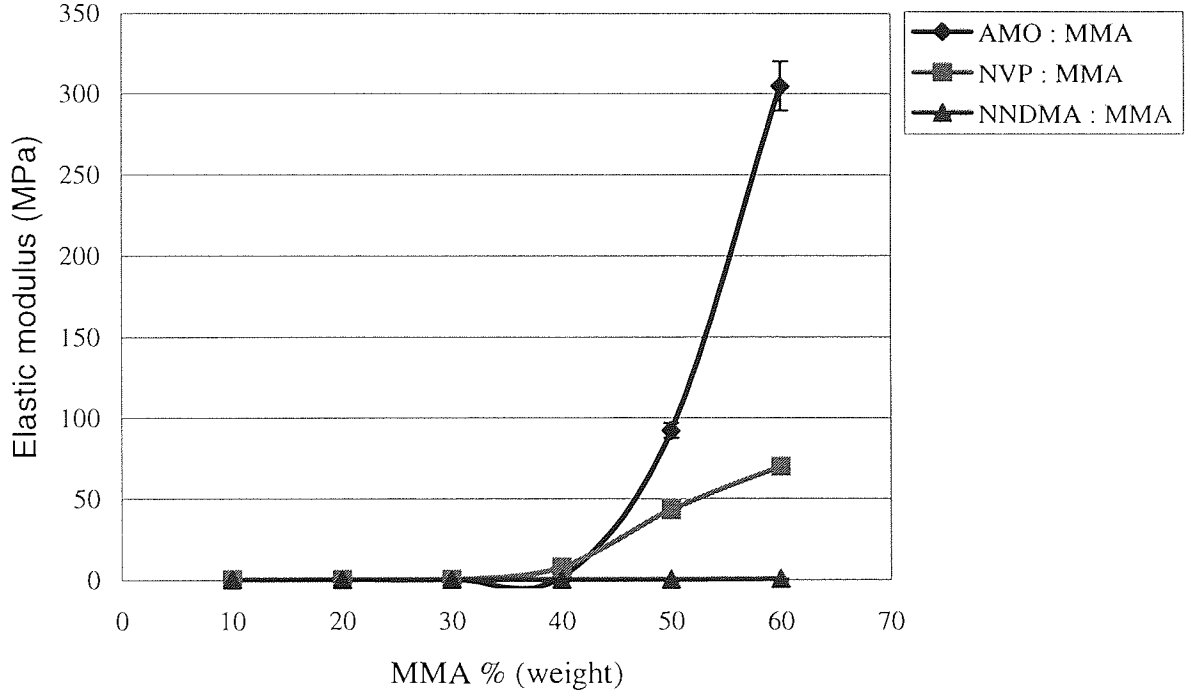

Figure 4.2 The effect of MMA content on the elastic modulus of MMA copolymers

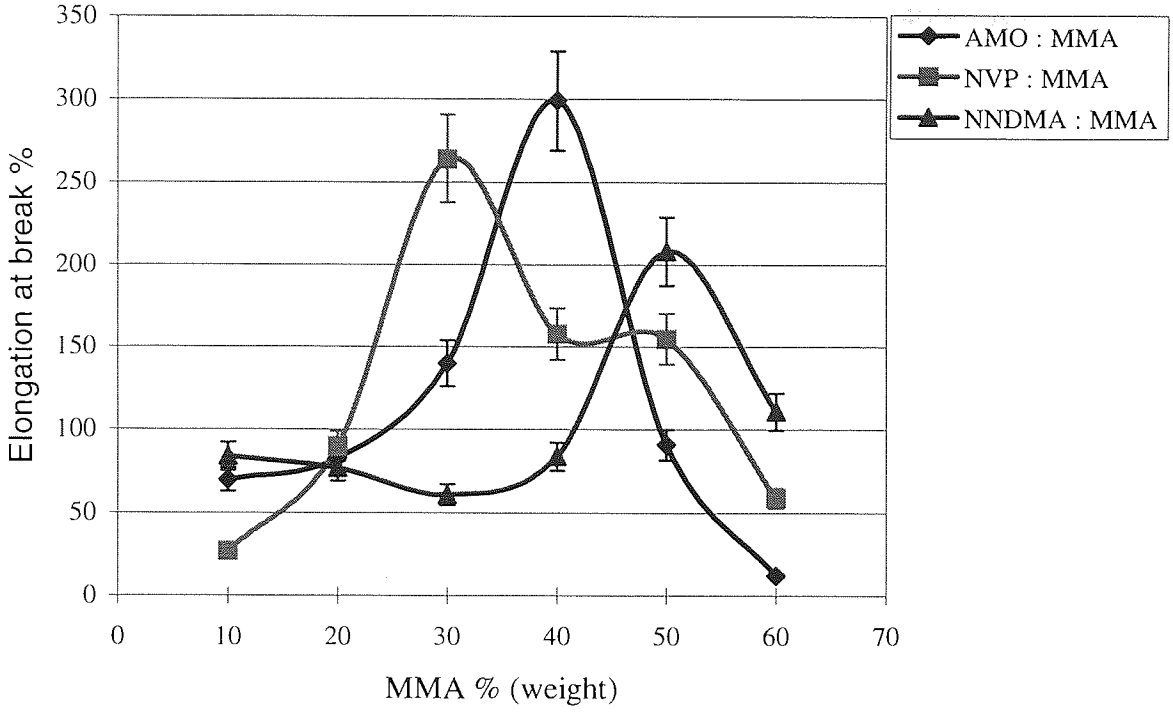

Figure 4.3 The effect of MMA content on the elongation at break of MMA copolymers

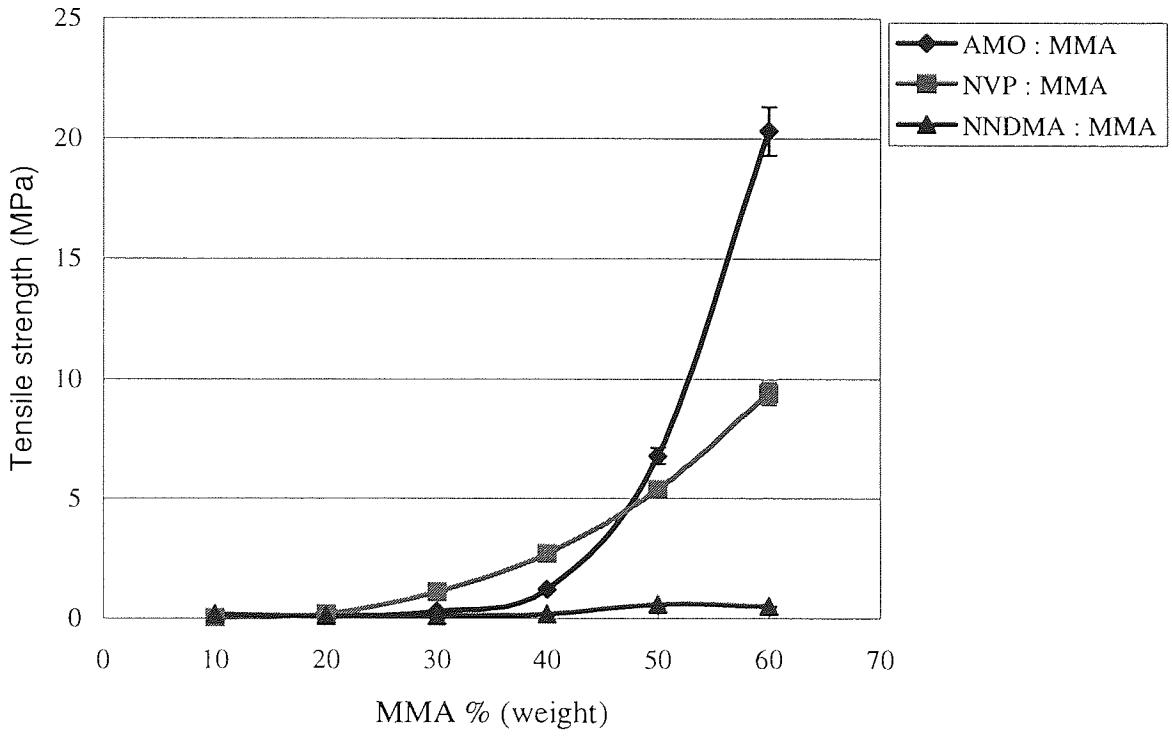

Figure 4.4 The effect of MMA content on the tensile strength of MMA copolymers

The tensile strength of AMO-MMA copolymer increases steadily with the increase in the concentration of MMA after the concentration of MMA is more than 40%. And for NVP-MMA copolymer the same phenomenon turns up when the concentration of MMA is more than 20%. The highest value of tensile strength of AMO-MMA is over 20 MPa.

For NNDMA-MMA copolymer, the elastic modulus and tensile strength are quite low and change only slightly even with a change in concentration of MMA from 10% to 60%. A likely reason for this difference with NNDMA is that the readily abstractable hydrogens on the methyl groups lead to chain transfer during polymerisation, which manifests itself in imperfect and mechanically weak networks and produces polymers with a low tear strength.

With the increase in concentration of MMA, the elongation at break of these three kinds of copolymers increases steadily to a maximum value firstly and then decreases. The maximum value appears with the addition of 30% MMA for the NVP-MMA copolymers, 40% MMA for AMO-MMA copolymers and 50% MMA for NNDMA-MMA copolymers. In the range between 10% MMA and 40% MMA, the elongation at break of NNDMA-MMA copolymer changes slightly with the increase of the concentration of MMA.

It is shown from Figure 4.2 to Figure 4.4 that an obvious transition in mechanical properties of NVP-MMA copolymers and AMO-MMA copolymers occurs after the addition of 40% MMA. AMO-MMA copolymers have outstanding mechanical properties over NVP-MMA and NNDMA-MMA copolymers due to its good sequence distribution. And NNDMA-MMA copolymer has the lowest value for each of these mechanical properties. Three mechanical properties can be obtained during the tensile test in this thesis, tensile strength, elastic modulus and elongation at break. If these three mechanical properties have relatively high values at the same time, we can consider this hydrogel as having good mechanical properties. Considering the combination of these three different aspects of mechanical properties, these three kinds of copolymers in which the concentration of MMA is between 40% and 50% show very strong mechanical properties.

4.2.2 Effect of EWC on Mechanical Properties

Water plays a major part in determining the mechanical properties of the hydrogels, generally making them soft and compliant and not dissimilar in feel to those of some

natural body tissues, such as skins. So it is necessary to investigate the effect of EWC on the mechanical properties of these MMA based copolymers. The results are displayed in Figures 4.5, 4.6 and 4.7.

With an increase in EWC, a decrease in both tensile strength and elastic modulus for the AMO-MMA and NVP-MMA copolymers occur. When the EWC of the NVP-MMA copolymer is greater than 60%, the elastic modulus becomes very low (less than 0.5 MPa). The same phenomenon can be observed when the AMO-MMA copolymer contains 35% or more water. For the NNDMA-MMA copolymer, the elastic modulus and tensile strength are very low and do not change with the increase of EWC.

With increasing EWC, the elongation at break of these three kinds of copolymers increases steadily to maximum value firstly and then decreases. For the NVP-MMA copolymer the maximum value appears when the EWC reaches 65%, for the AMO-MMA copolymer it appears when the EWC reaches 53%.

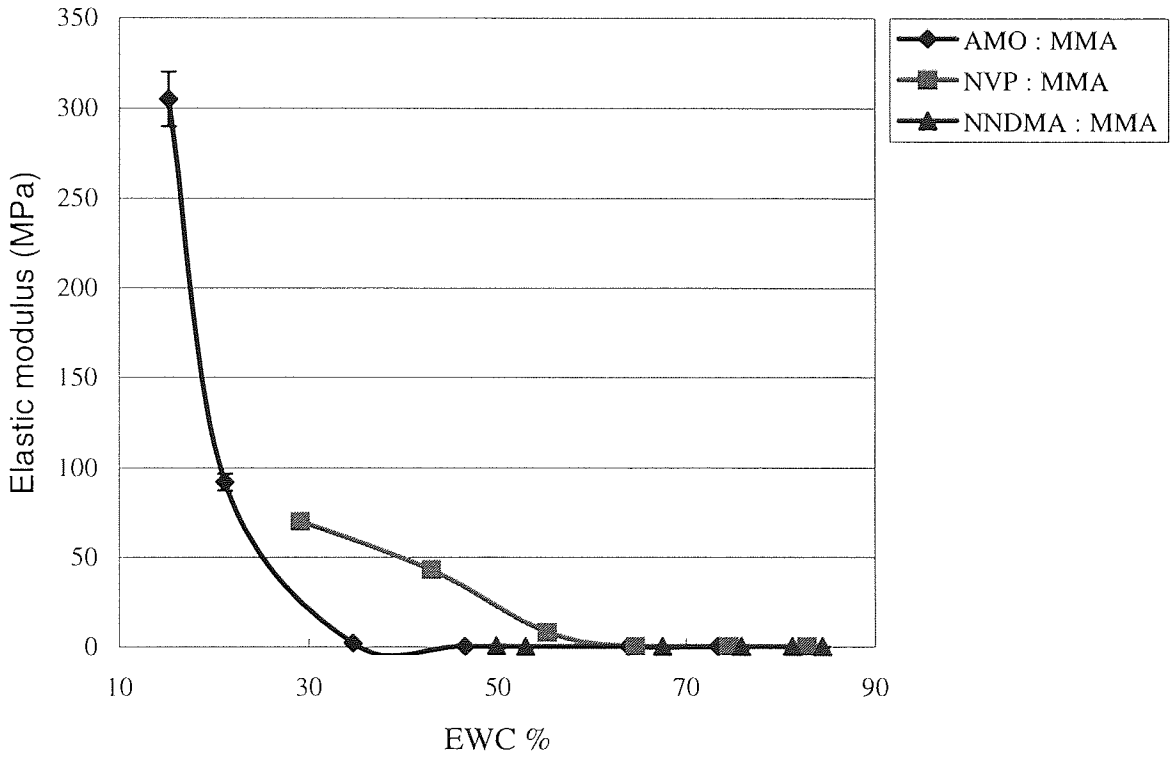

Figure 4.5 The effect of EWC on the elastic modulus of MMA copolymers

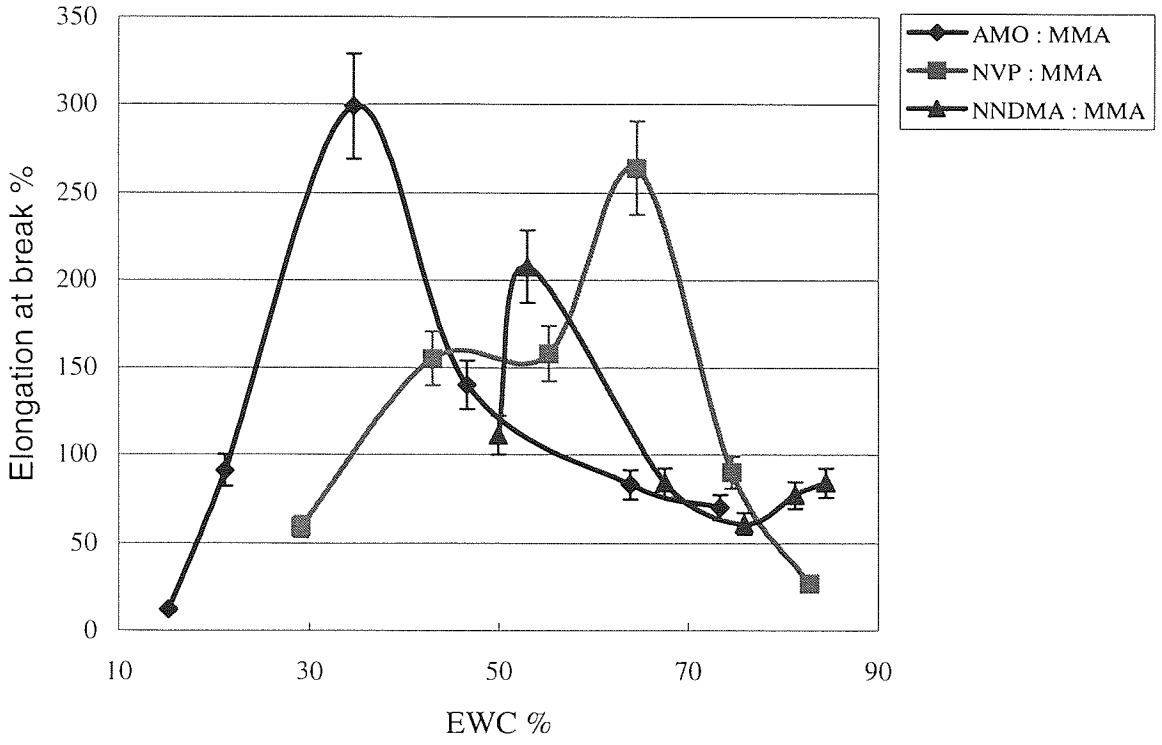

Figure 4.6 The effect of EWC on the elongation at break of MMA copolymers

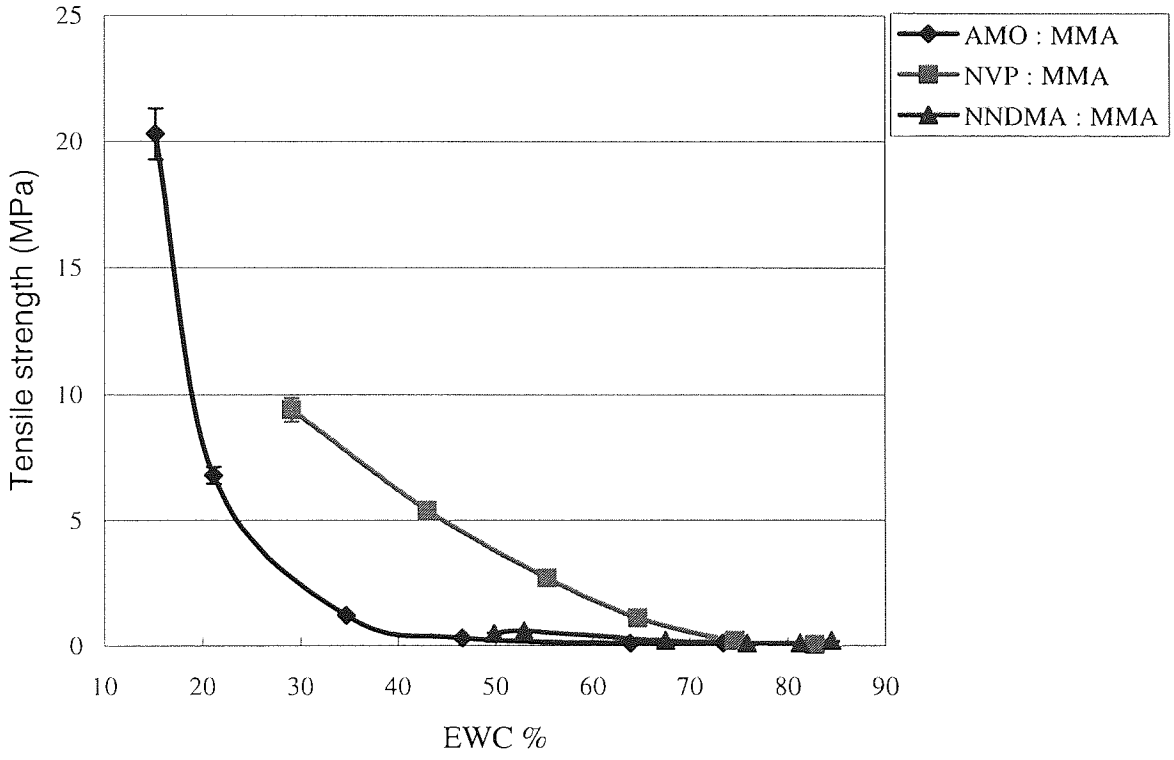

Figure 4.7 The effect of EWC on the tensile strength of MMA copolymers

It is shown in Figures 4.5, 4.6 and 4.7 that the EWC does influence the mechanical properties of the hydrogels. Considering the combination of these three different aspects of mechanical properties, tensile strength, elastic modulus and elongation at break, the most suitable EWC for good mechanical properties is between 20% and 35% for the AMO-MMA copolymers, between 55% to 70% for the NNDMA-MMA copolymers and between 45% to 55% for the NVP-MMA copolymers.

4.2.3 Effect of FWC on Mechanical Properties

Despite the fact that water structuring plays an important part in controlling the permeation properties of the hydrogel, the usefulness of this fact is, in many cases, compromised by undesirable changes in mechanical strength. The elastic modulus of the material indicates the stiffness of the material. With increasing incorporation of a hydrophilic monomer, it would be expected that the stiffness would decrease due to an increase in the amount of plasticising, freezing water content. The effect of freezing water content on the mechanical properties is shown in Figures 4.8, 4.9 and 4.10.

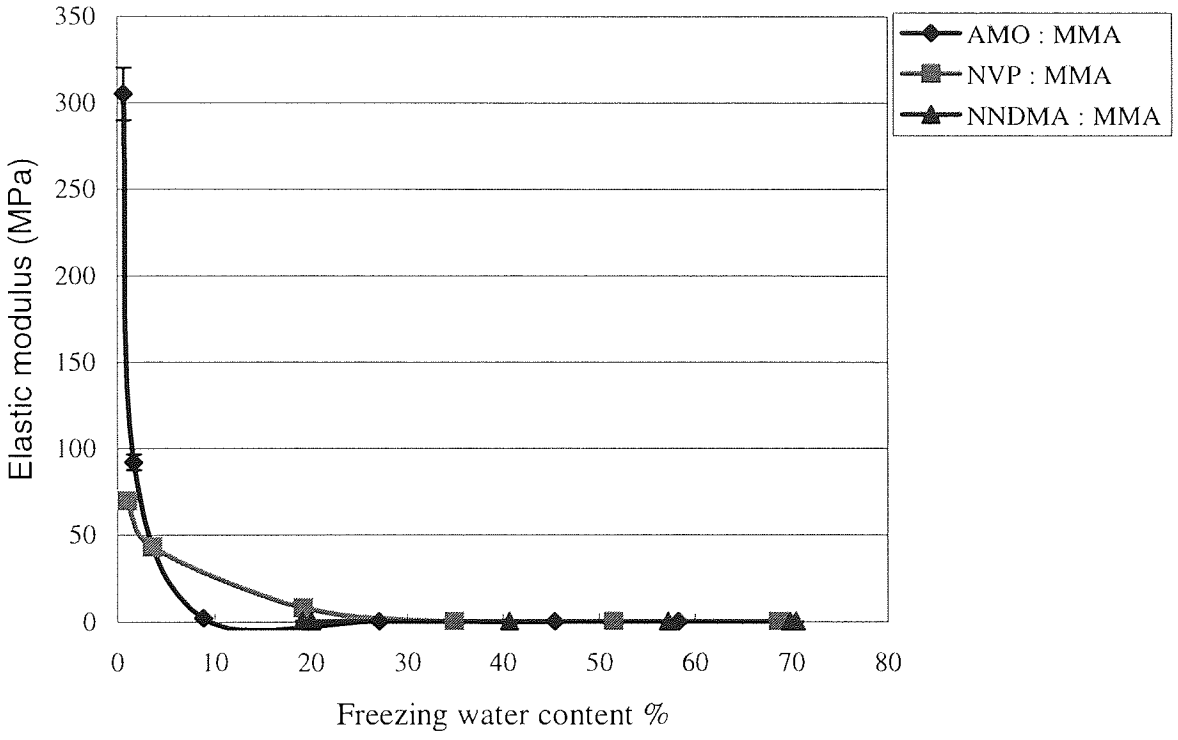

Figure 4.8 The effect of freezing water content on the elastic modulus of MMA copolymers

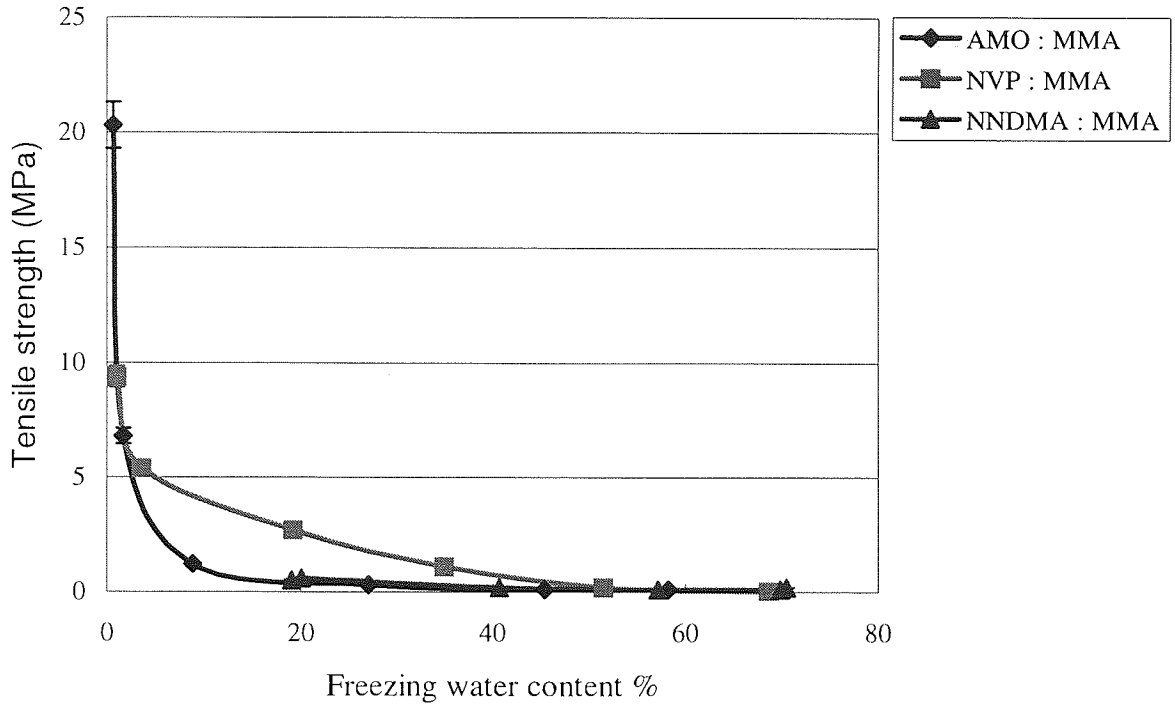

Figure 4.9 The effect of freezing water content on the tensile strength of MMA copolymers

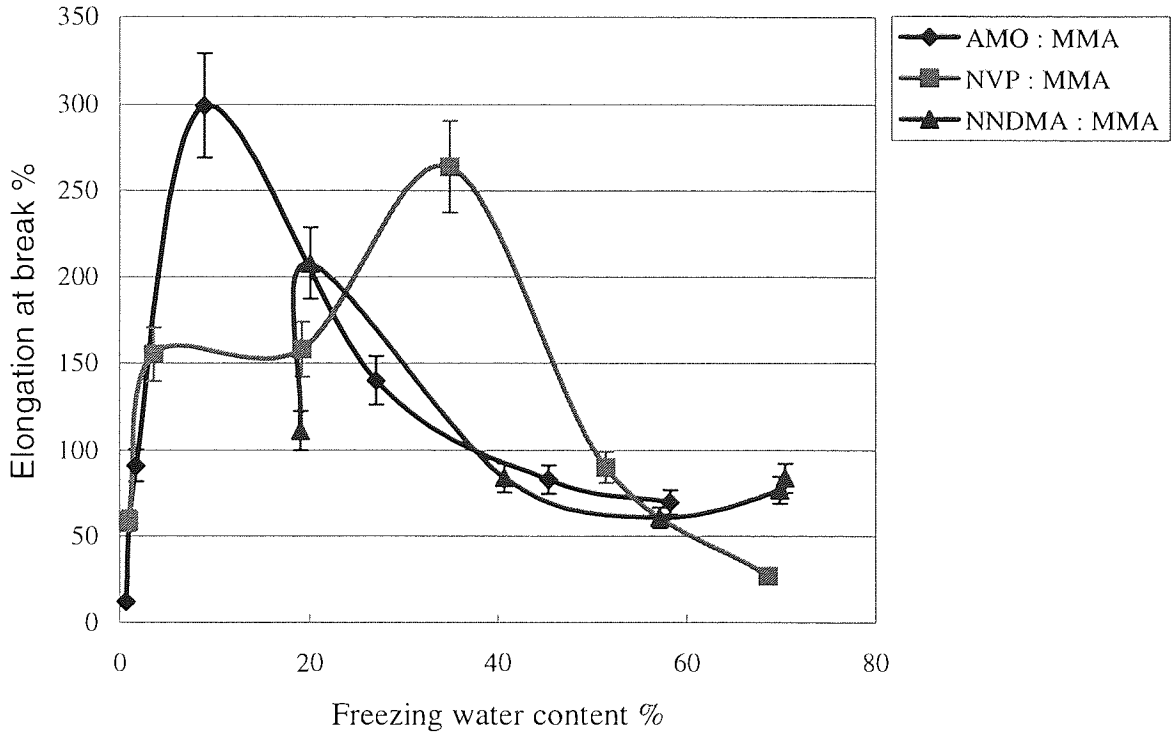

Figure 4.10 The effect of freezing water content on the elongation at break of MMA copolymers

With an increase in freezing water content, the decrease in both tensile strength and elastic modulus for the AMO-MMA and NVP-MMA copolymers occurs as expected. When the freezing water content in NVP-MMA copolymers is 25% or more, the elastic modulus becomes very low (less than 0.5 Ma). The same phenomenon can be observed when AMO-MMA copolymers contain 10% or more freezing water. For NNDMA-MMA copolymers, the elastic modulus and tensile strength are quite low and do not change with the increase of freezing water content.

With an increase in freezing water content, the elongation at break for these three types of copolymers increases steadily to a maximum value and then decreases. For the NVP-MMA copolymers the maximum value appears when the FWC reaches 33%, for AMO-MMA copolymer it appears when the FWC reaches 9% and for the NNDMA-MMA copolymer it appears when the FWC reaches 19%.

It is shown in Figures 4.8, 4.9 and 4.10 that the freezing water content does influence the mechanical properties of the hydrogels. Considering the combination of these three different aspects of mechanical properties, tensile strength, elastic modulus and elongation at break, the good mechanical properties occur when the freezing water content is between 3% and 15% for AMO-MMA copolymers, between 20% to 40% for NNDMA-MMA copolymers and between 5% to 20% for NVP-MMA copolymers.

4.3 Semi-interpenetrating Polymer Networks

The mechanical properties of SIPNs have attracted a great deal of interest because an important advantage of SIPNs is the ability to reinforce the hydrogel. The mechanical properties of the same SIPNs clear and porous hydrogels as described in Chapter 3 were measured by the technique described in Chapter 2 and the results are displayed graphically from Figure 4.11 to Figure 4.34 and in Table 4.1. This section illustrates the effect of monomer nature, equilibrium water content and freezing water content, on the mechanical properties of the SIPNs.

4.3.1 Effect of Monomer Composition on Mechanical Properties

4.3.1.1 Effect of Hydrophilic Component on Mechanical Properties of Clear SIPNs

It is shown in Figures 4.11 to 4.16 that the effect of the components on the mechanical properties of three series of clear SIPNs, AMO SIPNs, NVP SIPNs and NNDMA SIPNs.

It has been shown in Chapter 3 that for the same composition ratio, NNDMA SIPNs have the highest water content and AMO SIPNs have the lowest water content in these three families of SIPNs synthesized in this work.

It can be seen from Figure 4.11 that for the same composition ratio, NNDMA SIPNs have the lowest elastic modulus at the highest water content. When the hydrophilic component increases, the elastic modulus of these three types of SIPNs decreases. However, when the proportion of hydrophilic component to PU and THFMA is over a certain value (about 1.2), the elastic modulus does not decrease greatly with increasing the hydrophilic component.

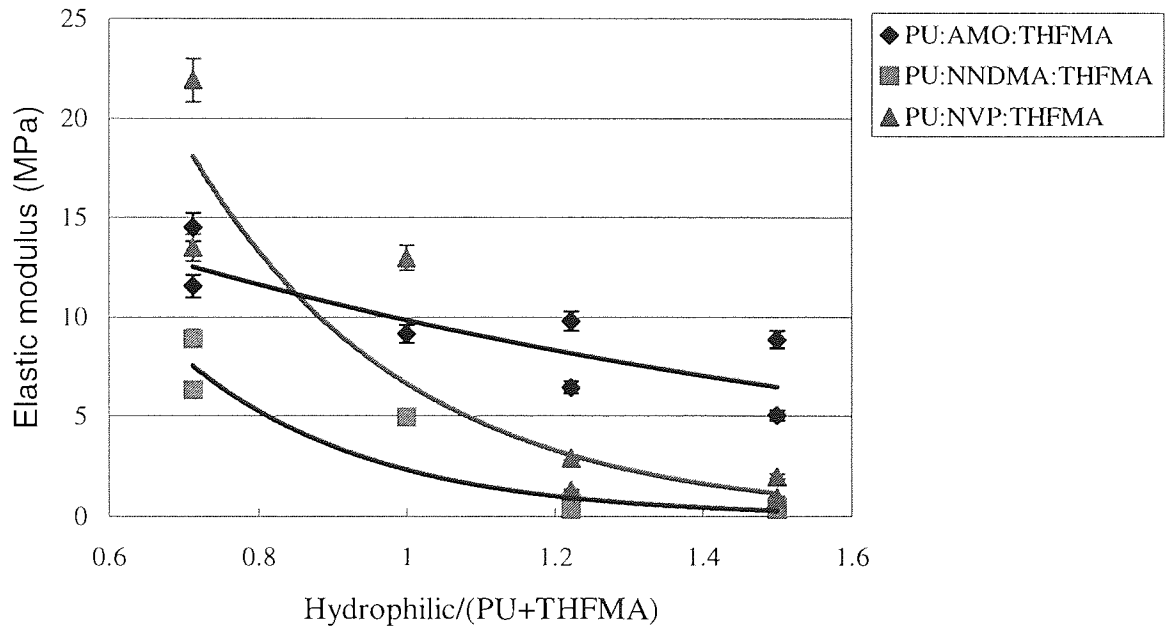

Figure 4.11 The effect of hydrophilic components on the elastic modulus of clear SIPNs (composition details shown in Table 3.1)

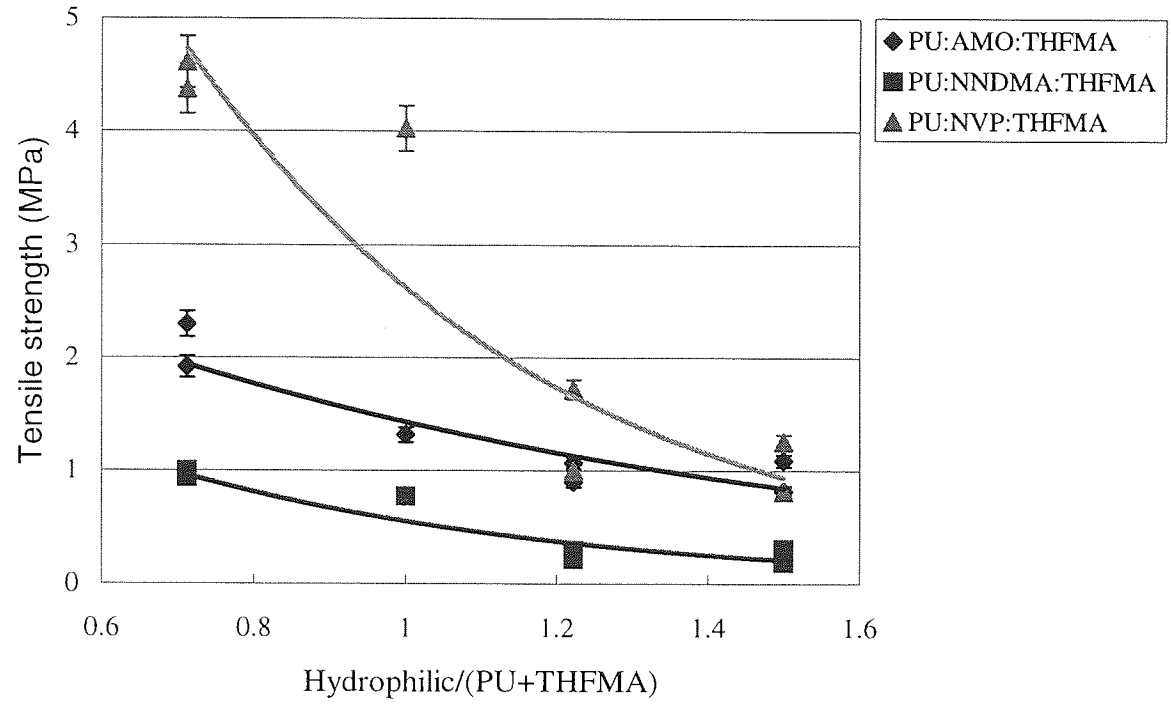

Figure 4.12 The effect of hydrophilic components on the tensile strength of clear SIPNs (composition details shown in Table 3.1)

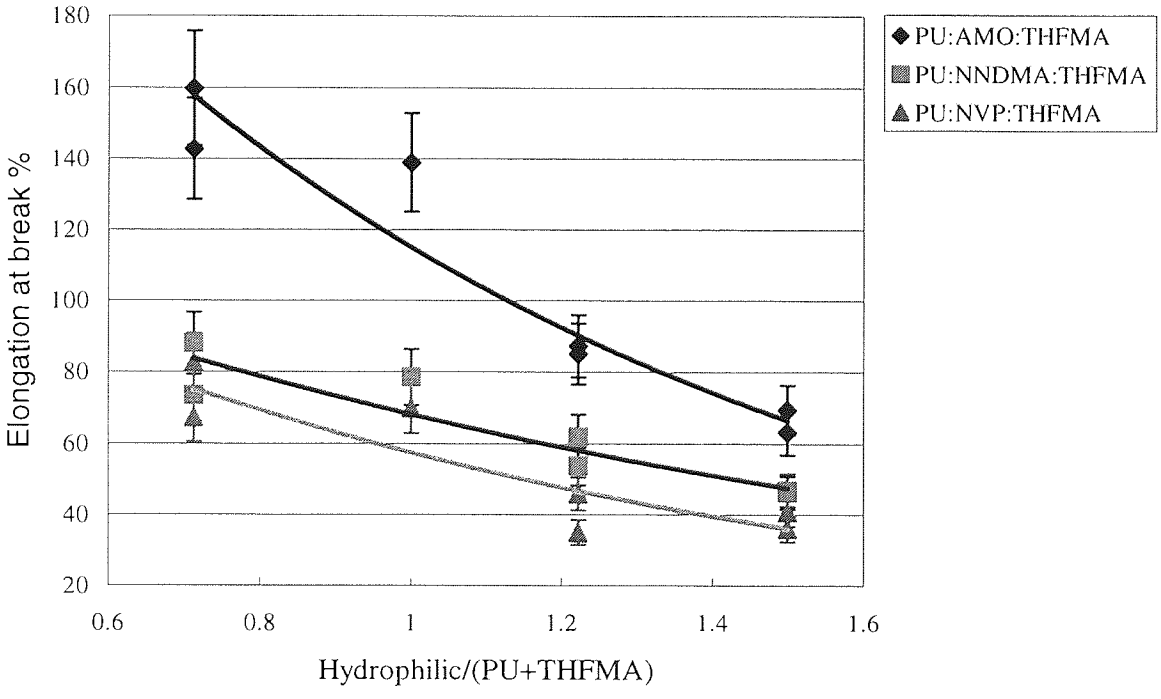

Figure 4.13 The effect of hydrophilic components on the elongation at break of clear SIPNs (composition details shown in Table 3.1)

It is shown in Figure 4.12 that the NNDMA SIPNs have the lowest tensile strength at the highest water content and NVP copolymers have the highest tensile strength at the intermediate water content. When the hydrophilic component increases, the tensile strength decreases. However, when the proportion of hydrophilic component to PU and THFMA is over a certain value (about 1.2), the tensile strength does not decrease greatly with increasing the hydrophilic component.

Figure 4.13 shows that an increase in the hydrophilic component leads to a decease in the elongation at break. The AMO SIPNs have the highest elongation at break at the lowest water content and the NVP SIPNs have the lowest elongation at break just at the intermediate water content. When the hydrophilic component increases, the elongation at break decreases until a certain ratio value (about 1.2); the elastic modulus decreases slightly as hydrophilic component increases.

At the same concentration of the hydrophilic component, even if the proportion of PU5 to THFMA is different, the mechanical properties of these three families of SIPNs are not dissimilar. It seems that the hydrophilic component dominates the mechanical properties of these three families of SIPNs. It is shown from Figure 4.11 to Figure 4.13 that an obvious transition in mechanical properties of these three kinds of SIPNs occurs after the proportion of hydrophilic component to PU and THFMA component reaches 1.2.

4.3.1.2 Effect of Interpenetrant on Mechanical Properties of Clear SIPNs

PU5 as an interpenetrant is a very important component in SIPNs to reinforce the mechanical properties. An investigation of its effect on the mechanical properties is required. Graphs are shown from Figure 4.14 to Figure 4.16.

At PU5 contents of less than 15% (by weight), the tensile strength and elongation at break of AMO-SIPNs and the elastic modulus, tensile strength and elongation at break of NVP-SIPNs and NNDMA-SIPNs do not change significantly with the increase of PU5 content. However, above 15%, they increase with undulation with the increase of PU5 content.

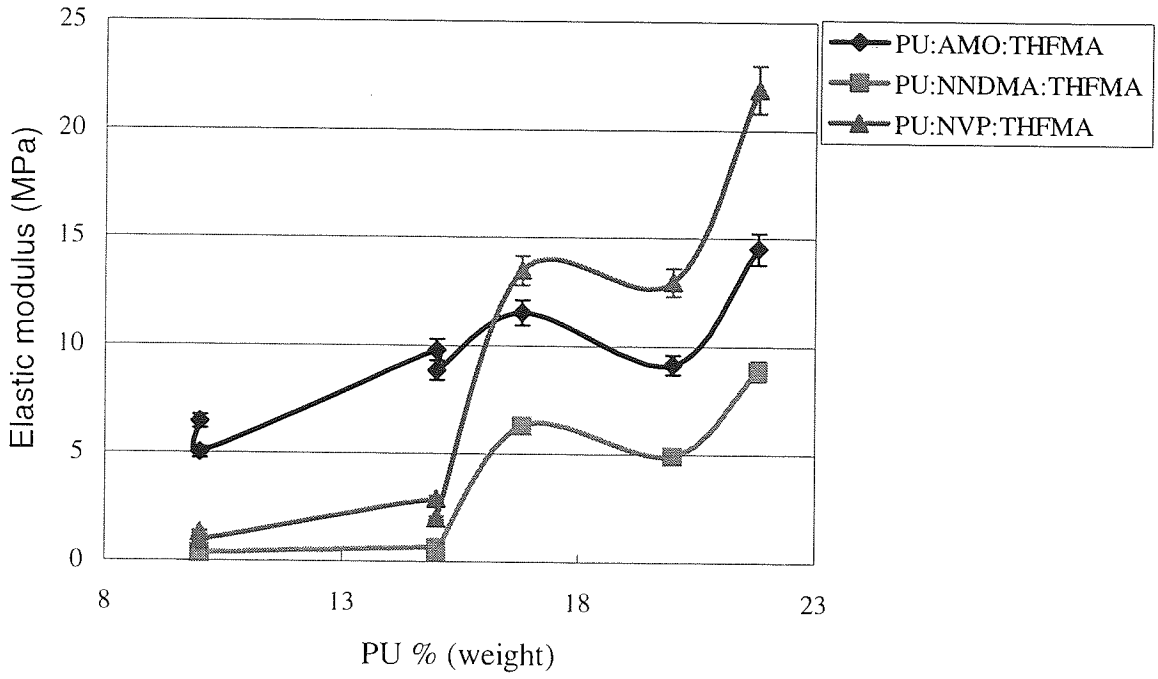

Figure 4.14 The effect of PU5 content on the elastic modulus of clear SIPNs (composition details shown in Table 3.1)

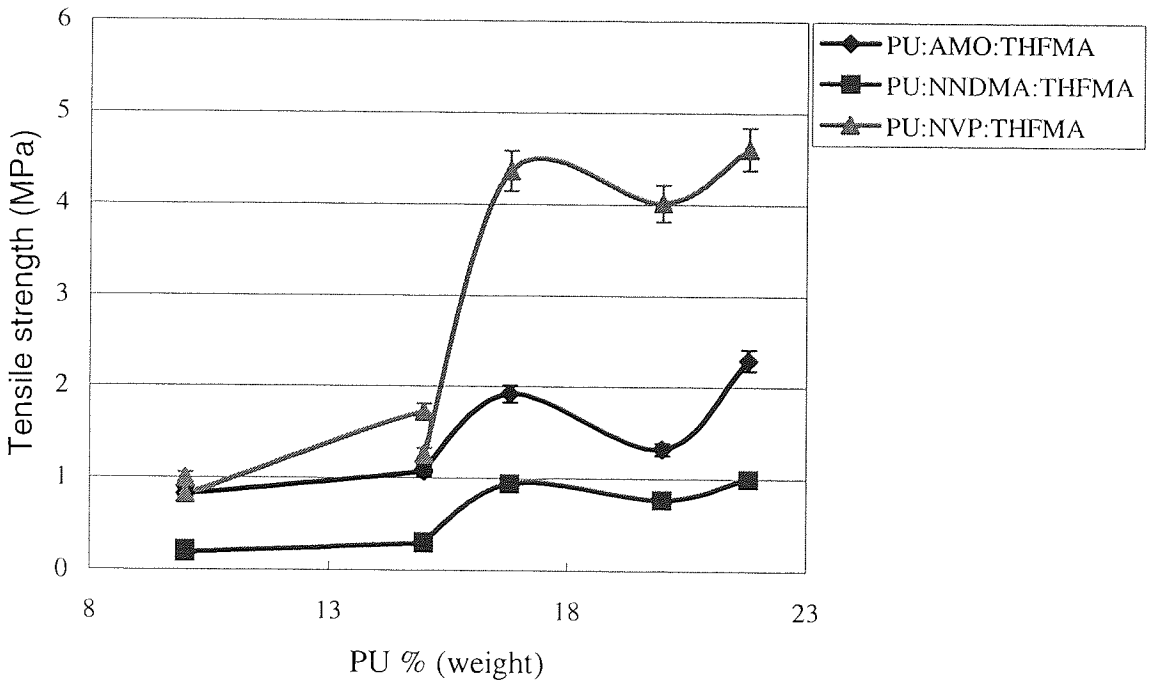

Figure 4.15 The effect of PU5 content on the tensile strength of clear SIPNs (composition details shown in Table 3.1)

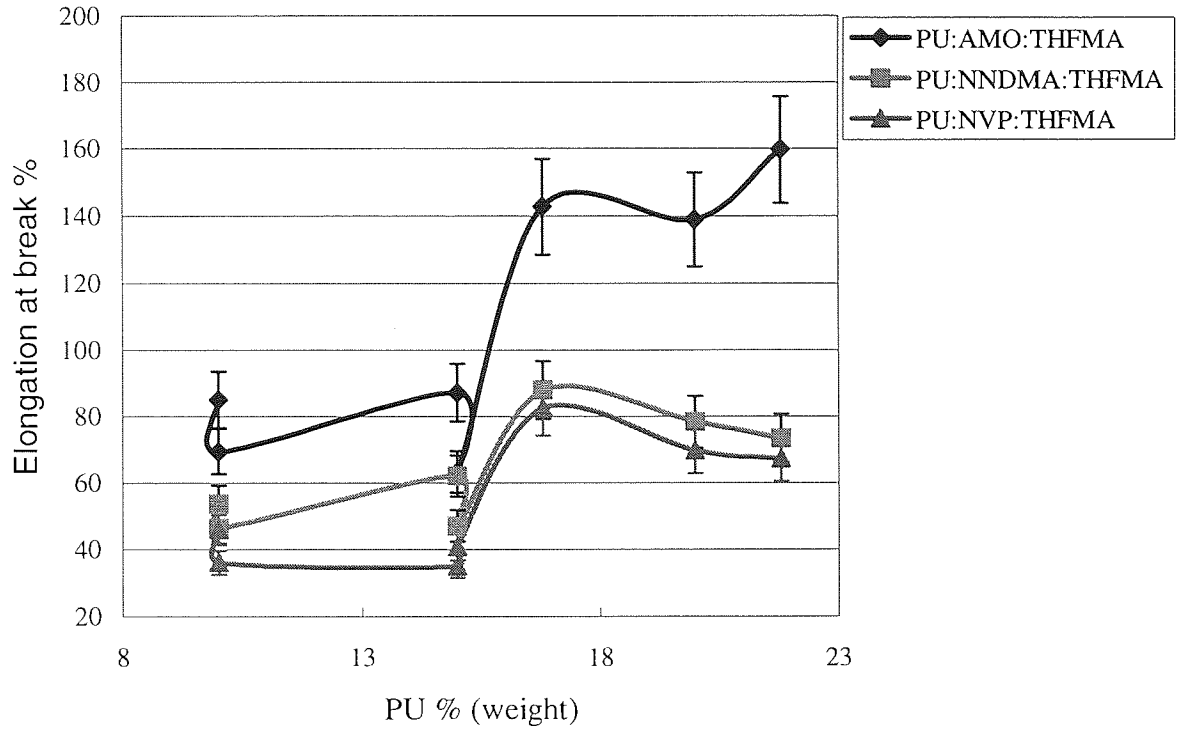

Figure 4.16 The effect of PU5 content on the elongation at break of clear SIPNs (composition details shown in Table 3.1)

From Figure 4.14 to Figure 4.16, it can been seen that the values of mechanical properties for each of these three SIPNs, elastic modulus, tensile strength and elongation at break, are almost same when they contain same concentration of PU5, even the proportions of the hydrophilic component to THFMA are different.

It is shown from Figure 4.14 to Figure 4.16 that an obvious transition in mechanical properties of these three SIPNs, AMO SIPNs, NVP SIPNs and NNDMA SIPNs occurs after the addition of 15% PU5.

It must be remembered in interpreting Figures 4.14 to 4.16, which show the change in mechanical properties with increasing PU5, that the ratio of hydrophilic component to THFMA also changes in each series of SIPNs (shown in Table 3.1). When the effect of the ratio of hydrophilic component to hydrophobic component on mechanical properties (Figures 4.11 to 4.13) is taken into account, it can be seen that the "transition" at 15% PU5 is caused largely by a change in the constituent monomer ratios. In general, increasing PU5 produces steadily increasing tensile strength and elastic modulus.

4.3.1.3 Effect of Hydrophilic Component on Mechanical Properties of Porous SIPNs

Porous hydrogels are potential candidates for the skirt material in the "core-and-skirt" KPro model. It is the primary stress bearing section during the surgical procedure and should also withstand the *in situ* stresses such as the deforming force of the eyelid during the blink cycle. The mechanical properties are thus very important parameters of the porous materials. The mechanical properties of the same porous materials as described in Chapter 3 are illustrated from Figure 4.17 to Figure 4.22 and Table 4.1.

Comparing the mechanical properties of the clear SIPNs (Figure 4.11, 4.12 and 4.13) with those of the porous SIPNs made using dextrin (Figures 4.17, 4.18 and 4.19) and using both dextrin and dextran (Figure 4.20, 4.21 and 4.22), the rule of diversification of elastic modulus and tensile strength of both porous SIPNs with diversifying the ratio of hydrophilic component to PU5 and THFMA is similar with clear SIPNs. However, the elongation at break curves for both types of porous materials appear more random. The reason for this could be that the heterogeneous nature of the porous hydrogels causes inconsistencies in the results.

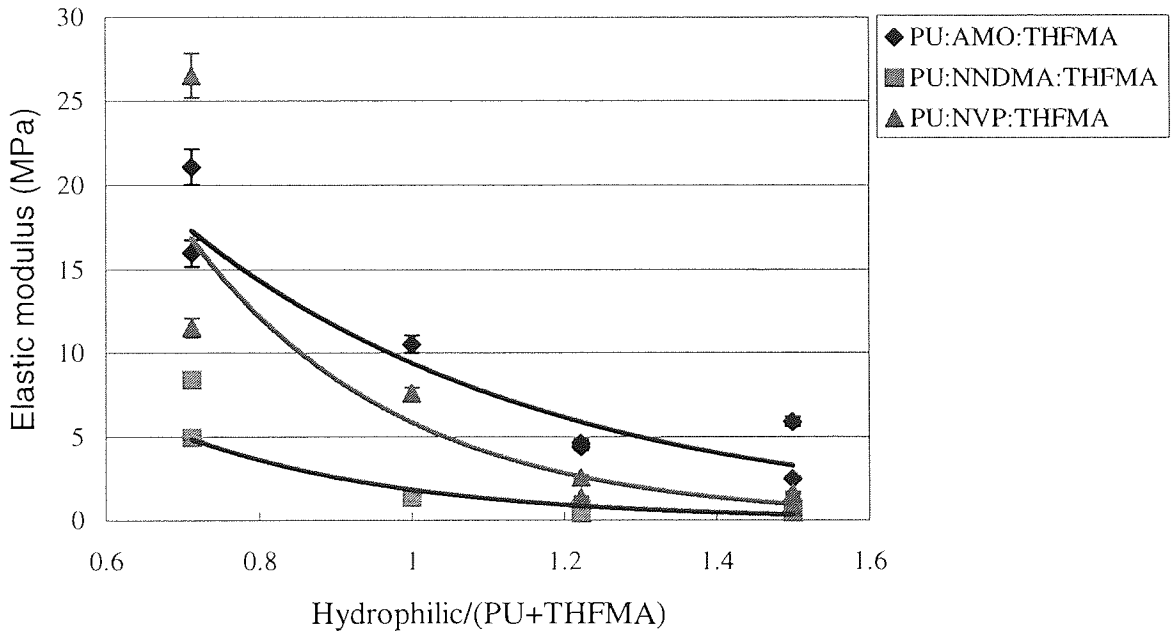

Figure 4.17 The effect of hydrophilic components on the elastic modulus of porous (Dextrin) SIPNs (composition details shown in Table 3.1)

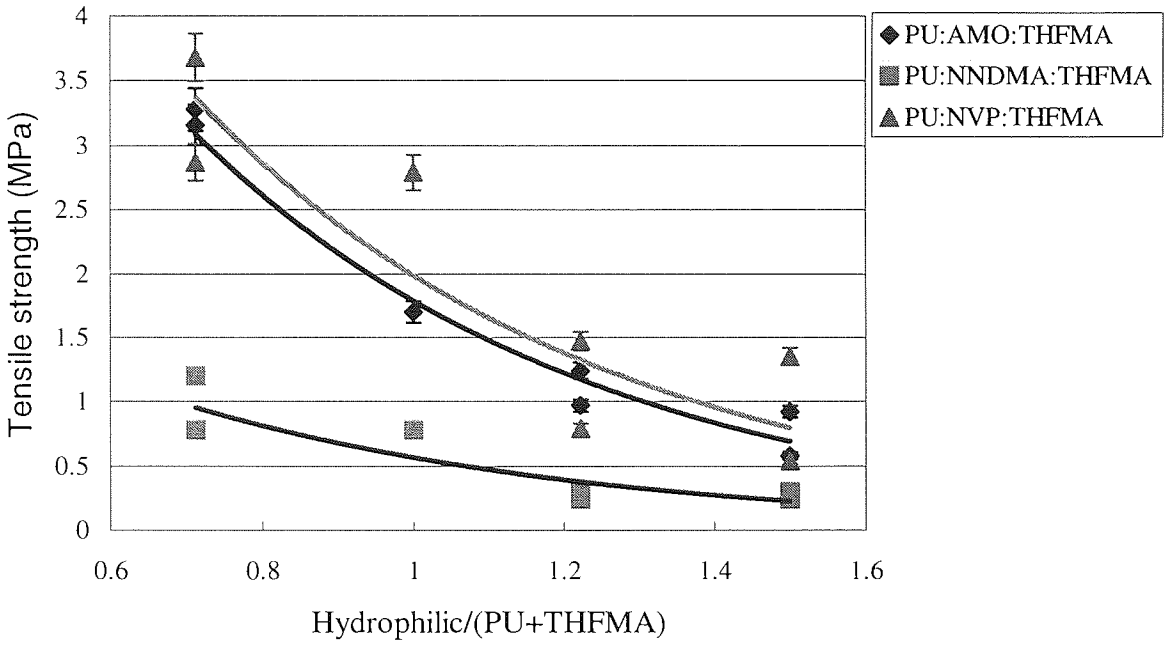

Figure 4.18 The effect of hydrophilic components on the tensile strength of porous (Dextrin) SIPNs (composition details shown in Table 3.1)

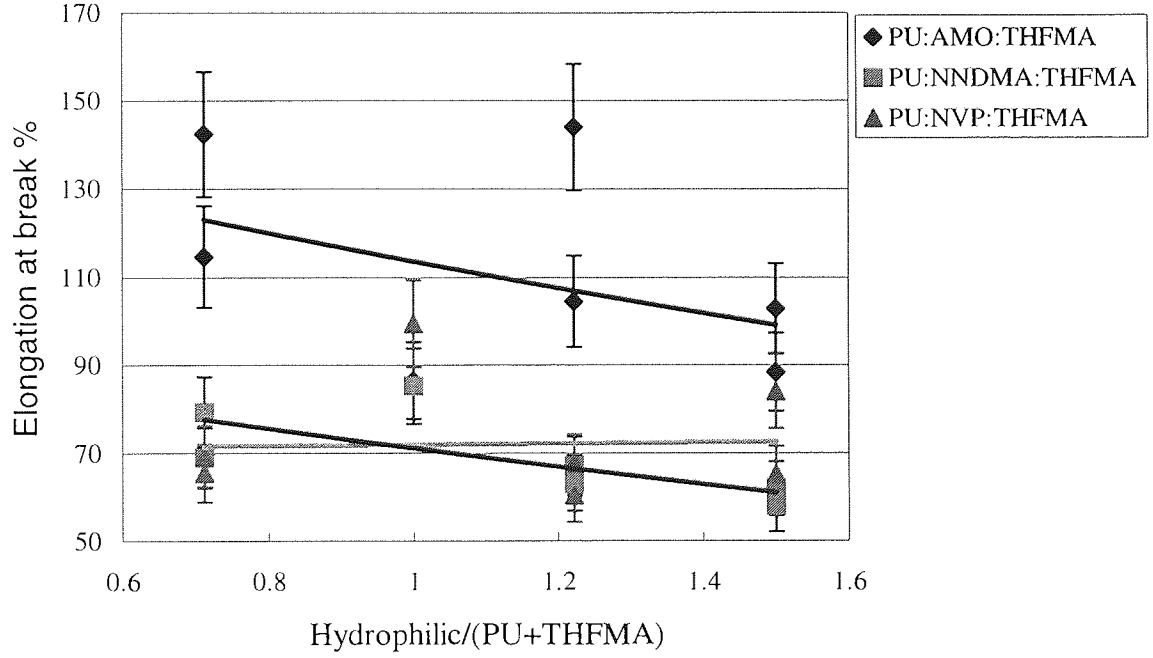

Figure 4.19 The effect of hydrophilic components on the elongation at break of porous (Dextrin) SIPNs (composition details shown in Table 3.1)

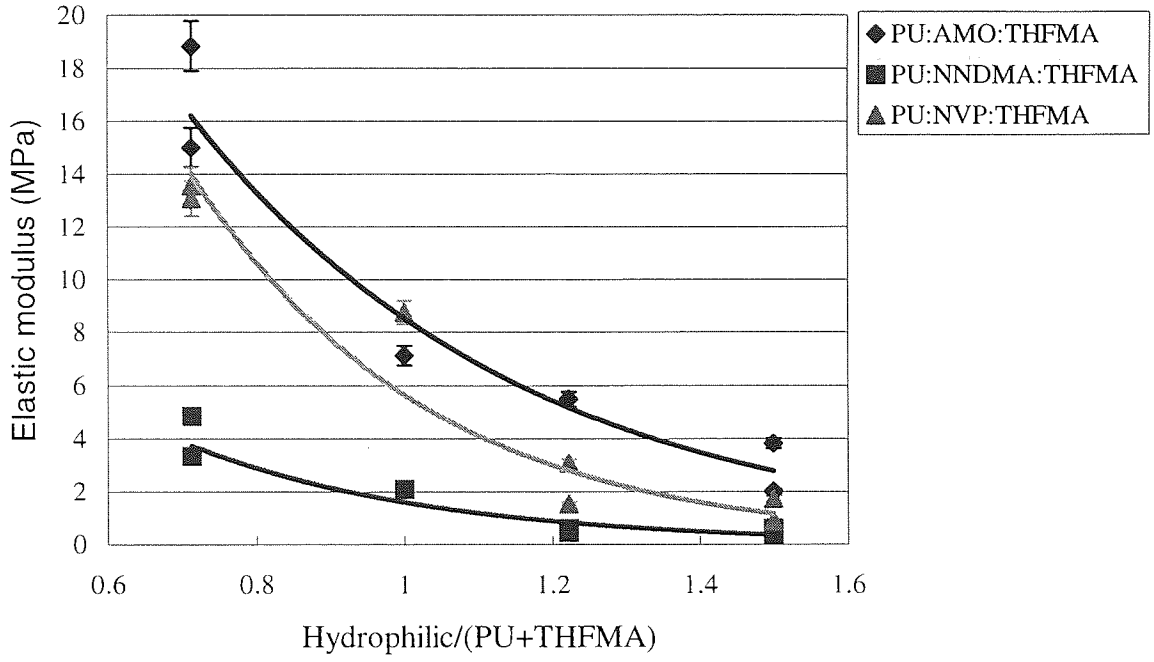

Figure 4.20 The effect of hydrophilic components on the elastic modulus of porous (Dextran + Dextrin) SIPNs (composition details shown in Table 3.1)

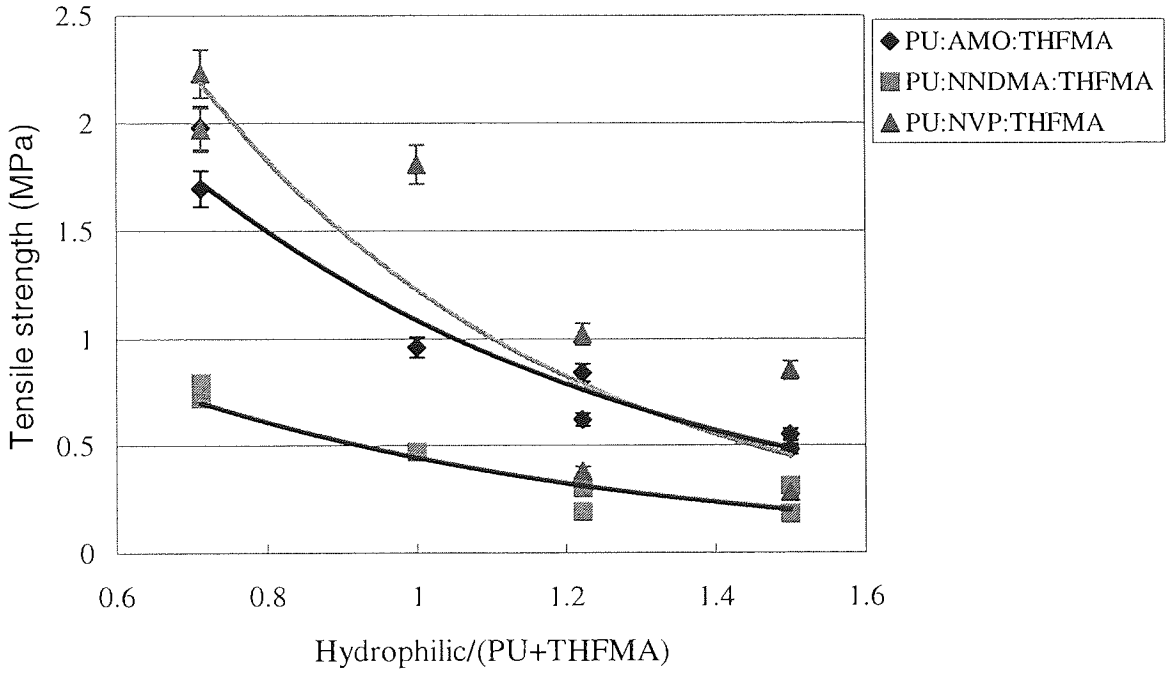

Figure 4.21 The effect of hydrophilic components on the tensile strength of porous (Dextran + Dextrin) SIPNs (composition details shown in Table 3.1)

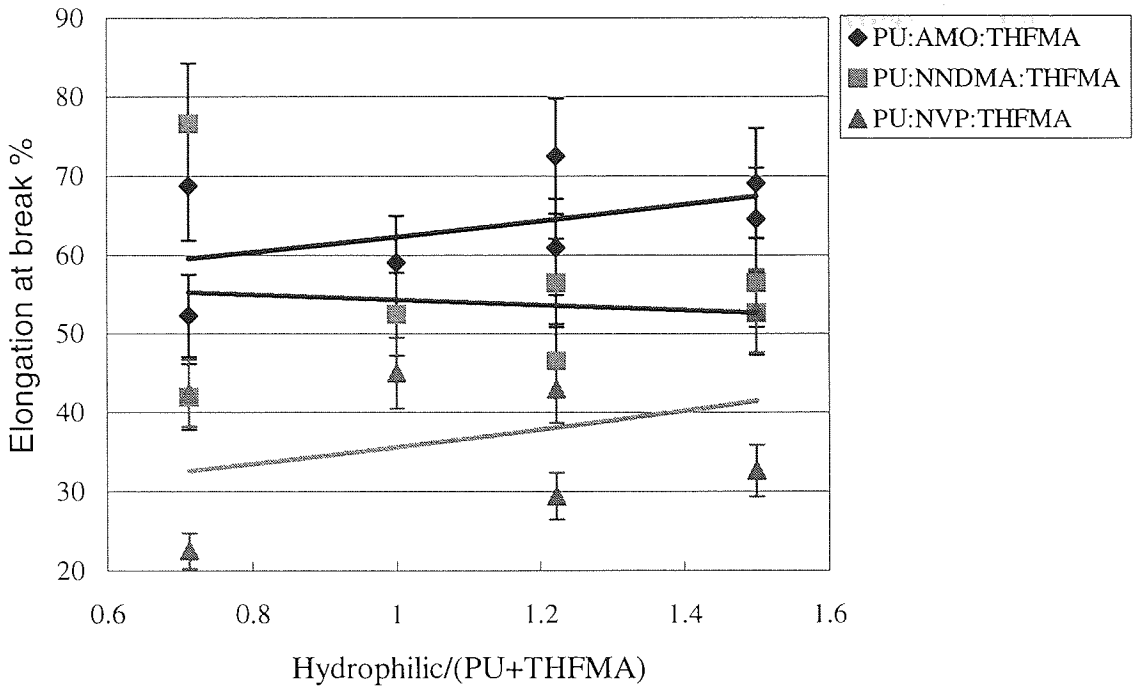

Figure 4.22 The effect of hydrophilic components on the elongation at break of porous (Dextran + Dextrin) SIPNs (composition details shown in Table 3.1)

Generally, the elastic modulus of porous materials made using dextrin is slightly lower than the corresponding clear material, though when both dextrin and dextran were used, the elastic modulus of AMO and NVP containing materials was slightly higher than that of the clear material, especially at lower levels of hydrophilic monomers. The tensile strength of both kinds of NVP SIPN porous materials is slightly lower than that of the clear material. The elongation at break of the porous materials are lower than that of the corresponding clear materials, with dextrin and dextran having a marked effect.

The clear material and porous materials are identical chemically, and as discussed in Chapter 3, both materials have similar water contents, but it is evident that the porosigen has some effect on the mechanical properties of the porous material. Hydrogels are amorphous polymers; there are inevitably defects, such as loops, entanglements, in the network. All these defects affect the mechanical properties of the hydrogel. The irregular pores created by the addition of porosigens increase the defects in the network further. The size and shape of the pores also affect the mechanical properties of the hydrogel.

Gel ID	PU5 : AMO : THFMA	E.Mod (MPa)	Ts (MPa)	Eb %
J10A	15 : 55 : 30	8.4	1.1	106
J10B	15 : 55 : 30	8.2	1.1	110
J10C	15 : 55 : 30	5.8	0.8	85
J10D	15 : 55 : 30	10.8	1.0	73
J10	15 : 55 : 30	9.8	1.1	87
J18A	16.8 : 41.6 : 41.6	22.1	3.2	157
J18B	16.8 : 41.6 : 41.6	14.9	3.1	151
J18C	16.8 : 41.6 : 41.6	14.8	2.4	132
J18D	16.8 : 41.6 : 41.6	15.1	1.9	87
J18	16.8 : 41.6 : 41.6	11.5	1.9	143

Gel ID	PU5 : NNDMA : THFMA	E.Mod (MPa)	Ts (MPa)	Eb %
J2A	20 : 50 : 30	2.7	0.5	65
J2B	20 : 50 : 30	3.5	0.5	65
J2C	20 : 50 : 30	2.9	0.5	63
J2D	20 : 50 : 30	3.4	0.4	56
J2	20 : 50 : 30	5.0	0.8	79
J3A	10 : 55 : 35	0.4	0.2	61
J3B	10 : 55 : 35	0.4	0.2	64
J3C	10 : 55 : 35	0.4	0.2	53
J3D	10 : 55 : 35	0.4	0.1	41
J3	10 : 55 : 35	0.6	0.2	54

Gel ID	PU5 : NVP : THFMA	E.Mod (MPa)	Ts (MPa)	Eb %
J7A	10 : 55 : 35	0.8	1.0	101
J7B	10 : 55 : 35	0.8	0.7	86
J7C	10 : 55 : 35	0.8	0.8	91
J7D	10 : 55 : 35	1.0	0.5	52
J7	10 : 55 : 35	1.3	1.0	46
J13A	21.8 : 41.6 : 36.6	18.7	4.6	110
J13B	21.8 : 41.6 : 36.6	18.6	4.7	108
J13C	21.8 : 41.6 : 36.6	20.5	4.2	88
J13D	21.8 : 41.6 : 36.6	21.4	2.5	35
J13	21.8 : 41.6 : 36.6	21.9	4.6	67

A: Add salt pore size between 38-63 μm 20% (by weight)

B: Add salt pore size between 63-90 μm 20% (by weight)

C: Add salt pore size between 90-125 μm 20% (by weight)

D: Add salt pore size between 38-63 μm 20% + Dextran 4% (by weight)

Table 4.1 The mechanical properties of porous materials made using salt

If a pore is present at the edge of cut sample, the sample maybe tear easily during the test. Thus an important requirement for the measurement of mechanical properties of porous materials is that no pores should be present at the edge of the cut sample.

Table 4.1 illustrates the mechanical properties of SIPNs with pores of different sizes created using salt. No clear trend is visible, probably because of the heterogeneous nature of the material. Perhaps surprisingly, the mechanical properties do not seem to depend on pore size. Usually, a larger pore size would be expected to cause more defects in the network, thereby affecting the mechanical properties to a greater extent.

4.3.2 Effect of EWC on Mechanical Properties of Clear SIPNs

One important feature of SIPNs is that they can reinforce the mechanical properties whilst maintaining relatively high water contents. Therefore it is interesting to investigate how the EWC affects the mechanical properties of SIPNs. The results are displayed from Figure 4.23 to Figure 4.25.

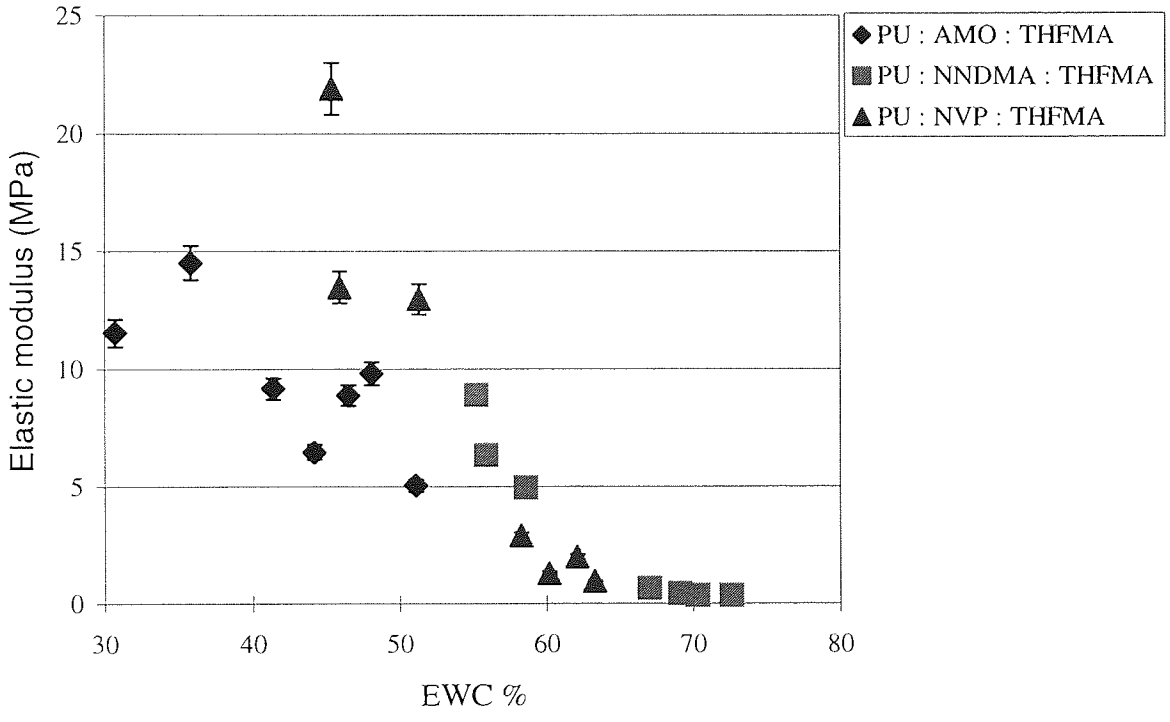

Figure 4.23 The effect of equilibrium water content on the elastic modulus of clear SIPNs

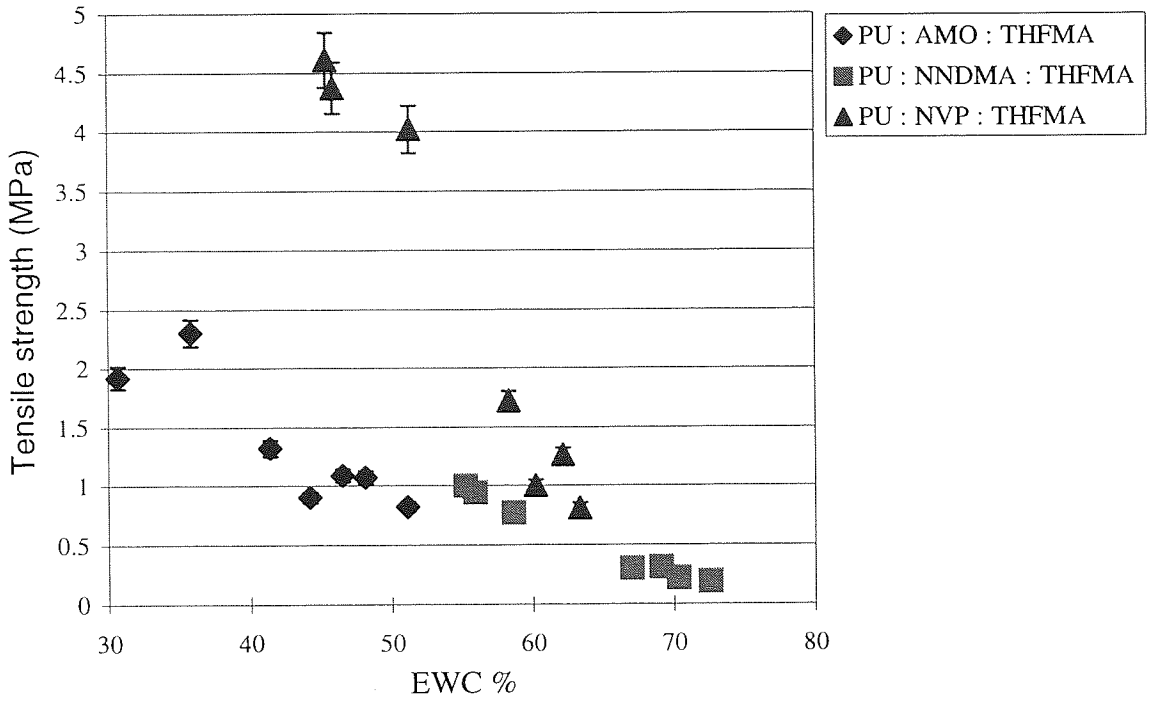

Figure 4.24 The effect of equilibrium water content on the tensile strength of clear SIPNs

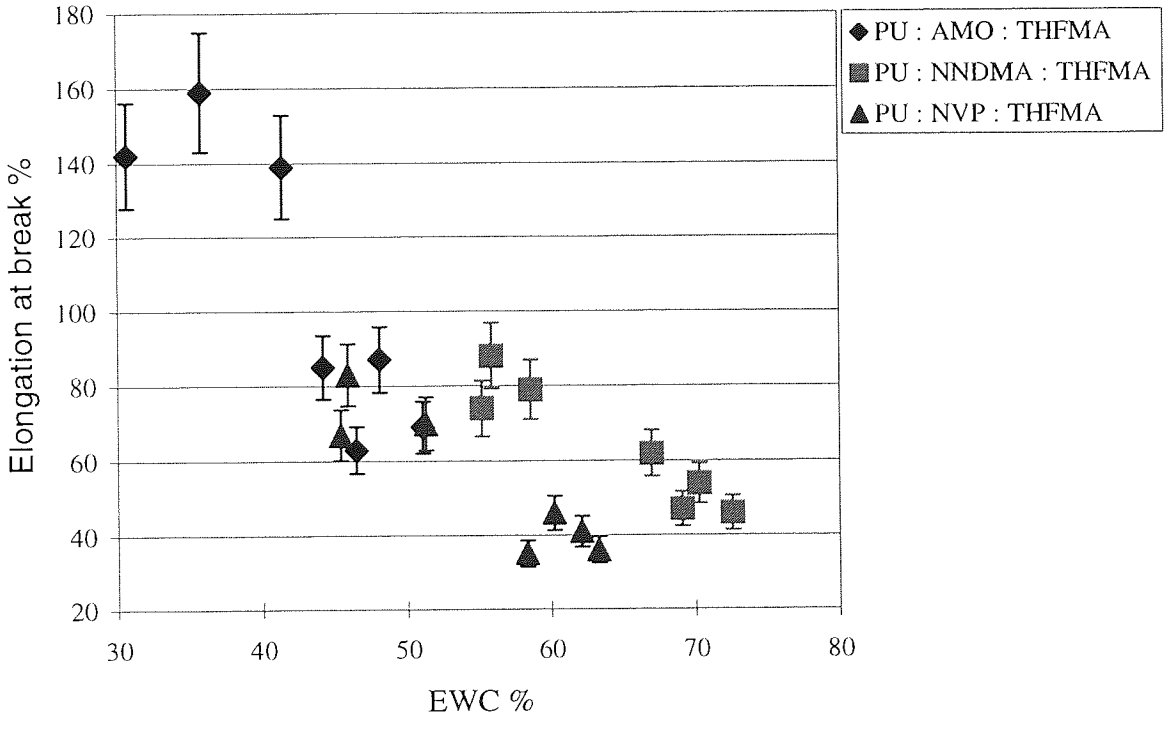

Figure 4.25 The effect of equilibrium water content on the elongation at break of clear SIPNs

It can be seen from Figure 4.23 to Figure 4.25 that an increase in the EWC leads to a decrease in elastic modulus, tensile strength and elongation at break.

At 50% EWC, the elastic modulus, tensile strength and elongation at break of the AMO-MMA copolymer are 0.5 MPa, 0.3 MPa and 125% respectively and the corresponding AMO SIPNs has values of 5 MPa, 0.8 MPa and 70%. The elastic modulus and tensile strength of AMO SIPNs are higher than AMO-MMA copolymer's but the elongation at break is lower. The same phenomenon can be observed for NNDMA polymers and NVP polymers at high water contents.

The elastic modulus and tensile strength of SIPNs having high water content are higher than the conventional copolymer hydrogels having the same water content, but the elongation at break is lower. Because the elastic modulus of the material indicates the stiffness of the material, the SIPNs are much stiffer than the conventional copolymer hydrogels even when they have high water content.

An abnormal phenomenon which should be mentioned here is that the elastic modulus and the tensile strength of NVP SIPNs are unusually high when their equilibrium water content is between 45% and 55%. A possible explanation is that the sequence distribution of NVP/THFMA causes the huge increase in the elastic modulus and the tensile strength. NVP/THFMA copolymer may have a blocky sequence distribution at later stage in the polymerisation.

4.3.3 Effect of FWC on Mechanical Properties of Clear SIPNs

The effect of freezing water content on mechanical properties of clear SIPNs is displayed from Figure 4.26 to Figure 4.28.

As expected, a decrease in freezing water content leads to an increase in the elastic modulus of the clear SIPNs. It is also shown in Figures 4.27 and 4.28 that with an increase of freezing water content, the tensile strength and elongation at break decrease.

At 25% freezing water content, the elastic modulus, tensile strength and elongation at break of the AMO-MMA copolymer are 0.3 MPa, 0.5 MPa and 150% respectively and the values

for the corresponding AMO SIPN are 7 MPa, 0.9 MPa and 85%. The elastic modulus and tensile strength of the AMO SIPN are higher than the AMO-MMA copolymer but the elongation at break is lower. The same phenomenon can be observed for the NNDMA polymers and NVP polymers.

The elastic modulus and tensile strength of SIPNs are higher than MMA based copolymers having the same freezing water content, but the elongation at break is lower.

The same abnormal phenomenon with NVP SIPNs as in section 4.3.2 is noticed here when its freezing water content is between 45% and 55%. A possible explanation may be the effect of sequence distribution as described in section 4.3.2.

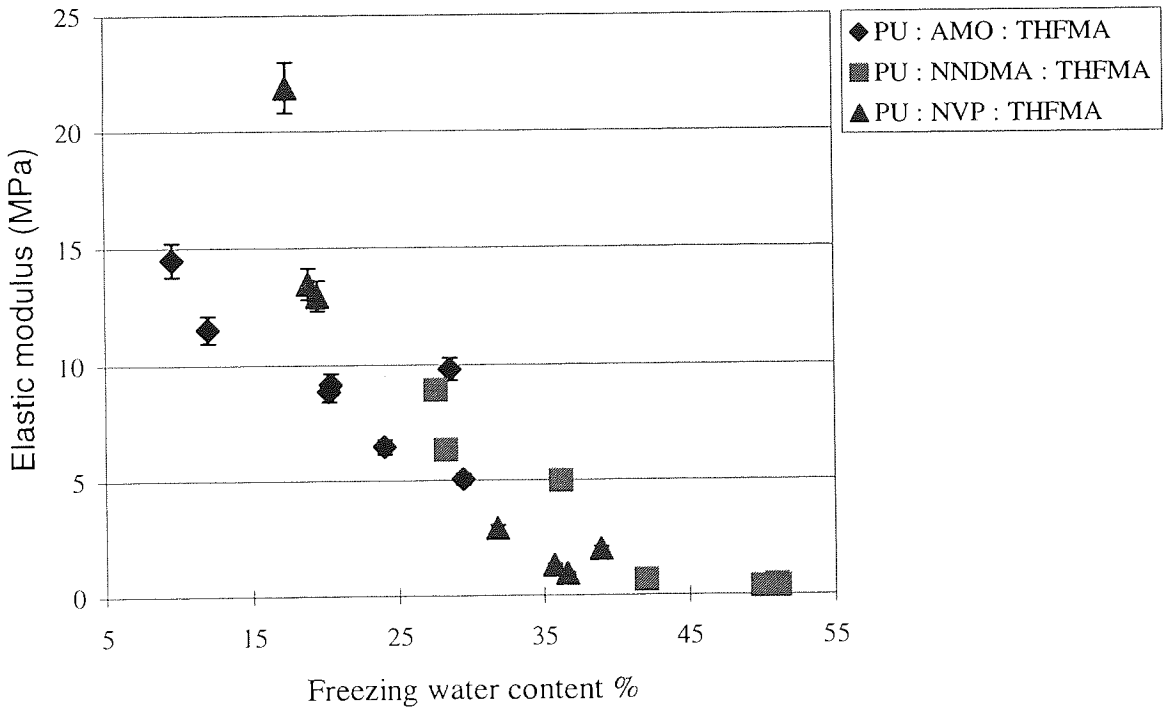

Figure 4.26 The effect of freezing water content on the elastic modulus of clear SIPNs

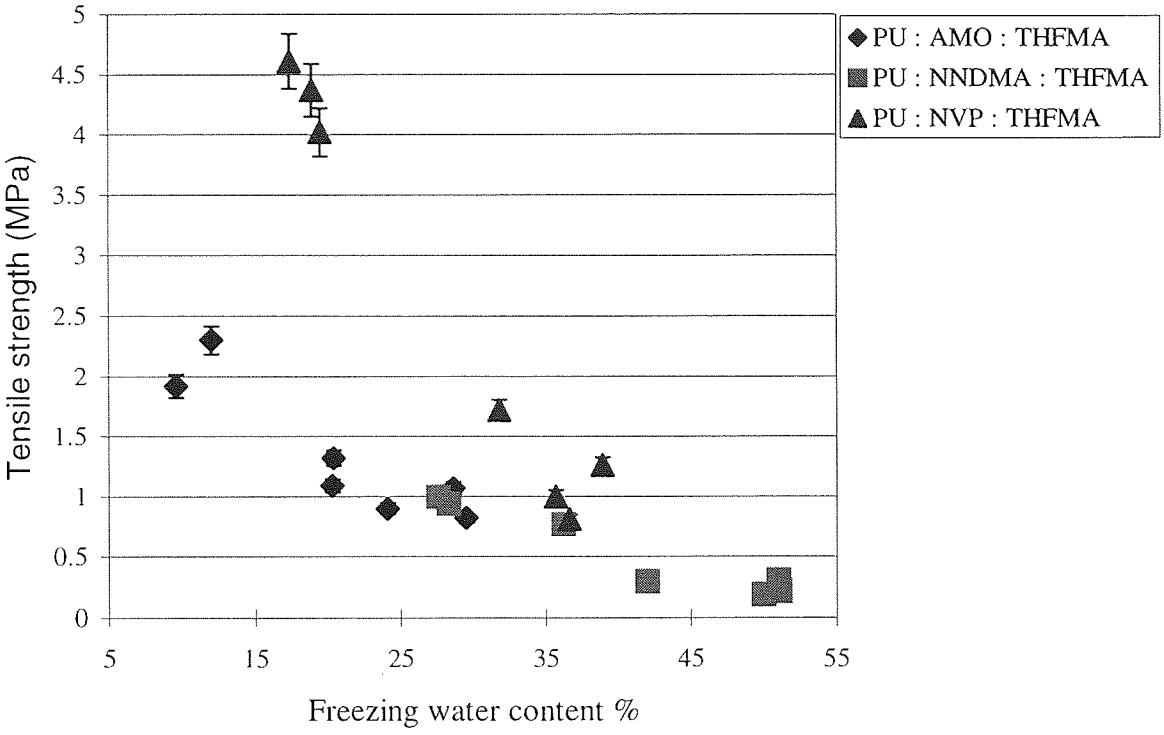

Figure 4.27 The effect of freezing water content on the tensile strength of clear SIPNs

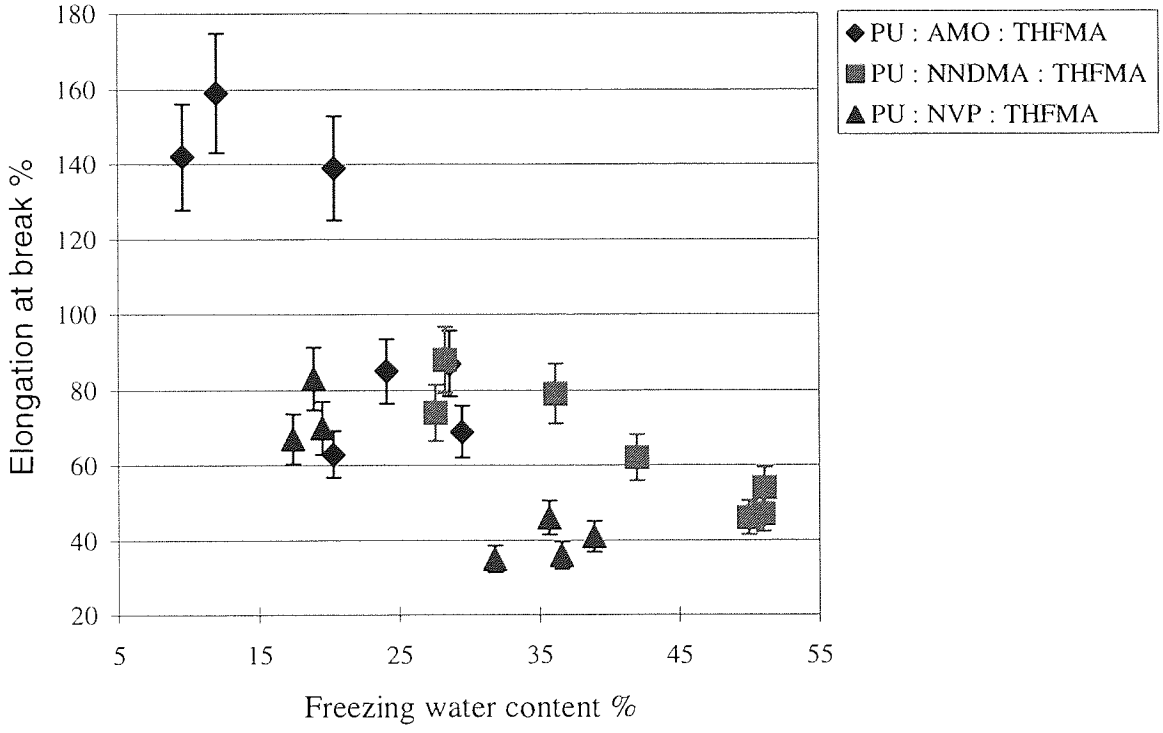

Figure 4.28 The effect of freezing water content on the elongation at break of clear SIPNs

4.4 Effect of PEG MA on Mechanical Properties of Clear SIPNs

As stated in Chapter 3, polyethylene glycol (PEG) is known to effectively reduce protein deposition and cell adhesion. A SIPN containing PEG MA is a good potential hydrogel for making optically transparent core material in the "core and skirt" KPro model. It should have suitable mechanical properties to withstand the forces applied to it once it is in the eye (such as blink deformation). The mechanical properties of clear SIPN hydrogels containing PEG MA were measured and the results are shown from Figure 4.29 to Figure 4.36.

4.4.1 AMO SIPNs

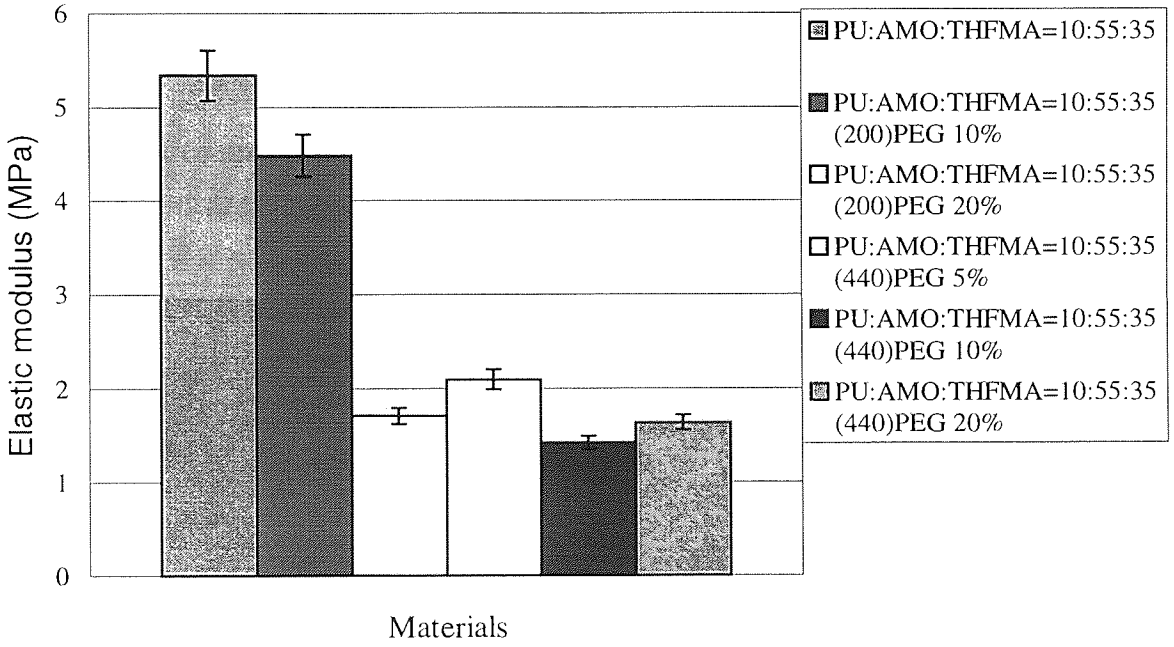

Figure 4.29 A comparison of the elastic modulus of AMO based SIPNs with and without PEG MA

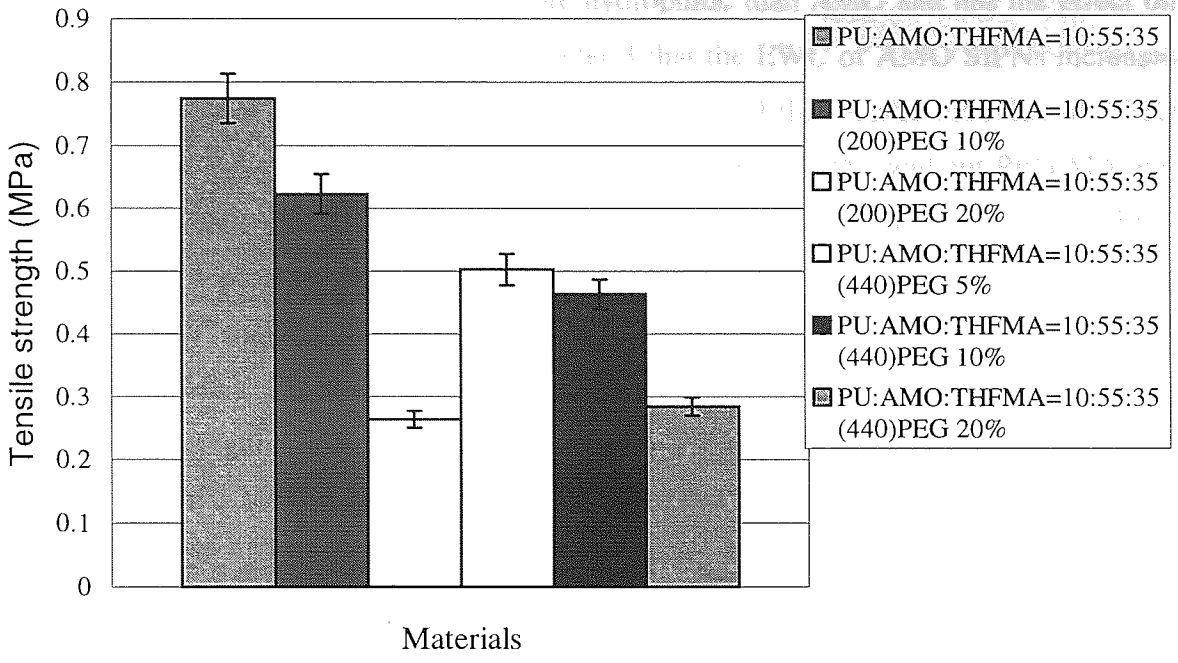

Figure 4.30 A comparison of the tensile strength of AMO based SIPNs with and without PEG MA

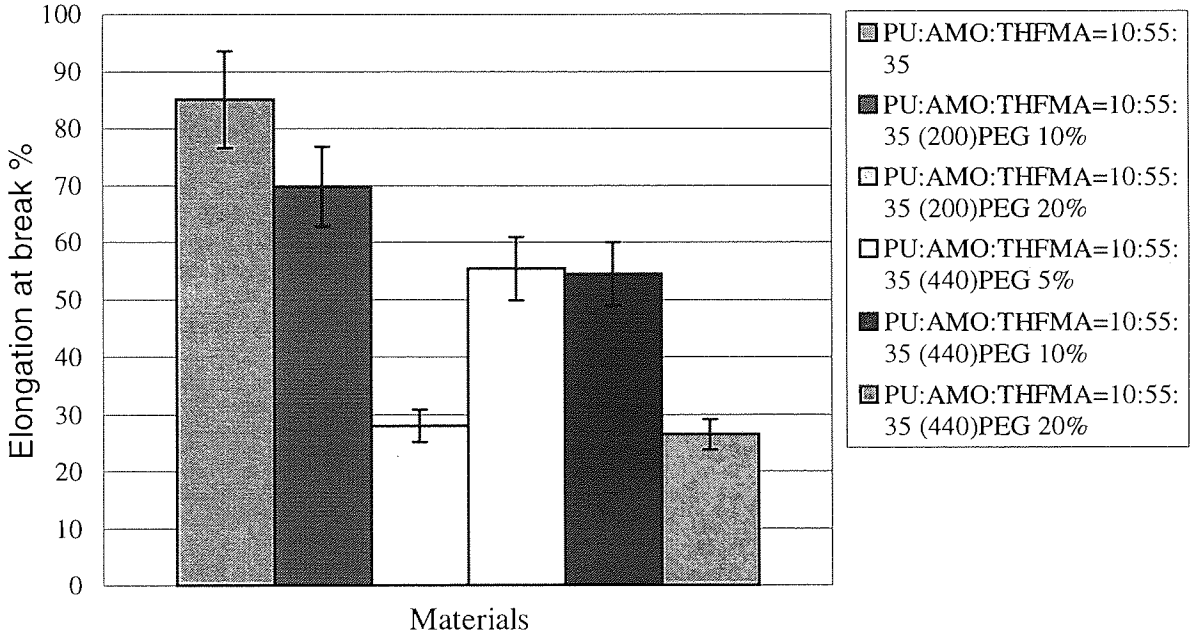

Figure 4.31 A comparison of the elongation at break of AMO based SIPNs with and without PEG MA

As discussed in Chapter 3, PEG MA is more hydrophilic than AMO and has the effect on the crosslink density. It is known from Chapter 3 that the EWC of AMO SIPNs increases with the addition of PEG MA. It is shown in Figure 4.29 that elastic modulus of AMO SIPNs containing PEG MA is much lower than that of AMO SIPNs without PEG MA and with the increase in PEG MA content, the elastic modulus of AMO SIPNs containing PEG MA decreases. A possible explanation could be that the addition of PEG MA has a greater effect on the EWC than on the crosslink density.

It can be seen in Figure 4.30 that the tensile strength of AMO SIPNs containing PEG MA is lower than that of AMO SIPNs without PEG MA and with the increase in PEG MA content, the tensile strength of AMO SIPNs with PEG MA decreases.

From Figure 4.31, the elongation at break of AMO SIPNs containing PEG MA is lower than that of AMO SIPNs without PEG MA and with the increase in PEG MA content, the elongation at break of AMO SIPNs with PEG MA decreases. This is because at high extension the increase in crosslink density due to the effect of PEG MA becomes more important.

4.4.2 NNDMA SIPNs

In Chapter 3 it was shown that PEG MA is less hydrophilic than NNDMA and the EWC does not change with the addition of PEG MA. It is shown in Figure 4.32 that the elastic modulus of NNDMA SIPNs containing PEG MA is similar to that of NNDMA SIPNs without PEG MA and with the increase in PEG MA content, the elastic modulus of NNDMA SIPNs with PEG MA does not significantly change. But the addition of EGDMA crosslinker does have a progressive effect noticeably because the gel network is so dilute.

Figure 4.33 shows that the tensile strength of NNDMA SIPNs is not affected by PEG MA.

Figure 4.34 shows that the elongation at break of NNDMA SIPNs containing PEG MA is lower than that of NNDMA SIPNs without PEG MA and the decreasing elongation at break with increasing PEG MA content. This is because at high extension the increase in crosslink density due to the effect of PEG MA becomes more important.

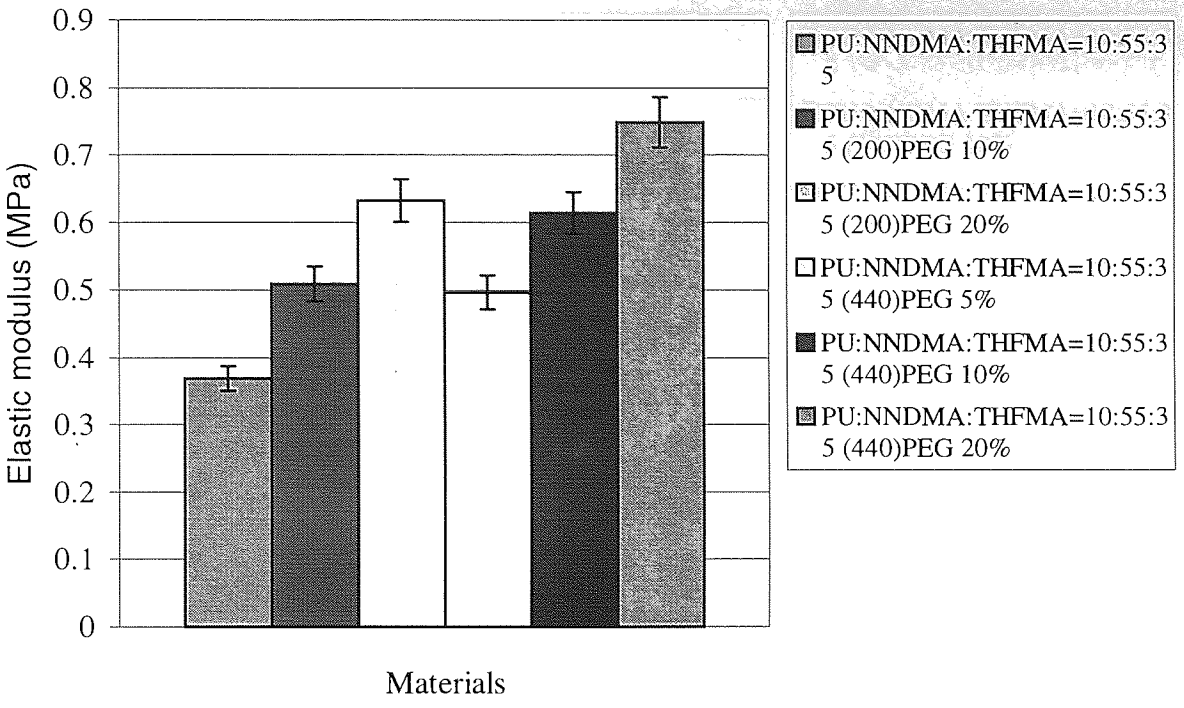

Figure 4.32 A comparison of the elastic modulus of NNDMA based SIPNs with and without PEG MA

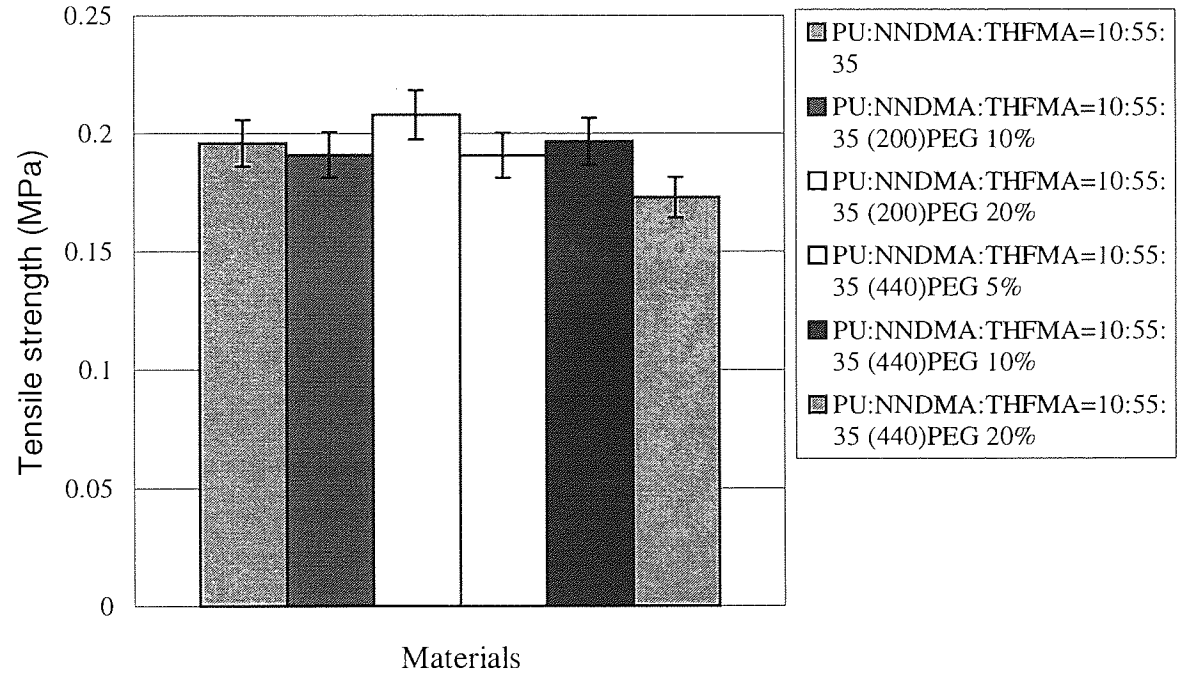

Figure 4.33 A comparison of the tensile strength of NNDMA based SIPNs with and without PEG MA

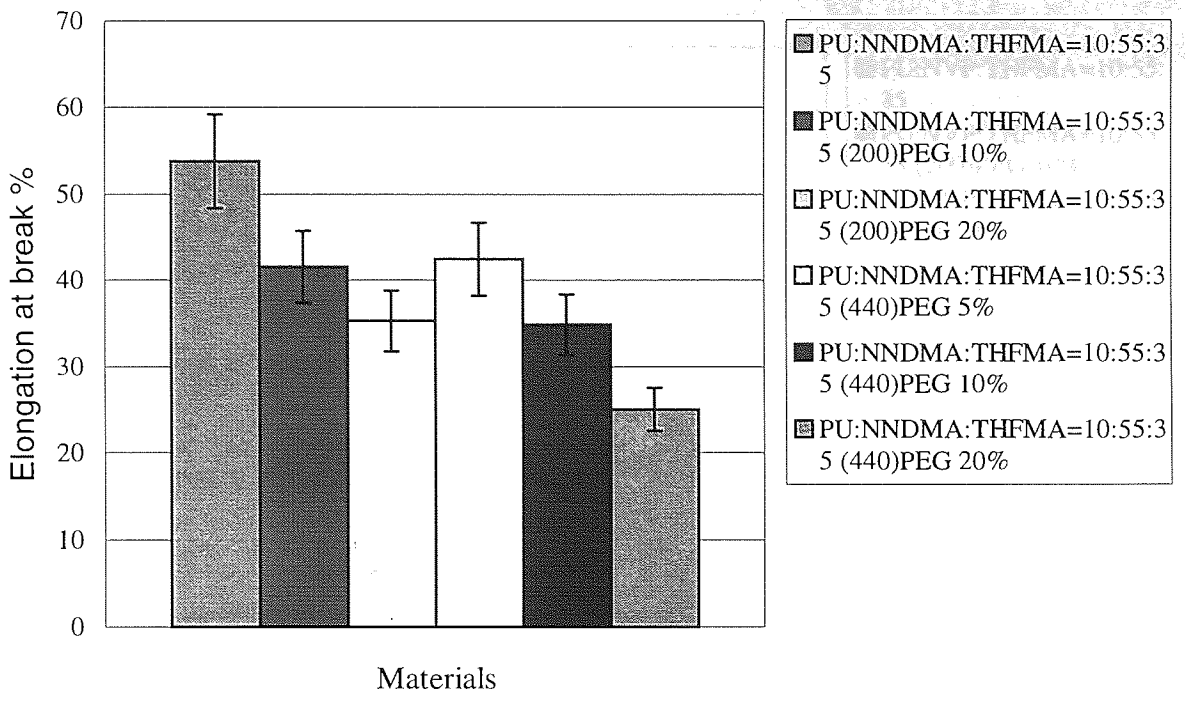

Figure 4.34 A comparison of the elongation at break of NNDMA based SIPNs with and without PEG MA

4.4.3 NVP SIPNs

As discussed in Chapter 3, PEG MA is more hydrophilic than NVP and the EWC of NVP SIPNs increases with the addition of PEG MA. In contrast to the NNDMA polymers and in accordance with AMO polymers, PEG MA has the effect of deceasing the elastic modulus (Figure 4.35). The possible explanation could be that the effect of the addition of PEG MA on EWC is more than on the crosslink density.

It can be seen in Figure 4.36 that the tensile strength of NVP SIPNs with PEG MA is lower than that of NVP SIPNs without PEG MA and with the increase in PEG MA content, the tensile strength of NVP SIPNs with PEG MA decreases.

As with AMO and NNDMA, the elongation at break of NVP SIPNs with PEG MA is lower than that of NVP SIPNs without PEG MA and with the increase in PEG MA content, the elongation at break of NVP SIPNs with PEG MA decreases (see Figure 4.37). This is for the same reason as described for AMO and NNDMA SIPNs.

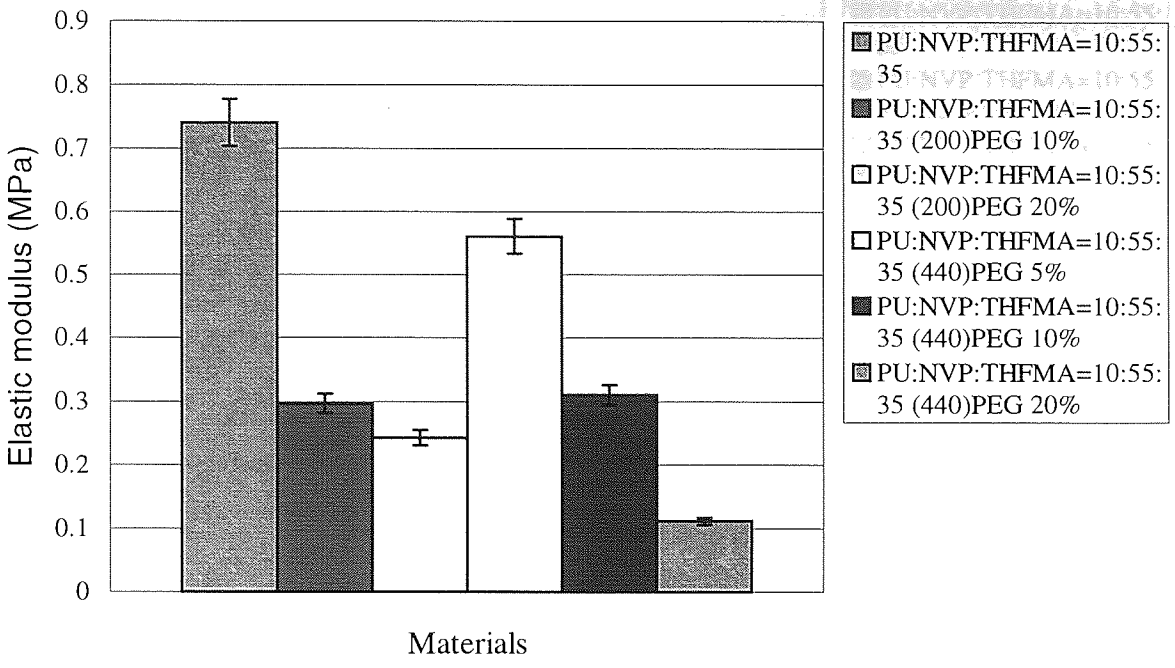

Figure 4.35 A comparison of the elastic modulus of NVP based SIPNs with and without PEG MA

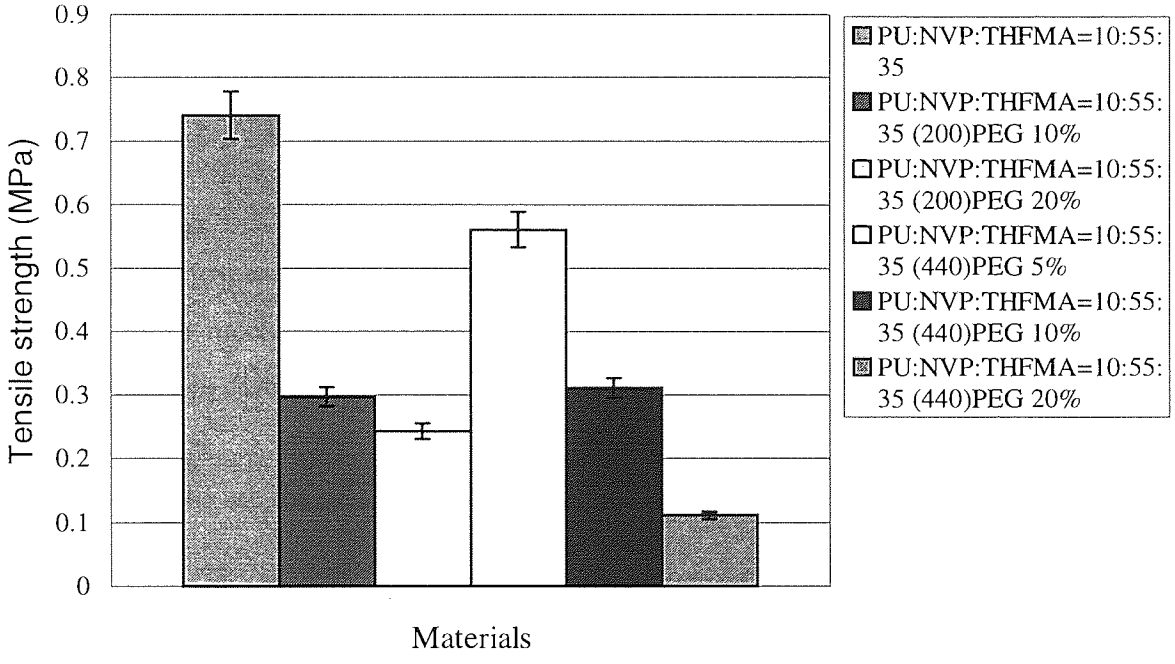

Figure 4.36 A comparison of the tensile strength of NVP based SIPNs with and without PEG MA

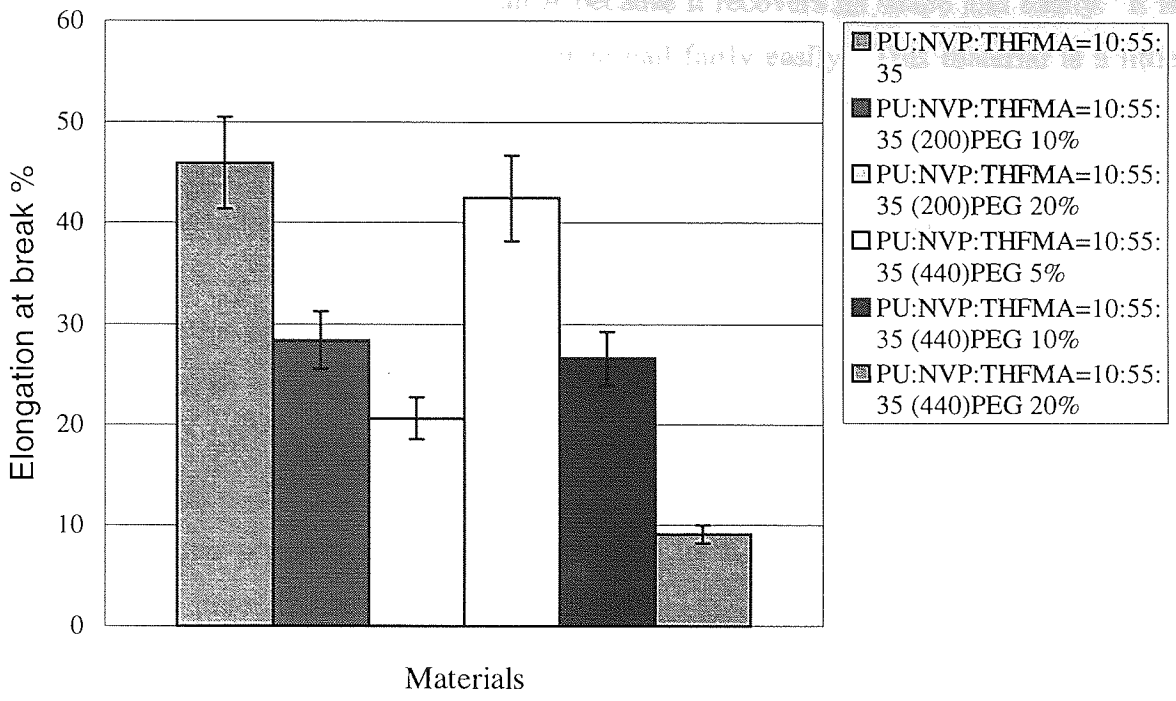

Figure 4.37 A comparison of the elongation at break of NVP based SIPNs with and without PEG MA

4.5 Handling Test

A blind handling blind test was operated by an experienced surgeon Dr. Liu after the mechanical properties of SIPNs were measured. Five different hydrogels with contrasting mechanical properties were selected carefully and were labelled A, B, C, D, or E. The surgeon did not know the identity of the formulations of the hydrogels nor the equilibrium water content or mechanical properties. The samples were cut by a size seven core-borer and were stored in distilled water before the test.

The testing results are displayed below:

A: The sample is thin in comparison to human cornea and it is stiffer and more elastic than the human cornea. No surface deformation of artificial cornea would occur if the KPro model was made with this material. But this material is friable.

B: This material is more deformable than A because it recovers its shape less easily. It is quite easily broken and can be cut with a fingernail fairly easily. This material is a little stiffer than A in terms of elasticity.

C: The sample is quite tough. However, it still can be cut with a fingernail.

D: This sample has good memory of shape and better recovery from bending. It is the toughest material so far in terms of elasticity. But it still can be cut with a fingernail.

E: It is the toughest of the five materials. It is very difficult to bend and is stiff enough for normal intraocular pressure to be able to maintain its shape. The material needs to be deformable by intraocular pressure or be hard like PMMA so that it retains its shape in the eye.

Sample ID	Gel ID	Formulations	EWC %	E.Mod (MPa)	Ts (MPa)	Eb%
A	J20	PU5 : AMO : THFMA 15 : 60 : 35	46.5	8.9	1.1	63
B	J2	PU5 : NNDMA : THFMA 20 : 50 : 30	58.6	5.0	0.8	79
C	J1	PU5 : AMO : THFMA 10 : 55 : 35	44.2	6.5	0.9	85
D	J14	PU5 : NVP : THFMA 15 : 60 : 25	62.1	2.0	1.3	41
E	J6	PU:NVP:THFMA 20 : 50 : 30	51.3	13.0	4.0	70

Table 4.2 The hydrogels prepared for the handling test

After testing these five kinds of hydrogels, comparable materials, a HEMA contact lens, porous poly HEMA and clear poly HEMA were supplied. The results are listed below:

HEMA contact lens: It is quick to go back to its structure after stretching. It deforms but cannot be cut with a fingernail.

Porous polyHEMA: It behaves like a rubber band under stretching.

PolyHEMA: It is broken quite easily.

From the clinical point of view the optical stability even with blinking and rubbing which retains its shape is due to intraocular pressure. Ideally, the material should allow measurement of intraocular pressure, as does a natural cornea. The best choice from these five materials is D. PolyHEMA is too floppy, elastic and soft. There is of course thickness dependence. An optimal material would be able to deform and recover quickly during the blink cycle, and would be slightly stiffer than polyHEMA.

4.6 Conclusions

MMA based copolymers and semi-interpenetrating network have a wide range of mechanical properties. Monomer composition, equilibrium water content and freezing water content do influence the mechanical properties of these hydrogels. The tensile strength and elastic modulus of NNDMA-MMA copolymers were consistently low because of chain transfer. The fact that AMO-MMA copolymers have the highest tensile strength and elastic modulus is due to their good sequence distribution. NNDMA-MMA copolymers have consistently the lowest mechanical properties because of its chain transfer.

As expected, the SIPN materials are stiffer and stronger than simple hydrogel copolymers in high water content, but are less elastic. Interpenetrant PU5 does have the major effect on the mechanical properties of SIPNs.

Generally the introduction of the pores into a hydrogel does not alter the mechanical properties in comparison to the corresponding clear material significantly. Neither does the pore size. However, the randomly porous nature of the hydrogels causes inconsistencies in the results.

The addition of PEG MA has an effect on the mechanical properties of SIPNs. PEG MA has more effect on the crosslink density of the AMO SIPNs and NVP SIPNs than on the hydrophilicity but the reverse is true for NNDMA SIPNs.

The conclusion drawn from the handling test with several SIPNs with different mechanical properties is that the material which can deform and recover quickly during the blink and is

slightly stiffer than polyHEMA would be best suited to surgery and would be the most effective in the eye. The simple MMA copolymers and SIPNs are not ideal KPro materials.

Chapter 5

Surface Properties Of Novel Hydrogels

5.1 Introduction

A successful keratoprosthesis material will be one which is chemically stable and non-toxic, and which does not act as an immunological or inflammatory stimulus which would cause an allergic response. In other words, the device must be biotolerant. Several workers have suggested that the surface free energy of a hydrogel is an important property in determining the biotolerence of the material[53, 54, 55]. Surface chemistry is also an important determining factor of the collagenase response of corneal epithelial and keratocyte cells to hydrogels[228]. Corneal collagenases are produced by injured epithelium and stroma tissue as part of the normal wound healing response following surgery[229].

In this Chapter the measured surface energies of three series of clear semi-interpenetrating networks described in Chapter 3 and Chapter 4 in both their hydrated and dehydrated states are presented in an attempt to correlate molecular structure with surface free energy. The results are presented graphically in this Chapter and the precise values of surface free energy, and its polar and dispersive components can be found in Appendix 3. It has been shown in Chapter 3 that AMO, NVP and NNDMA are more hydrophilic than PU5 and THFMA in the semi-interpenetrating polymer networks studied. In this section, the hydrophilic component shown in the figures indicates AMO, NVP or NNDMA.

It is very difficult to obtain consistent and accurate surface energy measurements of hydrogel materials. The actual values for each component of surface free energy can vary quite considerably when experiments are carried out by different operators.

In the dehydrated state, the use of measurements involving water droplets on freshly blotted gel surfaces suffer from the disadvantage that the surface layer dehydrates rapidly and becomes relatively hydrophobic. If a residual aqueous film is left intact before the water droplet is applied the surface is unrepresentatively hydrophilic. The essence of the problem lies in the fact that the interface between a hydrogel surface and water is much more diffuse than that between conventional hydrophobic polymers and water. It should also be remembered that due to effects such as sedimentation, evaporation of the liquid and other chemical or physical interactions at the solid surface, the contact angle is time dependent. The flatness of the sample and manual determination of the contact angles also influence the accuracy of the results obtained.

The determination of surface energies in the dehydrated state provides useful information about the surface of the polymer. However when hydrogel materials are swollen as they are in biomedical applications, the surface energies change dramatically. The determination of contact angles of hydrated hydrogels is a difficult process due to dehydration of the polymer surface during measurement, although the use of inverted droplet methods has eliminated these problems.

In the hydrated state, the use of water immersion (captive air bubble and octane droplet) techniques can maintain the surface in a hydrated state but makes it difficult for the inverted droplet probes to displace the adsorbed water layers. For this reason the results are modified by this water layer. In other studies on adsorbed species on polymer surfaces the fact that the values of the surface energy components of such systems are a function of both adsorbed and substrate layers has been demonstrated[230]. The deformation of the air bubble or octane droplet also leads to variations in values obtained for similar materials. Therefore, this technique is useful to make comparisons between materials where trends may be seen, but actual values for contact angles may vary considerably with operator.

5.2 Dehydrated State

The measured surface free energies of the dehydrated polymer surface are a function of the interactions that take place both at the surface and in the bulk of the polymer. The orientation of the chemical functional groups at the polymer surface, which may be affected by the nature of the adjacent phase, will have a bearing on the values obtained for the surface free energy.

5.2.1 Effect of PU5 on the Surface Free Energy

The effect of PU5 on the total surface free energy of three series of SIPNs, as well as the polar and dispersive components of the surface free energy, is illustrated in Figures 5.1, 5.2 and 5.3.

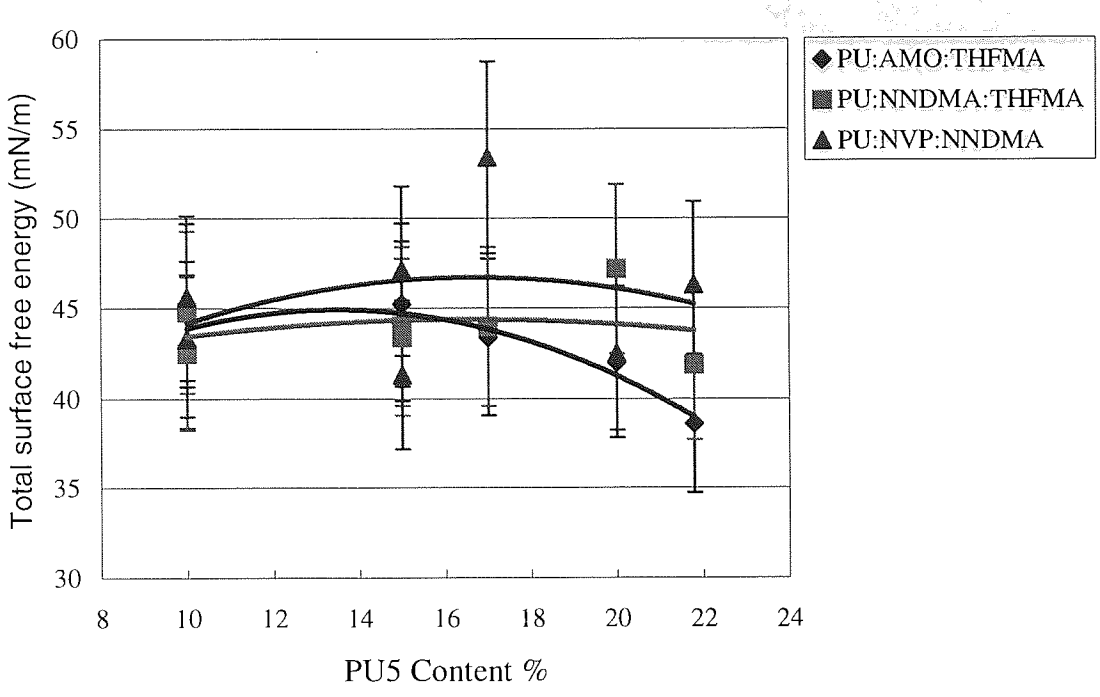

Figure 5.1 The effect of PU5 content on the total surface free energy of clear SIPNs in the dehydrated state

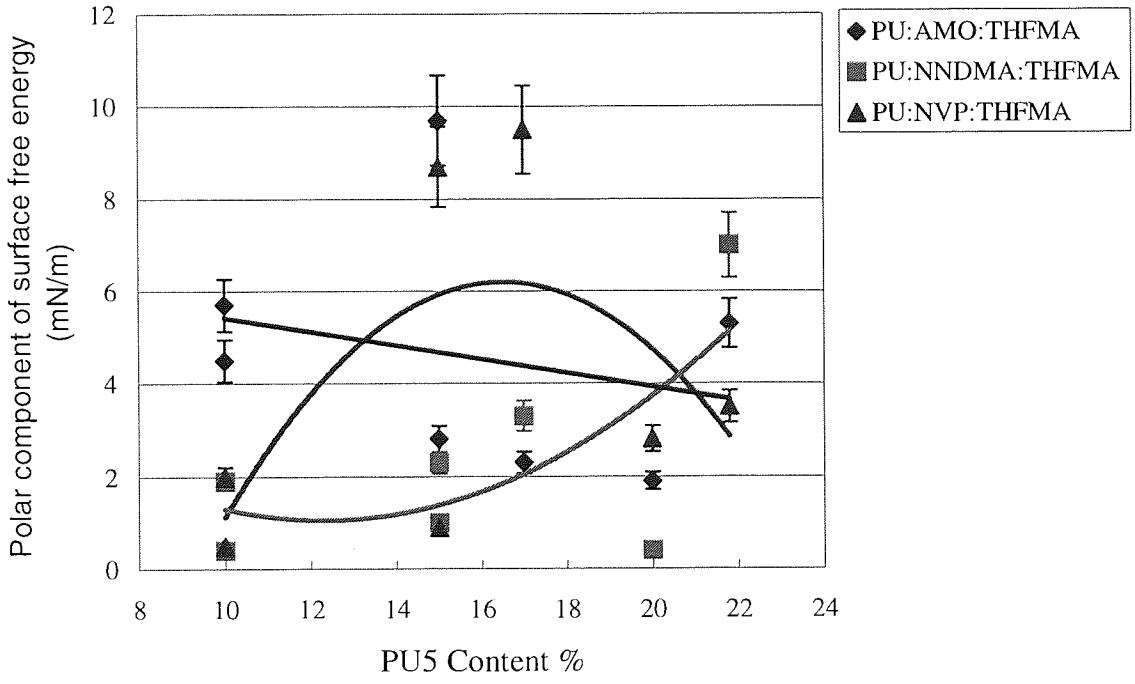

Figure 5.2 The effect of PU5 content on the polar surface free energy of clear SIPNs in the dehydrated state

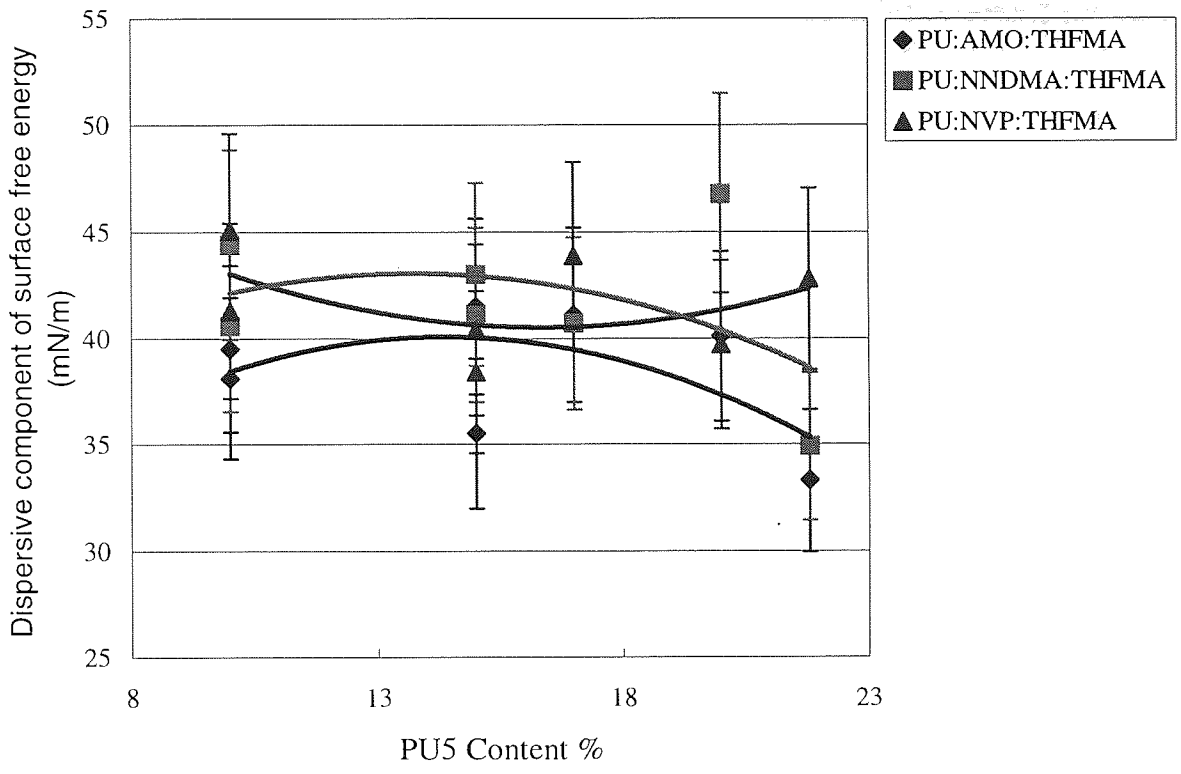

Figure 5.3 The effect of PU5 content on the dispersive surface free energy of clear SIPNs in the dehydrated state

It is shown from Figures 5.1 to 5.3 that there is no real evidence of any progressive contribution of PU5 to the surface energies of the dehydrated membrane for these three series of SIPNs. With the increase in PU5 content, the total surface free energy, and the polar and dispersive components of surface free energy change slightly, but it appears that the PU5 content does not greatly influence their values. The phenomenon could be due to the fact that the polymeric "surfactant" (Polyurethane 5) cannot easily diffuse through the dehydrated polymer.

5.2.2 Effect of Hydrophilic Component on the Surface Free Energy

The effect of hydrophilic component (AMO, NVP or NNDMA) on the total surface free energy of three series of SIPNs, as well as the polar and dispersive components of the surface free energy, is illustrated in Figures 5.4, 5.5 and 5.6.

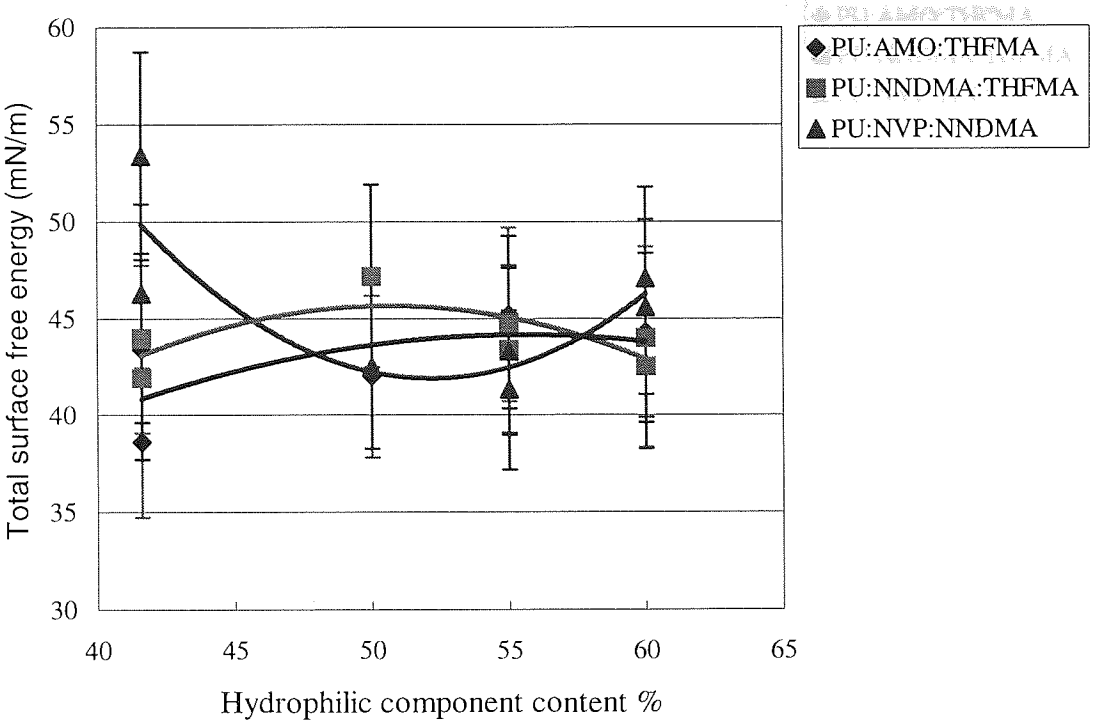

Figure 5.4 The effect of hydrophilic component content on the total surface free energy of clear SIPNs in the dehydrated state

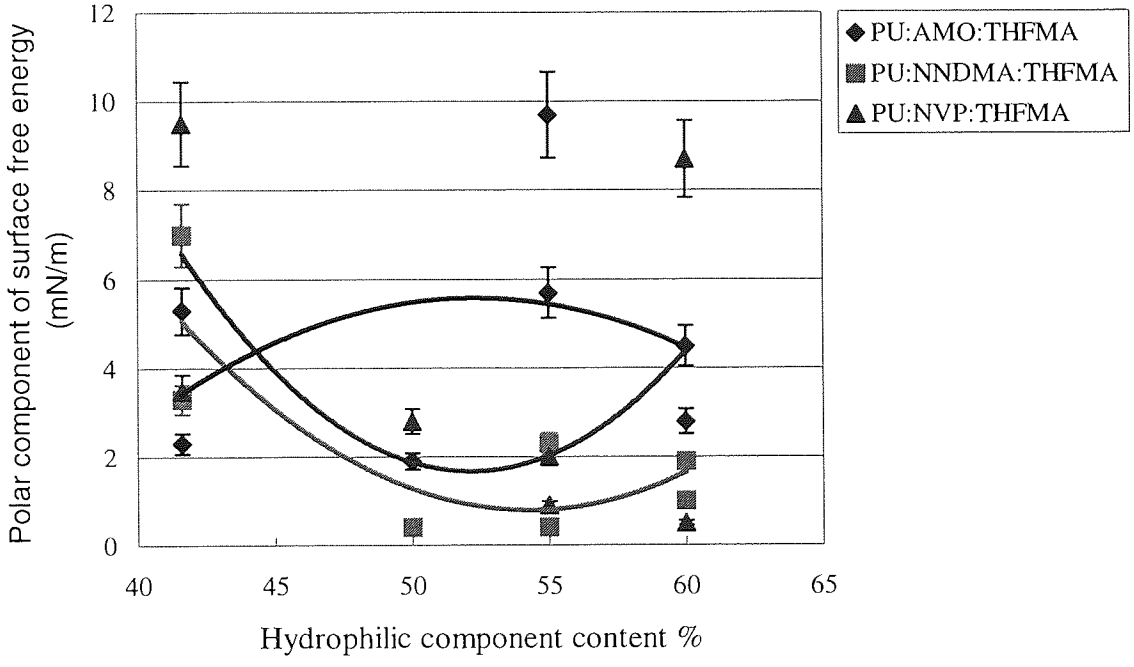

Figure 5.5 The effect of hydrophilic component content on the polar surface free energy of clear SIPNs in the dehydrated state

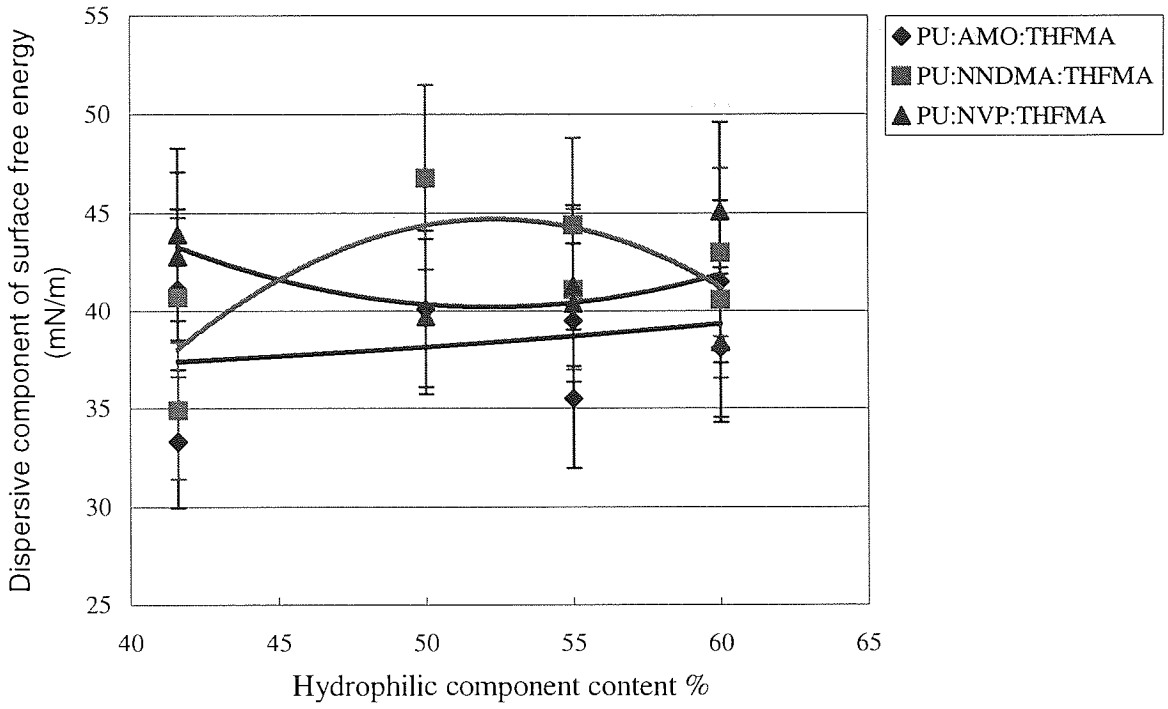

Figure 5.6 The effect of hydrophilic component content on the dispersive surface free energy of clear SIPNs in the dehydrated state

It is shown from Figure 5.4 to Figure 5.6 that with the increase in the hydrophilic component content, the total surface free energy, the polar component of surface free energy and the dispersive component of surface free energy of these three series of SIPNs only change slightly and these three series of SIPNs have similar surface free energies. It appears that hydrophilic component content does not influence the surface free energy greatly.

In the dehydrated state, SIPNs have low polar components of surface energy, the values for the dispersive component being much higher. This observation is consistent with the effect of hydrophobic group expression at the air interface and the orientation of the hydrophilic groups towards the polymer bulk. This results in the surface of the polymer being dominated by hydrophobic groups and the value of the surface energy being dominated by the dispersive component.

As discussed in Chapter 3, the EWC increases with the increase of hydrophilic component content in SIPNs. When measurements are carried out in the dehydrated state, the amount of water contained in the hydrated SIPNs does not influence the surface free energy greatly.

5.3 Hydrated State

5.3.1 Effect of PU5 on the Surface Free Energy

The effect of PU5 content on the total surface free energy of three series of SIPNs, as well as the polar and dispersive components of the surface free energy, is illustrated in Figures 5.7, 5.8 and 5.9.

It can be seen from Figure 5.7 to Figure 5.9 that there is generally a regular and progressive effect of increasing PU5 content on the surface free energies of the hydrated membranes. When the PU5 content increases, the total surface free energy, the polar component and the dispersive component of surface free energy all decrease.

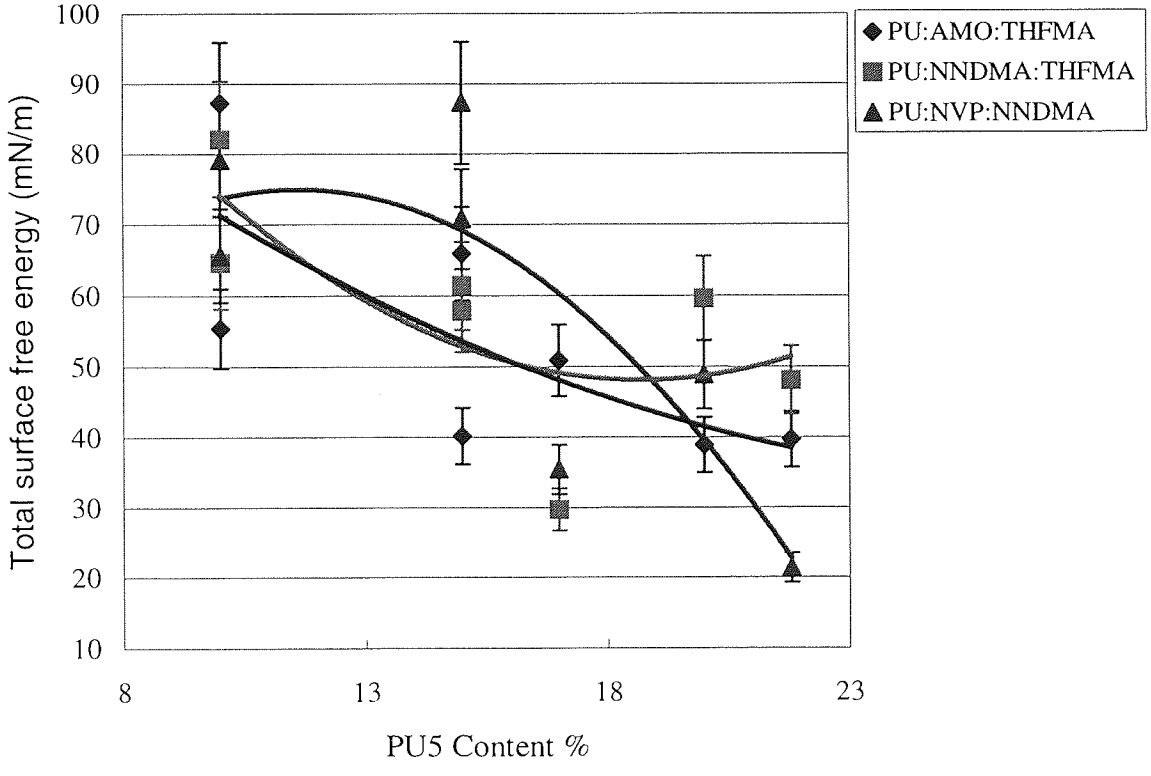

Figure 5.7 The effect of PU5 content on the total surface free energy of clear SIPNs in the hydrated state

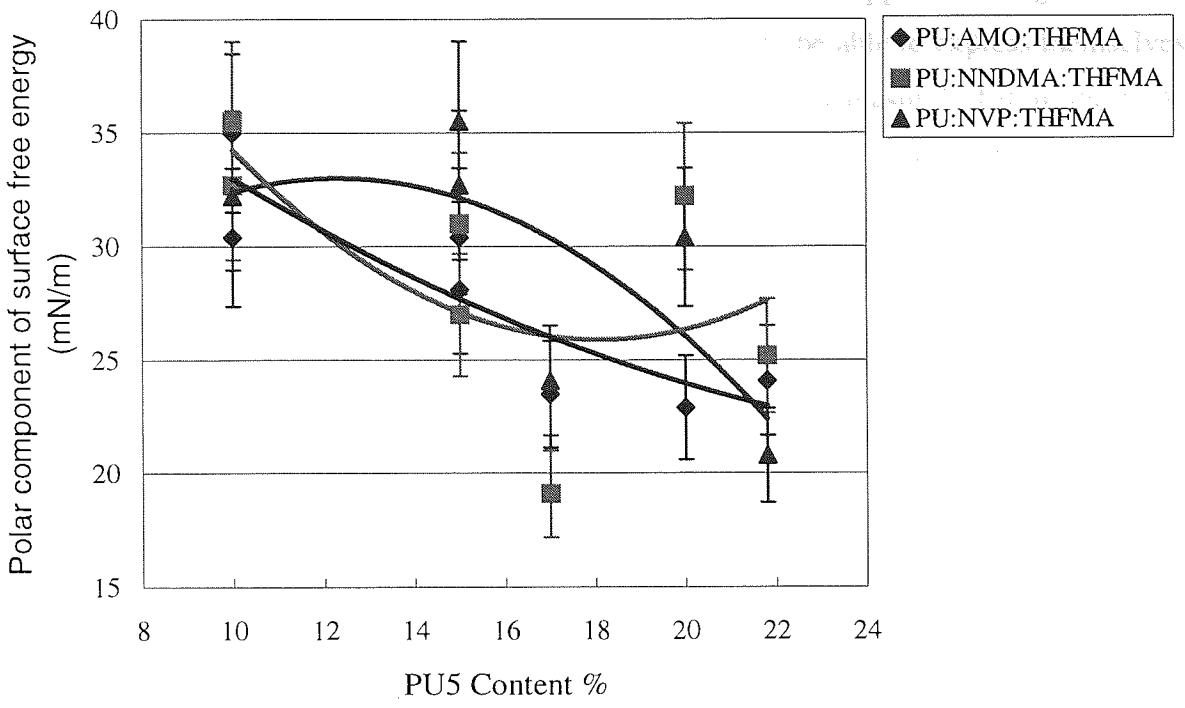

Figure 5.8 The effect of PU5 content on the polar surface free energy of clear SIPNs in the hydrated state

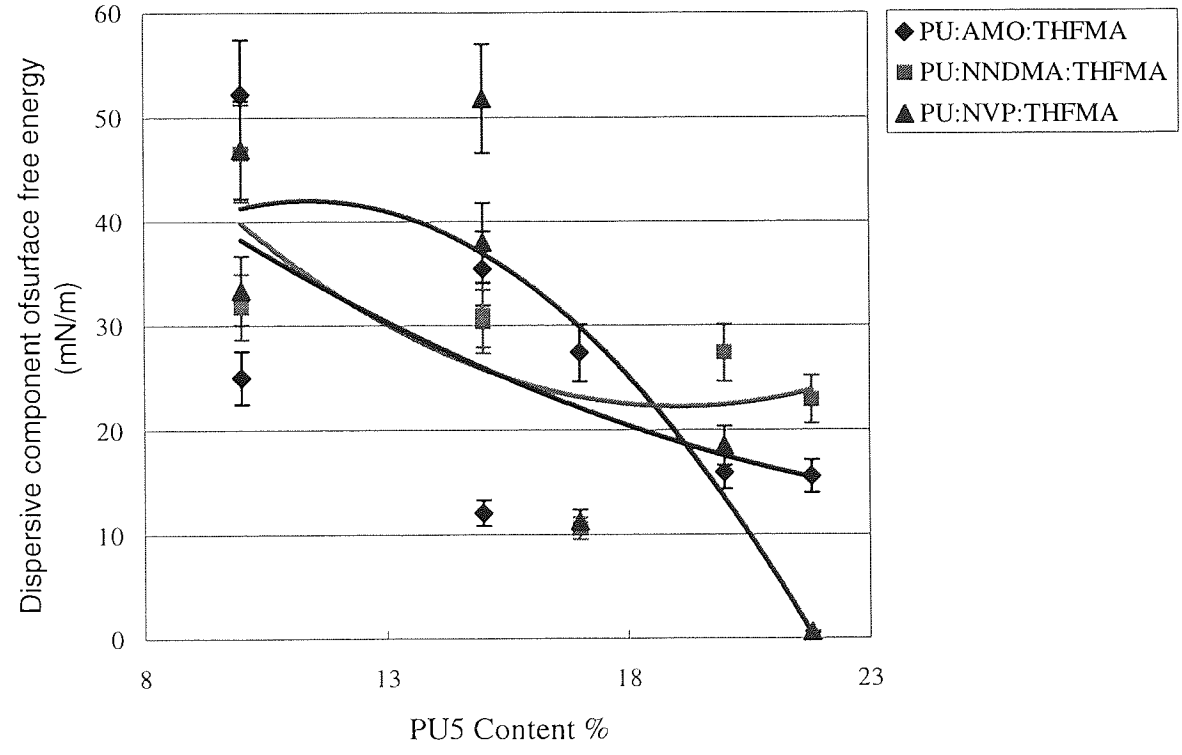

Figure 5.9 The effect of PU5 content on the dispersive surface free energy of clear SIPNs in the hydrated state

Comparing with the behaviour of PU5 in dehydrated state, PU5 appears to migrate to the surface in the hydrated SIPNs and the polar groups appear to be able to express themselves at the surface independent of the hydrophobic interpenetrant increasingly filling the bulk. Hydrophobic groups then may dominate surface and hydrophilic groups can rotate away from the surface when it is exposed to air during contact angle measurement. The factors which might cause a difference of surface free energy between the contribution of hydrophilic monomers and the hydrogel SIPNs with polyurethane are firstly chain variation of monomer and secondly less surface segregation of polyurethane.

5.3.2 Effect of Hydrophilic Component on the Surface Free Energy

Figures 5.10, 5.11 and 5.12 illustrate the effect of hydrophilic component on the total surface free energy, the polar and dispersive components of the surface free energy.

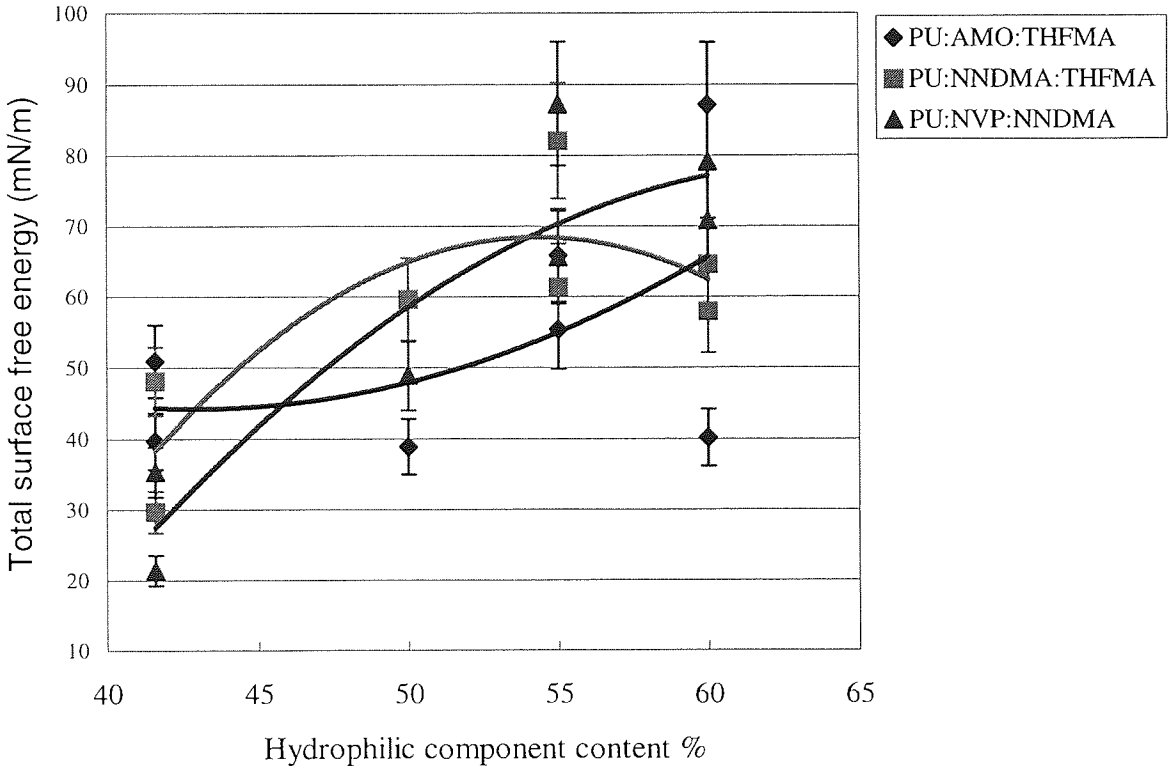

Figure 5.10 The effect of hydrophilic component content on total surface free energy of clear SIPNs in hydrated state

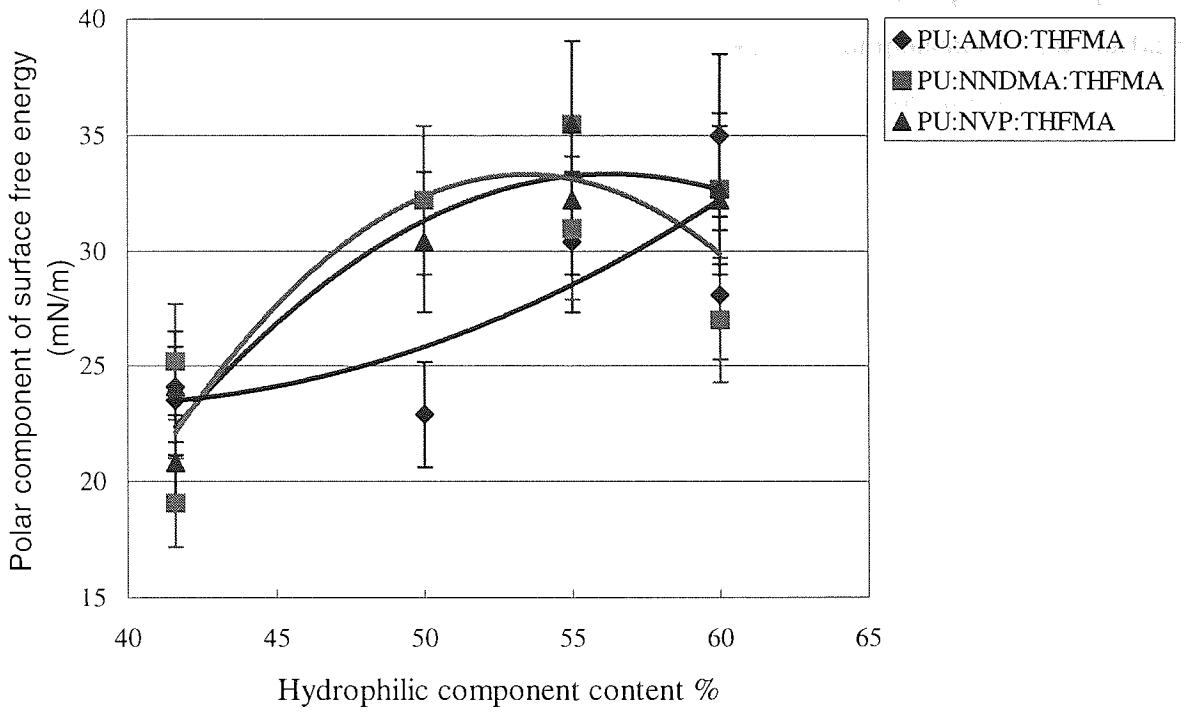

Figure 5.11 The effect of hydrophilic component content on polar surface free energy of clear SIPNs in hydrated state

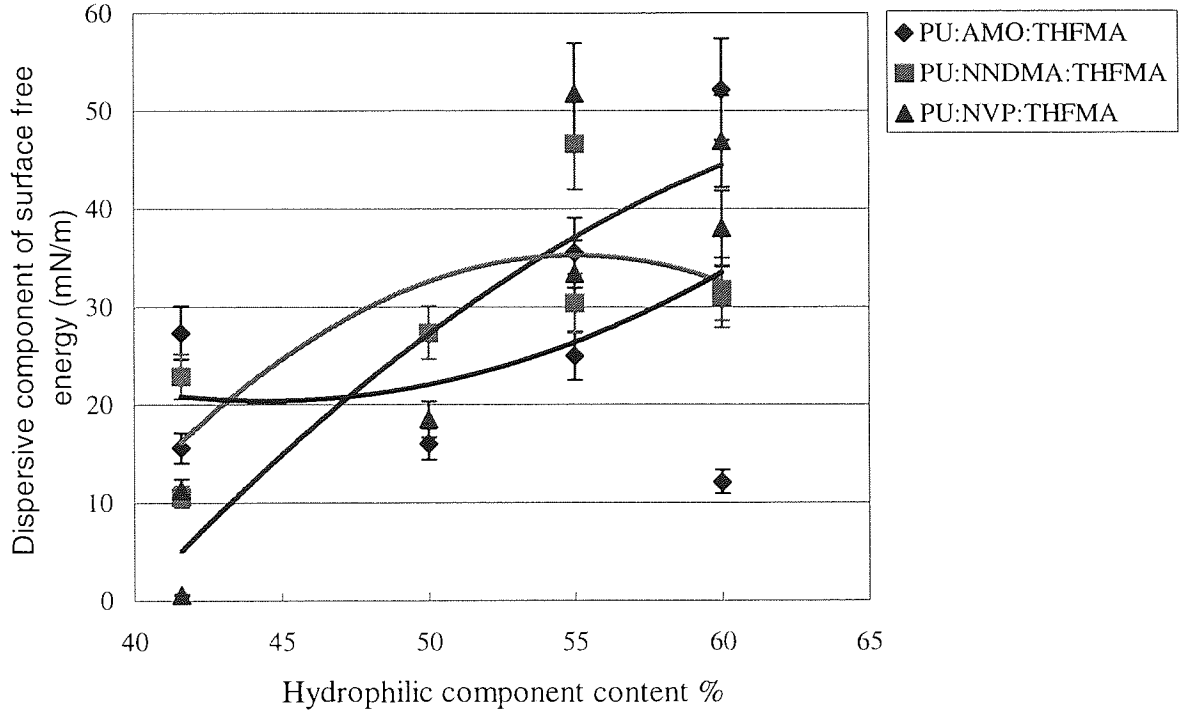

Figure 5.12 The effect of hydrophilic component content on dispersive surface free energy of clear SIPNs in hydrated state

It is shown from Figures 5.10 to 5.12 that with the increase in hydrophilic component content the total surface free energy, the polar and dispersive components of the surface free energy increase steadily. In the hydrated state, surface group rotation is more freely than in dehydrated state. The increase of polar groups along with the increase of hydrophilic component content causes the increase in the surface free energy although the structural features of the monomers used in these experiments, AMO, NVP, NNDMA and THFMA, all having either a ring or an α-methyl group may restrict the freedom of rotation around the backbone of the polymer. Thus in the hydrated state it seems likely that the surface of the material remains dominated by the hydrophilic groups at the surface.

The polymer structure is capable of influencing the detailed surface energy components. The results support the view that the direct measurement techniques currently available for hydrated surfaces suggest the presence of a surface layer of water that dominates the measured values. Molecular processes at hydrogel surfaces (e.g. biological interaction and protein deposition) indicate that surface changes, inadequately detected by these macroscopic droplet techniques, take place as the nature of the polymer matrix and the volume fraction of water are varied. The measured surface energies of the hydrated hydrogels presented in this thesis are all higher than the values obtained from the same hydrogels in the dehydrated state. This phenomenon has been reported by other workers[14, 226, 231].

The surface energy of water at 72.8 mN/m with a high polar component of surface free energy (51.0 mN/m) should be higher than those of polymers and particularly the dispersive component of the polymers should never fall below around 18 mN/m. There do appear to be some minor anomalies in the data obtained here, possibly due to the experimental error described previously.

5.3.3 Effect of the EWC on Surface Free Energy

The effect of the EWC on the surface properties of three kinds of clear SIPNs is illustrated in Figures 5.13, 5.14 and 5.15.

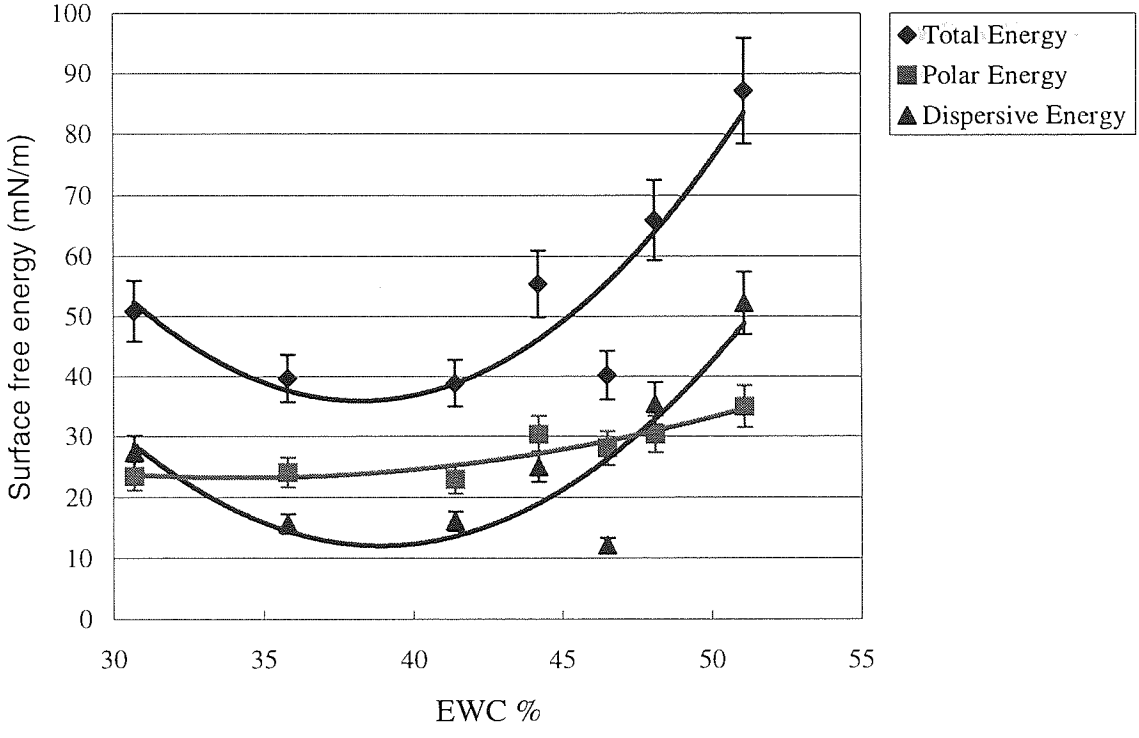

Figure 5.13 The effect of equilibrium water content on the surface free energy of clear AMO based SIPNs

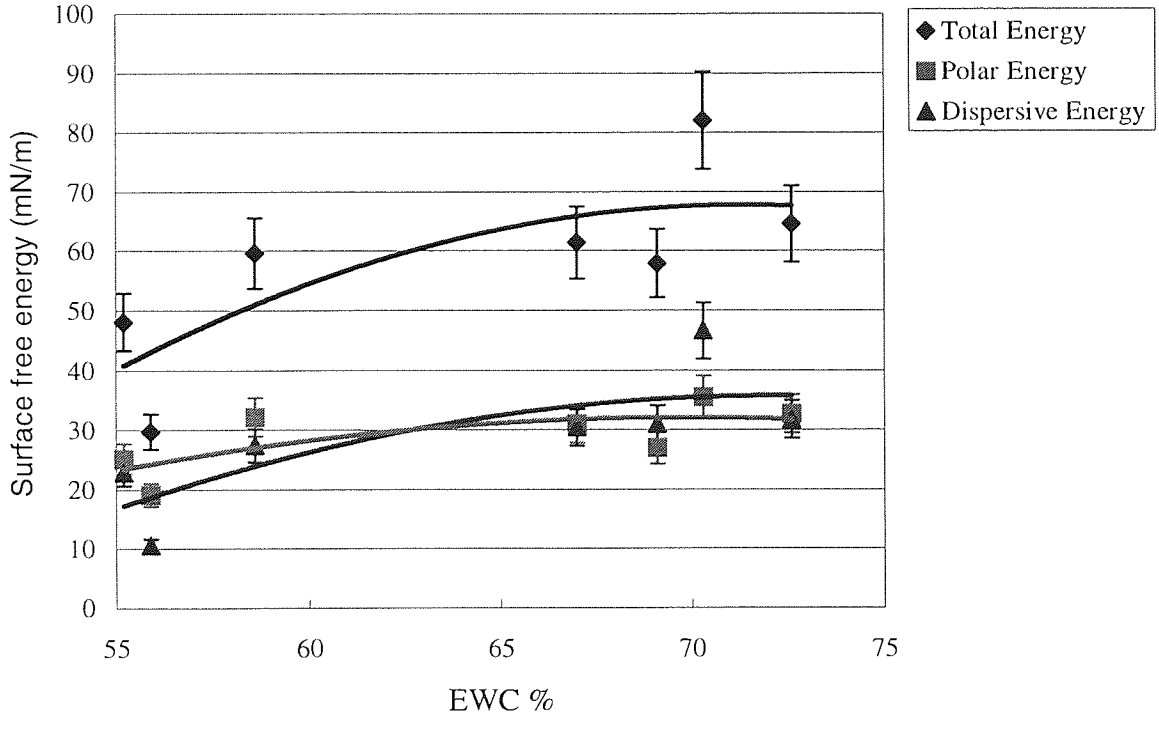

Figure 5.14 The effect of equilibrium water content on the surface free energy of clear NNDMA based SIPNs

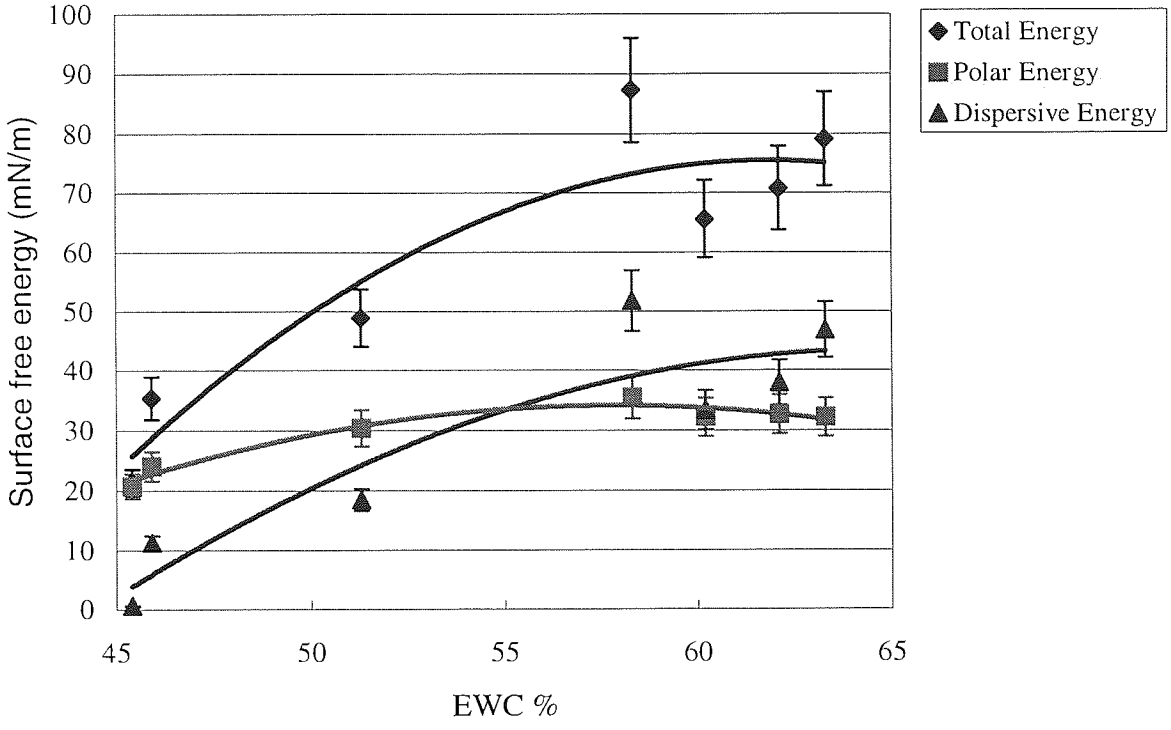

Figure 5.15 The effect of equilibrium water content on the surface free energy of clear NVP based SIPNs

In the hydrated state, as the EWC increases, the polar and dispersive components of the surface free energy and thus the total surface free energy of the NVP and NNDMA SIPNs increase steadily. The total surface free energy and the dispersive component of the surface free energy of the AMO SIPNs decrease slightly and then increase with further increase in the EWC. The change in the polar component of the surface free energy (γ^p) is to a less extent than the change in the dispersive component of the surface free energy (γ^d). For biological fluids, such as blood and tears, the total surface free energy of the fluid is about 45 mN/m, the polar component being about 22 mN/m and the dispersive component being about 23 mN/m. From Figures 5.13 – 5.15, it appears that in each case a total surface free energy of about 45-50 mN/m can be achieved with a range of EWC from 45% to 55%. When the total surface free energy is 45 mN/m, the γ^p and γ^d of AMO SIPNs, NVP SIPNs and NNDMA SIPNs are 27 mN/m and 18 mN/m, 28 mN/m and 17 mN/m, 25 mN/m and 20 mN/m respectively. The polar component usually must equal the dispersive component for the materials to be successful in biological systems. The NNDMA SIPNs is better than the AMO SIPNs and NVP SIPNs in this respect.

5.4 Conclusions

In the dehydrated state the surface free energy is dominated by the dispersive component whereas in the hydrated state the polar component is dominant due to the presence of water and the effect of rotation of the surface groups around the carbon backbone chain.

An increase in hydrophilic monomer concentration does not significantly influence the surface free energy of the SIPNs tested and these three SIPNs have similar surface free energies in the dehydrated state. However, in the hydrated state with the increase of the hydrophilic component, the surface free energy of the SIPNs increases steadily.

In the dehydrated state, PU5 content does not greatly influence the surface free energy of the SIPNs because it cannot easily diffuse through the dehydrated polymer. However, in the hydrated state with the increase of PU5 content, the surface free energy of the SIPNs decreases because it can migrate to the surface in the hydrated SIPNs.

It appears that the three series of semi-interpenetrating networks have similar total surface free energies to the biological fluid in the hydrated state when they have about 45% to 55% equilibrium water content. The NNDMA SIPNs show better biocompatibility than the AMO SIPNs and the NVP SIPNs.

Chapter 6

Cellular Response To Novel Hydrogels

6.1 Introduction

A hydrogel used as a biomaterial must be well tolerated when placed in the biological environment, to avoid rejection of the implant. The material must not be recognised as foreign by the host if the material is to be retained.

Cell biology provides a powerful tool which can be used to study the interface between a synthetic material and the biological system. Cells can differentiate small changes in surface characteristics that cannot be detected by other means[14]. Evaluation under *in vitro* conditions can provide rapid and inexpensive data about biological interactions. Single cell culture models have the advantage that the effects of single factors can be isolated and studied far more easily than is the case with *in vivo* experimentation. The *in vitro* cell culture techniques can also minimize the use of animals in research.

All KPros currently used produce serious complications such as implant extrusion, retroprosthetic membrane formation, infection and glaucoma[121]. The incorporation of biocompatible materials which are conducive to implant integration with the host cornea could limit these complications. While the central optical cylinder should hinder cellular ingrowth, the peripheral skirt should enhance host keratocyte adhesion and spreading. These cells will anchor the KPro to the surrounding tissue and induce controlled matrix remodelling so that the implant becomes an integral component of the cornea.

Numerous studies have considered the ability of various biomaterials to encourage cell adhesion and growth. The process is complex and involves the interaction of a number of factors including surface group expression, surface charge, surface energy, surface morphology, wettability (hydrophilicity/hydrophobicity), sequence distribution and equilibrium water content, porosity, and roughness[224]. According to these workers, cell adhesion and spreading tend to favour moderately hydrophilic materials which incorporate a positive charge and depend on initial protein adsorption by the polymer[214, 232, 233].

The aim of this chapter is, therefore, to investigate the cell adhesion of a number of hydrogels described in previous chapters. The results are displayed in Figures 6.2 to 6.4 and the precise values can be found in Appendix 4.

6.2 Cell Adhesion

The majority of mammalian cells, including fibroblasts, require a suitable substratum in order to grow. Such cells are called anchorage-dependent cells because they must adhere to the substrate before they will grow[234]. Complex molecular interactions that determine and regulate cell behaviour are established when the cells come into contact with the substrate.

Four major classes of adhesion receptors on the cell surface have been identified: cadherins, immunoglobulin superfamily receptors, selectins, and integrins. Cadherins are Ca^{2+} dependent, homophilic cell-cell adhesion molecules. Immunoglobulin (Ig) superfamily receptors are a large group of receptors, including antibodies and T cell receptors, which bind to integrin type receptors on other cells and homophilic receptors. Selectins are calcium dependent receptors involved in the regulation of leucocyte binding to endothelium at sites of inflammation. Integrins are heterodimeric receptors with ligand specificities controlled by divalent cations, binding to extracellular matrix proteins and Ig and some integrin receptors on other cells.

The integrins mediate adhesion to proteins such as fibronectin (Fn), vitronectin (Vn) and laminin which can be absorbed to material surfaces from tissue fluids and serum.

There are two theories of cell adhesion. The first is the colloid stability theory which describes a balance between electrostatic repulsion, due to negative charges on the cell surface, and electromagnetic attraction, due to varying dipole moments in the surface layers and intervening medium[235]. No contact is involved in these interactions. This theory does not explain the preferred adhesion to more negatively charged surfaces such as modified polystyrene.

An alternative theory claims that close range intermolecular forces such as hydrogen bonds are necessary for cell adhesion[236, 237]. This theory predicts that cells will adhere more strongly to hydrophilic surfaces than hydrophobic surfaces, and in general this is found to be the case experimentally[238, 239].

6.3 Calcein AM Assay for Viable Cell Adhesion

Previous works indicate that calcein AM (calcein acetoxy methyl ester) best satisfies the criteria for assaying cell adhesion[240, 241, 242], with the least effect on cell viability and other cell functions. Calcein AM (Figure 6.1) also avoids the use of radioactive material[243, 244]; it is better retained by viable cells than are fluorescein, carboxyfluorescein and BCECF (2', 7'-bis-(2-carboxyethyl) -5-(and-6)-carboxyfluorescein) and tends to have brighter fluorescence in a number of mammalian cell types[245].

.

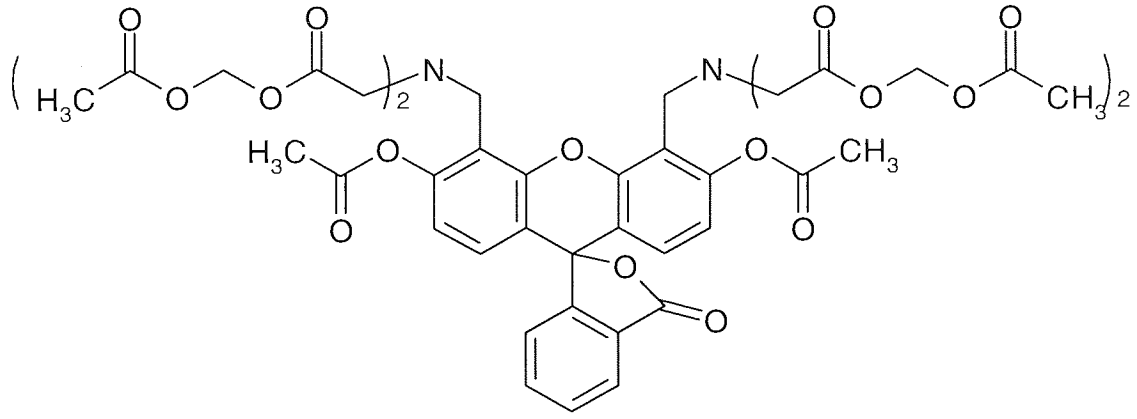

Figure 6.1 Structure of calcein AM

Calcein AM is cleaved by cellular esterases present within viable cells to form a fluorescent green product which is membrane impermeable.

Calcein AM assays were carried out by Dr. Sandeman in the Department of Pharmacy and Biomolecular Sciences at the University of Brighton using Ek1.Br human foetal keratocytes established in the department[246].

6.3.1 Clear SIPNs with PEG MA or without PEG MA

The presence of small amounts of PEG on biomaterial surfaces may prove useful to switch the balance between cell growth and differentiation. The incorporation of polyethylene glycol (PEG) onto biomaterials is expected to effectively reduce protein deposition and cell adhesion[224]. It is necessary to investigate the effect of PEG MA on the cell adhesion of the clear SIPNs which used as the central optical cylinder should hinder cellular ingrowth. A

number of clear SIPNs with or without PEG MA described in previous chapters is investigated for cell adhesion in this section. Their compositions and equilibrium water contents are displayed in Table 6.1 and the results of cell adhesion assays are illustrated in Figure 6.2.

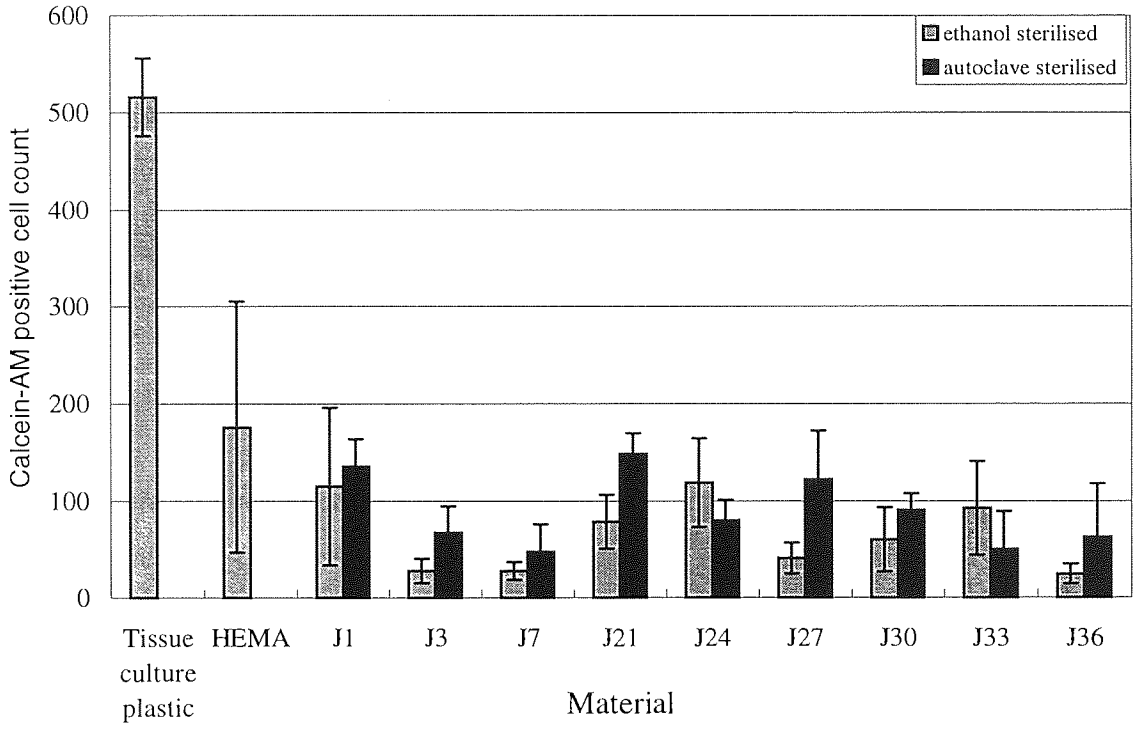

Figure 6.2 The calcein AM assay of clear SIPNs (autoclaved versus ethanol sterilised), using EK1.Br cells (n=3, mean +/- SEM)

Gel ID	Composition (by weight)	EWC %
J1	PU5 : AMO : THFMA = 10 : 55 : 35	44.2
J3	PU5 : NNDMA : THFMA = 10 : 55 : 35	70.3
J7	PU5 : NVP : THFMA = 10 : 55 : 35	60.2
J21	PU5 : AMO : THFMA = 10 : 55 : 35 (200) PEG 5%	49.1
J24	PU5 : NNDMA : THFMA = 10 : 55 : 35 (200) PEG 5%	72.6
J27	PU5 : NVP : THFMA = 10 : 55 : 35 (200) PEG 5%	64.0
J30	PU5 : AMO : THFMA = 10 : 55 : 35 (440) PEG 5%	47.8
J33	PU5 : NNDMA : THFMA = 10 : 55 : 35 (440) PEG 5%	71.5
J36	PU5 : NVP : THFMA = 10 : 55 : 35 (440) PEG 5%	63.8

Table 6.1 The composition and EWC of the clear SIPNs used in the calcein AM assay

It is obvious that materials implanted into the body of a human or an animal must be sterile to avoid subsequent infection that can lead to serious illness or death. There were two sterilisation methods used in the work described in this thesis, autoclaving and ethanol sterilisation.

The effect of autoclaving versus ethanol sterilisation was assessed using duplicate disks and 72-hour incubation of the EK1.Brs with the materials followed by calcein AM staining. The autoclave protocol involved the sterilisation of samples in water at 115 ^{o}C for 5 minutes in a glass universal bottle. The ethanol protocol involved placing all samples into 70% ethanol in a 24 well plate for 10-20 minutes. To allow the samples to deswell, the samples are left in distilled water for 10 minutes. The samples are then left in PBS overnight in the incubator.

20 fields were counted under the fluorescence microscope for each disc. Higher cell counts were observed on materials sterilised by autoclaving, so the same method should be used for all samples if meaningful comparative data is to be obtained. The difference could be explained by residual ethanol causing lower cell adhesion when ethanol sterilisation has been used, or perhaps surface group modification due to the heat of autoclaving.

Cell culture plastic exhibits approximately 3 times the number of adhered cells than poly HEMA. Adhesion can be seen with all SIPNs materials in Figure 6.2 but all attached fewer cells than polyHEMA and tissue culture plastic. Previous researchers have shown that 100% polyHEMA hydrogels discourage cell attachment[247, 248] and they generally can be considered to be non cell adhesive hydrogels. All the hydrogels displayed in Figure 6.2 do not support cell adhesion. This means that they do show good potential for KPro core materials.

Hydrogels with –OH as the water structuring group (poly HEMA based hydrogels)[249] containing between 35% and 60% water do not support cell attachment. As the water content is reduced below 40% (by copolymerisation with a hydrophobic monomer), cell attachment and cell spreading increases. Hydrogels containing more than 60% water (by copolymerisation with ionic monomers) show an increase in cell attachment, however no cell spreading was observed. The EWC of polyHEMA used as the negative control is around 38%. From Table 6.1, it can be seen that all clear SIPNs tested have a higher EWC

than polyHEMA. This could be one possible explanation why these clear SIPNs attach fewer cells than polyHEMA. Another possible explanation is that there are no strong donor or acceptor groups such as acrylamide or methacrylic acid in these three nitrogen containing monomers, AMO, NVP and NNDMA. J1 shows the best cell adhesion result in three clear SIPNs without PEG MA. It may be due to the presence of oxygen in the ring structure.

Cell adhesion decreases with increased EWC within a family when these hydrogels were sterilised by autoclaving. J21 (49.1%) has the highest cell adhesion and J24 (72.6%) has the lowest cell adhesion in J21, J24 and J27. The same phenomenon can be seen in the series J30, J33 and J36.

When AMO SIPNs were sterilised by 70% ethanol, comparing J1, J21 and J30, the number of cells attached on the surface decreases with the addition of PEG MA. PEG MA does protect the surface of the SIPNs and reduce the cell adhesion. This could be due to the presence of the hydrophilic PEG, causing a net reduction in the degree of hydrophobic-hydrophobic interactions between the biomaterial and adsorbed cell adhesion protein. On the contrary, in the same conditions, the addition of PEG MA enhances the cell adhesion compared with the NNDMA clear material greatly, but the addition of PEG MA does not affect the cell adhesion of NVP clear materials significantly. It is known that the chemical and physical surface structure of polymers is mainly responsible for the reactions in biological systems[250]. It suggested that cell attachment is promoted by the presence of polar surface groups such as hydroxyl and carbonyl[251]. With increasing oxygen content, the cell attachment increased, which implied that a high surface polarity was evidently of most benefit for cell attachment[252]. The increased polarity improved surface hydrophilicity, and subsequently enhanced the cell spreading on the surface and increased the growth rate. PEG MA, NNDMA, NVP and AMO all contain carbonyl groups and so would be expected to increase the cell adhesion. Therefore, the difference in the effect of PEG MA on the cell adhesion for these three kinds of SIPNs may be caused by the sequence distribution of the polymers.

Comparing J21 with J30, J24 with J33, J27 with J36 using both sterilisation methods, 70% ethanol and autoclaving, the number of cells attached on the clear SIPNs containing PEG MA 200 is greater than those containing PEG MA 440. This indicates that the longer chain PEG MA is better at protecting the surface from cell adhesion, i.e. 440 is better than 200.

Some uncommon phenomena are observed in Figure 6.2 for hydrogels sterilised using autoclaving. For example, J3 adhered more cell than J7 even if it has a higher EWC; the number of cells attached on J21 was also greater than on J1. This may be caused by the harsh autoclaving. Autoclaving is the simplest method of sterilisation but this involves subjecting the materials to a very high temperature and pressure. It was thought that this treatment could perhaps modify the polymers in some way, thereby changing the surface properties of the materials. If the materials become blocky, regions of different phases will alter the materials properties. An increase in temperature and mobility will lead to phase separation. Therefore autoclaving may aid cell adhesion as some of the materials exhibited visible lines on their surface (evidence of phase separation) after sterilisation with this method. The influence of PU5 on the surface energies may contribute to this abnormal phenomenon.

6.3.2 Low Water Content SIPNs

As mentioned previously, low water content materials can increase cell adhesion. Two low water content clear SIPNs are investigated in this section. Their composition and EWC are shown in Table 6.2 and the result of cell adhesion assays are displayed in Figure 6.3.

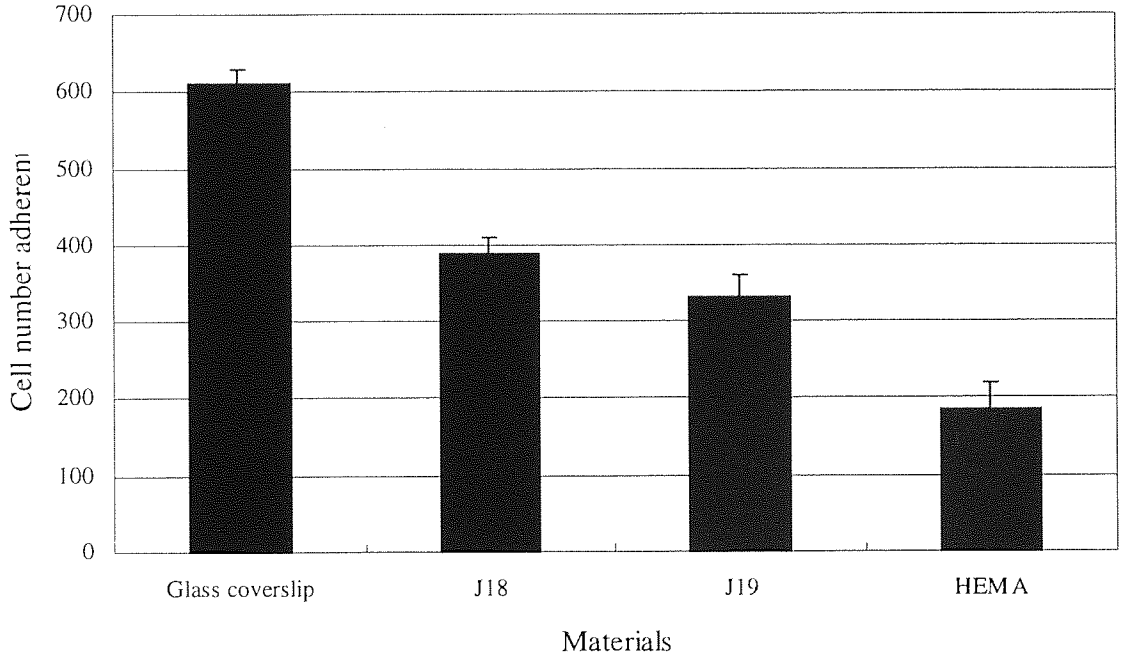

Figure 6.3 The calcein AM assay of low water content hydrogels, using EK1.Brs cells (n=5, mean +/- SEM)

Gel ID	Composition (by weight)	EWC %
J18	PU5 : AMO : THFMA = 16.8:41.6:41.6	30.7
J19	PU5 : AMO : THFMA = 21.8:41.6:36.6	35.8

Table 6.2 The composition and EWC of the low water content hydrogels used in calcein AM test

Figure 6.3 shows that the number of cells attached on the low water content J18 and J19 materials are much higher than on poly HEMA as expected. The EWC of J19 is only 3% less than that of poly HEMA, but the number of cells attached on J19 is approximately twice the number on polyHEMA. This proves that the EWC plays a very important part in the cell adhesion of hydrogels. It should be mentioned, however, that only two low water content SIPNs were tested, and that EWC is only one of a number of factors likely to affect cell adhesion, the others include surface chemical groups, surface energy and surface topology.

6.3.3 Porous SIPNs

The porous SIPNs used as the peripheral skirt of the KPro should enhance host keratocyte adhesion and spreading. Several porous SIPNs synthesized using different porosigens and pore sizes are investigated in this section. Their compositions are displayed in Table 6.3 and the results are illustrated in Figure 6.4.

Gel ID	**Composition**
F1	PU5 : AMO : THFMA = 10 : 60 : 30 20% Dextrin (Pore size < 38 μm)
F2	PU5 : AMO : THFMA = 10 : 60 : 30 20% Dextrin (Pore size < 38 μm) + 4% Dextran
F3	PU5 : AMO : THFMA = 10 : 60 : 30 20% Salt (Pore size > 90 μm)
F4	PU5 : AMO : THFMA = 10 : 60 : 30 20% Salt (Pore size: 63 - 90 μm)
F5	PU5 : AMO : THFMA = 10 : 60 : 30 20% Salt (Pore size > 90 μm) + 4% Dextran
F6	PU5 : AMO : THFMA = 10 : 60 : 30 20% Salt (Pore size: 63 - 90 μm) + 4% Dextran

Table 6.3 The composition of the porous SIPNs used in calcein AM test

Gel ID	Composition
J5A	PU5 : NNDMA : THFMA = 10 : 60 : 30 20% Dextrin (Pore size < 38 μm)
J5B	PU5 : NNDMA : THFMA = 10 : 60 : 30 20% Dextrin (Pore size < 38 μm) + 4% Dextran
J5C	PU5 : NNDMA : THFMA = 10 : 60 : 30 20% Salt (Pore size: 38 – 63 μm)
J5D	PU5 : NNDMA : THFMA = 10 : 60 : 30 20% Salt (Pore size: 63 - 90 μm)
J5E	PU5 : NNDMA : THFMA = 10 : 60 : 30 20% Salt (Pore size: 90 - 125 μm)
J9A	PU5 : NVP : THFMA = 10 : 60 : 30 20% Dextrin (Pore size < 38 μm)
J9B	PU5 : NVP : THFMA = 10 : 60 : 30 20% Dextrin (Pore size < 38 μm) + 4% Dextran
J9C	PU5 : NVP : THFMA = 10 : 60 : 30 20% Salt (Pore size: 38 – 63 μm)
J9D	PU5 : NVP : THFMA = 10 : 60 : 30 20% Salt (Pore size: 63 - 90 μm)
J9E	PU5 : NVP : THFMA = 10 : 60 : 30 20% Salt (Pore size: 90 - 125 μm)

Table 6.3 continued. The composition of the porous SIPNs used in calcein AM test

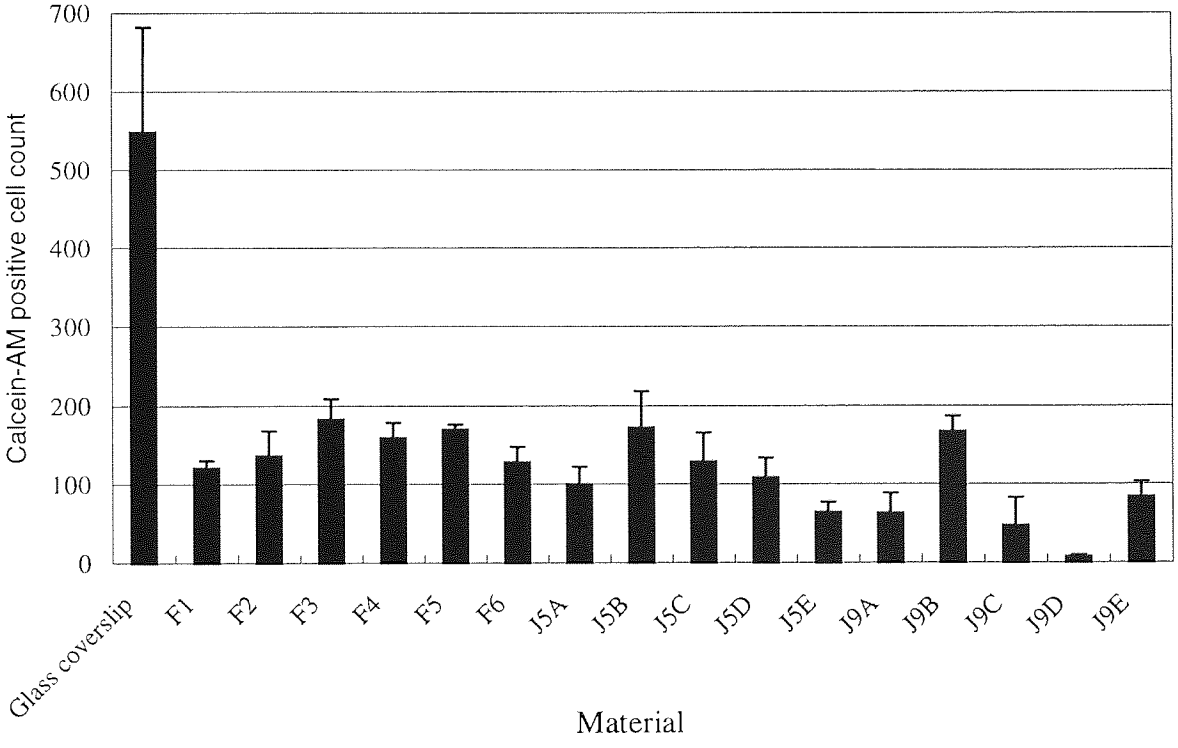

Figure 6.4 The calcein AM assay of porous SIPNs, using EK1.Brs cells (n=3, mean +/- SEM)

It is shown in Figure 6.4 that cells attached to all porous materials except J9D and the number of cells attaching on the same composition porous material is different. As discussed in Chapter 3, the addition of porosigen does not affect the EWC significantly, therefore, the effect of EWC on the cell adhesion for these porous materials with the same composition can be ignored. It does indicate, however, that pore formers alter the cell adhesion.

When the porous materials were synthesized using both dextrin and dextran, the addition of dextran enhanced the cell adhesion. This phenomenon can be observed by comparing the number of cells attached on F1 and F2, J5A and J5B, J9A and J9B. It appears that the channels created by dextran have a great effect on the cell adhesion while the pore size of dextrin is very small (less than 38 μm). However, when the pore size becomes larger (larger than 63 μm), the channels created by dextran have a minor effect on the cell adhesion of the porous materials. For example, the number of cells adhered on J3 is similar to the number adhered on J5, and J4 is similar to J6.

For the AMO porous materials, when the pore size increases from smaller than 38 μm to larger than 90 μm (F1, F3, and F5), the number of cells adhered on the surface increase; an expected result based on the hypothesis that cells can migrate into larger pores more easily than into small ones. However, for NNDMA porous materials, when the pore size increases from less than 38 μm to 125 μm (J5A, J5C, J5D and J5E), the number of cells attached on the surface decreases. An irregular pattern can be observed for the NVP porous materials (J9A, J9C, J9D and J9E). A possible explanation could be that when the pore size of porosigen increases, the shape of the pores becomes more and more irregular, thereby altering the cell adhesion significantly.

6.4 Conclusions

The "core and skirt" KPro requires both a cell adhesive material and a non cell adhesive material. Several techniques for controlling the cell adhesion have been investigated in this chapter. A desirable goal is to be able to switch the cell adhesion on or off depending on the specific requirements.

The sterilisation method has an important effect on the cell adhesion of the materials. Autoclaving may change the surface properties of the materials and aid cell adhesion as some of the materials exhibit white streaks on their surface after autoclaving.

PolyHEMA is generally considered to be non cell adhesive. However, the clear AMO, NNDMA and NVP SIPNs with water content higher than polyHEMA exhibited a lower level of cell adhesion than polyHEMA. Low water content clear SIPNs were synthesized which exhibited higher cell counts than polyHEMA. This indicates that the equilibrium water content is an important factor in affecting the cell adhesion of the hydrogels.

The presence of small amounts of PEG on biomaterial surfaces alters the cell adhesion of the hydrogel. PEG MA protects the surface of clear AMO SIPNs from the cell adhesion. However the addition of PEG MA enhances the cell adhesion on the clear NNDMA SIPNs and has a minor effect on the NVP clear SIPNs. This may be due to the difference in chemical structure of the hydrophilic monomer and the reactive ratios with PEG MA, resulting in less even sequence distribution in the NNDMA and NVP polymers than the AMO system. The longer chain PEG MA provides better protection for the surface of the hydrogel and reduces cell adhesion than the short chain PEG MA, i.e. 440 is better than 200.

The nature of porosigen has an effect on the cell adhesion. The addition of dextran has the greatest effect on the cell adhesion when the pore size of dextrin is smaller than 38 μm. With the increase in size of porosigen, the shape of the pore becomes more and more irregular, thereby altering the cell adhesion on the porous materials.

Chapter 7

Mesh Reinforced Materials

7.1 Introduction

Many biological tissues consist of a charged, organic extracellular matrix infused with an ionic interstitial fluid that may flow through matrix intermolecular spaces during tissue deformation. The mechanical strength of the cornea is provided by its collagen matrix, which is different from that of skin or the contiguous sclera and which requires the presence of mechanisms that regulate hydration to maintain transparency.

Collagen constitutes about 71 percent of the dry weight of the cornea and is the structural macromolecule providing tissue transparency and mechanical resistance to intraocular pressure[253, 254]. In the quiescent cornea, both procollagen and collagen are secreted at a low basal rate; however, in the initial phase of healing of corneal wounds, collagen secretion may be greatly increased[255]. Although there is some disagreement about which collagen types are found in the corneas of various species, there is agreement that type I collagen predominates[256]. Additionally, there is strong evidence that types III and V collagen are found in the human cornea[257].

The epithelium of the cornea is unlikely to contribute to the stiffness of the total cornea because it constitutes less than 10% of the total corneal thickness and consists of five or six layers of cells. The corneal stroma, which constitutes about 90% of the total corneal thickness, is thought to contribute significantly to the mechanical properties of the cornea. Its structure is composed of insoluble collagen fibrils and stromal fluid. This allows the corneal stroma to experience large deformations over a relatively short period of time.

The collagen fibrils, which are packed in parallel arrays[258], make up the 300 to 500 lamellae of the stroma. The lamellae extend from limbus to limbus and are oriented at various angles to one another, less than 90 degrees in the anterior stroma but nearly orthogonal in the posterior stroma[254]. A random cross-sectional electron micrograph of the stroma, therefore, reveals some fibrils cut nearly perpendicularly and other fibrils cut tangentially (Figure 7.1). Viewed using electron microscopy, the fibrils appear to have uniform diameters; however, various studies have found mean diameters ranging from 22 to 32 nm[259, 260]. At high magnification, the fibrils appear to have several small filaments, which may be precursor subunits. In longitudinal view, the fibrils have a macroperiodicity of 64 nm, which is

constant throughout the cornea. There is little variation in fibril size at different depths in the central cornea.

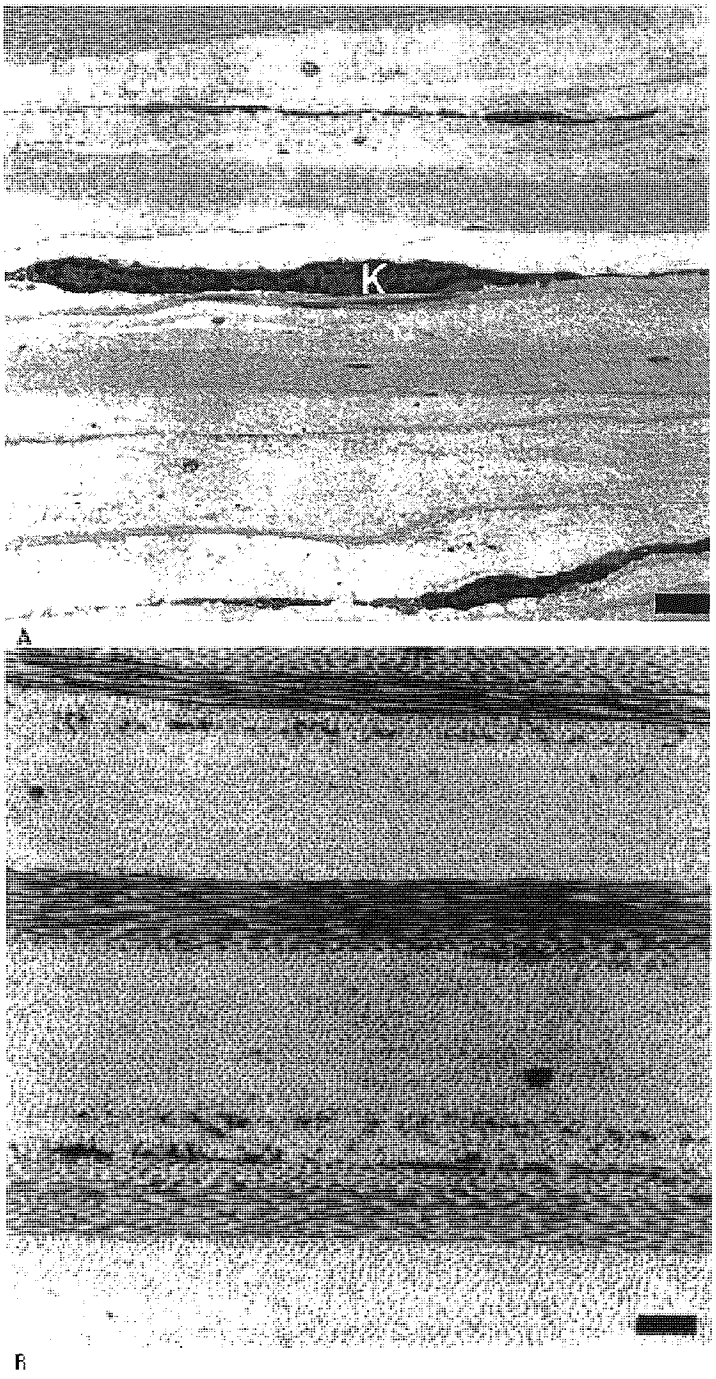

Figure 7.1[65] *(A) Electron micrograph demonstrating the alternating orientation of collagen lamellae in the midcentral stroma. K, keratocyte cell body. (Bar, 2 μm) (B) Higher-power electron micrograph illustrating the regular arrangement of individual collagen fibrils within various lamellae. Each fibril is composed of several smaller subunits. (Bar, 0.5 μm)*

The collagen fibrils are surrounded by a polyanionic extracellular matrix, which may be important in maintaining the fairly constant separation distance of 60 nm between the centres of the fibrils[261]. The primary glycosaminoglycans of the stroma are keratan sulphate and chondroitin sulphate, which occur in a ratio of 3:1[262]. In culture, human keratocytes can be induced to produce dermatan sulphate and heparan sulphate, which may be analogous to the naturally produced sulphates for wound healing[263]. Some regional differences may exist in the distribution of these substances. The concentration of keratan sulphate appears to be greatest in the central anterior stroma and least peripherally, where the concentration of chondroitin sulphate is increased. There is a rough correlation between the increase in the diameter of collagen fibrils (60 to 70 nm) peripherally and the decrease in keratan sulphate[264]. Thus the cornea can be described as a "collagen in jelly" model. The intraocular pressure deforms the cornea in a balance of the tension and compression forces.

There are about 200 lamellae in any radial section through the human cornea. The collagen fibril distribution varies throughout the cornea. Thus cornea's mechanical properties are anisotropic in nature. At Aston, oscillation of the human cornea was investigated by Dr. Lydon using a Bohlin rheometer. At a frequency of 5 Hz, the complex modulus, the storage (elastic) modulus and the viscous (loss) modulus of the human cornea are 6.5 KPa, 6.4 KPa and 0.7 KPa respectively. However, at the same frequency, a conventional hydrogel lens (Acuvue) gives values of 14 KPa, 13.5 KPa and 2.5 KPa respectively, and an extended wear lens (Night & Day) gives respective values of 88 KPa, 87 KPa and 10 KPa. This information demonstrates that to mimic the cornea such high modulus may not be necessary but that the material may need strength under tension. Corneal assessment has shown the dynamic properties in tension of the cornea are due to the collagen fibrils and so it makes the natural cornea appear stiffer than it is, especially in flexure.

A simple handling test is a measurement of the flexibility and deformation described in Chapter 4. It demonstrated that an ideal KPro material should be stiffer than polyHEMA and should be able to deform and recover quickly during the blink. The core of the KPro needs to be sufficiently stiff to overcome astigmatism and to overcome corneal irregularity, but sufficiently flexible to permit measurement of intraocular pressure. Thus a hybrid of a soft elastic centre and a stiff collagen upper layer to form a laminar structure would be an ideal structure.

The mechanical properties of two different kinds of hydrogels, the MMA based copolymers and SIPNs polymers, have been examined in detail in Chapter 4. The elastic modulus and tensile strength of polyHEMA are known to be approximately 0.5 MPa and 0.25 MPa respectively[15]. The elastic modulus and tensile strength of most SIPNs synthesized for the current project are over 1 MPa and 0.5 MPa respectively: much stiffer than polyHEMA. Direct handling test by an experienced surgeon indicated that these SIPNs polymers are too stiff to be used for the KPro model. The elastic modulus and tensile strength of most of the simple MMA copolymers synthesized in this work are around 0.5 MPa and 0.5 MPa; these are similar to or lower than polyHEMA which means that they are not stiff enough for the KPro. None of these materials seems to be ideal for KPro use. A new kind of novel hydrogel which can overcome the problem on the mechanical properties should be considered to take place of the hydrogels stated above, and to provide strength under tension combined with flexibility.

Mesh materials made from polymers such as high density polyethylene or poly amide, are very flexible but very strong under tension. When incorporated into a conventional hydrogel they may mimic the collagen matrix in the natural cornea. Hydrogels will dominate the oscillation properties and mesh materials will dominate the tensile properties. This kind of hydrogel can be treated as a laminar structure which is formed from a hybrid of a soft elastic centre and collagen stiff upper layer. An optimal balance of flexibility and stiffness can be achieved.

The hydrogels reinforced mesh materials should not only overcome the mechanical problems identified in this work, but also possess some other advantages, such as enhancing the integration of the skirt and core materials. The lack of adequate integration between the optic and its surrounding skirt, and between the skirt and the host tissue, underlies most of the complications associated with KPros. Some researchers believe that biointegration of the skirt in an artificial donor button KPro could never provide sufficient mechanical strength, and are evaluating more complex methods of fixation[123, 265, 266]. A polymer mesh should be able to act as a "bridge" to help anchor the core and skirt together.

In this chapter, the mechanical properties of hydrogels reinforced mesh materials are investigated. The results are shown in Figures 7.2 to 7.4. A conventional contact lens mould, similar in shape to the cornea, was used to make the model of the hydrogel

containing mesh material. The spoilation test of several hydrogels used in the model was carried out by Dr. Franklin and the results are displayed from Figures 7.5 to 7.8. All the precise values used in the chapter can be found in Appendix 5.

7.2 The Effect of Diluent on the KPro Model

When the hydrogels are immersed in an aqueous solution, they will imbibe solvent and swell until an equilibrium is established between swelling forces and elastic restoring forces in the crosslinked polymer network that tends to restrict swelling. Factors that determine the overall amount of swelling include (1) thermal motion of matrix molecules (polymer excluded volume effects), (2) interactions between solvent and polymer molecules, (3) stretching of the molecular chains between crosslinks, and (4) electrostatic (electrical double layer) repulsion forces between the charged groups along the polymer chains[267].

The mesh materials used in this work are based on high density polyethylene with different coatings. They do not swell or expand in distilled water. However, when the hydrogel containing mesh is soaked in distilled water, it will cause an uneven or even destroyed surface due to the hydrogel expanding around the mesh. To avoid this problem, the same amount of diluent as the equilibrium water content of the hydrogel should be mixed with monomers before synthesis in order to fix the shape of the mesh reinforced hydrogel before soaking in the distilled water. The diluent occupies the volume of water in the network during polymerisation. The diluent is then exchanged for distilled water when the hydrogel is soaked in distilled water to reach equilibrium, thereby keeping the original shape of the hydrogel unchanged. In the contact lens industry a mixture of ethylene glycol and water or boric acid ester is used to achieve this effect. The basic requirements for a diluent are that it can dissolve the monomer and that it will not react with the monomers in the experimental conditions used.

Several diluents such as N-methyl pyrrolidone (NMP), ethylene glycol and pure water, were employed in the work and these are all found to be suitable diluents for HEMA. But water is not a good solvent for MMA as it leads to heterogeneous solution. A mixture of water and NMP is a good diluent for the MMA containing comonomers.

The technique for making the mesh reinforced hydrogel KPro model is described below:

1. Cut mesh template.
2. Put mesh template into mould. The mesh should be a little bit larger than the mould.
3. Pour monomer mixture with diluent into mould (make mixture in 14 ml glass vial) and fill to the top.
4. Push lid into place in mould. Push gently and let monomer mixture overflow.
5. Put moulds into the rack and into the oven and polymerise at 60 °C for three days and then at 90 °C for three hours.
6. Remove from oven, and allow the mould to cool down slightly.
7. Separate the hydrogels from the mould carefully and soak in distilled water for at least one week prior to use.

7.3 Mechanical Properties of Mesh Reinforced Hydrogels

Membranes of mesh containing polyHEMA was synthesized using the same basic technique described in Chapter 2 with the additional step of cutting the mesh to the same size as the membrane mould and placing it in the mould before injection of the monomer mixture. Four different types of mesh materials were used in this work and their properties are shown in Appendix 6. The mechanical properties were investigated using a Hounsfield Hti tensometer described in Chapter 2 and the results are displayed below.

It can be seen from Figures 7.2, 7.3 and 7.4 that the incorporation of mesh material reinforces the elastic modulus and tensile strength of the hydrogels, but sacrifices the elongation at break. The polyHEMA with different mesh materials show similar mechanical properties. The four different mesh materials themselves have the similar mechanical properties (see Appendix 6); this indicates that mesh materials dominate the tensile properties.

Comparing with the mechanical properties of MMA based copolymers and SIPNs described in Chapter 4, at the same equilibrium water content (40%), the tensile strength, elastic modulus and elongation of SIPNs are 1.5 MPa, 10 MPa and over 100%, respectively and those of MMA based copolymers are 0.5 MPa, 1.0 MPa and over 150%. The elastic modulus governs the stiffness of the materials. So the hydrogels with mesh materials are more flexible than SIPNs and stronger than MMA based copolymers.

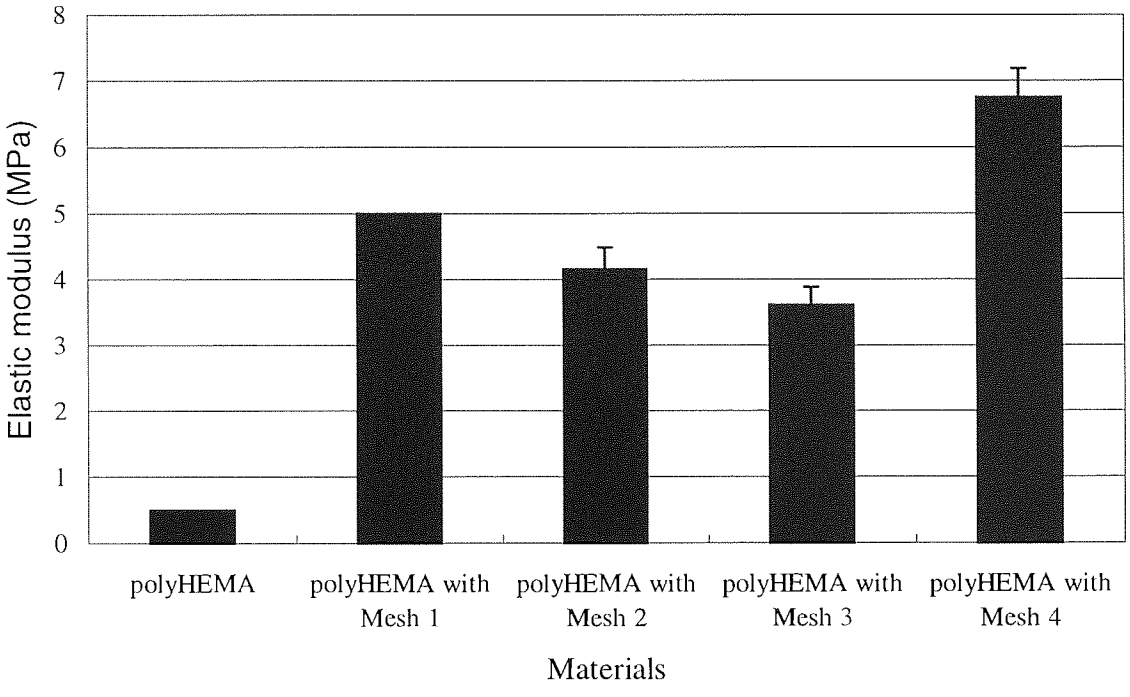

Figure 7.2 A comparison of the elastic modulus of polyHEMA with and without mesh materials

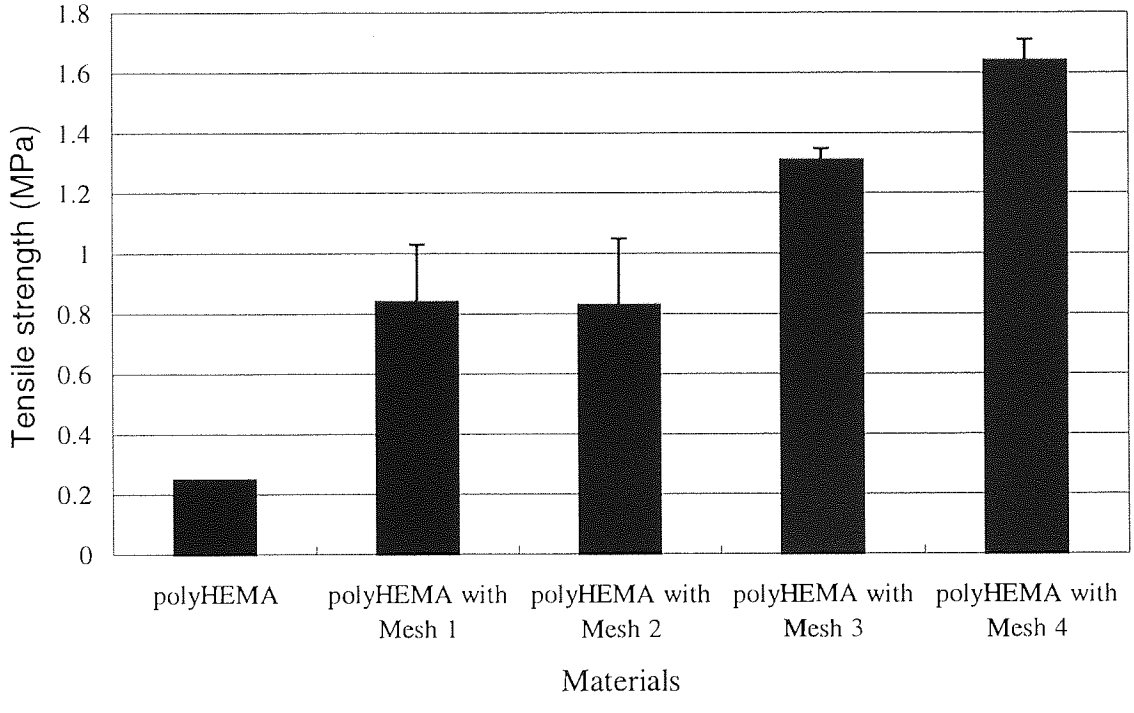

Figure 7.3 A comparison of the tensile strength of polyHEMA with and without mesh materials

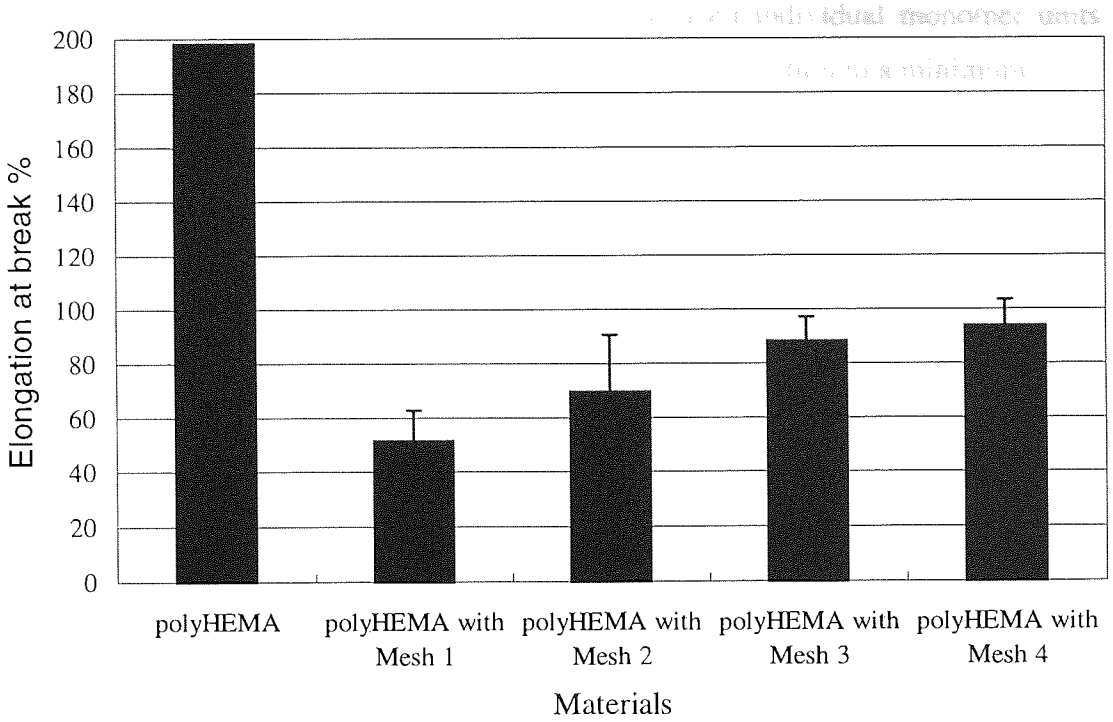

Figure 7.4 A comparison of the elongation at break of polyHEMA with and without mesh materials

It was shown in Chapter 4 how the mechanical properties of the hydrogel decrease with an increase in EWC. The advantage of the hydrogels containing mesh materials is that with the increase of the EWC, the mechanical properties of the hydrogels do not change greatly because the mesh materials contribute the majority of mechanical strength. However, the mechanical properties of the hydrogels with mesh depend on the type, shape and thickness of the mesh. Further work was carried out to develop a KPro material based on MMA copolymers with N-containing monomers (e.g. NVP, NNDMA, AMO). That would combine good mechanical properties with good ocular compatibility.

7.4 A Modified Hydrogel KPro Model Combined with Mesh Material

Work done at Aston, has found that polymers with long repeat units or extensive segments of individual monomer units (which may contain charged or uncharged groups), have a greater tendency to produce non-specific protein adsorption than polymers that mimic the molecular architecture of naturally occurring polymers (regular, short sequences of monomers)[58]. Thus polymers synthesized by more than two monomers can have less

protein adsorption on the surface because more dispersed individual monomer units are created. In the design of the KPro, it is important to keep spoilation to a minimum.

A low water content, non-ionic hydrogel material called Aston Biomimetic Hydrogel (ABH) composed of HEMA, NVP, MMA and PEG200 MA has been used as the basis of a proprietary material that has been through clinical trials and is commercially supplied through optometrists in Europe in the form of contact lenses. This material has been successfully worn in eyes for ten years[190]. Starting with a HEMA base, to increase the water content, NVP was added. The mechanically weak and fragile materials produced were strengthened by the addition of the hydrophobic monomer MMA. Finally, the PEG200 MA was added as a 'swinging arm' to reduce the deposition.

A contact lens mould was used to make the mesh reinforced hydrogel model in the initial stage for its similar shape to the cornea. Several other hydrogels which have similar composition to ABH, modified with AMO and NNDMA, have been used to make the model as well. Their compositions and equilibrium water content are shown in Table 7.1.

Gel ID	Composition	EWC %
J81	HEMA : AMO : MMA :PEG200 MA = 55 : 12 : 13 : 20	36.4
J82	HEMA : NNDMA : MMA : PEG200 MA = 55 : 12 : 13 : 20	40.2
J83	HEMA : NVP : AMO : MMA : PEG200 MA = 45 : 15 : 12 : 13 : 20	46.0
J84	AMO : MMA : PEG200 MA = 80 : 10 : 10	68.5
J85	NVP : MMA : PEG200 MA = 70 : 20 : 10	68.3
J86	NNDMA : MMA : PEG200 MA = 60 : 30 : 10	70.8
ABH	HEMA : NVP : MMA : PEG200 MA = $55\,^{3}/_{7} : 11\,^{7}/_{10} : 12\,^{3}/_{5} : 20\,^{1}/_{5}$	40.1

Table 7.1 The composition and equilibrium water content of the hydrogel used in the contact lens mould

7.5 Spoilation Test

The spoilation test was carried out by Dr. Franklin. The technique is described in Chapter 2 in detail. The *in vitro* spoilation model has been shown to produce an accelerated spoilation equivalent to approximately six months extended wear *in vivo*. Spoilation is dependent on

the patient, the wear regime and the material so there is no single correlation factor between *in vivo* wear and the *in vitro* model. There are many factors that contribute to the levels of spoilation, such as the polarity of the surface, the monomer structure and the water content of the hydrogel. Hydrophobic clusters on the surface and monomers with methyl side groups also increase the potential spoilation levels by providing an area capable of blocking proteins and adsorbing lipids.

Some of the hydrogels used for the model stated above were investigated and the results are shown in Figures 7.5 to 7.8. PolyHEMA was included above as a comparison as it is a starting material for making the mesh reinforced hydrogel model. J83 was too brittle to survive the duration of the test, thus the experiment for J83 ended at 21 days.

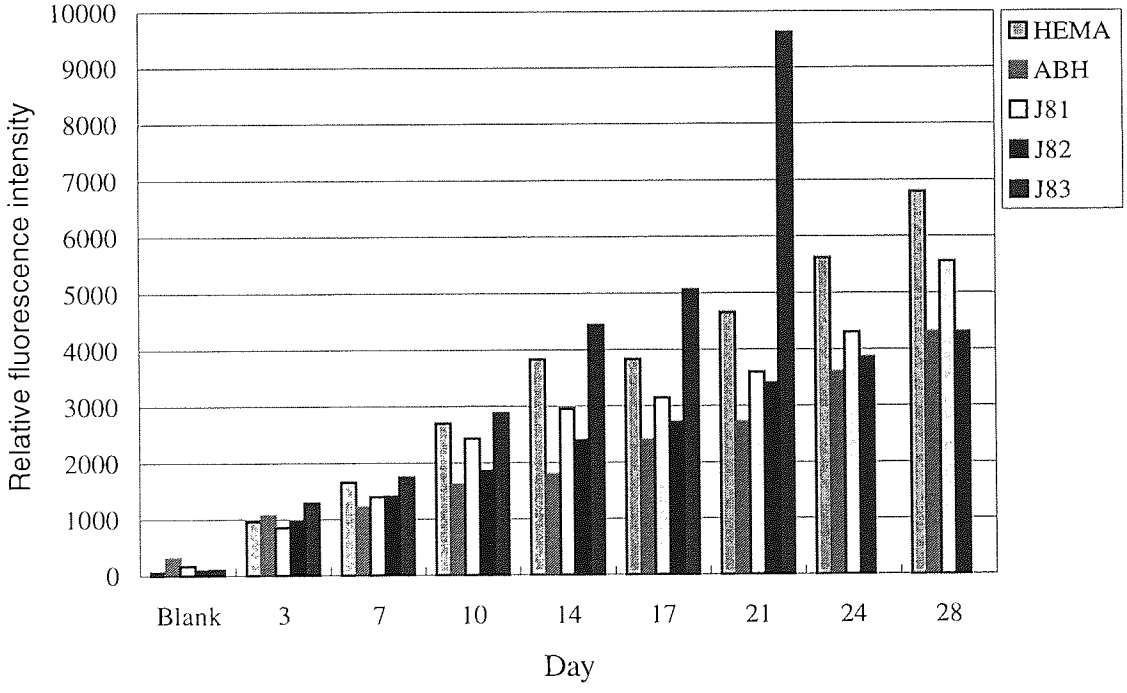

Figure 7.5 Progressive build up of protein spoilation measured using fluorescence spectroscopy at an excitation wavelength of 280nm for the hydrogels used in the model

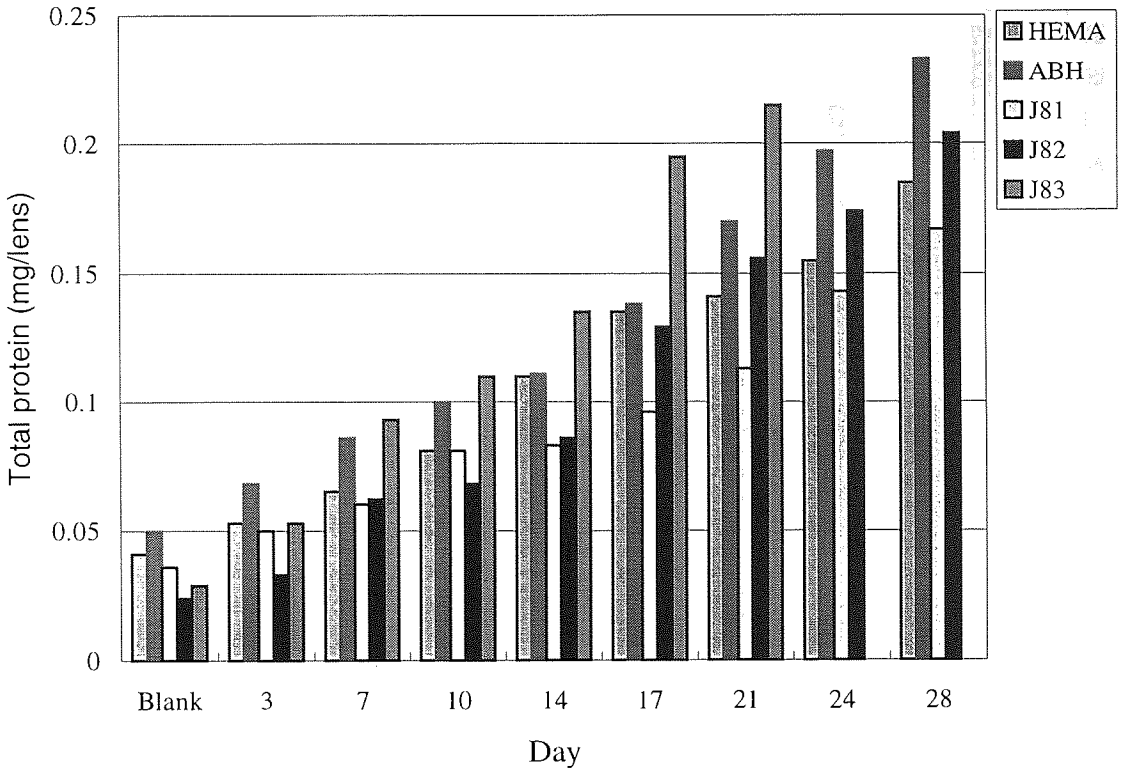

Figure 7.6 The total protein spoilation profile of the hydrogels used in the model

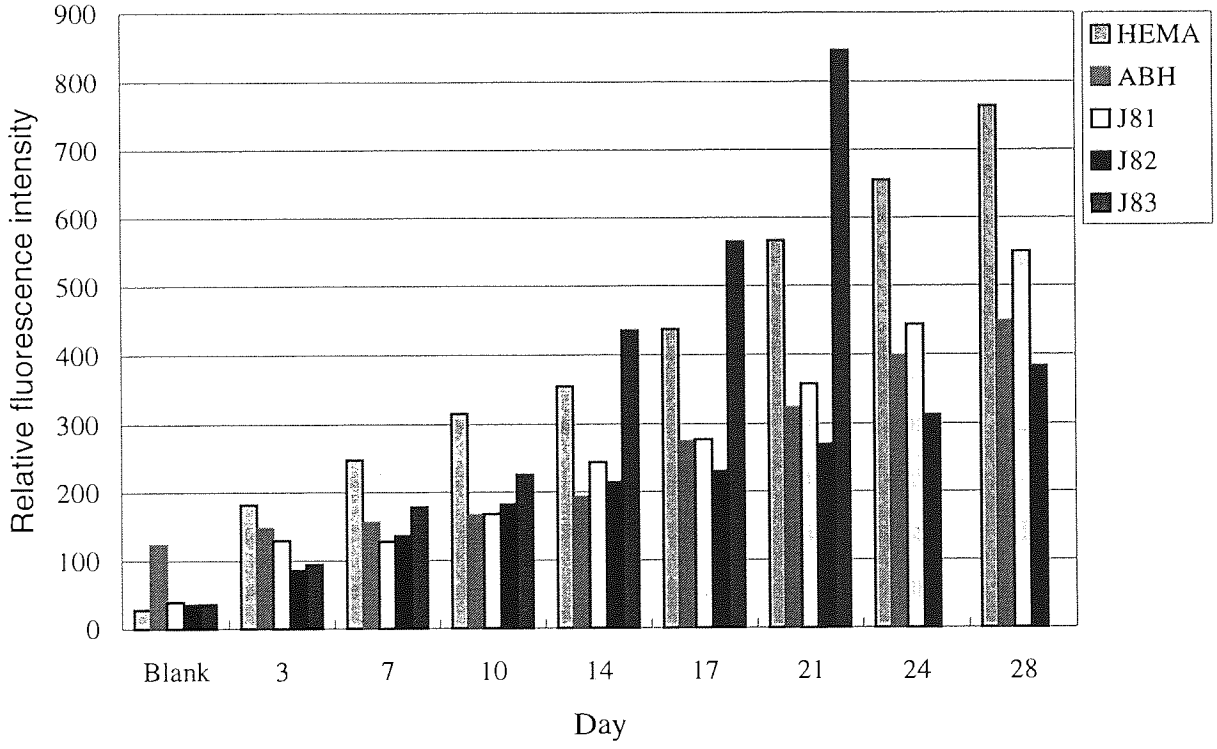

Figure 7.7 Progressive build up of lipid spoilation measured using fluorescence spectroscopy at an excitation wavelength of 280nm for the hydrogels used in the model

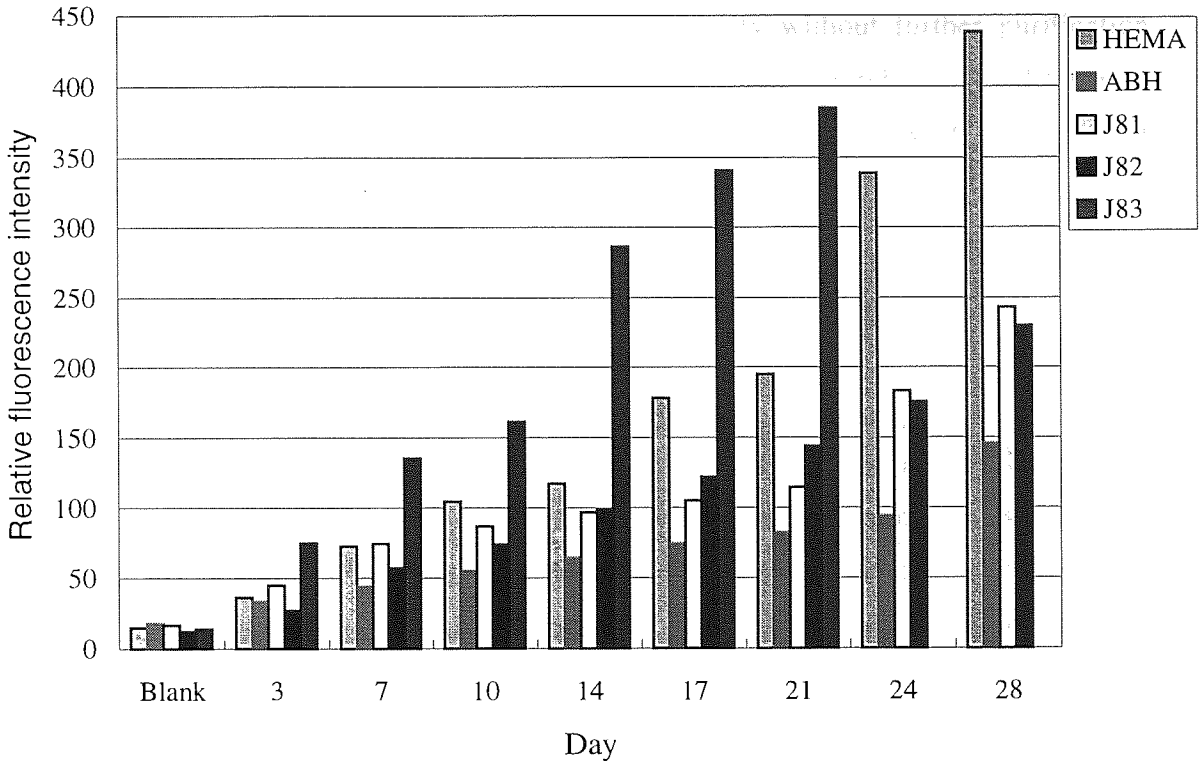

Figure 7.8 Progressive build up of lipid spoilation measured using fluorescence spectroscopy at an excitation wavelength of 360nm for the hydrogels used in the model

Figure 7.6 displays the surface protein deposition using fluorescence spectroscopy and Figure 7.7 shows the total protein spoilation using UV analysis. UV analysis provides a means to examine the total protein in and on the surface of a hydrogel and is unable to distinguish location. Fluorescence spectroscopy allows the amount of protein to be quantified on the surface of the hydrogel, expressed as an amount of fluorescence.

Fluorescence spectrophotofluorimetry can also be used to obtain comparative data on the relative degree of lipid spoilation. By applying an incident beam at a certain wavelength, the conjugated species fluoresce and the intensity of the resultant peak is determined. Conjugated double bonds are present in the majority of lipids found in tears, such as in cholesterol and cholesterol esters. Figures 7.8 and 7.9 display the surface lipid deposition detected at the 280 nm wavelength and 360 nm wavelength respectively.

As HEMA is well known to undergo a disproportionation reaction to produce methacrylic acid (MAA), polyHEMA will possess differing degrees of ionicity depending on the

amount of acid it contains. Optical grades of HEMA monomer were used in the work described in this thesis in an effort to reduce the impurity without further purification performed, though obtaining monomer completely free of methacrylic acid, MAA is a major difficulty. The residual MAA leads to an increase in the anionicity of the surface of the lenses, which in turn leads to the accumulation of the positively charged protein lysozyme[268]. Thus it is not surprising to see the higher levels of protein and lipid adsorption on polyHEMA. The MMA impurity in HEMA also affects the levels of spoilation of the other (HEMA containing) hydrogels investigated here.

The NVP monomer can result in 'blocky' polymers when the comonomer has poorly matched reactivity ratios, with these sites leading to increased spoilation. It is neutral at physiological pH though the pendant pyrrolidone ring presents a relatively hydrophobic external surface which leads to an increase in albumin (negatively charged) deposition. The amphiphilic nature of the pyrrolidone ring is the underlying reason for its susceptibility to lipid accumulation[303]. The results shown above indicate the enhanced spoilation that is associated with NVP copolymers, such as ABH and J83.

AMO monomer is more polar than NVP, and its copolymers when polymerised with MMA have a good controlled sequence distribution, with short, regular repeat units mimicking those found in nature, due to its higher reactivity ratio. However, because the amount of AMO in J81 and J83 equates to only about 12% of the weight of the polymer, it does not greatly affect the levels of spoilation.

The high level of spoilation seen with J83 could also be explained by sample fragility, with deposition occurring at a higher rate than expected because of surface irregularities.

7.6 Conclusions

This chapter investigates the mesh reinforced hydrogels. Mesh reinforced hydrogels have more appropriate properties than non reinforced hydrogels. Mesh materials govern the tensile mechanical properties of these hydrogels. They offer a promising approach to making a hydrogel that is very flexible but strong under tension, thereby having mechanical properties closer to the natural cornea than has been previous possible. The advantage of a hydrogel incorporated with mesh materials is that it still can have very good mechanical

properties at the high equilibrium water content. The thickness, type and shape of the mesh materials all affect the mechanical properties of the hydrogels.

The diluent is a very important component in the mesh reinforced hydrogels. It allows the original shape of the hydrogel to remain unchanged when the hydrogel is soaked in distilled water. It is necessary to select the most suitable diluent depending on the monomers used. The basic requirement is that the diluent can dissolve the monomer and that it will not react with the monomers in the certain experimental condition.

Some hydrogels used in the contact lens mould were tested using the spoilation test. MAA impurity enhances the level of spoilation on the hydrogels containing HEMA. It is very important to remove all impurities from the monomer to avoid the high protein and lipid deposition.

The colour of the mesh materials is also a very important factor in the model of mesh reinforced hydrogels designed for KPro. Fully opaque would be more desirable than translucent as this would avoid scatter problems caused by light as it would pass through. Thus black is better than white for the mesh material and cosmetically looks better.

Although the problem of the core and skirt integration in potential KPro material has not been solved in this work, a promising future in which mesh materials will help anchor the core and skirt materials together still can be predicted. The mesh materials can be treated as the "bridge" to connect the core and skirt materials, and will be present in both sections of the KPro.

Mesh material could be allowed to protrude from the KPro skirt edge if it was felt that this would aid integration into the host pocket by stitching through surrounding mesh. It depends on the mould designed for KPro.

The mesh should also assist cell integration. A cell promoter could be coated on the mesh materials and would be expected to leach into the pores of the porous materials and be anchored inside them. Furthermore, a mesh positioned closer to the anterior rather than the posterior surface would also be beneficial because inhibition of cell adhesion on the posterior face is required in order to prevent retroprosthetic membrane formation.

Chapter 8

Conclusions And Suggestions For Future Work

8.1 Conclusions

The aim of this thesis was to investigate the use of novel synthetic hydrogels for keratoprosthesis. The restoration of vision in patients with corneal blindness has become increasingly successful because of advances in standard penetrating keratoplasty (PK) and ocular surface reconstruction achieved during the past century. However, there remains a subset of patients with severe corneal opacity in whom PK and ocular surface reconstruction techniques have either failed, or carry a poor prognosis, owing to past or ongoing chronic inflammation. Such cases include patients suffering from Stevens-Johnson syndrome (SJS), chemical burns, ocular cicatricial pemphigoid (OCP), severe keratoconjunctivitis sicca, stem cell deficiencies, and severe vascularization resulting from other causes. In addition, there exists another, larger group of patients with repeated graft failures for unknown reasons, in whom the likelihood of successful subsequent corneal allografting is low. For these two categories of patients with complicated corneal blindness and with a world shortage of donated corneas, keratoprosthesis (KPro) surgery may be the only hope of any visual improvement. For the purpose of synthetic KPro design, it is useful to categorise the patients in two classes, one with a functional tear film and the other with a dry ocular surface. Most of the work in this thesis is based on the hydrogels, which are water-containing polymers and are therefore directed to patients with a functioning tear film.

The most commonly used KPro model consists of a transparent central stem with a porous peripheral skirt. A major cause of keratoprosthesis failure has been the absence of healing between the periphery of the artificial device and the rim of the host cornea. As a result, tissue necrosis, wound leakage, epithelial downgrowth and intraocular infection often occur. Therefore, it is apparent that for long term success, secure healing of the device into the surrounding cornea must occur via a porous periphery into which stromal fibroblasts (keratocytes) and penetrate, proliferate and synthesis connective tissue proteins. This in turn requires integration with an optically transparent centre and ideally an anterior surface that will support the adherence and proliferation of epithelium and/or resist substantial contamination by denatured tear components. Attempts to date to achieve this goal have been almost exclusively based on commercially-available rather than purpose-designed polymers.

Hydrogels have been utilised in many biomedical applications; there is the potential to manipulate the properties for a given application by changing the chemical structure of the constituent monomers. The only fully hydrogel-based keratoprosthesis to be developed has been fabricated from 2-hydroxyethyl methacrylate (HEMA) which is known not to support cell adhesion and spreading. The major problem that has limited the use of this homogeneous synthetic hydrogel in this application is due to the fact that polyHEMA has a fixed EWC (about 40%), relatively poor mechanical strength and limited control of properties. HEMA also has poor solvent properties which restrict its use in interpenetrating polymer network formation, which would otherwise be a convenient method of evaluating its properties.

Clear PMMA core material has been used in KPro for many years, such as in the Strampelli KPros prosthesis (OOKP) which has not caused the failure found in other core and skirt prostheses; the OOKP approach has been particularly valuable when there is tear film dysfunction. However, epithelialization of this kind of solid, rigid optic material is clearly impossible and thus it is not ideal for patients with a stable tear film. The approach to the development of a hydrogel for potential KPro application adopted in this work is to develop soft core materials to mimic the properties of the natural cornea; this can then be used in patients with a good tear film. This studies have been based on hydrophilic monomers, such as N,N-dimethyacrylamide (NNDMA), N-vinyl pyrrolidone (NVP) and acryloylmorpholine (AMO) in combination with methyl methacrylate (MMA). They may therefore be regarded as an extension of the PMMA-based prosthesis to soft hydrogel corneal analogue.

The above three nitrogen monomers have the similar chemical structure, all containing a Nitrogen atom linked a C=O group, and give predictable sequences when polymerised with methacrylate. NVP/MMA copolymers have previously been investigated for use in synthetic cartilage at Aston[23]. They have a blocky sequence distribution, especially at later stage in the polymerisation, rather than the desired alternating sequence distribution that has been demonstrated to show enhanced compatibility. Replacing NVP with AMO in MMA overcomes this problem. AMO contains a highly polar disubstituted amide group coupled with apolar methylene and methane groups. It shows a good alternating sequence distribution when copolymerised with MMA due to the increased reactivity of AMO to radical polymerisation[23]. NNDMA also has a structural resemblance to NVP but it does

give early blockiness when polymerised with MMA. The presence of two methyl groups can confer hydrolytic stability and it can offer a potential increase in equilibrium water content over HEMA.

The hydrogel to be used in keratoprosthesis must be able to withstand the stresses involved in the surgical procedure involved with the KPro and the *in situ* stresses such as the deforming force of the eyelid during the blink cycle and intraocular pressure. Conventional synthetic hydrogels such as simple MMA copolymers can be produced with a similar water content to that of biological organs (often as high as 85%), however the mechanical properties are poor. The semi-interpenetrating polymer networks (SIPNs) synthesized in this work were designed to obtain much improved mechanical properties with similar water contents to conventional hydrogels. SIPNs had been investigated as a potential synthetic cartilage and cellulose acetate butyrate (CAB) was used as the interpenetrant. However CAB would not be successful in this KPro as the polymers produced at higher water content were opaque[200], which is not important in cartilage application.

An ester-based polyurethane (PU) was used as an interpenetrant in this thesis because it can form a clear system with AMO and THFMA. PU has excellent mechanical properties, high elongation capacity, good abrasion resistance, high flexibility and hardness, and good biocompatibility. Hydrophilic monomers, AMO, NVP and NNDMA, and THFMA were also used to produce SIPNs in this work for the synthetic cornea. THFMA has been used in dental applications for some years; its biotolerance has been studied and was found to be relatively non-irritant in dental applications[216]. These nitrogen-containing monomers have better solvent-power than HEMA, in part because of the absence of an alpha methyl group, so they can be used to assess the solubility of the interpenetrant thereby making SIPNs.

The natural cornea has been known to contain about 80% water[74] and is a reaction site for a series of complex biological processes. The materials designed for KPro should allow the ready diffusion of macromolecular nutrients to maintain the epithelium and keratocytes. The function is mainly executed by the water contained in the hydrogels. Thus the water content is an important factor that should be considered for potential materials used in the KPro. The equilibrium water content of the MMA copolymers synthesized in this work varies from 15% to 85% and that of the SIPNs varies from 30% to 73% (Figure 8.1). The freezing water content of the MMA copolymers varies from 1% to 70% and that of the

SIPNs varies from 10% to 50%. A wide range of hydrogels which have different EWC and freezing water contents can be chosen for the potential KPro material. PolyHEMA is known to have about 40% EWC and cannot be increased. It seems that the more water contained in the hydrogel the more beneficial is the effect on the nutrients' transport.

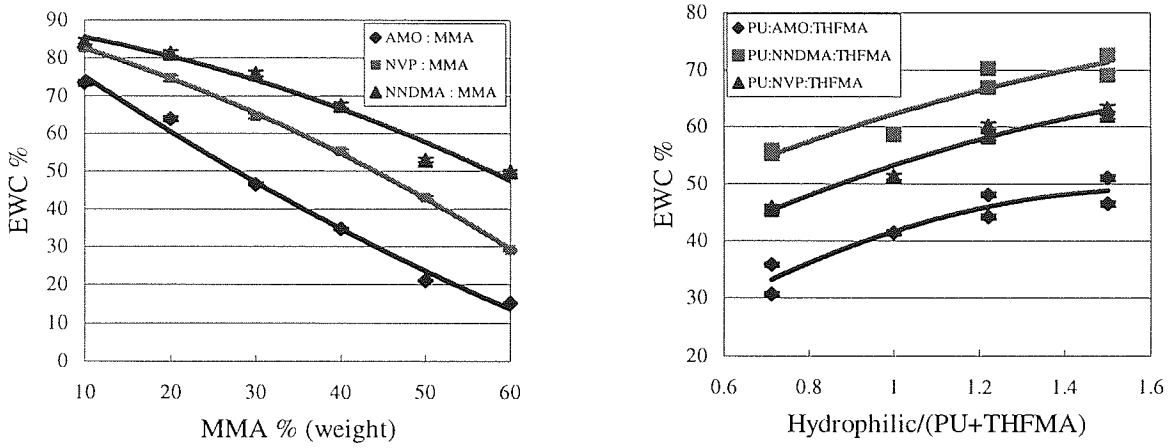

Figure 8.1 The EWC of simple MMA copolymers and SIPNs

The hydrophilicity order of the monomers used in this work is: NNDMA > NVP > AMO > PU5 > MMA > THFMA. The increase of hydrophilic component, NNDMA, NVP and AMO, can lead the increase in EWC and freezing water content in MMA copolymers and SIPNs. Hydrogels with even higher water contents than those hydrogels synthesized in this work can be produced by carefully selecting the ratio of hydrophilic component and hydrophobic component.

The literature values relating to the mechanical properties of the human cornea have caused some confusion. Papers in recent years have quoted the value of the shear modulus of the natural human cornea is 13MPa. Our initial work was based on this quoted value where a polyHEMA is only 0.5 MPa. These suggested that it was necessary to produce hydrogels much stiffer than polyHEMA in order to match the corneal properties. Our early studies were designed, therefore, to produce hydrogels with a wide range of mechanical properties. It was only at a later stage in the progress that both samples of human cornea and the methodology needed to measure dynamic mechanical properties became available. As a result of this work the target properties required for a functioning hydrogel analogue of the cornea changed as the studies progressed.

The AMO, NNDMA and NVP hydrogels synthesized in this work have a wide range of mechanical properties; the elastic modulus of the simple MMA copolymers vary from 305 to 0.2 MPa and the tensile strength varies from 20 to 0.1 MPa. The elastic modulus of the SIPNs synthesized in this work vary from 22 to 0.3 MPa and the tensile strength varies from 4.5 to 0.2. However, with the increase of EWC, the tensile strength, elastic modulus of MMA copolymers and SIPNs all decrease. Thus some part of mechanical properties of hydrogel must be sacrificed in order to achieve higher water content. At higher water contents, the mechanical properties of MMA copolymer deteriorate. As stated above, the use of semi-interpenetrating network technology can help to solve this problem. SIPN materials have higher values of tensile strength and elastic modulus than the simple hydrogel copolymers with the same water content, but they are less elastic. They can not, therefore, be used as true corneal analogue.

A simple handling test was performed by an experienced surgeon. A series of SIPN hydrogel with mechanical properties matched to the modulus values of the human natural cornea quoted from the literature were selected for this test. Unfortunately, these indicated that SIPNs were not suitable for KPro core materials because of their high stiffness. They cannot therefore be used as true corneal analogue. The ideal KPro core material should possess the ability to deform and recover quickly during the blink and should be slightly stiffer than polyHEMA. The elastic modulus and tensile strength of most simple MMA copolymers synthesized in this work are around 0.5 MPa and 0.5 MPa, similar or less than polyHEMA. These information indicates that the MMA copolymers and SIPNs synthesized in this work which show isotropic mechanical behaviour are not suitable for KPro core materials since they do not mimic the anisotropic behaviour of natural cornea. It was clear that another strategy was required to match the combination of stiffness intension combined with flexicity.

The KPro device must be biotolerant. The surface free energy of a hydrogel is an important property in determining the biotolerence of the material. The surface properties of SIPNs have been investigated in this work. In the dehydrated state the surface free energy is dominated by the dispersive component whereas in the hydrated state the polar component is dominant due to the presence of water and the effect of rotation of the surface groups around the carbon backbone chain. An increase in hydrophilic monomer does not significantly influence the surface free energy of the SIPNs tested and these three SIPN

families studied (AMO, NNDMA, and NVP containing) have similar surface free energies in the dehydrated state. However, in the hydrated state with an increase in the hydrophilic component, the surface free energy of the SIPNs increases steadily. In the dehydrated state, the PU5 content does not greatly influence the surface free energy of the SIPNs because it cannot easily diffuse through the dehydrated polymer. However, in the hydrated state with the increase in PU5 content, the surface free energy of the SIPNs decreases because it can migrate to the surface in the hydrated SIPNs. It appears that in the hydrated state the three series of semi-interpenetrating networks have similar total surface free energies to the biological fluid when they have an equilibrium water content in the range between 45% and 55%.

All KPros currently used produce serious complications such as implant extrusion, retroprosthetic membrane formation, infection and glaucoma. The incorporation of biocompatible materials which are conductive to implant integration with the host cornea could limit these complications. In the "core and skirt" KPro, the central optical cylinder should hinder cellular ingrowth. It would be a desirable goal to be able to switch the cell adhesion on or off depending on the specific requirements. The cell adhesion of some hydrogels was investigated in this thesis. The cell adhesion is affected by the protein deposited on the surface of the hydrogel, which can be affected by the sequence distribution. The polymers with long repeat units or extensive segments of individual monomer units were found to have a greater tendency to produce non-specific protein adsorption than polymers that mimic the molecular architecture of naturally occurring polymers (regular, short sequences of monomers). Thus the polymers synthesized with more than two monomers can have less protein adsorption on the surface, thereby having less cell adhesion.

PolyHEMA is generally considered to be a non cell adhesive hydrogel. However, the AMO, NNDMA and NVP clear SIPNs whose water content is higher than polyHEMA exhibited a lower level of cell adhesion than polyHEMA. Low water content clear SIPNs were synthesized which exhibited higher cell counts than polyHEMA. This indicates that the equilibrium water content is an important factor in affecting the cell adhesion of the hydrogels. The simple MMA copolymers and SIPNs synthesized in this work have a wide range of EWCs. Thus it would be possible to modulate to some extent the cell adhesion on the surface of hydrogel.

The core material in the KPro should inhibit the deposition of lipid and protein and should either not promote cell adhesion at all or be able to support a functioning epithelium (this is the ultimate goal for a corneal analogue). Polyethylene glycol monomethacrylate (PEG MA) known as an effective monomer to modulate protein deposition and cell adhesion was incorporated with SIPNs. PEG MA is also a hydrophilic monomer. The incorporation of PEG MA into both AMO and NVP-based SIPNs does lead to an increase in the EWC but will not affect the EWC of NNDMA-based SIPNs. The chain length of PEG MA (either 200 or 440 has little effect on the EWC of the hydrogel tested. The addition of PEG MA also has the effect on the mechanical properties of SIPNs. The presence of small amounts of PEG MA on biomaterial surfaces alters the cell adhesive properties of the hydrogel. PEG MA protects the surface of clear AMO SIPNs from cell adhesion, as one would expect due to the mobility of the long chains blocking adhesion sites. However the addition of PEG MA enhances the cell adhesion on the clear NNDMA SIPNs and did not have a significant effect on the clear NVP SIPNs. This may be due to the difference in chemical structure of the hydrophilic monomer and the reactivity ratios with PEG MA, resulting in less even sequence distribution in the NNDMA and NVP polymers than the AMO system. The longer chain PEG MA provides better protection for the surface of the hydrogel and reduces cell adhesion than the short chain PEG MA, i.e. 440 is better than 200.

The KPro currently used usually consists of two parts, an optical core and a porous periphery. One of the major problems encountered in this device has been the lack of integration between the core and periphery. In an attempt to overcome this, the porous periphery was made from the same material as the core, with the addition of porosigen. In the hydrogels described in this thesis, different sizes of salt or dextrin were added to form the different pore sizes and dextran was used to create the channels.

The incorporation of porosigen only slightly increases the EWC of porous hydrogels compared to the clear materials having the same chemical composition. Generally the introduction of pores into a hydrogel does not significantly alter the mechanical properties in comparison to the equivalent clear material. Neither does the pore size. However, the randomly porous nature of the hydrogels may cause apparent inconsistencies in the mechanical results. The porous peripheral skirt should enhance host keratocyte adhesion and spreading in the KPro model. The nature of the porosigen has an effect on the cell adhesion. The addition of dextran has the greatest effect on the cell adhesion when the pore

size of made using dextrin is smaller than 38 μm. With the increase in size of the porosigen, the shape of the pore size becomes more and more irregular, thereby altering the cell adhesion on the porous materials. In this work two problems were encountered, however. dextrin produced polymers with too small a pore size and a high density of salt was found to precipitate at the underside of the membrane so as to create two completely different surfaces of the membrane. Other porosigens should therefore be considered for the contribution to this project.

The mechanical properties of the natural human cornea in oscillation were measured on a Bohlin rheometer in the final stage of this work because the natural human cornea was not available until then. The information obtained from the rheometer demonstrates that to mimic the cornea we do not need supply high modulus but need strength under tension combined with a relatively low modulus instead. The cornea can be described as a "collagen in jelly" model. The intraocular pressure deforms the cornea in a balance of the tension and compression forces. Corneal assessment has shown that the dynamic properties in tension of the cornea are due to the collagen fibrils and so it makes it appear stiffer than it is, especially in flexure.

Thus the mesh reinforced hydrogels which make the hydrogel much stronger and less stiff so that their mechanical properties are much closer to the natural cornea were investigated in final stage of this work. This kind of hydrogel can be treated as a laminar structure which is formed from a hybrid of a soft elastic centre and collagen stiff upper layer. The mesh can make the conventional synthetic hydrogel stiff enough, in the meantime, it can still keep the hydrogel very flexible. Mesh material was found to govern the tensile mechanical properties of the hydrogels since they contribute almost all of the strength. The advantage of the mesh reinforced hydrogels is that they still can have very good mechanical properties at the high equilibrium water content. The thickness, type and shape of mesh materials all affect the mechanical properties of the hydrogels.

The diluent is a very important component in the mesh reinforced hydrogel. The use of a diluent helps to maintain the original shape of the hydrogel unchanged when swollen. A suitable diluent must be chosen depending on the composition of the hydrogel. The basic requirement for a diluent is that it can dissolve the monomer yet doesn't react with the monomers in the experimental conditions used.

Because the stiffness of the hydrogel itself does not make a major contribution to the mechanical stiffness of a mesh-reinforced hydrogel, an alternative hydrogel study was examined based on previous experience in this project and with hydrogel compatibility in the eye. A low water content hydrogel called Aston Biomimetic Hydrogel (ABH) composed of HEMA, NVP, MMA and PEG200 MA which has been successfully worn in eyes for ten years[190] but was not strong and stiff enough to be used in KPro was examined with mesh materials. Several other hydrogels which have similar composition to ABH, modified with AMO and NNDMA, have been examined with mesh materials as well. THFMA was replaced by MMA because the stiffness is not necessary. PEG MA was used to protect the surface and a combination of HEMA and Nitrogen-containing monomers was employed to produce a batch of EWC and sequence distribution (which is affected by both concentration and reactivity ratios of compositions). These hydrogels have similar equilibrium water contents and mechanical properties with ABH, are very flexible but not strong and stiff enough. They all can polymerise with mesh materials with a suitable diluent (in this case it is a mixture of pure water and N-methyl pyrrolidione (NVP) in the ratio of 50:50 by weight) and these mesh reinforced hydrogels show stronger and stiffer mechanical properties.

The hydrogels reinforced with mesh materials should not only overcome the mechanical problems identified in this work, but also possess some other advantages, such as enhancing the integration of the skirt and core materials. The lack of adequate integration between the optic and its surrounding skirt, and between the skirt and the host tissue, underlies most of the complications associated with KPros. A polymer mesh should be able to act as a "bridge" to help anchor the core and skirt together. The mesh material could be allowed to protrude from the KPro skirt edge if it was felt that this would aid integration into the host pocket by stitching through the surrounding mesh. It depends on the mould designed for KPro. The mesh should also assist cell integration. Thus, by careful choice of mesh material and hydrogels it should be possible to "design" mesh reinforced materials for use in keratoprosthesis successfully.

8.2 Future Work

The aim of this thesis is to develop novel hydrogels to mimic the natural human cornea. The mechanical properties of the natural human cornea constitute a very important factor

that should be considered. At Aston, a rheometer has been used to measure the dynamic mechanical property of the human cornea. Some workers have described the mechanical behaviour of the cornea as a continuum poroelastic material model and used computer methods to calculate theoretical mechanical properties. However, no literature has been found which overviews the comprehensive mechanical properties of the natural human cornea. Thus the swollen cornea's mechanical properties and how the liquid in the cornea affects the mechanical properties should be studied further. This will set a criterion for the development of novel hydrogels for keratoprosthesis.

MMA copolymers and SIPNs have been investigated in this thesis. None of these materials are ideal KPro materials. Mesh material as an alternative material was investigated in the initial stage in this thesis. It exhibited a promising future and seems that it can overcome the limitation in the mechanical properties of the conventional hydrogels. Different kinds of mesh materials in various aspects, such as the thickness, density and colour, should be studied. Surface treatment of mesh to increase the bond between the polymer and mesh, and to overcome water interface properties and boundary effects may be useful.

Hydrophilic groups on the surface will be important for the longevity of the final KPro. Various surface modification techniques and covalent attachment of cell adhesion proteins need to be employed to promote epithelialization.

The peripheral section is a very important component in KPro model. Two porosigens were used to make the porous material in this work but neither is ideal. An alternative porosigen should be found and the optimum pore size, distribution, density and depth into the material should be studied further.

The integration of core and skirt materials remains a technical problem although the mesh material can act as a "bridge" to help anchor both materials. The conventional contact lens mould may not be an ideal device to fabricate the KPro model. Other KPro moulds should be designed and studied in the future.

A cell-promoting material for the skirt may be worth considering. A cell promoter such as Fibronectin can be bound inside of pores to encourage cellular integration. There are two possible ways to achieve it. One is to coat the cell enhancer onto the porosigen. It would

be possible to anchor the cell promoter into the pores to inhibit it from leaching out. Another method would be to coat the cell promoter onto the mesh material. The cell promoter may then infiltrate into the pores.

The ideal KPro material should be non degradable. A degradation study should be undertaken in the next step. An autoclave or a high pressure cooker can be used to study the degradation and the EWC, mechanical properties and surface properties need be assessed before and after this treatment.

It would be necessary to undertake some implantation studies. They may show whether the material selection is correct and how it reacts when inserted into the body. The implantation work can indicate the modifications that may be required regarding the surgical procedure. Most importantly, implantation will indicate the viability of the device, whether or not extrusion, retroprosthetic membrane formation or tissue melting occurs.

References

1. Williams, D.F., Definitions in Biomaterials, Proceedings of a Consensus Conference of the European Society for Biomaterials, Chester, England, 1986, **4**, Elsevier, New York

2. Wichterle, O. and Lim, D., Hydrophilic gels for biological use, Nature, 1960, **185**, 117-118

3. Mackay, T.G., Wheatley, D.J., Bernacca, G.M. *et al.*, New polyurethane heart valve prostheses, Biomaterials, 1996, **17**, 19, 1857-1863

4. Ambrosio, L., Netti, P.A., Iannace, S. *et al*, Composite hydrogels for intervertebral disc prostheses, J. Mat. Sci.: Mats. in Med., 1996, **7**, 251-254

5. Netti, P.A., Shelton, J.C., Revell, P.A. *et al*, Hydrogels as an interface between bone and an implant, Biomaterials, 1993, **14**, 14, 1098-1104

6. Tighe, B.J., Towards the bionic man; A new biomedical technology?, Biomedical technology., 1992, 186-192

7. Oxley, H.R., Corkhill, P.H., Fitton, J.H. *et al*, Macroporous hydrogels for biomedical applications: methodology and morphology, Biomaterials, 1993, **14**, 14, 1064-1072

8. Packard, R.B.S., Garner, A. and Arnott, E.J., PolyHEMA as a material for intraocular lens implantation: a preliminary report, Br. J. Ophthalmol., 1981, **65**, 585-587

9. Pedley, D.G., Skelly, P.J. and Tighe, B.J., Hydrogels in biomedical applications, Br. Polym. J., 1980, **12**, 99-110

10. Tighe, B.J., Hydrogel materials: The Patents and the products, part I and II, Optician, 1989, June 2, 17-24, and July 7, 17-22

11. Sperling, L.H., Interpenetrating networks and related materials, Plenum Press, New York, 1981

12. Aylsworth, J.W., U.S. Patent No. 1,111,284, 1914

13. Corkhill, P.H., Fitton, J.H. and Tighe, B.J., Towards a synthetic articular cartilage, J. Biomat. Sci.: Polym. Ed., 1993, **4**, 6, 615-630

14. Corkhill, P.H., Novel hydrogel polymers, Ph.D thesis, Aston University, 1988

15. Corkhill, P.H., Jolly, A.M., Ng, C.O. *et al*, Synthetic hydrogels 1: Hydroxyalkyl acrylate and methacrylate copolymers–water binding studies, Polymer, 1987, **28**, 1758-1766

16. Mathur, A.M. and Scranton, A.B., Characterization of hydrogels using nuclear magnetic resonance spectroscopy, Biomaterials, 1996, **17**, 547-557

17. Larsen, D.W., Huff, J.W. and Holden, B.A., Proton NMR relaxation in hydrogel contact lenses: correlation with *in vivo* lens dehydration data, Current Eye Research, 1990, **9,** 7, 697-706

18. Sung, Y.K., Gregonis, D.E., John, M.S. *et al*, Thermal and pulse NMR analysis of water in poly(2-hydroxyethyl methacrylate), J. Appl. Polym. Sci., 1981, **26**, 3719-3728

19. Yamada-Nosaka, A., Ishikiriyama, K. *et al*, ^{1}H-NMR studies on water in methacrylate hydrogels. I, J. Appl. Polym. Sci, 1990, **39**, 2443-2452

20. Roorda, W.E., de Bleyser, J., Junginger, H.E. *et al*, Nuclear magnetic relaxation of water in hydrogels, Biomaterials, 1990, **11**, 17-23

21. Pathmanathan, K. and Johari, G.P., Dielectric and conductivity relaxations in poly (HEMA) and of water in its hydrogel, J. Polym. Sci.: Part B: Polym. Physics, 1990, **28**, 675-689

22. Roorda, W.E., Bouwstra, J.A., de Vries, M.A. *et al*, Thermal analysis of water in p(HEMA) hydrogels, Biomaterials, 1998, **9**, 494-499

23. Ma, J.J., Novel hydrogel polymers, Ph.D thesis, Aston University, 1996

24. Cha, W.I., Hyon, S.H. and Ikada, Y., Microstructure of poly(vinly alcohol) hydrogels investigated with differential scanning calorimetry, Makromol. Chem., 1993, **194**, 2433-2442

25. Khare, A.R. and Peppas, N.A., Investigation of hydrogel water in polyelectrolyte gels using differential scanning calorimetry, Polymer, 1993, **34**, 22, 4736-4739

26. Takigami, S., Kimura, T. and Nakamura, Y., The state of water in nylon-6 membranes grafted with hydrophilic monomers: 2. Water in acrylic acid, acrylamide and p-styrenesulphonic acid grafted nylon-6 membranes, Polymer, 1993, **34,** 3, 604-609

27. Hatakeyema, T., Yamaucho, A. and Hatakeyema, H., Studies on bound water in poly(vinyl alcohol), Eur. Polym. J., 1984, **20,** 1, 61-64

28. Tighe, B.J. and Trevett, A.S., Characterisation of mechanical properties of soft contact lenses, BCLA Annual Clinical Conference, Glasgow, May 1990, reprinted in BCLA Transactions 1990, **13**, 2, 57-61

29. John, M.S. and Andrade, J.D., Water and hydrogels, J. Biomed. Mater. Res., 1973, **7**, 509-552

30. Smith, L., Doyle, C., Gregonis, D.E. *et al*, Surface oxidation of cis-trans polybutadiene, J. Appl. Polym. Sci., 1982, **27**, 1269-1276

31. Andrade, J.D., Smith, L.M. and Gregonis, D.E., The contact angle and interface energetics in biomedical polymers, Vol. 1., J.D. Andrade Ed., New York, Plenum, 1985, 249-292

32. Tretinnikov, O.N. and Ikada, Y., Dynamic wetting and contact angle hysteresis of polymer surfaces studied with the modified Wilhelmy balance method, Langmuir, 1994, **10**, 1606-1614

33. Yasuda, H. and Sharma, A.K., Effect of orientation and mobility of polymer molecules at surfaces on contact angle and its hysteresis, J. Polym. Sci.: Polym. Phys. Ed., 1981, **19**, 1285-1291

34. Young, T., On the cohesion of fluids, Phil. Trans. Roy. Soc. (London), 1805, **95**, 65-87

35. Dupre, A., Theorie mechanique de la chaleur, Guthier Villars, Paris, 1869, 369

36. Fowkes, F.M., Determination of interfacial tensions, contact angles and dispersion forces in surfaces by assuming additivity of intermolecular interactions in surfaces, J. Phys. Chem., 1962, **66**, 382

37. Good, R.J. and Girifalco, L.A., A theory for the estimation of surface and interfacial energies III: Estimation of surface energies of solids from contact angles, J. Phys. Chem., 1960, **64**, 561-565

38. Owens, D.K. and Wendt, R.C., Estimation of the surface free energy of polymers, J. Appl. Polym. Sci., 1969, **13**, 1741-1747

39. Hamilton, W.C., A technique for the characterization of hydrophilic solid surfaces, J. Colloid and Interface Sci., 1972, **40**, 2, 219-222

40. Hamilton, W.C., Measurement of the polar force contribution to adhesive bonding, J. Colloid and Interface Sci., 1974, **47**, 3, 672-675

41. Fowkers, F.M., Attractive forces at interfaces, Ind. End. Chem., 1964, **56**, 40

42. Tamai, Y., Makuuchi, K. and Suzuki, M., Experimental analysis of interfacial forces at the plane surface of solids, J. Phys. Chem., 1967, **71**, 4176-4179

43. Adamson, A.W., Physical chemistry of surfaces, 3rd Edn., Wiley-Interscience, New York, 1976

44. Andrade, J.D., King, R.N., Gregonis, D.E. *et al*, Surface characterization of p(HEMA) and related polymers I: Contact angle methods in water, J. Appl. Polym. Sci.: Polym. Symp., 1979, **66**, 313-336

45. Franklin, V.J., Lipoidal species in ocular spoilation processes, Ph.D thesis, Aston University, 1990

46. Sariri, R., Tear protein interaction with hydrogel contact lenses, Ph.D thesis, Aston University, 1995

47. Ikada, Y., Suzuki, M. and Tamada, Y., Polymer surfaces possessing minimal interaction with blood components, in Polymers as biomaterials, Shalaby, S., Hoffman, A., Ratner, B. and Horbett, T., Eds., Plenum, New York, 1984, 135-147

48. Baker, D.A., Corkhill, P.H., Ng, C.O. *et al*, Synthetic hydrogels 2: Copolymers of carboxyl, lactam and amide-containing monomers: structure/property relationships, Polymer, 1988, **29**, 691-700

49. Barnes, A., Corkhill, P.H. and Tighe, B.J., Synthetic hydrogels 3: Hydroxylalkyl acrylate and methacrylate copolymers: Surface and mechanical properties, Polymer, 1988, **29**, 2191-2202

50. Franklin, V.J., Bright, A.M. and Tighe, B.J., Hydrogel polymers and ocular spoilation processes, TRIP, 1993, **1**, 1, 9-16

51. Baker, D. and Tighe, B.J., Polymers in contact lens applications (VIII): Problem of biocompatibility, Contact Lens J., 1981, **10**, 3, 3-14

52. French, K.A., Novel cationic polymers for use at biological interfaces, Ph.D thesis, Aston University, 1996

53. Baier, R.E., Dutton, R.C. and Gott, V.L., Surface chemical features of blood vessels walls and of synthetic materials exhibiting thromboresistance, in Advances in Experimental Medicine, Surface chemistry of biological surface, Plenum press, New York, 1970, **7**, 235-260

54. Andrade, J.D., Interfacial phenomena and biomaterials, Medical Instrumentation, 1973, **7**, 110-120

55. Coleman, D.L., Gregonis, D.E. and Andrade, J.D., Blood-materials interactions: the minimum interfacial free energy and the optimum polar/apolar ratio hypotheses, J. Biomed. Mater. Res., 1982, **16**, 381-398

56. Ratner, B.D., Hoffman, A.S., Hanson, S.R. *et al*, Blood compatibility-water content relationships for radiation grafted hydrogels, J. Polym. Sci.: Polym. Symp., 1979, **66**, 363-375

57. Okano, T., Nishiyama, S., Shinohara, I. *et al*, Interaction between plasma protein and microphase separated structure of copolymers, Polymer J. (Tokyo), 1978, **10**, 223-228

58. Asharf, N., Sequence distribution in free radical polymerisations, Ph.D thesis, Aston University, 1995

59. Ma, J.J., Franklin, V.J., Tonge, S.R. *et al*, Ocular compatibility of biomimetic hydrogels, Poster presented at BCLA 9th Annual Clinical Conference, Torquay, 1994, May

60. Alfrey, T. and Goldfinger, G., The mechanism of copolymerisation, J. Chem. Phys., 1944, **12**, 205-209

61 Mayo, F.R. and Lewis, F.M., Copolymerisation I. A basis for comparing the behaviour of monomers in copolymerisation; the copolymerisation of styrene and methyl methacrylate, J. Am. Chem. Soc., 1944, **66**, 1594-1601

62. Alfrey, T. and Price, C.C., Relative reactivities in vinyl copolymerisation, J. Polym. Sci., 1947, **2,** 1, 101-106

63. Laurier, G.C., O'Driscoll, K.F. and Reilly, P.M., Estimating reactivity in free radical copolymerizations, J. Polym. Symp., 1985, **72**, 17-26

64. O'Driscoll, K.F., Comments on "Relative reactivities in vinyl copolymerisation," Turner Alfrey, Jr. and Charles C. Price, J. Polym. Scil, 2, 101 (1947), J. Polym. Sci.: Part A: Polym. Chem., 1996, **34**, 155-156

65. Kaufman, H.E., Barron, B.A., McDonald, M.B. *et al*, The Cornea, 2nd Edn., Butterworth-Heinemann, 1999

66. Sharma, A., Energetics of corneal epithelial cell-ocular mucus-tear film interactions: some surface-chemical pathways of corneal defence, Biophys. Chem., 1993, **47**, 87-99

68. Maurice, D.M., The eye, ed. Davson, H., 2nd Edn., Academic Press, New York, 1969, **1**, 489-600

68. Fini, M.E. and Gerard, M.T., The pattern of metalloproteinase expression by corneal fibroblasts is altered by passage in cell culture, J. Cell Sci., 1990, **97**, 373-383

69. Geroshi, D.H., Matsuda, M. and Yee, R.W., Pump function of the human corneal endothelium, Ophthalmology, 1995, **92**, 1

70. Joyce, N.C., Navon, S.E., Sayon, R. *et al*, Expression of cell-cycle associated proteins in human and rabbit corneal endothelium in situ, Invest. Ophthalmol. Vis. Sci., 1996, **37**, 1566

71. Faragher, R.G.A., Mulholland, B., Tuft, S.J. *et al*, Aging and the cornea, Br. J. Ophthalmol., 1997, **81**, 814-817

72. Intraocular lens implantation, NIH consensus Statement 1979, **2**, 37-42

73. Chirila, T.V., Modern artificial corneas the use of porous polymers, TRIP, 1994, **2**, 296-300

74. Corkhill, P.H., Hamilton, C.J. and Tighe, B.J., Design of hydrogels for medical applications, Critical Reviews in Biocompatibility, 1990, **5**, 4, 363-436

75. Hogan, M.J. and Zimmerman, L.E., Ophthalmic Pathology, An Alta and Textbook, Saunders, Philadelphia, PA, 1962, 277-343

76. Greer, C.H., Ocular Pathology, 3rd Edn., Blackwell Scientific, Oxford, 1979, 79-115

77. Barraquer, J.I., Binder, P.S., Buxton, J.N. *et al*, Symposium on Medical and Surgical Diseases of the Cornea, Mosby, St Louis, MO, 1980

78. Leibowitz, H.M. (ed.), Corneal Disorders, Clinical Diagnosis and Management, Saunders, Philadelphia, PA, 1984

79. Oslen, R.J., Corneal transplantation techniques in Kaufman, H.E., Barron, B.A., McDonald, M.B., Waltman S.R., (ed), The Cornea, New York, Churchill Livingston, 1988, 743-784

80. Khan, B., Dudenhoefer, E.J. and Dohlman, C.H., Keratoprosthesis: an update, Current Opinion in Ophthalmology, 2001, **12**, 282-287

81. Hirschberg, J., The History of ophthalmology, Wayenborgh, Bonn, 1984, **3**, 1, 380

82. Nussbaum, J.N., Zeitschr. Wiss. Zool., 1854, **5**, 179-187 (within reference: Chirila, T.V., Hicks, C.R., Dalton, P.D. *et al*, Artificial Cornea, Prog. Polym. Sci., 1998, **23**, 447-473)

83. Maurice, D.M., The Eye, Davson, H. (ed), 2nd Edn, Academic Press, New York, 1969, **1**, 489-600

84. Cardona, N., Keratoprostheses, Am. J. Ophthalmol., 1962, **54**, 284-294

85. Giles, C.L. and Henderson, J.W., Keratoprosthesis: current status, Am. J. Med. Sci., 1967, **253**, 239-242

86. Heusser, T., Denkschr. Med. Chir. Ges. Kant. Zurich, 1860, 127-129 (within reference: Chirila, T.V., Hicks, C.R., Dalton, P.D. *et al*, Artificial Cornea, Prog. Polym. Sci., 1998, **23**, 447-473)

87. Forster, A.E., A review of keratoplastic surgery and some experiments in keratoplasty, Am. J. Ophthalmol., 1923, **6**, 366-375

88. Baker, A.R., Am. J. Ophthalmol. (Ser. 2), 1889, **6**, 1-10 (within reference: Chirila, T.V., Hicks, C.R., Dalton, P.D. *et al*, Artificial Cornea, Prog. Polym. Sci., 1998, **23**, 447-473)

89. Dimmer, F., Ber. Versamml. Ophthalmol. Ges. Heidelberg, 1889, **20**, 148-163 (within reference: Chirila, T.V., Hicks, C.R., Dalton, P.D. *et al*, Artificial Cornea, Prog. Polym. Sci., 1998, **23**, 447-473)

90. Dimmer, F., Klin. Monatsbl Augenheilk., 1891, **29**, 104-105 (within reference: Chirila, T.V., Hicks, C.R., Dalton, P.D. *et al*, Artificial Cornea, Prog. Polym. Sci., 1998, **23**, 447-473)

91. Lang, W., Trans. Ophthalmol. Soc. U.K., 1887, **7**, 286-291 (within reference: Chirila, T.V., Hicks, C.R., Dalton, P.D. *et al*, Artificial Cornea, Prog. Polym. Sci., 1998, **23**, 447-473)

92. Salzer, F., Zeitschr. Augenheilk., 1900, **3**, 504-509 (within reference: Chirila, T.V., Hicks, C.R., Dalton, P.D. *et al*, Artificial Cornea, Prog. Polym. Sci., 1998, **23**, 447-473)

93. Salzer, F., Arch. Augenheilk., 1937, **101**, 450-481 (within reference: Chirila, T.V., Hicks, C.R., Dalton, P.D. *et al*, Artificial Cornea, Prog. Polym. Sci., 1998, **23**, 447-473)

94. Hess, V.R., Klin. Montasbl. Augenheilk., 1940, **104**, 334 (within reference: Chirila, T.V., Hicks, C.R., Dalton, P.D. *et al*, Artificial Cornea, Prog. Polym. Sci., 1998, **23**, 447-473)

95. Vogt, A., Klin. Montasble. Augenheilk, 1941, **106**, 243-244 (within reference: Chirila, T.V., Hicks, C.R., Dalton, P.D. *et al*, Artificial Cornea, Prog. Polym. Sci., 1998, **23**, 447-473)

96. Davson, H., The Physiology of the Eye, 3rd Edn. Churchill Livingstone, Edinburgh, 1972, 68-85

97. Sommer, G., Klin. Montasbl. Augenheilk., 1953, **122**, 545-554 (within reference: Chirila, T.V., Hicks, C.R., Dalton, P.D. *et al*, Artificial Cornea, Prog. Polym. Sci., 1998, **23**, 447-473)

98. Anderson, O.E.E., Theoretical considerations for an artificial corneal implant, Br. J. Ophthalmol., 1951, **35**, 628-630

99. Cuperus, P.L., Jongebloed, W.L., Van Andel, P. *et al*, Doc. Ophthalmol., 1989, **71**, 29-47

100. Van Andel, P., Singh, I., Worst, J. *et al*, The 4th World Biomaterials Congress, Abstracts, Berlin, Germany, 1992, 486

101. Singh, I.R., The 2nd KPro Study Group Meeting, Abstracts, Rome, Italy, 1995, 16

102. Van Andel, P., Worst, J. and Singh, I., The 2nd KPro Study Group Meeting, Abstracts, Rome, Italy, 1995, 17-18

103. Stone, W. and Herbert, E., Experimental study of plastic materials as replacement for the cornea, Am. J. Ophthalmol., 1953, **36**, 168-173

104. Ridley, H., Intra-ocular acrylic lenses: a recent development in the surgery of cataract, Br. J. Ophthalmol., 1952, **36**, 113-122

105. Chirila, T.V., Constable, I.J., Russo, A.V. *et al*, Ridley intraocular lens revisited: chemical analysis of residuals in the original lens material, J. Cata. Refr. Surg., 1989, **15**, 283-288

106. Gyorffy, I., Acrylic corneal implant in keratoplasty, Am. J. Ophthalmol., 1951, **34**, 757-758

107. Wunshce, G., Arztliche Forsch., 1947, **1**, 345-348 (within reference: Chirila, T.V., Hicks, C.R., Dalton, P.D. *et al*, Artificial Cornea, Prog. Polym. Sci., 1998, **23**, 447-473)

108. Vanysek, J.V., Iserle, J. and Altman, J., Csl. Oftal., 1954, **10**, 108-120; Ophthalmic Lit., 1954, **8**, 1187 (within reference: Chirila, T.V., Hicks, C.R., Dalton, P.D. *et al*, Artificial Cornea, Prog. Polym. Sci., 1998, **23**, 447-473)

109. Thompson, K.P., Hanna, K. and Waring, G.O., *et al.* Current status of synthetic epikeratoplasty, J. Refract. Surg., 1991, **7**, 240-248

110. Trinkaus-Randall, V., Wu, X.Y., Tablante, R. *et al*, Implantation of a synthetic cornea: design, development and biological response, Artificial Organs, 1997, **21**, 1185-1191

111. Hicks, C.R., Chirila, T.V., Clayton, A.B. *et al.*, Clinical results of implantation of the Chirila keratoprosthesis in rabbits, Br. J. Ophthalmol., 1998, **82**, 18-25

112. Legeais, J.M. and Renard, G., A second generation of artificial cornea (Biokpro II), Biomaterials, 1998, **19**, 1517-1522

113. Jacob-LaBarre, J.T. and Caldwell, D.R., Development of a new type of artificial cornea for treatment of end stage corneal diseases, in Gebelein, C.G., Dunn, R.L., Progress in Biomedical Polymers, New York, Plenum Press, 1990, 27-39

114. Kain, H.L. and Thoft, R.A., A new approach to keratoprosthesis (abstract), Invest. Ophthalmol. Vis. Sci., 1987, **28**, 231

115. Trinkaus-Randall, V., Capecchi, J., Vadaz, A. *et al*, Development of a biopolymeric keratoprosthesis: epithelial adhesion *in vitro* and *in vivo* (abstract), Invest. Ophthalmol. Vis. Sci., 1987, **28**, 54

116. Capecchi, J.T., Trinkaus-Randall, V., Vadaz, A. *et al*, Development of a biopolymeric keratoprosthesis material (abstract), Invest. Ophthalmol. Vis. Sci., 1987, **28**, 160

117. Leibowitz, H., Trinkaus-Randall, V., Capecchi, J. *et al*, Development of a biopolymeric keratoprosthesis: stromal fibroblast ingrowth and synthesis (abstract), Invest. Ophthalmol. Vis. Sci., 1988, **29**, 452

118. Chirila, T.V., Chen, Y.C., Griffin, B.J. *et al*, Hydrophilic sponges based on 2-hydroxyethyl methacrylate I: Effect of monomer mixture composition on the pore size, Polym. Int., 1993, **32**, 221-232

119. Cardona, H., The Cardona keratoprosthesis: 40 years experience, Refract. Corneal Surg., 1991, **7**, 468-471

120. Wilson, S.E., Li, Q., Weng, J. *et al*, The Fas-Fas ligand system and other modulators of apoptosis in the cornea, Invest. Ophthalmol. Vis. Sci., 1996, **37**, 1582-1592

121. Hicks, C.R., Fitton, J.H., Chirila, T.V. *et al*, Keratoprostheses: Advancing toward a true artificial cornea, Survey of ophthalmology, 1997, **42**, 175-189

122. Kain, H.L., The development of the silicone-carbon keratoprosthesis, Refract. Corneal Surg. 1993, **9**, 209-210

123. Trinkaus-Randall, V., Capecchi, J., Sammon, L. *et al*, *In vitro* evaluation of fibroplasia in a porous polymer, Invest. Ophthalmol. Vis. Sci., 1990, **31**, 1321-1326

124. Trinkaus-Randall, V., Banwatt, R., Capecchi, J. *et al*, *In vivo* fibroplasia of a porous polymer in the cornea, Invest. Ophthalmol. Vis. Sci., 1991, **32**, 3245-3251

125. Capecchi, J.T., Franzblau, C., Gibbons, D.F. *et al*, U.S. Patent No. 5,108,428, 1992

126. Trinkaus-Randall, V., Banwatt, R., Wu, X.Y. *et al*, Effect of pretreating porous webs on stromal fibroplasia *in vivo*, Biomed. Mater. Res., 1994, **28**, 195-202

127. Aysta, J.E., Capecchi, J.T., Franzblau, C. *et al*, U.S. Patent No. 5,032,131, 1991

128. Lamberts, D.W. and Grandon, S.C., A new alloplastic material for ophthalmic surgery, Ophthalmic Surg., 1978, **9**, 35-42

129. Shea, J.J. and Homsy, C.A., The use of Proplast in otologic surgery, Laryngoscope, 1974, **84**, 1835-1845

130. Barber, J.C., Feaster, F. and Priour, D., The acceptance of a vitreous carbon alloplastic material, Proplast, in the rabbit eye, Invest. Ophthalmol. Vis. Sci., 1980, **19**, 182-191

131. White, J.H. and Gona, O., Proplast" for keratoprosthesis, Ophthalmic Surg., 1988, **19**, 331-333

132. Caldwell, D.R. and Jacob-Labarre, J.T., U.S. Paten No. 4,865,601, 1989

133. Caldwell, D.R. and Jacob-Labarre, J.T., U.S. Patent No. 4,932,968, 1990

134. Kim, H.C., The experimental Seoul-type keratoprosthesis, Korean J. Ophthalmol., 1992, **6**, 55-61

135. Legeais, J.M., Renard, G. and Anton, M., Fr. Patent No. 2,649,605, 1991

136. Legeais, J.M., Rossi, C., Renard, G. *et al*, A new fluorocarbon for keratoprosthesis, Cornea, 1992, **11**, 538-545

137. Legeais, J.M., Renard, G., Parel, J.M. *et al*, Expanded fluorocarbon for keratoprosthesis cellular ingrowth and transparency, Exp. Eye Res., 1994, **58**, 41-52

138. Renard, G., Cetinel, B., Legeais, J.M. *et al*, Incorporation of a fluorocarbon polymer implanted at the posterior surface of the rabbit cornea, J. Biomed. Mater. Res., 1996, **31**, 193-199

139. Matsuda, S., Iwata, H. and Ikada, Y., Biomedical materials in the Far East –II (Proceeding of the 2nd Far-Eastern Symposium on Biomedical Materials), ed. Ikada, Y. and Zhang, X., Kyoto, Japan, 1995, 179-180

140. Sieck, E.A., Uyemura, M.J. and Miller, J.R., Porous polyethylene (medpor) as an intrastromal corneal support for a keratoprosthesis, Invest. Ophthalmol. Vis. Sci., 1995, **36(Suppl.)**, 314

141. Pintucci, S., Pintucci, F., Cecconi, M. *et al*, New Dacron tissue colonisable keratoprosthesis: clinical experience, Br. J. Ophthalmol., 1995, **79**, 825-829

142. Chirila, T.V., Constable, I.J., Crawford, G.J. *et al*, Australian Patent No. 650,156, 1994

143. Chirila, T.V., Constable, I.J., Crawford, G.J. *et al*, U.S. Patent No. 5,300,16, 1994

144. Chirila, T.V., Constable, I.J., Crawford, G.J. *et al*, U.S. Patent No. 5,458,819, 1995

145. Yasuda, H., Gochin, M. and Stone, W., Hydrogels of poly(hydroxyethyl methacrylate) and hydroxyethyl methacrylate-glycerol monomethacrylate copolymers, J. Polym. Sci. Part A, 1966, **4**, 2913-2927

146. Dusek, K., Phase separation during the formation of three-dimensional polymers, J. Polym. Sci., Part C, 1967, **16**, 1289-1299

147. Chirila, T.V., Constable, I.J., Crawford, G.J. *et al*, Poly(2-hydroxyethyl methacrylate) sponges as implant materials: *in vivo* and *in vitro* evaluation of cellular invasion, Biomaterials, 1993, **14**, 26-38

148. Crawford, G.J., Constable, I.J., Chirila, T.V. *et al*, Tissue interaction with hydrogel sponges implanted in the rabbit cornea, Cornea, 1993, **12**, 348-357

149. Fyodorov, S.N., Moroz, Z.I. and Zuev, V.K., Keratoprostheses, London, Churchill, Livingstone, 1987, **7**, 54

150. Cardona, H., Keratoprosthesis with a plastic fibre meshwork supporting plate, Am. J. Ophthalmol., 1967, **64**, 228-233

151. Cardona, H., Keratoprosthesis: acrylic optical cylinder with supporting intralamellar plate, Am. J. Ophthalmol., 1962, **54**, 284-294

152. Polack, F.M., Corneal optical prostheses, Br. J. Ophthalmol., 1971, **55**, 838-843

153. Roper-Hall, M.J., Why are keratoprostheses not given more importance [letter], Eur. J. Ref. Surg., 1991, **3**, 79

154. Polack, F.M., Clinical results with ceramic keratoprosthesis, Cornea, 1983, **2**, 185-196

155. Kozarsky, A.M., Knight, S.H. and Waring, G.O., Clinical results with a ceramic keratoprosthesis placed through the eyelid, Ophthalmology, 1987, **94**, 904-911

156. Strampelli, B., Keratoprosthesis with osteodontal tissue, Am. J. Ophthalmol., 1963, **89**, 1029-1039

157. Strampelli, B., Nouvelle orientation biologique dans la keratoprosthese, Bull Mem. Soc. Fr. Ophthalmol., 1964, **77**, 145-161

158. Hatt, M., Experimental osteokeratoprosthesis, Ophthalmol. Res., 1979, **11**, 40-51

159. Caiazza, S., Falcinelli, G. and Pintucci, S., Exceptional case of bone resorption in an osteo-odonto-keratoprosthesis, A scanning electron microscopy and xray microanalysis study, Cornea, 1990, **9**, 23-27

160. Gristina, A.G., Biomaterial-centered infection: microbial adhesion versus tissue integration, Science, 1987, **237**, 1588-1595

161. Oga, M., Sugioka, Y., Hobgood, C.D. *et al*, Surgical biomaterials and differential colonization by staphylococcus epidermidis, Biomaterials, 1988, **9**, 285-289

162. Moller, J.K., Drug resistance and plasmid profiles in Staphylococcus epidermidis in 1964 and 1986, J. Hosp. Infect., 1988, **12**, 19-27

163. Turss, R., Friend, J. and Dohlman, C.H., Effect of corneal fluid barrier on nutrition of the epithelium [letter], Exp. Eye. Res., 1970, **9**, 254

164. Knowles, W., Effect of intralamellar plastic membranes on corneal physiology, Am. J. Ophthalmol., 1961, **51**, 274-284

165. Alberts, B., Bray, D., Lewis, J. *et al*, Cell growth and division, Molecular biology of the cell, New York, Garland, 1983, 618-619

166. Stone, W., Study of potency of openings in corneas anterior to intralamellar plastic artificial discs, Am. J. Ophthalmol., 1955, **39**, 185-196

167. Kornmehl, E.W., Bredvik, B.K., Kelman, C.D. *et al*, *In vivo* evaluation of a collagen corneal allograft derived from rabbit dermis, J. Refr. Surg., 1995, **11**, 502-507

168. Green, D. W., A biological-inspired support frame for an artificial cornea, Ph.D thesis, Aston University, 2000

169. Chirila, T.V., Hicks, C.R., Dalton, P.D. *et al*, Artificial Cornea, Prog. Polym. Sci., 1998, **23**, 447-473

170. Ricci, R., Pecorella, I., Ciardi, A. *et al*, Strampelli's osteo-odonto-keratoprosthesis: Clinical and histological long-term features of these prostheses, Br. J. Ophthalmol., 1992, **76**, 232-234

171. Falcinelli, G., Barogi, G. and Taloni, M., Osteo-odonto-keratoprosthesis: Present experience and future prospects, Refr. Corneal Surg., 1993, **9**, 193-194

172. Liu, C. and Pagliarini, S., Long-term results of the Falcinelli osteo-odonto keratoprosthesis (OOKP) (abstract), Fourth World Congress on the Cornea Abstracts, The Castroviejo Society, 1996, 91

173. Lee, J.H., Wee, W.R., Chung, E.S. *et al.*, Development of a newly designed double-fixed Seoul-type keratoprosthesis, Arch. Ophthalmol., 2000, **118**, 1673-1678

174. Hicks, C., Crawford, G., Chirila, T.V. *et al.*, Development and clinical assessment of an artificial cornea, Prog. in Ret. and Eye Res., 2000, **19**, 149-170

175. Langefeld, S., Kompa, S. and Redbrake, C., Aachen keratoprosthesis as temporary implant for combined vitreoretinal surgery and keratoplasty: report on 10 clinical applications, Graefes. Arch. Clin. Exp. Ophthalmol., 2000, **238**, 722-726

176. Dohlman, C.H., Schneider, H.A. and Doane, M.G., Prosthokeratoplasty, Am. J. Ophthalmol., 1974, **77**, 694-700

177. Cardona, H., Mushroom transcorneal keratoprosthesis, Am. J. Ophthalmol., 1969, **68**, 604-612

178. Castroviejo, R., Cardona, H. and DeVoe, A.G., The present status of prosthokeratoplasty, Trans. Am. Ophthalmol. Soc., 1969, **67**, 204-234

179. Vijayasekaran, S., Chirila, T.V., Robertson, T.A. *et al*, Calcification of poly (2-hydroxyethyl methacrylate) hydrogel sponges implanted in the rabbit cornea: a 3-month study, J. Biommater. Sci.: Polymer Edn., 2000, **11**, 6, 599-615

180. Coleman, D.L., Hsu, H.C., Dong, D.E. and Olsen, D.B., Calcium in biological systems, Plenum Press, New York, 1985, 653

181. Hamon, R.F., Khan, A.S. and Chow, A., The cation-chelation mechanism of metal-ion sorption by polyurethanes, Talanta, 1982, **29**, 313

182. Pfister, R.R., Chemical injuries of the eye, Ophthalmology, 1983, **90**, 1246-1253

183. Lloyd, A.W., Faragher, R.G.A. and Denyer, S.P., Ocular biomaterials and implants, Biomaterials, 2001, **22**, 769-785

184. Wu, X.Y., Tsuk, A., Leibowitz, H.M. *et al*, *In vivo* comparison of three different porous materials intended for use in a keratoprosthesis, Br. J. Ophthalmol., 1998, **82**, 569-576

185. Trinkaus-Randall, V. and Nugent, M.A., Biological response to a synthetic cornea, J. Controlled Release, 1998, **53**, 205-214

186. Yocum, R.H. and Nyquist, E.B. (ed), Functional Monomers, Vols. 1 and 2, Marcel Dekker, New York, 1973

187. Young, R., Synthesis and characterisation of hydrogel polymers for medical applications, Ph.D thesis, Aston University, 1998

188. Lai, Q., Protein and cell adhesion to block polymer microdomains, Conference proceedings, Fourth World Biomaterials Congress, Berlin, 1992, 450

189. Minoura, N., Aiba, S., Fujiwara, Y. *et al*, Interactions of culture cells with membranes composed of random and block copolypeptides, J.Biomed. Mater. Res., 1989, **2,** 2, 139-146

190. Benning, B., Novel high water content hydrogels, Ph.D thesis, Aston University, 2000

191. Lee, V.H.L., In peptide and protein drug delivery, Marcel Dekker Inc., New York, 1991, 831-864

192. Pato, J., Azori, M., Ulbrich, K. *et al*, Polymers containing enzymatically degradable bonds, 9. chymotrypsin catalysed hydrolysis of an p-nitroanilide drug model, bound *via* oligopeptides onto poly(vinylpyrrolidone-co-maleic anhydride), J. Makromol. Chem., 1984, **185**, 231

193. Azori, M., Szinai, I., Veres, Z. *et al*, Polymeric prodrugs, 3. synthesis elimination and whole-body distribution of ^{14}C-labelled drug carrier, Makromal. Chem., 1986, **187**, 297

194. Artoni, G., Gianazza, E., Zanoni, M. *et al*, Fractionation techniques in hydro-organic environment II. Acryloylmorpholine polymers as matrix for electrophoresis in hydro-organic solvents, Analytical Biochemistry, 1984, **137**, 420-428

195. Evans, K., Ocular biomaterials and the anterior eye, Ph.D thesis, Aston University, 1997

196. Kim, E.H., Jeon, S.I., Yoon, S.C. *et al*, The nature of water in tactic poly (2-hydroxyethyl methacrylate) hydrogels, Bull. Korean Chem. Soc. 1981, **2**, 60-66

197. Lee, H.B., Jhon, M.S. and Andrade, J.D., Nature of water in synthetic hydrogels I. Dilatometry, specific conductivity and differential scanning calorimetry of polyhydroxyethyl methacrylate, J. Colloid Interface Sci. 1975, **51**, 225-231

198. Pedley, D.G. and Tighe, B.J., Water binding properties of hydrogel polymers for reverse osmosis and related applications, Br. Polym. J. 1979, **11**, 130-136

199. Xie, H.Q., Zhang, C.X. and Guo, J.S., In: Kempner, D., Sperling, L.H., Utracke, L.A. (ed), Interpenetrating polymer networks, Washington DC: American Chemical Society, 1994, 557

200. Young, R., Lydon, F. and Tighe, B., Polyurethane based hydrogel IPNs for ophthalmic application, Presented at the 8th symposium on the materials science and chemistry of contact lenses, New Orleans, 1996

201. Lelah, M.D. and Cooper, S.L., Polyurethanes in medicine, Boca Raton, FL: CRC Press, 1986

202. Francois, P., Vaudaux, P., Nurdin, A. *et al*, Physical and biological effects of a surface coating procedure on polyurethane catheter, Biomaterials, 1996, **17**, 667

203. Gorman, S.P., Tunney, M.M., Keane, P.F. *et al*, Characterization and assessment of a novel poly (ethylene oxide)/polyurethane composite hydrogel as a uretal sent biomaterial, J. Biomed. Mater. Res., 1998, **39**, 642

204. Elma, H., de Groot, J.H. and Nijenhuis, A.J., Use of porous biodegradable polymer implants in meniscus reconstruction: 2. Biological evaluation of porous biodegradable polymer implants in menisci, Colloid Polym. Sci., 1990, **268**, 1082

205. Messner, K. and Gillquist, J., Prosthetic replacement of the rabbit medial meniscus, J. Biomed. Mater. Res., 1993, **27**, 1165-1173

206. Messner, K. and Gillquist, J., Synthetic implants for the repair of osteochondral defects of the medial femoral condyle: a biomechanical and histological evaluation in the rabbit knee, Biomaterials, 1993, **14**, 513-521

207. Messner, K. and Gillquist, J., Cartilage repair: a critical review, Acta. Orthop. Scand., 1996, **67**, 523

208. Klompmaker, J., Jansen H.W.B. and Veth, R.P.H., Porous polymer implants for repair of full-thickness defects of articular cartilage: an experimental study in rabbit and dog, Biomaterials, 1992, **13**, 625

209. Radder, A.M., Leenders, H. and van Blitterswijk, C.A., Application of porous PEO/PBT copolymers for bone replacement, J. Biomed. Mater. Res., 1996, **30**, 341-351

210. Szycher, M., U.S. Patent No. 4,285,073, 1981

211. Szycher, M., U.S. Patent No. 4,386,039, 1983

212. Szycher, M., U.S. Patent No. 4,424,335, 1984

213. Bruin, P., Meeuwsen, E.A.J., Van Andel, M.V. *et al*, Autoclavable highly cross-linked polyurethan network in ophthalmology, Biomaterials, 1993, **14**, 1089-1097

214. Lydon, M. J., Minett, T. W. and Tighe, B. J., Cellular interactions with synthetic polymer surfaces in culture, Biomaterials, 1985, 6, **11**, 396-402

215. Patel, M. P. and Braden, M., Heterocyclic methacrylates for clinical applications 1: Mechanical properties, Biomaterials, 1991, **12**, 9, 645-648

216. Patel, M. P. and Braden, M., Heterocyclic methacrylates for clinical applications 2: Room temperature polymerising systems for potential clinical use, Biomaterials, 1991, **12**, 9, 649-652

217. Patel, M. P. and Braden, M., Heterocyclic methacrylates for clinical applications 3: Water absorption characteristics, Biomaterials, 1991, **12**, 9, 653-657

218. Labella, R., Braden, M., Clarke, R. L. and Davy, R. W. M., THFMA in dental monomer systems, Biomaterials, 1996, **17**, 4, 431-436

219. Chirila, T.V., Vijayasekaran, S., Horne, R. *et al*, Interpenetrating polymer network (IPN) as a permanent joint between the elements of a new type of artificial cornea, J. Biomed. Mater. Res., 1994, **28**, 745-753

220. Lin, F.H., Yao, C.H., Sun, J.S. *et al*, Biological effects and cytotoxicity of the composite composed by tricalcium phosphate and glutaraldehyde crosslinked gelation, Biomaterials, 1998, **19**, 905-917

221. Drubaix, I., Legeais, J.M., Malek-Cherhire, N. *et al*, Collagen synthesized in fluorocarbon polymer implant in the rabbit cornea, Exp. Eye Res., 1996, 367-376

222. Cima, L., Polymer substrates for controlled biological interactions, J. Cell Biochem., 1994, **56**, 155-161

223. Drumheller, P. and Hubbell, J., Polymer networks with grafted cell adhesion peptides for highly biospecific cell adhesive substrates, Anal. Biochem., 1994, **222**, 380-388

224. Fitton, J.H., Cells, surfaces and adhesion, PhD thesis, Aston University, 1993

225. Drumheller, P. and Hubbell, J., Densely crosslinked polymer networks of poly(ethylene glycol) in trimethylolpropane triacrylate for cell-adhesion-resistant surfaces, J. Biomed. Mater. Res., 1995, **29**, 207-215

226. Oxley, H.R., Hydrogel polymers containing linear and cyclic polyesters, Ph.D thesis, Aston University, 1990

227. Sariri, R., Evans, K. and Tighe, B.J., Protein mobility and activity in hydrogel polymers, Poster presented at 11th European conference on Biomaterials, Pisa, 1994

228. Ziegelaar, B.W., Fitton, J.H., Clayton, A.B. *et al*, The modulation of corneal keratocyte and epithelial cell responses to poly(2-hydroxyethyl methacrylate) hydrogel surfaces: phosphorylation decreases collagenase production *in vitro*, Biomaterials, 1999, **20**, 1979-1988

229. Grillo, H.C. and Gross, J., Collagenolytic activity during mammalian wound repair, Dev. Biol., 1966, **15**, 300-316

230. Clay, C.S., Lydon, M.J. and Tighe, B.J., Biomaterials and clinical applications, (Eds. Pizzoferrato, A., Marchetti, P.G., Ravaglioli, A. and Lee, A.J.C.), Elsevier Science, Amsterdam, 1987, 535

231. Lydon, F.J., Novel hydrogel copolymers and semi-interpenetrating polymer networks, Ph.D thesis, Aston University, 1996

232. Smetana, K., Lukas, J., Paleckova, V. *et al*, Effect of chemical structure of hydrogels on the adhesion and phenotypic characteristics of human monocytes such as expression of galectins and other carbohydrate-binding sites, Biomaterials, 1997, **18**, 14, 1009-1014

233. Kunzler, J. and McGee, J., Contact lens materials, Chem. Ind., 1995, **16**, 651-655

234. Stoker, M., O'Neill, C., Berryman, S. *et al*, Anchorage and growth regulation in normal and virus-transformed cells, International Journal of Cancer, 1968, **3**, 683-693

235. Verwey, E.J.W. and Overbeek, J., Theory of the stability of lyophobic colloids, Elsevier, Amsterdam, 1948

236. Kauzman, W., Some factors in the interpretation of protein denaturation, Advances in Protein Chemistry, 1959, **14**, 1-63

237. Baier, R.E, Shafrin, E.G., and Zisman, W.A., Adhesion: Mechanisms that assist or impede it, Science, 1968, **162**, 1360-1368

238. Altankov, G. and Groth, T.H., Reorganization of substratum-bound fibronectin on hydrophilic and hydrophobic materials is related to biocompatibility, Journal of Materials Science: Materials in Medicine, 1994, **5**, 732-737

239. Maroudas, N.G., Adhesion and spreading of cells on charged surfaces, Journal of Theoretical Biology, 1975, **49**, 417-424

240. Braut-Boucher, F., Pichon, J. and Rat, P., A non-isotopic, highly sensitive, fluorimetric, cell-cell adhesion microplate assay using calcein AM-labeled lymphocytes, Journal of Immunological Methods, 1995, **178,** 1, 41-51

241. Rat, P., Korwin-Zmijowska, C., Warnet, J.M. *et al*, New *in vitro* fluorimetric microtitration assays for toxicological screening of drugs, Cell Biology and Toxicology, 1994, **10,** 5, 329-337

242. De Clerck, L.S., Bridts, C.H., Mertens, A.M. *et al*, Use of fluorescent dyes in the determination of adherence of human leucocytes to endothelial cells and effect of the fluorochromes on cellular function, Journal of Immunological Methods, 1994, **172,** 1, 115-124

243. Aparicio, C.L., Strong, L.H., Yarmush, M.L. *et al*, Correction for label leakage in fluorimetric assays of cell adhesion, Biotechniques, 1997, **23**, 6, 1056-1060

244. Akeson, A.L. and Woods, C.W., A fluorometric assay for the quantitation of cell adherence to endothelial cells, Journal of Immunological Methods, 1993, **163,** 2, 181-185

245. Haugland, R.P., Handbook of fluorescent probes and research chemicals, 7th Edn, Molecular Probes. Inc. Eugene, Oregon, 1999

246. Dropcova, S., Denyer, S.P., Lloyd, A.W. *et al*, A standard strain of human ocular keratocytes, Ophthalmic Research, 1999, **31,** 1, 33-41

247. Brandley, B.K., Weisz, O.A. and Schnaar, R.L., Cell attachment and long-term growth on derivatizable polyacrylamide surfaces, Journal of Biological Chemistry, 1987, **262**, 6431-6437

248. Peluso, G., Petillo, O., Anderson, J.M. *et al*, The differential effects of poly(2-hydroxyethyl methacrylate) and poly(2-hydroxyethyl methacrylate)/ poly(caprolactone) polymers on cell proliferation and collagen synthesis by human lung fibroblasts, J. Biomed. Mater. Res., 1997, **34**, 327-336

249. Minett, W.T., Cell adhesion on synthetic polymer substrates, Ph.D thesis, Aston University, 1986

250. Ratner, B.D., The synthesis, characterisation, applications of polymer, Vol. 7, Specially polymers and polymer processing, Pergamon Press, Oxford, 1989

251. Guan, J., Gao, C., Feng, L. *et al*, Surface photo-grafting of polyurethane with 2-hydroxyethyl acrylate for promotion of human endothelial cell adhesion and growth, J. Biomater. Sci.: Polymer Edn, 2000, **11**, 5, 523-536

252. Ito, Y., Sisido, M. and Imanishi, Y., Synthesis and antithrombogenicity of anionic polyurethanes and heparin-bound polyurethanes, J. Biomed. Mater. Res. 1986, **20**, 1157-1177

253. Newsome, D.A., Foidart, J.M., Hassell, J.R. *et al*, Detection of specific collagen types in normal and keratoconus corneas, Invest. Ophthalmol. Vis. Sci., 1981, **20**, 738

254. Maurice, D.M., The cornea and sclera. p. 1. In Davson, H. (ed): The Eye, Vol. 1B. Vegetative Physiology and Biochemistry. 3rd Edn. Academic Press, Orlando, FL, 1984

255. Cintron, C., Schneider, H. and Kublin, C., Corneal scar formation, Exp. Eye Res., 1973, **17**, 251

256. Freeman, I.L., Collagen polymorphism in mature rabbit cornea, Invest. Ophthalmol. Vis. Sci., 1978, **17**, 171

257. Newsome, D.A., Gross, J. and Hassell, J.R., Human corneal stroma contains three distinct collagens, Invest. Ophthalmol. Vis. Sci., 1982, **22**, 376

258. Hamada, R., Giraud, J.P., Graft, B. *et al*, Etude analytique et statistique des lamelles, des keratocytes, des fibrilles de collagene de la region centrale de la cornee humaine normale, Arch. Ophtalmol. (Paris), 1972, **32**, 563

259. Giraud, J.P., Pouliquen, Y., Offret, G. *et al*, Statistical morphometric studies in normal human and rabbit corneal stroma, Exp. Eye Res., 1975, **21**, 221

260. Hogan, M.J., Alvarado, J.A. and Weddell, E., Histology of the Human Eye. WB Saunders, Philadelphia, 1971

261. Kuwabara, T., Current concepts in anatomy and histology of the cornea, Contact Intraocular Lens Med. J., 1979, **4**, 101

262. Praus, R. and Brettschneider, I., Glycosaminoglycans in embryonic and postnatal human cornea, Ophthalmic Res., 1975, **7**, 542

263. Yue, B., Baum, J.L. and Silbert, J.E., Synthesis of glycosaminoglycans by cultures of normal human corneal endothelial and stromal cells, Invest. Ophthalmol. Vis. Sci., 1978, **17**, 523

264. Borcherding, M.S., Blacik, L.J., Sittig, R.A. *et al*, Proteoglycans and collagen fibre organization in human corneoscleral tissue, Exp. Eye Res., 1975, **21**, 59

265. Py, D.C., Debiccari, A. and Caldwell, D., Keratoprosthesis: engineering and safety assessment, Refract. Corneal Surg., 1993, **9**, 206-208

266. Guo, A., Rife, L.L., Rao, N.A. *et al*, Anterior segment prosthesis development: evaluation of expanded polytetrafluoroethylene as a sclera-attached prosthetic material, Cornea, 1996, **15**, 210-214

267. Flory, P.J., Principles of Polymer Chemistry, Cornell University Press, Ithaca, N.Y., 1953

268. Sariri, R., Mann, A.M., Franklin, V.J. *et al*, Acidic and basic impurities in soft contact lenses, Poster presented at BCLA, London, 1995

Appendix 1

Water Contents Of Novel Hydrogels

Gel ID	AMO : MMA	EWC %	Freeing water content %	Non freezing water content %
J66	40 : 60	15.2	0.7	14.5
J50	50 : 50	21.1	1.7	19.4
J49	60 : 40	34.7	8.9	25.8
J57	70 : 30	46.6	27.1	19.5
J60	80 : 20	63.9	45.4	18.5
J63	90 : 10	73.4	58.3	15.1

Gel ID	NVP : MMA	EWC %	Freeing water content %	Non freezing water content %
J68	40 : 60	29.1	1.0	28.1
J54	50 : 50	43.0	3.6	39.4
J53	60 : 40	55.3	19.2	36.1
J59	70 : 30	64.6	34.9	29.7
J62	80 : 20	74.6	51.5	23.1
J65	90 : 10	82.8	68.7	14.1

Gel ID	NNDMA : MMA	EWC %	Freeing water content %	Non freezing water content %
J67	40 : 60	49.9	19.1	30.8
J52	50 : 50	53.0	20.1	32.9
J51	60 : 40	67.5	40.7	26.8
J58	70 : 30	75.9	57.2	18.7
J61	80 : 20	81.3	69.9	11.4
J64	90 : 10	84.5	70.5	14.0

Gel ID	AMO : MMA	Total Grams of Water / Gram of Polymer	Grams of Freezing Water / Gram of Polymer	Grams of Non-freezing Water / Gram of Polymer
J66	40 : 60	0.18	0.01	0.17
J50	50 : 50	0.27	0.02	0.25
J49	60 : 40	0.53	0.14	0.39
J57	70 : 30	0.87	0.51	0.36
J60	80 : 20	1.77	1.26	0.51
J63	90 : 10	2.76	2.19	0.57

Gel ID	NVP : MMA	Total Grams of Water / Gram of Polymer	Grams of Freezing Water / Gram of Polymer	Grams of Non-freezing Water / Gram of Polymer
J68	40 : 60	0.41	0.01	0.40
J54	50 : 50	0.75	0.06	0.69
J53	60 : 40	1.24	0.43	0.81
J59	70 : 30	1.82	0.99	0.83
J62	80 : 20	2.94	2.03	0.91
J65	90 : 10	4.81	3.99	0.82

Gel ID	NNDMA : MMA	Total Grams of Water / Gram of Polymer	Grams of Freezing Water / Gram of Polymer	Grams of Non-freezing Water / Gram of Polymer
J67	40 : 60	1.00	0.38	0.62
J52	50 : 50	1.13	0.43	0.70
J51	60 : 40	2.08	1.25	0.83
J58	70 : 30	3.15	2.37	0.78
J61	80 : 20	4.35	3.74	0.61
J64	90 : 10	5.45	4.55	0.90

Gel ID	PU5 :AMO:THFMA	EWC %	Freezing water content %	Non-freezing water content %
J18	16.8 : 41.6 : 41.6	30.7	12.0	18.7
J19	21.8 : 41.6 : 36.6	35.8	9.6	26.2
A14	20 : 50 : 30	41.4	20.4	21.0
J1	10 : 55 : 35	44.2	24.1	20.1
J10	15 : 55 : 30	48.1	28.6	19.5
J11	10 : 60 : 30	51.1	29.5	21.6
J20	15 : 60 : 25	46.5	20.3	26.2

Gel ID	PU5 : NNDMA : THFMA	EWC %	Freezing water content %	Non-freezing water content %
J15	16.8 : 41.6 : 41.6	55.9	28.3	27.6
J16	21.8 : 41.6 : 36.6	55.2	27.6	27.6
J2	20 : 50 : 30	58.6	36.2	22.4
J3	10 : 55 : 35	70.3	51.1	19.2
J4	15 : 55 : 30	67.0	42.0	25.0
J5	10 : 60 : 30	72.6	50.0	22.6
J17	15 : 60 : 25	69.1	51.0	18.1

Gel ID	PU5 : NVP : THFMA	EWC %	Freezing water content %	Non-freezing water content %
J12	16.8 : 41.6 : 41.6	45.9	18.9	27.0
J13	21.8 : 41.6 : 36.6	45.4	17.4	28.0
J6	20 : 50 : 30	51.3	19.5	31.8
J7	10 : 55 : 35	60.2	35.7	24.5
J8	15 : 55 : 30	58.3	31.8	26.5
J9	10 : 60 : 30	63.3	36.6	26.7
J14	15 : 60 : 25	62.1	38.9	23.2

Gel ID	PU5 :AMO:THFMA	Total Grams of Water / Gram of Polymer	Grams of Freezing Water / Gram of Polymer	Grams of Non-freezing Water / Gram of Polymer
J18	16.8 : 41.6 : 41.6	0.44	0.17	0.27
J19	21.8 : 41.6 : 36.6	0.56	0.15	0.41
A14	20 : 50 : 30	0.71	0.35	0.36
J1	10 : 55 : 35	0.79	0.42	0.37
J10	15 : 55 : 30	0.93	0.55	0.38
J11	10 : 60 : 30	1.04	0.60	0.44
J20	15 : 60 : 25	0.87	0.38	0.49

Gel ID	PU5 : NNDMA : THFMA	Total Grams of Water / Gram of Polymer	Grams of Freezing Water / Gram of Polymer	Grams of Non-freezing Water / Gram of Polymer
J15	16.8 : 41.6 : 41.6	1.27	0.64	0.63
J16	21.8 : 41.6 : 36.6	1.23	0.62	0.61
J2	20 : 50 : 30	1.42	0.87	0.55
J3	10 : 55 : 35	2.37	1.72	0.65
J4	15 : 55 : 30	2.03	1.27	0.76
J5	10 : 60 : 30	2.65	1.82	0.83
J17	15 : 60 : 25	2.24	1.65	0.59

Gel ID	PU5 : NVP : THFMA	Total Grams of Water / Gram of Polymer	Grams of Freezing Water / Gram of Polymer	Grams of Non-freezing Water / Gram of Polymer
J12	16.8 : 41.6 : 41.6	0.85	0.35	0.50
J13	21.8 : 41.6 : 36.6	0.83	0.32	0.51
J6	20 : 50 : 30	1.05	0.40	0.65
J7	10 : 55 : 35	1.51	0.90	0.61
J8	15 : 55 : 30	1.40	0.76	0.64
J9	10 : 60 : 30	1.72	1.00	0.72
J14	15 : 60 : 25	1.64	1.03	0.61

PU5 :AMO:THFMA (porous)	EWC % (with dextrin)	EWC% (with dextrin and dextran)
16.8 : 41.6 : 41.6	29.6	32.3
21.8 : 41.6 : 36.6	33.1	37.3
20 : 50 : 30	37.9	42.0
10 : 55 : 35	42.2	40.7
15 : 55 : 30	40.1	43.1
10 : 60 : 30	46.2	46.8
15 : 60 : 25	45.3	48.9

PU5 : NNDMA : THFMA (porous)	EWC % (with dextrin)	EWC % (with dextrin and dextran)
16.8 : 41.6 : 41.6	54.2	54.3
21.8 : 41.6 : 36.6	52.7	52.6
20 : 50 : 30	60.8	62.1
10 : 55 : 35	68.5	67.7
15 : 55 : 30	66.9	67.2
10 : 60 : 30	69.9	73.0
15 : 60 : 25	70.2	68.3

PU5 : NVP : THFMA (porous)	EWC % (with dextrin)	EWC % (with dextrin and dextran)
16.8 : 41.6 : 41.6	44.5	46.2
21.8 : 41.6 : 36.6	43.1	43.6
20 : 50 : 30	50.4	50.4
10 : 55 : 35	59.3	58.9
15 : 55 : 30	56.5	54.5
10 : 60 : 30	63.4	64.5
15 : 60 : 25	59.4	60.3

Gel ID		EWC %
J21	PU5 : AMO : THFMA = 10 : 55 : 35 (200) PEG 5%	49.1
J22	PU5 : AMO : THFMA = 10 : 55 : 35 (200) PEG 10%	50.5
J23	PU5 : AMO : THFMA = 10 : 55 : 35 (200) PEG 20%	53.3
J24	PU5 : NNDMA : THFMA = 10 : 55 : 35 (200) PEG 5%	72.6
J25	PU5 : NNDMA : THFMA = 10 : 55 : 35 (200) PEG 10%	72.2
J26	PU5 : NNDMA : THFMA = 10 : 55 : 35 (200) PEG 20%	70.4
J27	PU5 : NVP : THFMA = 10 : 55 : 35 (200) PEG 5%	64.0
J28	PU5 : NVP : THFMA = 10 : 55 : 35 (200) PEG 10%	63.6
J29	PU5 : NVP : THFMA = 10 : 55 : 35 (200) PEG 20%	63.1
J30	PU5 : AMO : THFMA = 10 : 55 : 35 (440) PEG 5%	47.8
J31	PU5 : AMO : THFMA = 10 : 55 : 35 (440) PEG 10%	50.4
J32	PU5 : AMO : THFMA = 10 : 55 : 35 (440) PEG 20%	52.6
J33	PU5 : NNDMA : THFMA = 10 : 55 : 35 (440) PEG 5%	71.5
J34	PU5 : NNDMA : THFMA = 10 : 55 : 35 (440) PEG 10%	70.8
J35	PU5 : NNDMA : THFMA = 10 : 55 : 35 (440) PEG 20%	70.0
J36	PU5 : NVP : THFMA = 10 : 55 : 35 (440) PEG 5%	63.8
J37	PU5 : NVP : THFMA = 10 : 55 : 35 (440) PEG 10%	64.4
J38	PU5 : NVP : THFMA = 10 : 55 : 35 (440) PEG 20%	63.4

Appendix 2

Mechanical Properties Of Novel Hydrogels

Gel ID	AMO : MMA	E.Mod (MPa)	Ts (MPa)	Eb %
J66	40 : 60	305.0	20.3	12
J50	50 : 50	92.0	6.8	91
J49	60 : 40	2.1	1.2	299
J57	70 : 30	0.3	0.3	140
J60	80 : 20	0.2	0.1	83
J63	90 : 10	0.2	0.1	70

Gel ID	NVP : MMA	E.Mod (MPa)	Ts (MPa)	Eb %
J68	40 : 60	70.0	9.4	59
J54	50 : 50	43.0	5.4	155
J53	60 : 40	8.1	2.7	158
J59	70 : 30	0.5	1.1	264
J62	80 : 20	0.2	0.2	90
J65	90 : 10	0.2	0.04	27

Gel ID	NNDMA : MMA	E.Mod (MPa)	Ts (MPa)	Eb %
J67	40 : 60	0.6	0.5	111
J52	50 : 50	0.3	0.6	208
J51	60 : 40	0.3	0.2	84
J58	70 : 30	0.2	0.1	61
J61	80 : 20	0.2	0.1	77
J64	90 : 10	0.2	0.2	84

Gel ID	PU5 : AMO : THFMA	E.Mod (MPa)	Ts (MPa)	Eb %
J18	16.8 : 41.6 : 41.6	11.5	1.9	142
J19	21.8 : 41.6 : 36.6	14.5	2.3	159
A14	20 : 50 : 30	9.2	1.3	139
J1	10 : 55 : 35	6.5	0.9	85
J10	15 : 55 : 30	9.8	1.1	87
J11	10 : 60 : 30	5.0	0.8	69
J20	15 : 60 : 25	8.9	1.1	63

Gel ID	PU5 : NNDMA : THFMA	E.Mod (MPa)	Ts (MPa)	Eb %
J15	16.8 : 41.6 : 41.6	6.3	0.9	88
J16	21.8 : 41.6 : 36.6	8.9	1.0	74
J2	20 : 50 : 30	5.0	0.8	79
J3	10 : 55 : 35	0.4	0.2	54
J4	15 : 55 : 30	0.7	0.3	62
J5	10 : 60 : 30	0.4	0.2	46
J17	15 : 60 : 25	0.5	0.3	47

Gel ID	PU5 : NVP : THFMA	E.Mod (MPa)	Ts (MPa)	Eb %
J12	16.8 : 41.6 : 41.6	13.5	4.4	83
J13	21.8 : 41.6 : 36.6	21.9	4.6	67
J6	20 : 50 : 30	13.0	4.0	70
J7	10 : 55 : 35	1.3	1.0	46
J8	15 : 55 : 30	2.9	1.7	35
J9	10 : 60 : 30	1.0	0.8	36
J14	15 : 60 : 25	2.0	1.3	41

Gel ID	PU5 : AMO : THFMA (with dextrin)	E.Mod (MPa)	Ts (MPa)	Eb %
J18	16.8 : 41.6 : 41.6	21.1	3.3	142
J19	21.8 : 41.6 : 36.6	16.0	3.2	115
A14	20 : 50 : 30	10.5	1.7	87
J1	10 : 55 : 35	4.4	1.0	144
J10	15 : 55 : 30	4.6	1.2	105
J11	10 : 60 : 30	2.5	0.6	89
J20	15 : 60 : 25	5.9	0.9	103

Gel ID	PU5 : NVP : THFMA (with dextrin)	E.Mod (MPa)	Ts (MPa)	Eb %
J12	16.8 : 41.6 : 41.6	11.5	2.9	69
J13	21.8 : 41.6 : 36.6	26.5	3.7	65
J6	20 : 50 : 30	7.6	2.8	100
J7	10 : 55 : 35	1.4	0.8	60
J8	15 : 55 : 30	2.6	1.5	68
J9	10 : 60 : 30	0.8	0.5	65
J14	15 : 60 : 25	1.6	1.4	84

Gel ID	PU5 : NNDMA : THFMA (with dextrin)	E.Mod (MPa)	Ts (MPa)	Eb %
J15	16.8 : 41.6 : 41.6	5.0	0.8	69
J16	21.8 : 41.6 : 36.6	8.4	1.2	79
J2	20 : 50 : 30	1.4	0.8	85
J3	10 : 55 : 35	0.4	0.2	63
J4	15 : 55 : 30	0.6	0.3	67
J5	10 : 60 : 30	0.5	0.2	58
J17	15 : 60 : 25	0.5	0.3	62

Gel ID	PU5 : AMO : THFMA (with dextrin and dextran)	E.Mod (MPa)	TS (MPa)	Eb %
J18	16.8 : 41.6 : 41.6	18.8	2.0	69
J19	21.8 : 41.6 : 36.6	15.0	1.7	52
A14	20 : 50 : 30	7.1	1.0	59
J1	10 : 55 : 35	5.5	0.6	61
J10	15 : 55 : 30	5.5	0.8	72
J11	10 : 60 : 30	2.0	0.5	65
J20	15 : 60 : 25	3.8	0.6	69

Gel ID	PU5 : NVP : THFMA (with dextrin and dextran)	E.Mod (MPa)	TS (MPa)	Eb %
J12	16.8 : 41.6 : 41.6	13.6	2.0	43
J13	21.8 : 41.6 : 36.6	13.1	2.2	23
J6	20 : 50 : 30	8.8	1.8	45
J7	10 : 55 : 35	1.5	0.4	29
J8	15 : 55 : 30	3.1	1.0	43
J9	10 : 60 : 30	0.9	0.3	33
J14	15 : 60 : 25	1.7	0.9	53

Gel ID	PU5 : NNDMA : THFMA (with dextrin and dextran)	E.Mod (MPa)	TS (MPa)	Eb %
J15	16.8 : 41.6 : 41.6	2.3	0.7	77
J16	21.8 : 41.6 : 36.6	4.9	0.8	42
J2	20 : 50 : 30	2.1	0.5	52
J3	10 : 55 : 35	0.5	0.2	47
J4	15 : 55 : 30	0.6	0.3	57
J5	10 : 60 : 30	0.4	0.2	53
J17	15 : 60 : 25	0.6	0.3	57

Gel ID		E.Mod (MPa)	Ts (MPa)	Eb%
J22	PU5 : AMO : THFMA = 10 : 55 : 35 (200) PEG 10%	4.5	0.6	70
J23	PU5 : AMO : THFMA = 10 : 55 : 35 (200) PEG 20%	1.7	0.3	28
J25	PU5 : NNDMA : THFMA = 10 : 55 : 35 (200) PEG 10%	0.5	0.2	42
J26	PU5 : NNDMA : THFMA = 10 : 55 : 35 (200) PEG 20%	0.6	0.2	35
J28	PU5 : NVP : THFMA = 10 : 55 : 35 (200) PEG 10%	1.1	0.3	28
J29	PU5 : NVP : THFMA = 10 : 55 : 35 (200) PEG 20%	1.4	0.2	21
J30	PU5 : AMO : THFMA = 10 : 55 : 35 (440) PEG 5%	2.1	0.5	55
J31	PU5 : AMO : THFMA = 10 : 55 : 35 (440) PEG 10%	1.4	0.5	55
J32	PU5 : AMO : THFMA = 10 : 55 : 35 (440) PEG 20%	1.6	0.3	27
J33	PU5 : NNDMA : THFMA = 10 : 55 : 35 (440) PEG 5%	0.5	0.2	43
J34	PU5 : NNDMA : THFMA = 10 : 55 : 35 (440) PEG 10%	0.6	0.2	35
J35	PU5 : NNDMA : THFMA = 10 : 55 : 35 (440) PEG 20%	0.8	0.2	25
J36	PU5 : NVP : THFMA = 10 : 55 : 35 (440) PEG 5%	1.4	0.6	42
J37	PU5 : NVP : THFMA = 10 : 55 : 35 (440) PEG 10%	1.3	0.3	27
J38	PU5 : NVP : THFMA = 10 : 55 : 35 (440) PEG 20%	1.5	0.1	9

Appendix 3

Surface Properties Of Novel Hydrogels

Dehydrated State Surface Properties

Gel ID	PU5 : AMO : THFMA	Water Contact Angles	Diiodomethane Contact Angles	γ^d (mN/m)	γ^p (mN/m)	γ (mN/m)
J18	16.8 : 41.6 : 41.6	83	32	41.1	2.3	43.4
J19	21.8 : 41.6 : 36.6	79	44	33.3	5.3	38.6
A14	20 : 50 : 30	85	35	40.1	1.9	42.0
J1	10 : 55 : 35	74	30	39.5	5.7	45.2
J10	15 : 55 : 30	68	35	35.5	9.7	45.2
J11	10 : 60 : 30	78	35	38.1	4.5	42.6
J20	15 : 60 : 25	81	30	41.5	2.8	44.3

Gel ID	PU5 : NNDMA : THFMA	Water Contact Angles	Diiodomethane Contact Angles	γ^d (mN/m)	γ^p (mN/m)	γ (mN/m)
J15	16.8 : 41.6 : 41.6	80	31	40.7	3.3	44.0
J16	21.8 : 41.6 : 36.6	74	39	34.9	7.0	41.9
J2	20 : 50 : 30	90	24	46.8	0.4	47.2
J3	10 : 55 : 35	91	30	44.4	0.4	44.8
J4	15 : 55 : 30	83	32	41.1	2.3	43.4
J5	10 : 60 : 30	85	34	40.6	1.9	42.5
J17	15 : 60 : 25	88	31	43.0	1.0	44.0

Gel ID	PU5 : NVP : THFMA	Water Contact Angles	Diiodomethane Contact Angles	γ^d (mN/m)	γ^p (mN/m)	γ (mN/m)
J12	16.8 : 41.6 : 41.6	63	20	43.9	9.5	53.4
J13	21.8 : 41.6 : 36.6	78	25	42.8	3.5	46.3
J6	20 : 50 : 30	82	34	39.7	2.8	42.5
J7	10 : 55 : 35	84	32	41.3	2.0	43.3
J8	15 : 55 : 30	90	37	40.4	0.9	41.3
J9	10 : 60 : 30	90	28	45.1	0.5	45.6
J14	15 : 60 : 25	68	29	38.4	8.7	47.1

Hydrated State Surface Properties (Clear Materials)

Gel ID	PU5 : AMO : THFMA	Air Contact Angles	N-Octane Contact Angles	γ^d (mN/m)	γ^p (mN/m)	γ^l (mN/m)
J18	16.8 : 41.6 : 41.6	136	111	27.4	23.5	50.9
J19	21.8 : 41.6 : 36.6	123	112	15.6	24.1	39.7
A14	20 : 50 : 30	125	110	16.0	22.9	38.9
J1	10 : 55 : 35	124	123	25.0	30.4	55.4
J10	15 : 55 : 30	133	123	35.5	30.4	65.9
J11	10 : 60 : 30	140	131	52.2	35.0	87.2
J20	15 : 60 : 25	114	119	12.1	28.1	40.2

Gel ID	PU5 : NNDMA : THFMA	Air Contact Angles	N-Octane Contact Angles	γ^d (mN/m)	γ^p (mN/m)	γ^l (mN/m)
J15	16.8 : 41.6 : 41.6	124	103	10.6	19.1	29.7
J16	21.8 : 41.6 : 36.6	129	114	22.9	25.2	48.1
J2	20 : 50 : 30	124	126	27.4	32.2	59.6
J3	10 : 55 : 35	135	132	46.6	35.5	82.1
J4	15 : 55 : 30	128	124	30.4	31.0	61.4
J5	10 : 60 : 30	127	127	31.8	32.7	64.6
J17	15 : 60 : 25	134	117	31.0	27.0	57.9

Gel ID	PU5 : NVP : THFMA	Air Contact Angles	N-Octane Contact Angles	γ^d (mN/m)	γ^p (mN/m)	γ^l (mN/m)
J12	16.8 : 41.6 : 41.6	118	112	11.3	24.1	35.4
J13	21.8 : 41.6 : 36.6	102	106	0.6	20.8	21.4
J6	20 : 50 : 30	118	123	18.5	30.4	48.9
J7	10 : 55 : 35	129	126	33.4	32.2	65.6
J8	15 : 55 : 30	139	132	51.8	35.5	87.3
J9	10 : 60 : 30	140	126	46.9	32.2	79.1
J14	15 : 60 : 25	132	127	38.0	32.7	70.8

Appendix 4

Cell Response To Novel Hydrogels

Sample ID		Cell Adhesion Number (ethanol sterilised)	Cell Adhesion Number (autoclave sterilised)
CS		516 ± 40	
HEMA		176 ±129	
J1	PU5 : AMO: THFMA = 10 : 55 : 35	115 ± 81	136 ± 28
J3	PU5 : NNDMA : THFMA = 10 : 55 : 35	28 ± 13	68 ± 27
J7	PU5 : NVP :THFMA = 10: 55 : 35	28 ± 9	47 ± 29
J21	PU5 : AMO : THFMA = 10 : 55 : 35 (200) PEG 5%	79 ± 28	149 ± 21
J24	PU5 : NNDMA : THFMA = 10 : 55 : 35 (200) PEG 5%	119 ± 46	80 ± 21
J27	PU5 : NVP : THFMA = 10 : 55 : 35 (200) PEG 5%	41 ± 16	122 ± 51
J30	PU5 : AMO : THFMA = 10 : 55 : 35 (440) PEG 5%	60 ± 33	91 ± 17
J33	PU5 : NNDMA : THFMA = 10 : 55 : 35 (440) PEG 5%	92 ± 48	50 ± 39
J36	PU5 : NVP : THFMA = 10 : 55 : 35 (440) PEG 5%	25 ± 10	63 ± 55

Sample ID		Cell Adhesion Number
CS		611 ± 20
J18	PU5 : AMO :THFMA = 16.8 : 41.6 : 41.6	388 ± 23
J19	PU5 : AMO : THFMA = 21.8 : 41.6 : 36.6	332 ± 28
HEMA		184 ± 34

Sample ID		Cell Adhesion Number
CS		548 ± 134
F1	PU5 : AMO : THFMA = 10 : 60 : 30 20% Dextrin (Pore size < 38 μm)	121 ± 10
F2	PU5 : AMO : THFMA = 10 : 60 : 30 20% Dextrin (Pore size < 38 μm) + 4% Dextran	136 ± 32
F3	PU5 : AMO : THFMA = 10 : 60 : 30 20% Salt (Pore size > 90 μm)	183 ± 26
F4	PU5 : AMO : THFMA = 10 : 60 : 30 20% Salt (Pore size: 63 - 90 μm)	159 ± 19
F5	PU5 : AMO : THFMA = 10 : 60 : 30 20% Salt (Pore size > 90 μm) + 4% Dextran	170 ± 6
F6	PU5 : AMO : THFMA = 10 : 60 : 30 20% Salt (Pore size: 63 - 90 μm) + 4% Dextran	128 ± 19
J5A	PU5 : NNDMA : THFMA = 10 : 60 : 30 20% Dextrin (Pore size < 38 μm)	100 ± 22
J5B	PU5 : NNDMA : THFMA = 10 : 60 : 30 20% Dextrin (Pore size < 38 μm) + 4% Dextran	172 ± 46
J5C	PU5 : NNDMA : THFMA = 10 : 60 : 30 20% Salt (Pore size: 38 – 63 μm)	129 ± 36
J5D	PU5 : NNDMA : THFMA = 10 : 60 : 30 20% Salt (Pore size: 63 - 90 μm)	109 ± 25
J5E	PU5 : NNDMA : THFMA = 10 : 60 : 30 20% Salt (Pore size: 90 - 125 μm)	64 ± 13
J9A	PU5 : NVP : THFMA = 10 : 60 : 30 20% Dextrin (Pore size < 38 μm)	63 ± 26
J9B	PU5 : NVP : THFMA = 10 : 60 : 30 20% Dextrin (Pore size < 38 μm) + 4% Dextran	167 ± 19
J9C	PU5 : NVP : THFMA = 10 : 60 : 30 20% Salt (Pore size: 38 – 63 μm)	48 ± 36
J9D	PU5 : NVP : THFMA = 10 : 60 : 30 20% Salt (Pore size: 63 - 90 μm)	7 ± 2
J9E	PU5 : NVP : THFMA = 10 : 60 : 30 20% Salt (Pore size: 90 - 125 μm)	84 ± 19

Appendix 5

Spoilation Test On Novel Hydrogels

Surface Protein Spoilation (fluorescence units) (280nm)					
Day	**HEMA**	**ABH** (HEMA : NVP : MMA : PEG200 MA = $55\,^{3}/_{7} : 11\,^{7}/_{10} : 12\,^{3}/_{5} : 20\,^{1}/_{5}$)	**J81** (HEMA : AMO : MMA :PEG200 MA = 55 : 12 : 13 : 20)	**J82** (HEMA : NNDMA : MMA : PEG200 MA = 55 : 12 : 13 : 20)	**J83** (HEMA : NVP : AMO : MMA : PEG200 MA = 45 : 15 : 12 : 13 : 20)
Blank	54.6	307.6	170.4	89.1	96.7
3	967.2	1067.6	852.5	965.4	1298.9
7	1663.0	1214.8	1399.3	1405.6	1757.0
10	2712.2	1610.2	2430.1	1871.4	2892.3
14	3846.5	1799.7	2959.0	2405.6	4444.8
17	3850.2	2402.5	3146.8	2714.6	5068.0
21	4664.3	2715.2	3610.8	3408.2	9619.0
24	5617.2	3604.2	4315.2	3868.0	
28	6790.8	4309.3	5547.2	4313.8	

Total Protein Spoilation (mg/lens) (UV)					
Day	**HEMA**	**ABH** (HEMA : NVP : MMA : PEG200 MA = $55\,^{3}/_{7} : 11\,^{7}/_{10} : 12\,^{3}/_{5} : 20\,^{1}/_{5}$)	**J81** (HEMA : AMO : MMA :PEG200 MA = 55 : 12 : 13 : 20)	**J82** (HEMA : NNDMA : MMA : PEG200 MA = 55 : 12 : 13 : 20)	**J83** (HEMA : NVP : AMO : MMA : PEG200 MA = 45 : 15 : 12 : 13 : 20)
Blank	0.041	0.050	0.036	0.024	0.029
3	0.053	0.068	0.050	0.033	0.053
7	0.065	0.086	0.060	0.062	0.093
10	0.081	0.100	0.081	0.068	0.110
14	0.110	0.111	0.083	0.086	0.135
17	0.135	0.138	0.096	0.129	0.195
21	0.141	0.170	0.113	0.156	0.215
24	0.155	0.197	0.143	0.174	
28	0.185	0.233	0.167	0.204	

Surface Lipid Spoilation (fluorescence units) (280nm)					
Day	**HEMA**	**ABH** (HEMA : NVP : MMA : PEG200 MA = 55 $^{3}/_{7}$: 11 $^{7}/_{10}$: 12 $^{3}/_{5}$: 20 $^{1}/_{5}$)	**J81** (HEMA : AMO : MMA :PEG200 MA = 55 : 12 : 13 : 20)	**J82** (HEMA : NNDMA : MMA : PEG200 MA = 55 : 12 : 13 : 20)	**J83** (HEMA : NVP : AMO : MMA : PEG200 MA = 45 : 15 : 12 : 13 : 20)
Blank	28.15	123.90	39.79	35.44	36.85
3	182.41	147.73	130.38	86.38	95.05
7	248.45	155.98	128.65	136.88	178.96
10	315.78	167.08	168.90	182.62	225.33
14	354.62	192.63	244.10	214.54	435.85
17	437.55	274.10	277.48	229.94	565.50
21	567.25	323.17	357.84	269.88	846.00
24	656.02	397.07	444.32	312.86	
28	763.90	448.67	550.43	383.04	

Surface Lipid Spoilation (fluorescence units) (360nm)					
Day	**HEMA**	**ABH** (HEMA : NVP : MMA : PEG200 MA = 55 $^{3}/_{7}$: 11 $^{7}/_{10}$: 12 $^{3}/_{5}$: 20 $^{1}/_{5}$)	**J81** (HEMA : AMO : MMA :PEG200 MA = 55 : 12 : 13 : 20)	**J82** (HEMA : NNDMA : MMA : PEG200 MA = 55 : 12 : 13 : 20)	**J83** (HEMA : NVP : AMO : MMA : PEG200 MA = 45 : 15 : 12 : 13 : 20)
Blank	14.87	18.02	16.89	12.21	13.92
3	36.45	33.73	44.89	27.38	75.07
7	72.66	44.31	74.70	57.35	135.23
10	104.87	55.19	86.82	74.31	161.04
14	117.65	64.79	97.22	98.91	286.28
17	178.07	74.82	105.07	122.11	340.77
21	195.06	82.51	114.58	143.78	385.00
24	338.67	94.21	183.08	175.38	
28	438.45	145.83	243.38	229.84	

Appendix 6

Datasheets Of Mesh Materials

Mesh 1

DELNET X 540 N-AA

PRODUCT DESCRIPTION

Delnet EP X 540 N-AA is made from HDPE with an amide skin layer on both surfaces.

PRODUCT PROPERTIES

Property		Target
Weight		19 g / m^2
Thickness		160 microns
Boss count	MD	27 per 2.5 cm
	CD	26 per 2.5 cm
Tensile strength	MD	30 N / 5 cm
	CD	33 N / 5 cm
Soft. Pt. Skin		105 °C
Processing range		> 120 °C

APPLICATIONS

Delnet X 540 N-AA is suitable for low temperature laminations and coating to a wide range of substrates including paper, wood, fibreboard, glass fibre, cotton textiles, cotton felt, polyester felt, polypropylene textile, polyurethane foam and other porous materials.

It should be noted that process temperatures will vary with substrates, insulation factors, line speeds, pressure and equipment geometry. These figures should be considered as a starting point when setting operation conditions for each application.

Mesh 2

DELNET EP X540N-E

PRODUCT DESCRIPTION

Delnet EP X 540 N-E is made from HDPE with a surface layer of EVA to provide a low temperature spot bonding system. All components of X540N-E comply with FDA21CFR177.1520 and CICFR177.1330. This grade is also available with a white (WHT) addictive package.

PRODUCT PROPERTIES

Property		Values
Weight		15 g / m^2
Thickness		119 microns
Boss count	MD	9.5 per cm
	CD	9.5 per cm
Maximum width		190 cm
Melting range		95 - 110 °C
Recommended bonding range		120 - 130 °C
Thermal resistance		90 °C

APPLICATIONS

Delnet EP X 540N-E is suitable for low temperature laminations and coating to a wide range of substrates including paper, wood, fibreboard, glass fibre, cotton textiles, cotton felt, polyester felt, polypropylene textile, polyurethane foam and other porous materials.

It should be noted that process temperatures will vary with substrates, insulation factors, line speeds, pressure and equipment geometry. These figures should be considered as a starting point when setting operation conditions for each application.

Mesh 3

DELNET P 520 N-SS

PRODUCT DESCRIPTION

Delnet EP P 520N-SS is made from HDPE with a surlyn skin layer on both surfaces. All components of P 520N-SS comply with 21CFR177.1520, 21CFR177.1330 and other regulations concerning the use of plastics in food contact applications.

PRODUCT PROPERTIES

Property		Target
Weight		27 g / m^2
Thickness		127 microns
Boss count	MD	63 per 5 cm
	CD	69 per 5 cm
Porosity		1700 l /sec / m^2
Tensile strength	MD	44 N / 5 cm
Soft. Pt. Skin		105 °C
Processing range		> 120 °C

APPLICATIONS

Delnet P 520 N-SS is suitable for low temperature laminations and coating to a wide range of substrates including paper, wood, fibreboard, glass fibre, cotton textiles, cotton felt, polyester felt, polypropylene textile, polyurethane foam and other porous materials.

It should be noted that process temperatures will vary with substrates, insulation factors, line speeds, pressure and equipment geometry. These figures should be considered as a starting point when setting operation conditions for each application.

Mesh 4

DELNET P 520 N-AA

PRODUCT DESCRIPTION

Delnet EP P 520N-AA is made from HDPE with an amide skin layer on both surfaces.

PRODUCT PROPERTIES

Property		Target
Weight		27 g / m^2
Thickness		127 microns
Boss count	MD	63 per 5 cm
	CD	69 per 5 cm
Porosity		1700 l / sec / m^2
Tensile strength	MD	44 N / 5 cm
Soft. Pt. Skin		105 °C
Processing range		> 120 °C

APPLICATIONS

Delnet P 520 N-AA is suitable for low temperature laminations and coating to a wide range of substrates including paper, wood, fibreboard, glass fibre, cotton textiles, cotton felt, polyester felt, polypropylene textile, polyurethane foam and other porous materials.

It should be noted that process temperatures will vary with substrates, insulation factors, line speeds, pressure and equipment geometry. These figures should be considered as a starting point when setting operation conditions for each application.